

AD-770 300

AIRCRAFT ANTISKID ANALYSIS VERIFICATION  
AND REFINEMENT

Byron H. Anderson

General Dynamics

Prepared for:

Air Force Flight Dynamics Laboratory

September 1973

DISTRIBUTED BY:

**NTIS**

National Technical Information Service  
U. S. DEPARTMENT OF COMMERCE  
5285 Port Royal Road, Springfield Va. 22151

**UNCLASSIFIED**

Security Classification

**DOCUMENT CONTROL DATA - R & D**

(Security classification of title, body of abstract and indexing annotation must be entered when the overall report is classified)

1. ORIGINATING ACTIVITY (Corporate author) <b>General Dynamics Corporation Convair Aerospace Division, Ft. Worth Operations P.O. Box 748, Fort Worth, Texas 76101</b>		2a. REPORT SECURITY CLASSIFICATION <b>UNCLASSIFIED</b>	
3. REPORT TITLE <b>AIRCRAFT ANTISKID ANALYSIS VERIFICATION AND REFINEMENT</b>			
4. DESCRIPTIVE NOTES (Type of report and inclusive dates) <b>Final Report (December 1970 thru April 1973)</b>			
5. AUTHOR(S) (First name, middle initial, last name) <b>Byron H. Anderson</b>			
6. REPORT DATE <b>September 1973</b>		7a. TOTAL NO. OF PAGES <b>351 365</b>	7b. NO. OF REFS <b>17</b>
8a. CONTRACT OR GRANT NO. <b>F33615-71-C-1109</b>		8b. ORIGINATOR'S REPORT NUMBER(S)	
b. PROJECT NO. <b>1369</b>		9b. OTHER REPORT NO(S) (Any other numbers that may be assigned this report) <b>AFFDL-TR-73-70</b>	
c. Task Area No. 01			
d. Work Unit No. 21			
10. DISTRIBUTION STATEMENT <b>Approved for Public Release - Distribution Unlimited</b>			
11. SUPPLEMENTARY NOTES		12. SPONSORING MILITARY ACTIVITY <b>Air Force Flight Dynamics Laboratory Wright-Patterson AFB, Ohio 45433</b>	
13. ABSTRACT <p>A program for verifying and refining a previously developed aircraft antiskid performance and system compatibility analysis procedure is described. Analysis verification was performed by comparing antiskid system operation as predicted by the analytical procedures with that recorded during laboratory testing. The laboratory tests were conducted at the Air Force Flight Dynamics Laboratory Landing Gear Test Facility at Wright-Patterson Air Force Base, Ohio using a set-up consisting of F-111 aircraft main landing gear, tire, wheel, brake, hydraulic brake actuation system and several antiskid control circuit variations. The aircraft landing gear equipment was mounted in a support fixture with movable load carriage installed over the 192 inch diameter brake test dynamometer. Analytical refinement consisted of modifying the mathematical equations describing antiskid operations to enhance computation economy and more accurately agree with test results. A discussion of parameters influencing antiskid operation is presented. Preliminary design of components for a fluidic controlled pneumatic brake actuation system is described.</p> <p>Reproduced by, <b>NATIONAL TECHNICAL INFORMATION SERVICE</b> U.S. Department of Commerce Springfield VA 22151</p>			

**DD FORM 1473**  
1 NOV 65

**UNCLASSIFIED**

Security Classification

**UNCLASSIFIED**

Security Classification

14. KEY WORDS	LINK A		LINK B		LINK C	
	ROLE	WT	ROLE	WT	ROLE	WT
Airplane Stopping Performance Antiskid Analysis Antiskid Dynamometer Testing Landing Gear Brake System Performance						
ib						

**UNCLASSIFIED**

Security Classification

## NOTICE

When Government drawings, specifications, or other data are used for any purpose other than in connection with a definitely related Government procurement operation, the United States Government thereby incurs no responsibility nor any obligation whatsoever; and the fact that the government may have formulated, furnished, or in any way supplied the said drawings, specifications, or other data, is not to be regarded by implication or otherwise as in any manner licensing the holder or any other person or corporation, or conveying any rights or permission to manufacture, use, or sell any patented invention that may in any way be related thereto.

ADDITIONAL		
ATIS		
10		
10		
APPROVAL		
BY		
UNITED STATES GOVERNMENT		
Dist.	FACIL. AND SP. CHAL	
A		

Copies of this report should not be returned unless return is required by security considerations, contractual obligations, or notice on a specific document.

# **AIRCRAFT ANTISKID ANALYSIS VERIFICATION AND REFINEMENT**

*BYRON H. ANDERSON*

Approved for public release; distribution unlimited

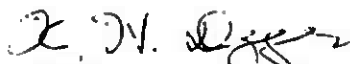
10

## FOREWORD

The Analytical and Experimental Aircraft Antiskid Analysis Verification and Refinement work reported herein was performed by the Fort Worth Operation of General Dynamics Convair Aerospace Division under U. S. Air Force Contract F33615-71-C-1109. The contract was initiated under Project No. 1369, "Mechanical Systems for Advanced Flight Vehicles," and Task No. 136901, "High Performance Landing Gear." This program was administered under the direction of the Air Force Flight Dynamics Laboratory. Mr. Paul M. Wagner (AFFDL/FEM) was the Air Force Project Engineer.

This report describes work conducted during the period from December 1970 thru April 1973. The Convair Project Leader was R. C. Churchill and B. H. Anderson was the principal investigator. The design and installation of the verification test set-up and overhead load carriage fixture on the AFFDL Landing Gear Test Facility at Wright-Patterson AFB, Ohio was accomplished by Mr. J. F. Maverick and Mr. W. I. Streiff. Mr. W. C. Kregar formulated some of the mathematical models. Digital computer programing was performed by Mr. C. W. Austin, Mrs. L. J. Schnacke and Mr. J. D. Price.

The author wishes to thank Mr. Wagner for his guidance and assistance throughout the program. The generous assistance and cooperation of AFFDL Landing Gear Test Facility personnel and members of the Systems Research Laboratories, Inc., during the Verification Test Phase of the program is appreciated. This report was submitted by the author in June 1973.



KENNERLY H. DIGGES  
Chief, Mechanical Branch  
Vehicle Equipment Division  
Air Force Flight Dynamics Laboratory

## ABSTRACT

A program for verifying and refining a previously developed aircraft antiskid performance and system compatibility analysis procedure is described. Analysis verification was performed by comparing antiskid system operation as predicted by the analytical procedures with that recorded during laboratory testing. The laboratory tests were conducted at the Air Force Flight Dynamics Laboratory Landing Gear Test Facility at Wright-Patterson Air Force Base, Ohio using a set-up consisting of F-111 aircraft main landing gear, tire, wheel, brake, hydraulic brake actuation system and several antiskid control circuit variations. The aircraft landing gear equipment was mounted in a support fixture with movable load carriage installed over the 192 inch diameter brake test dynamometer. Analytical refinement consisted of modifying the mathematical equations describing antiskid operations to enhance computation economy and more accurately agree with test results. A discussion of parameters influencing antiskid operation is presented. Preliminary design of components for a fluidic controlled pneumatic brake actuation system is described.

## CONTENTS

Section	Page
I        INTRODUCTION . . . . .	1
A. Objective . . . . .	1
B. Scope . . . . .	1
C. Background . . . . .	2
D. Problem Discussion . . . . .	24
II       VERIFICATION TESTING . . . . .	31
A. Total System Test Installation . . . . .	31
B. Test Conditions and Procedure . . . . .	41
C. Test Results . . . . .	49
III      ANALYSIS REFINEMENT . . . . .	52
IV       TEST DATA CORRELATION . . . . .	67
V        FLUIDIC CONTROLLED PNEUMATIC BRAKE ACTUATION SYSTEM DESIGN STUDY . . . . .	75
REFERENCES . . . . .	81
APPENDIX A   MATHEMATICAL MODELS . . . . .	83
APPENDIX B   DIGITAL COMPUTER PROGRAM FOR SIMPLIFIED ANTISKID ANALYSIS PROCEDURE . . . . .	316

# ILLUSTRATIONS

No.	Title	Page
1	Aircraft Antiskid Arrangement Block Diagram . .	3
2	Pneumatic Tire Slippage Versus Braking Force Characteristic . . . . .	6
3	Braked Wheel Forces . . . . .	8
4	Typical Brake Control/Antiskid Fluid Power System . . . . .	10
5	Typical Brake Characteristics . . . . .	11
6	Antiskid Cycle Events . . . . .	13
7	Comparison of Antiskid Cycle Conditions . . . .	16
8	Aircraft Landing Gear Vertical and Horizontal Loads . . . . .	20
9	Tire Friction Coefficient Functions . . . . .	27
10	Tire Friction Computation . . . . .	28
11	Total System Test Installation - Landing Gear and Support Fixture Viewed Looking North Inside Dynamometer Cage . . . . .	34
12	Total System Test Installation Support Fixture Viewed Looking East from Outside Dynamometer Cage . . . . .	35
13	Total System Test Installation - Dynamometer Control Console, Upper Carriage Control Unit and Data Recording Equipment . . . . .	36
14	Total System Test Installation - Aircraft Brake Metering Valve and Accumulator with Upper Carriage Loading System Components Viewed from Top of Dynamometer Cage . . . . .	37
15	Total System Test Installation - F-111 Main Landing Gear Left Wheel Installed Over Dynamometer Flywheel - Viewed Looking Outboard and Forward . . . . .	38
16	Total System Test Installation - F-111 Main Landing Gear Left Wheel Installed over Dynamometer Flywheel - Viewed Looking Inboard and Aft . . . . .	39
17	AFFDL 192 Inch Diameter Brake Test Dynamometer Prior to Total System Test Installation . . . .	40
18	Landing Gear Support Fixture Structural Proof Test for Side Load Condition . . . . .	42
19	Landing Gear Support Fixture Structural Proof Test for Landing Load Condition . . . . .	43
20	Test Condition No. 29 Oscillograph Recording . .	50
21	Simplified Brake Hydraulic System Schematic . .	53
22	Dynamometer Flywheel Setup . . . . .	57

## ILLUSTRATIONS

No.	Title	Page
23	Simplified Antiskid Analysis System Equation Flow Diagram . . . . .	59
24	Tire-To-Ground Friction Coefficient Versus Relative Velocity . . . . .	61
25	Expanded Time Scale Oscillograph Record of Test Condition No. 29 . . . . .	68
26	Analytically Predicted Antiskid Operation . . .	69
27	Antiskid Operation Recorded During Aircraft Landing . . . . .	71
28	Fluidic Controlled Pneumatic Braking System . .	76
29	Fluidic Wheel Speed Sensor . . . . .	77
30	Fluidic Wheel Speed Sensor Schematic/Circuit Diagram . . . . .	78
31	Adaption of an Electrical Antiskid Valve for Pneumatic Actuation . . . . .	80

### Appendix A

A1	Forces Acting on the Brake Discs . . . . .	93
A2	Keyway Friction Characteristic . . . . .	95
A3	Brake Assembly Equation Flow Diagram . . . . .	97
A4	Brake Pressure Volume Characteristic . . . . .	98
A5	Hydraulic System Components . . . . .	104
A6	Hydraulic System Schematic for Options 1, 2 and 3 . . . . .	104
A7	Hydraulic System Equation Flow Diagram for Options 1, 2 and 3 . . . . .	108
A8	Option 4 Hydraulic System Schematic . . . . .	109
A9	Option 4 Hydraulic System Equation Flow Diagram . . . . .	112
A10	Hydraulic Fluid Damping Characteristic . . . . .	117
A11	Flywheel System Model . . . . .	130
A12	Airplane System (Flywheel) Equation Flow Diagram . . . . .	132
A13	Main Gear Damping Curve . . . . .	133
A14	Main Gear Air Load Curve . . . . .	133
A15	Airplane Coordinates . . . . .	140
A16	Airplane Geometry . . . . .	141
A17	Airplane Dynamics . . . . .	143
A18	Main Strut Model . . . . .	144
A19	Airplane System (3 Degree) Equation Flow Diagram . . . . .	146

# ILLUSTRATIONS

No.	Title	Page
A20	Nose Gear Damping Curve . . . . .	147
A21	Nose Gear Air Load Curve . . . . .	148
A22	Main Gear Strut and Wheel Model . . . . .	149
A23	Airplane Initial Equilibrium Forces . . . . .	151
A24	Airplane Coordinates . . . . .	159
A25	Airplane Geometry . . . . .	160
A26	Airplane Dynamics (Pitch) . . . . .	162
A27	Airplane Dynamics (Yaw) . . . . .	163
A28	Airplane Dynamics (Roll) . . . . .	164
A29	Nose Tire Cornering Force . . . . .	165
A30	Side View of the Main Gear Strut . . . . .	167
A31	Main Gear Model . . . . .	168
A32	Airplane System (6 Degree) Equation Flow Diagram . . . . .	172
A33	Components of the Wheel and Tire System . . . . .	186
A34	Tire Horizontal Model . . . . .	187
A35	Tire Rotational Model . . . . .	188
A36	Wheel and Tire System (Flywheel) Equation Flow Diagram . . . . .	190
A37	Tire Tread Model . . . . .	192
A38	Tire Damping Models . . . . .	194
A39	Model Loss Factors . . . . .	196
A40	Tire Sliding Friction Coefficient . . . . .	198
A41	Components of the Wheel and Tire System . . . . .	204
A42	Tire Horizontal Model . . . . .	205
A43	Tire Rotational Model . . . . .	206
A44	Wheel and Tire System (3 Degree) Equation Flow Diagram . . . . .	208
A45	Footprint Friction Components . . . . .	215
A46	Wheel and Tire System (6 Degree) Equation Flow Diagram . . . . .	216
A47	Wheel Speed Signal System . . . . .	225
A48	Wheel Speed Sensor Equation Flow Diagram (Option 1) . . . . .	226
A49	Modulated Antiskid Control Functional Block Diagram . . . . .	233
A50	Modulated Antiskid Control Circuit Schematic . . . . .	235
A51	Modulated Antiskid Schematic with Mathematical Identification and Incorporating Equivalent Circuits for Transistors and Diodes . . . . .	238
A52	Modulated Antiskid Circuit Equation Flow Diagram . . . . .	262

## ILLUSTRATIONS

No.	Title	Page
A53	On-Off Antiskid Control Functional Block Diagram . . . . .	268
A54	Electrical On-Off Antiskid Control Circuit . . .	269
A55	Electrical On-Off Circuit Equation Flow Diagram . . . . .	275
A56	Mechanical On-Off Antiskid Device . . . . .	278
A56a	Mechanical On-Off Device Equation Flow Diagram . . . . .	284
A57	First Stage Spring Mass System . . . . .	285
A58	First Stage Control Pressure - Mass Position Relationship . . . . .	286
A59	Antiskid Valve Second Stage . . . . .	287
A60	Second Stage Spool Forces . . . . .	288
A61	Antiskid Control Valve Equation Flow Diagram (Option No. 1) . . . . .	291
A62	Antiskid Control Valve Equation Flow Diagram (Option No. 2) . . . . .	292
A63	Stability Augmentation System . . . . .	298
A64	Horizontal Tail Control Equation Flow Diagram .	301

## TABLES

No.	Title	Page
1	Test Condition Summary . . . . .	44
2	Simplified Antiskid Analysis System Parameters .	62
3	Computer Input Data for Test - Analysis Correlation . . . . .	70

## APPENDIX A

A1	Explanation of Mathematical Convention . . . . .	86
A2	Brake Assembly Parameters . . . . .	101
A3	Control Line Restrictions . . . . .	115
A4	Option 1, 2 and 3 Hydraulic System Parameters .	122
A5	Option 4 Hydraulic System Parameters . . . . .	127
A6	Vehicle and Wheel Structural Support (Flywheel) Parameters . . . . .	137
A7	3 Degree Airplane System Parameters . . . . .	154
A8	Airplane System (6 Degree) Parameters . . . . .	177
A9	Runway Friction Characteristics . . . . .	197
A10	Wheel and Tire System (Flywheel) Parameters . .	200
A11	Wheel and Tire System (3 Degree) Parameters . .	210
A12	Wheel and Tire System (6 Degree) Parameters . .	219
A13	Wheel Speed Sensor Parameters . . . . .	230
A14	Modulated Antiskid Circuit Conditions . . . . .	253
A15	Valve Amplifier Operating Mode Test Equations .	255
A16	Capacitor C4 Current Mode Test Equations . . . .	256
A17	Summary of Equations for Computing Current AD5 .	257
A18	Modulated Antiskid Circuit Equation Summary . .	259
A19	Modulated Control System Parameters . . . . .	263
A20	On-Off Control System Parameters . . . . .	276
A21	Antiskid Control Valve Parameters (Option No. 1) . . . . .	295
A22	Antiskid Control Valve Parameters (Option No. 2) . . . . .	297
A23	Horizontal Tail Control Parameters . . . . .	302
A24	Runway System Parameters (Flywheel and 3 Degree) . . . . .	306
A25	Three Track Elevation Profiles . . . . .	309
A26	Runway System Parameters (6 Degree) . . . . .	315

## SECTION I

### INTRODUCTION

#### A. OBJECTIVE

The objectives of this program as stated in the contract statement of work are: (1) to verify, correlate and refine the Aircraft Antiskid Performance - Total System Compatibility Analysis Procedures previously developed under U.S. Air Force Contract F33615-70-C-1004 and as described in AFFDL-TR-70-128, and (2) to establish the feasibility of a fluidic-controlled pneumatic braking system.

#### B. SCOPE

This program for Aircraft Antiskid Performance - Total System Compatibility Analysis Verification, Correlation and Refinement consisted of the following:

- (1) A total system verification test set-up was designed, fabricated and installed in the AFFDL Landing Gear Test Facility, Building 31, Area B, Wright-Patterson Air Force Base, Ohio. The test set-up is comprised of: (a) a structural steel framework attached to the 192 inch diameter inertia dynamometer, (b) a movable load carriage supported by the framework and providing simulated aircraft landing gear fuselage attachment provisions, (c) a carriage loading and positioning system, (d) one F-111 main landing gear tire-wheel-brake assembly assembled with the required aircraft landing gear structural components to complete an installation the same as that for the aircraft left wheel installation, (e) a mockup of the aircraft hydraulic brake actuation and control system including pilot's metering valve, accumulator, lines and fittings, (f) antiskid control circuits, an F-111 antiskid valve and wheel speed sensing unit and (g) instrumentation and recording equipment needed to measure and record parameter variations significant to antiskid operation.
- (2) Verification testing consisting of a number of braked stops was performed utilizing the total system verification test set-up for thirty-six test conditions having various combinations of landing gear loading, antiskid control circuit type, two different tire sizes, various tire inflation pressures and various amounts of hydraulic brake actuation system flow restriction. During these stops the following parameters

were measured and recorded with respect to time: dynamometer flywheel speed and distance, braked wheel speed, hydraulic pressure at the brake and at the antiskid valve inlet, brake torque, radial and tangential forces between the tire and dynamometer flywheel and antiskid valve electrical signal.

- (3) The results from some of the total system verification test runs were compared with analytically predicted parameter variations obtained from the antiskid performance and total system compatibility analysis procedures.
- (4) The Antiskid Performance and Total System Compatibility Analysis procedures have been refined to enhance computation economy and to achieve agreement with verification test results.
- (5) Components for a fluidic-controlled pneumatic braking system for operation with and skid control of an F-111 wheel/brake assembly have been designed. A comparison of fluidic to conventional brake control systems has been formulated.

#### C. BACKGROUND

The characteristics of modern high performance airplanes are such that there are many occasions where the pilot is very disadvantageously situated for perceiving the amount of wheel brake force which can be applied without causing tire skidding. Because of high airplane ground speeds required for takeoff or landing, relatively high wheel braking forces are frequently necessary for controlling the vehicle's velocity within the available runway distance. Since a relatively short duration tire skid at high speed may result in a blowout with consequent severe damage to other aircraft components or may cause loss of directional control, experience has established that a wheel brake antiskid feature is required for safe and predictable aircraft operation.

Figure 1 is a block diagram showing the typical arrangement of an aircraft landing gear wheel brake system and the relationship between the various elements within the total vehicle system. The brake system functions to inhibit wheel rotation in response to pilot command so that a force opposing aircraft motion is produced between the tires and runway surface. Most modern military aircraft are equipped with hydraulically actuated disc type brakes controlled by a full power brake control system which also incorporates an automatic antiskid feature as shown.



The antiskid function is accomplished by a group of components which automatically detect and alleviate incipient tire skidding by controlling brake torque. An incipient skid is alleviated by temporarily reducing brake torque to a value less than the torque being produced by the friction force at the tire-runway interface. Brake torque reduction is sustained for a time interval sufficiently long to allow the wheel to regain speed. After the wheel has regained speed, brake torque increase is initiated. Since brake torque is produced by applying fluid pressure to the brake actuating cylinders, torque is controlled indirectly by controlling actuation pressure.

Antiskid system components usually consist of wheel speed sensing units, antiskid control elements and antiskid brake torque control valves. For clarity, Figure 1 shows the arrangement of an aircraft having a tricycle landing gear arrangement with single wheel main gear configuration. For airplanes having multiple wheeled landing gears and/or multiple landing gears, the same basic arrangement prevails with the addition of additional similar type components as appropriate.

The reduction and subsequent reapplication of brake torque results in an oscillatory braking force being applied to the airplane. This oscillatory force has the potential for causing adverse dynamic loading of the airplane structure, for causing directional control difficulty and for degrading the aircraft's stopping performance. The need for evaluating antiskid operation to predict the effects of the potentially deleterious oscillatory braking force is now recognized because there have been a number of instances where failure to do so has resulted in severe operational difficulty and in some cases catastrophic landing gear failure.

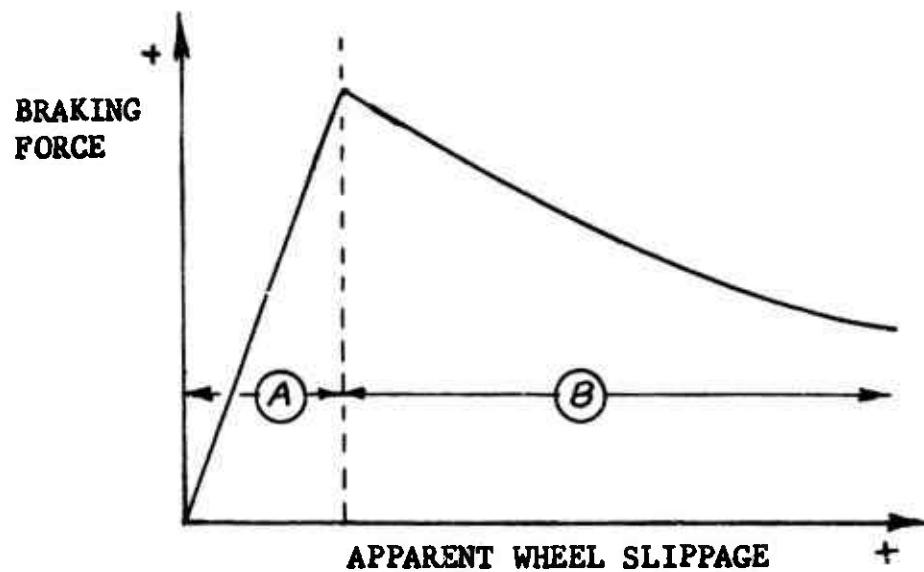
The overall resultant effects of antiskid operation are dependent upon the characteristics of the antiskid equipment components along with the characteristics of the airplane and many of its other systems as well as the operating environment into which the vehicle is placed. If during the airplane's usage, within its intended operating envelope instances of unsafe conditions resulting from antiskid operation frequently occur, the braking system is deficient with respect to the attempted operational circumstances and is relatively unacceptable. Braking system deficiencies are caused by incompatibilities within the overall vehicle system which result in antiskid operation being different than was intended or which result in the practically

achievable braking effectiveness being incorrectly predicted. These incompatibilities result from inadequate consideration of significant design parameters or of the aircraft's required operating environment.

It is intended that the analytical techniques described herein be used for establishing the influence of the individual total vehicle system elements upon antiskid operation. The behavior of each equipment item can thereby be established or its performance requirements defined so that the relative compatibility between individual elements and between equipment items and basic aircraft characteristics can be determined. Whenever the practically achievable performance for each equipment item is established considering the applicable prevailing cost, weight, volume or other inherent physical property restraints, the overall system can then be evaluated with respect to the braking system equipment's acceptability and proper utilization.

As with any system or device the degree to which a braking system or one of its components may be adjudged acceptable is established by how well it operates to provide the performance expected without causing any trouble. Therefore, it is evident that the braking system equipment's acceptability for a particular usage is influenced by how well expectation is tempered with reason and judgement. For instance, it is possible that some aerodynamic or other vehicle characteristic prevents achievement of the desired or expected wet runway stopping performance with any conceivable antiskid equipment configuration. If experiencing this type of disappointing circumstance is to be avoided the expected braking system effectiveness must be established from basic material properties and proven fundamental principles which have been verified by substantial experimental evidence rather than from optimistic estimates or unsupported claims. The antiskid analysis techniques utilized during this program may be employed for such realistic establishment of braking system effectiveness. The following discussion of some fundamental aspects of antiskid operation and antiskid evaluation is presented to help establish a rational basis for applying the analysis procedure.

The dominant factor influencing the operation of an antiskid brake control system is the well known characteristic behavior of a rolling tire while being subjected to braking forces. This characteristic behavior, as shown on Figure 2, is that as a small braking force is applied an apparent slippage develops between the tire and contacting surface. This apparent slippage is evidenced by the wheel angular velocity being less than the synchronous angular velocity by an amount proportional to the



Ⓐ ZONE OF NO TIRE FOOTPRINT SLIPPAGE

Ⓑ ZONE OF INCREASING TIRE FOOTPRINT SLIPPAGE

$$\text{APPARENT WHEEL SLIPPAGE} = \dot{X}_A - \dot{\Theta}_W R_e$$

WHERE:

$\dot{X}_A$  = AXLE TRANSLATIONAL VELOCITY

$\dot{\Theta}_W$  = WHEEL ANGULAR VELOCITY

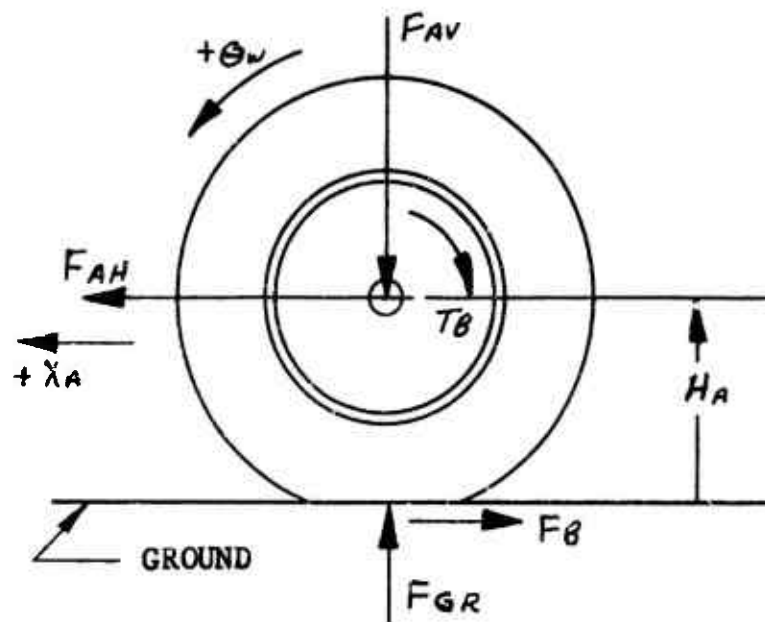
$R_e$  = TIRE UNBRAKED APPARENT ROLLING RADIUS

Figure 2 Pneumatic Tire Slippage Versus Braking Force Characteristic

the braking force. The tire synchronous angular velocity is the value which results from unbraked rolling. The initial apparent slippage proportional to the braking force occurs without appreciable relative motion between the tire footprint and contacting surface because of elastic deformations within the tire. If an increase in the braking force to a value exceeding the maximum achievable for prevailing friction conditions is attempted, an actual slippage between the tire footprint and contacting surface results. When the tire footprint is actually sliding relative to the contacting surface the friction coefficient decreases as sliding velocity increases which is the usual case with any two sliding objects.

When the characteristics of the braking force - slippage relationship are considered while examining the equation of the tire's angular motion with applied brake torque as shown by Figure 3, it can be seen that when the applied brake torque is less than the available friction torque, a friction torque equal and opposite to the brake torque will develop by the tire increasing its slippage along the positive-slope portion of the characteristic relationship. If the applied brake torque is increased or if the tire-to-ground friction force potential decreases so that a condition occurs where the brake torque exceeds the available friction torque, tire slippage will increase into the negative-slope region of the brake force - slippage characteristic variation resulting in an unstable ever increasing negative wheel angular acceleration. A full skid will result if the brake torque is not quickly reduced to some value less than the instantaneous friction torque so that a positive wheel angular acceleration is produced causing the wheel to regain speed. To satisfactorily control brake torque an antiskid system must be capable of distinguishing between a tire's slippage in the stable or unstable condition.

Several control concepts and a number of different type devices for implementing some of these concepts have been used for antiskid brake control. Because of very competitive market conditions and the achievement of relatively acceptable performance, practically all of the antiskid systems in current general usage are of the class previously described in Figure 1. These systems measure a braked wheel's speed, compare the measured speed magnitude and/or rate of change to an "index-of-acceptability", and control brake torque according to the results of the comparison. The primary differences between systems supplied by different airframe or antiskid equipment manufacturers is the "index-of-acceptability" utilized and the methods by which it is established. The usual "index-of-acceptability" is the amount of wheel slippage or the rate of increase in wheel slippage.



- $T_B$  = Brake torque
- $F_{GR}$  = Radial force on tire from ground
- $F_B$  = Braking force =  $\mu F_{GR}$
- $F_{AV}$  = Vertical force on wheel from axle
- $F_{AH}$  = Horizontal force on wheel from axle
- $H_A$  = Height of axle above ground
- $\mu$  = Friction coefficient between the footprints and ground
- $I_W$  = Tire-wheel assembly mass moment of inertia
- $\dot{x}_A$  = Horizontal axle displacement
- $\dot{\theta}_w$  = Horizontal axle velocity
- $\dot{\theta}_w$  = Wheel angular displacement
- $\ddot{\theta}_w$  = Wheel angular velocity
- $\ddot{\theta}_w$  = Wheel angular acceleration

Equation of wheel angular motion:  $I_W \ddot{\theta}_w = F_B H_A - T_B$

Figure 3 Braked Wheel Forces

Evaluating antiskid braking system performance and compatibility is aided by examining the physical operating characteristics of the applicable braking system equipment in the typical arrangement as shown schematically in Figure 4. The elements shown are: the pilot's metering valve, antiskid control valve, brake actuation cylinder, interconnecting fluid transmission lines with their flow resistances, brake discs, wheel and tire assembly, antiskid wheel speed sensor device and antiskid control circuit elements. The typical antiskid valve is a two element device having a control pressure producing first stage and a second stage power spool which controls the direction which fluid may flow thru the valve. Several different type first stage devices may be used and the range over which control pressure varies depends upon the type. Figure 4 shows the type where control pressure varies over the entire range between inlet port pressure and return port pressure. For other type first stage devices having different ranges of control pressure variation, the second stage spool areas upon which the control and brake port pressures act are sized so that a proper force balance is achieved. The antiskid valve operating principles are similar whichever type first stage type is used.

Figure 4 shows the antiskid valve second stage in the position for no antiskid control signal such that the fluid pressure as commanded by the pilot's pedal position is transmitted to the brake. The antiskid valve first stage produces a control pressure as a function of the antiskid valve control signal and inlet pressure. The control pressure is equal to antiskid valve inlet pressure with zero antiskid valve input signal and the control pressure is decreased as the valve signal increases. If the antiskid control valve input signal is increased the reduction in first stage control pressure imposes a pressure unbalance upon the second stage spool thereby causing spool movement to a position which allows fluid flow out of the brake cylinder to return. As the antiskid valve brake port pressure becomes equal to the first stage control pressure, the pressure balance on the second stage spool causes it to be repositioned to shut off fluid flow. Whenever the antiskid valve input signal is reduced, first stage control pressure increases to cause an opposite pressure unbalance in the second stage which results in the spool being positioned to allow fluid flow from the pilot's metering valve to the brake cylinder until a new pressure balance is achieved.

A typical aircraft brake has a characteristic cylinder pressure versus fluid volume relationship and a characteristic cylinder pressure versus torque relationship as shown on Figure 5.

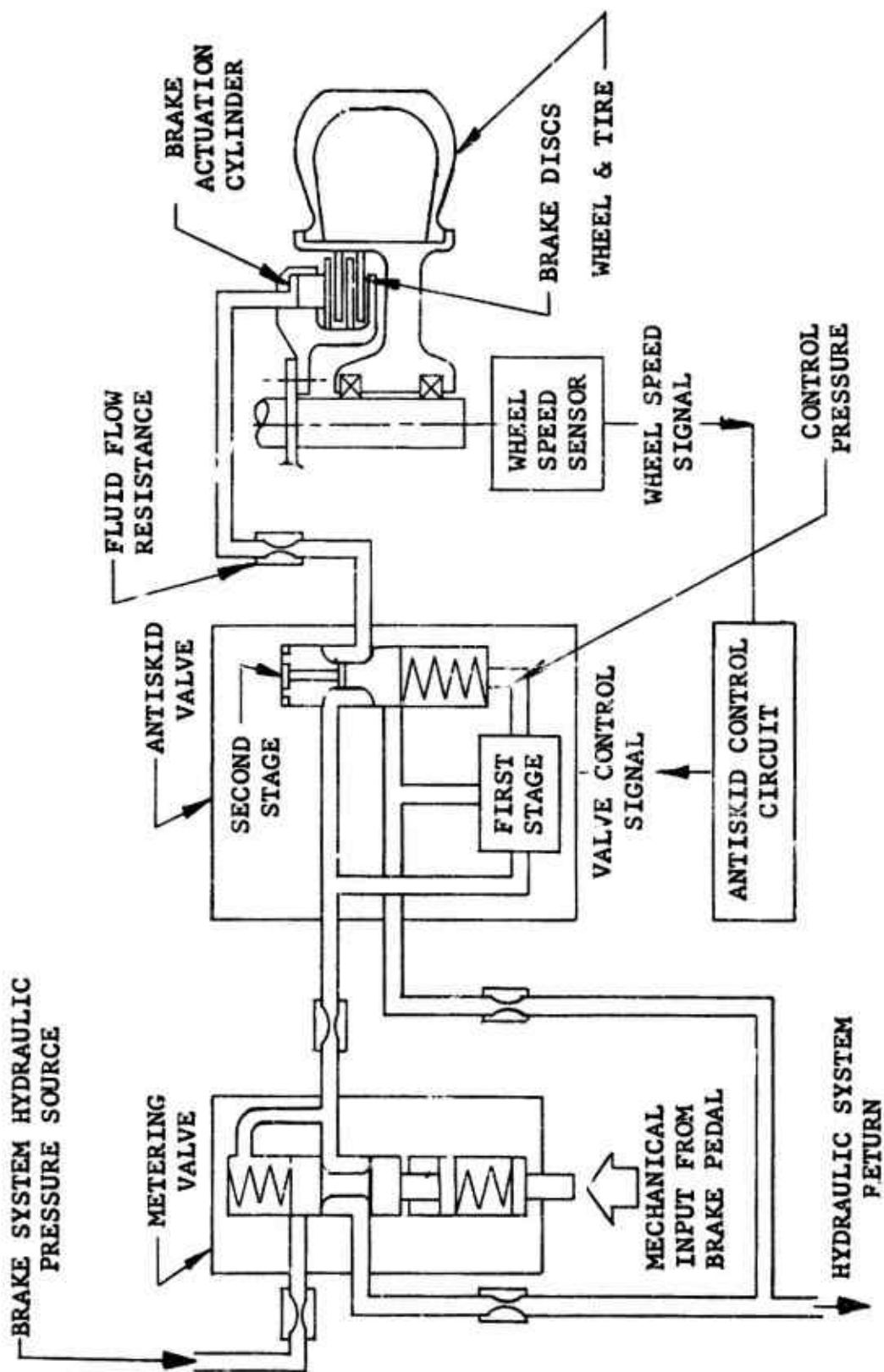


Figure 4 TYPICAL BRAKE CONTROL/ANTISKID FLUID POWER SYSTEM

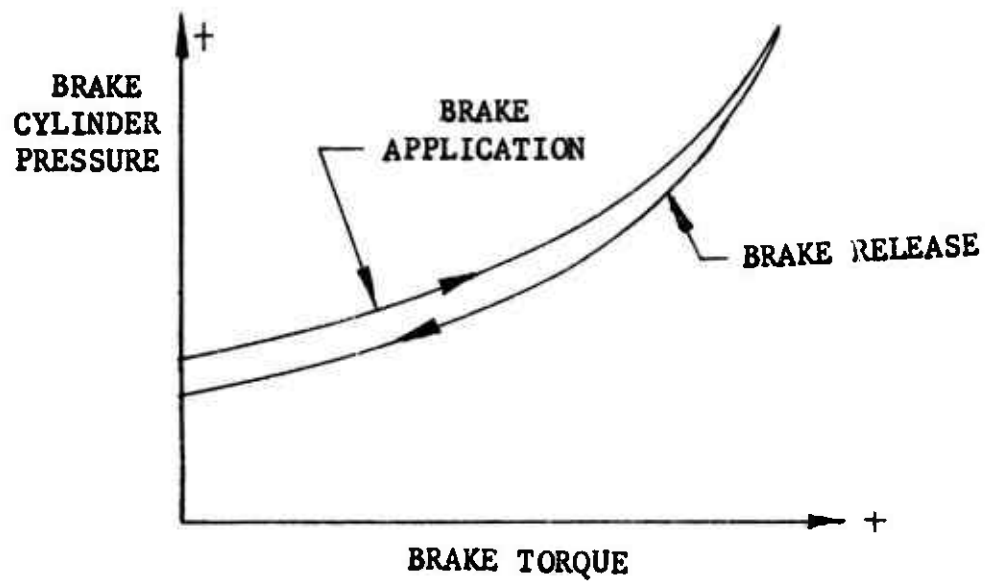
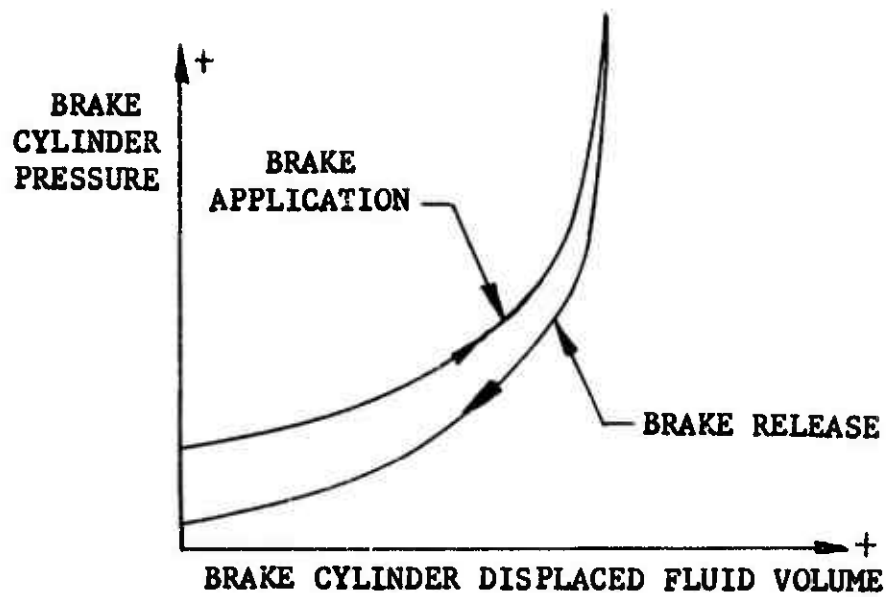
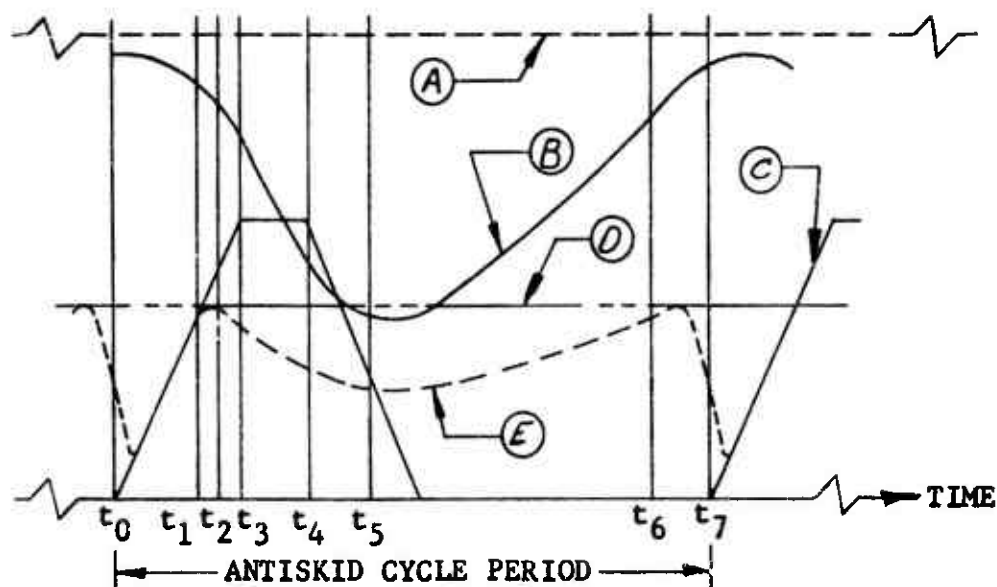


Figure 5 Typical Brake Characteristics

For occasions where the antiskid control circuit commands brake torque to be increased or decreased by changing the antiskid valve control signal, some amount of time must elapse during which sufficient fluid flow occurs to produce the change in brake cylinder volume corresponding with the required change in cylinder pressure. When changing brake cylinder pressure, the fluid flow rate at each instant is established by the difference between brake cylinder pressure and the system source pressure for brake application or by the difference between brake cylinder pressure and system return pressure for brake release and the combined resistance of the applicable fluid flow path. Since the antiskid valve is a mechanical device which must be positioned to permit fluid flow in the proper direction, some finite (usually small) time interval is required. Consequently, it must be recognized that the brake actuation system flow resistances, the antiskid valve dynamic response characteristics and the brake's characteristics have a very significant influence upon brake torque dynamic response to antiskid valve input control signals. In addition, the antiskid wheel speed sensing element and the control circuit elements usually have characteristics which result in the instantaneous values of the various signals lagging actual occurrences by some small amount. The relative compatibility of the brake actuation and control loop is established by how well the antiskid control element's characteristics are matched to the prevailing conditions of actuation fluid flow resistance, brake pressure-volume and pressure torque characteristics, and the dynamic response characteristics of the tire and wheel brake supporting structure.

Antiskid control has a cyclic nature because it involves detecting that braked wheel slippage has progressed from a stable condition to an unstable condition with subsequent brake torque adjustment in a manner such that wheel slippage returns to the stable condition. Figure 5 describes the sequential events which occur and the relative variation of wheel speed, brake torque and friction torque during a typical antiskid cycle. To emphasize the various events and fundamental characteristic variations, the magnitude and rate of the parameter changes shown have been arbitrarily assigned and are not intended to represent any specific case. The occurrences during the time intervals between events shown on Figure 5 are as follows:

TIME INTERVAL	OCCURRENCES
$t_0-t_1$	Brake torque increases and wheel angular velocity decreases in the stable region of the brake force - tire slippage characteristic producing an equal and opposite



#### PARAMETERS

- (A) Wheel synchronous angular velocity  $\dot{\chi}/R_e$
- (B) Wheel angular velocity  $\dot{\theta}_w$
- (C) Applied brake torque  $T_B$
- (D) Maximum available friction torque  $\mu_{\max}$
- (E) Achieved friction torque  $= \mu FGR$

#### EVENTS

- $t_0$  - Instant brake application is initiated
- $t_1$  - Instant when applied brake torque equals maximum available friction torque
- $t_2$  - Instant of incipient skid detection, i.e., wheel alipage or slippage rate becomes equal to skid detection threshold
- $t_3$  - Instant brake torque increase ceases (either because of brake torque reaching its applied value or because of skid control action preceding torque reduction)
- $t_4$  - Instant brake torque reduction is initiated
- $t_5$  - Instant brake torque equals friction torque and wheel negative acceleration ceases
- $t_6$  - Instant wheel angular velocity has regained the required portion of its initial value (value at  $t_2$ ) to cause initiation of brake reapplication, i.e., skid recovery signal threshold
- $t_7$  - Instant brake application is initiated for next antiskid cycle

Figure 6 Antiskid Cycle Events

friction torque until the maximum available friction torque is achieved at  $t_1$ . Brake torque increase rate is controlled by the brake, brake actuation control system (hydraulic flow restriction) and skid control system characteristics.

- $t_1-t_2$  Brake torque continues to increase producing increasing negative wheel acceleration into the unstable region of the brake force - tire slippage characteristic until wheel slippage or slippage increase rate reaches the skid-detection threshold.
- $t_2-t_3-t_4$  Brake torque increase continues until it is terminated by either (a) the torque reaching the value commanded or (b) skid control system terminates the torque increase in preparation for torque reduction. Friction torque and wheel speed continue to decrease (total interval may be called skid control reaction time).
- $t_4-t_5$  Brake torque decreases at a rate controlled by the brake, brake actuation system and antiskid control characteristics. Friction torque continues to decrease as wheel slippage increases. Wheel speed decreases to its minimum value.
- $t_5-t_6$  Brake torque decreases until it becomes zero or until antiskid control system initiates brake torque increase. Wheel speed increases from its minimum value to an amount required to initiate brake torque increase (skid recovery signal).
- $t_6-t_7$  Reaction time of the brake, brake actuation system and antiskid system between skid recovery signal and initiation of brake torque increase.

Figure 6 provides a graphic means for examining and evaluating the two most significant effects of antiskid cycling - the average braking force achieved (wheel braking system effectiveness) and the characteristics of dynamic forces being applied to the wheel supporting structure. From Figure 6 it can be seen that: the fundamental frequency of applied dynamic loading is established by the antiskid cyclic period (i.e., time interval  $t_0-t_7$ ), and assuming constant aircraft velocity during the cycle, the average braking force achieved is proportional to the area under the curve of friction torque versus time divided by the cyclic period.

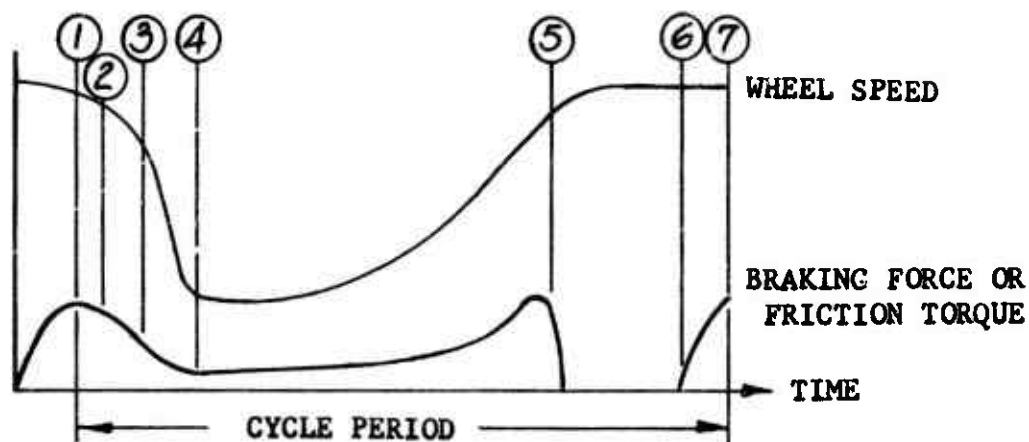
The dynamic loading and average achieved brake force are not independent of each other but rather have a very complex interrelationship influenced by antiskid component and other brake system equipment characteristics.

An examination of Figure 6 considering the parameters shown and the effects of their variation with respect to evaluating braking system performance reveals that braking effectiveness is increased by: (a) moderate rates of brake torque increase, (b) high rates of brake torque decrease, (c) lower values of wheel slippage or rate of wheel slippage increase for skid detection threshold, (d) short antiskid system reaction time, (e) smaller amounts of excess applied brake torque and (f) least possible fraction of initial cycle velocity for skid recovery signal. Since most of the above tend to diminish the cyclic period, increased antiskid performance usually results in higher cyclic frequency potential.

Some particularly important aspects of antiskid operation are exemplified by Figure 7 which shows a comparison of the characteristic variation in braked wheel speed and braking force (friction torque) throughout an antiskid cycle for two extreme circumstances:

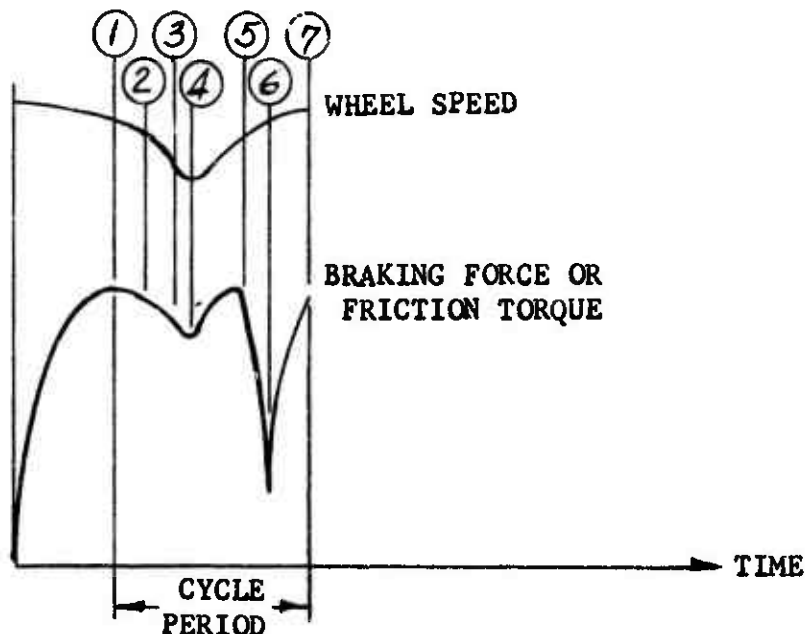
- (a) An instance where the applied brake torque is a very large percentage greater than the available friction torque and the available friction torque is low, and
- (b) An instance where the applied brake torque is a small percentage greater than the available friction torque and the available friction torque is high.

For both cases the interval between points ② and ③ is the time consumed by the required antiskid control circuit and antiskid valve actions, the interval between points ③ and ④ is the time required for sufficient fluid flow from the brake cylinders to cause brake torque reduction by an amount such that equality between brake torque and friction torque is achieved, the interval between points ④ and ⑤ is the time required for wheel spinup sufficiently to produce a skid recovery signal, the interval between points ⑤ and ⑥ is the time required for the antiskid control circuit and antiskid valve actions plus an interval required for sufficient fluid to flow such that the brake discs make contact if the brake was previously released to a degree for disc clearance to exist, and the interval between



CASE (A): HIGH BRAKE TORQUE - LOW AVAILABLE FRICTION TORQUE

- ① Brake torque application to an amount equal to instantaneous available friction torque
- ② Skid detection
- ③ Brake torque reduction initiated
- ④ Brake torque reduced sufficiently to allow wheel decel to cease and wheel accel to begin
- ⑤ Skid recovery signal - brake reapplication initiated
- ⑥ Brake torque increase starts
- ⑦ Brake reapplication to an amount equal to instantaneous available friction torque



CASE (B): HIGH BRAKE TORQUE - HIGH AVAILABLE FRICTION TORQUE

Figure 7 Comparison of Antiskid Cycle Conditions

points ⑥ and ⑦ is the time for sufficient fluid flow to the brake for causing brake torque increase by an amount such that equality between brake torque and friction torque is again achieved.

It should be noted that the time interval between points ② and ③ is approximately the same for both cases because the control circuit and antiskid valve consume about the same amount of operating time for any circumstance requiring brake pressure reduction. Since for case (a) the wheel has a much higher deceleration rate and a greater pressure reduction must be accomplished to prevent skidding with resultant greater time being consumed for removing fluid from the brake, the amount of wheel speed departure into the unstable slippage region is much greater. These factors along with the slower wheel spinup rate resulting from low available friction torque causes brake pressure reduction to be sustained for a longer time interval during which brake fluid volume usually decreases to an extent where clearance is produced between the friction surfaces. Upon brake reapplication a greater time interval is then required for replenishing the brake fluid volume to produce brake torque. The overall resultant effect is that the cyclic period for case (a) is greater than for case (b) and the average braking force achieved for case (a) is a smaller fraction of the maximum braking force produced than for case (b). Therefore, a major consequence of antiskid cycling is the trend toward reducing the achievable fraction of the instantaneous peak available braking force for conditions of low braking force potential (i.e., intensify the degradation of braking system effectiveness for conditions of reduced brake force potential). This inherent characteristic is unavoidable whenever any relatively "fixed time" elements are part of the control loop. The degree of degradation in braking system effectiveness is increased for larger amounts of excessive brake torque. This effect can be minimized if upon brake application the brake torque is reduced to more closely match the available friction torque. Modern "modulated" antiskid systems accomplish reduction of subsequent brake torque reapplication by using a servo type pressure regulating valve and providing a relatively slowly varying bias signal to the valve drive amplifier.

From the preceding discussion it can be established that the primary objectives of any brake control/antiskid system capable of achieving improved performance are: (1) to minimize the occurrence of antiskid cycles and (2) to minimize the amount of wheel speed departure into the unstable slippage region for cases where

cycling does occur. The degree to which these objectives are accomplished while permitting wheel brake application so as to achieve a large fraction of the potentially available friction force is a measure of the system's relative acceptability.

To accomplish its purpose an antiskid brake control system must function to cause a braked wheel's motion to be such that the relative velocity between the tire footprint and the ground is minimized for as much of the time as possible. An examination of the factors influencing tire footprint relative velocity reveals that the relative velocity between the tire footprint and the ground is equal to the horizontal velocity of the axle plus the horizontal velocity of the footprint relative to the axle, and that the horizontal velocity of the tire footprint relative to the axle is established by the rate of tire tread circumferential and radial displacement relative to the wheel and the wheel's angular velocity relative to the axle. At any instant all these velocity components are established by the relative distribution of elastic, thermal and kinetic energy resulting from the cumulative effects of the externally applied forces which have acted upon the tire-wheel assembly since spin-up and brake application.

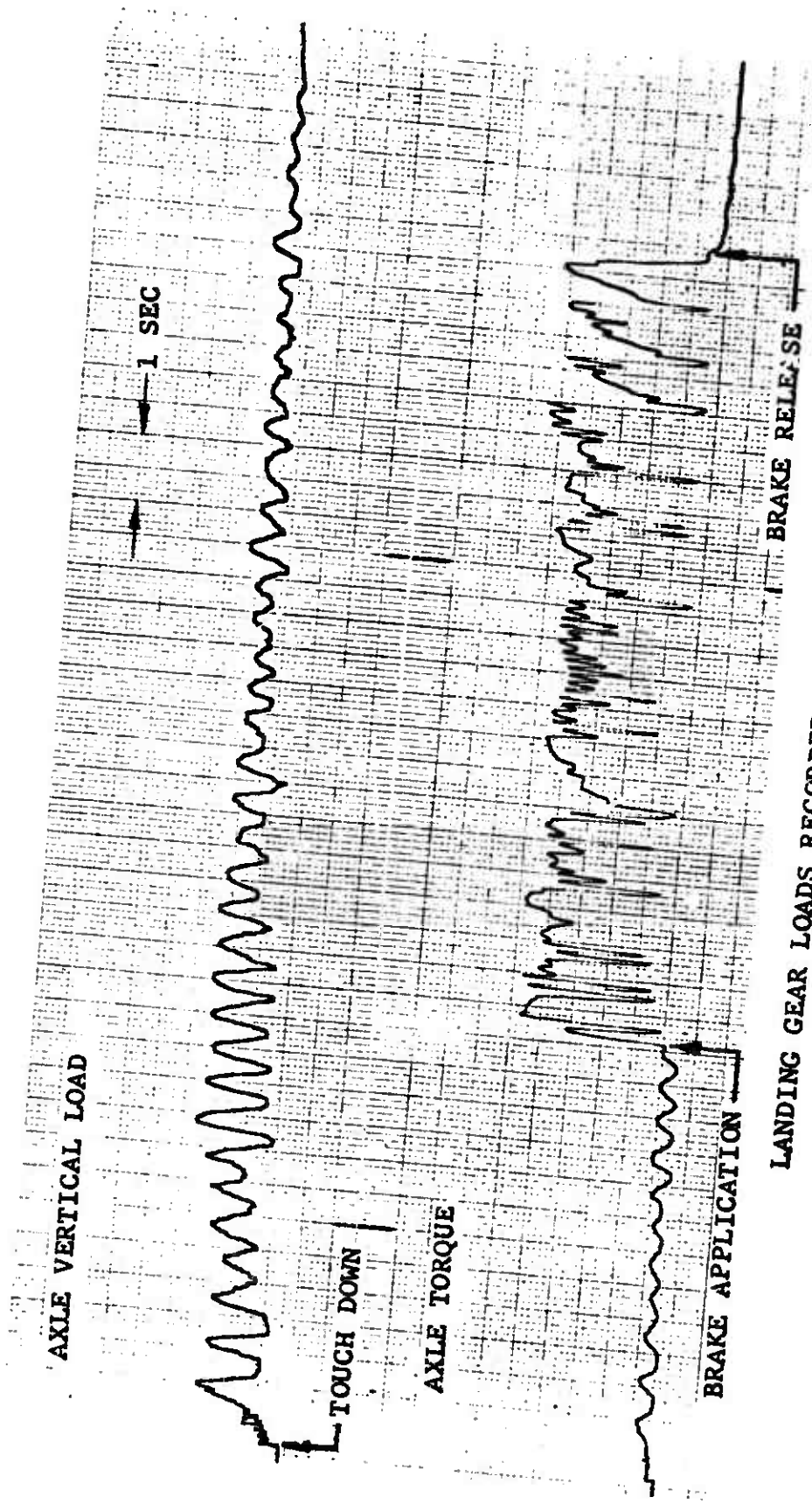
As shown on Figure 3 the externally applied forces acting upon the tire-wheel assembly are the horizontal and vertical force components between the wheel and the axle, the brake torque, the radial force between the tire footprint and the ground and the horizontal friction force between the footprint and the ground. The runway profile along with the individual and collective elastic and inertia properties of the tire, wheel, supporting structure and vehicle influence the amount and nature of variations in radial ground force acting upon the tire-wheel assembly. The horizontal friction force acting upon the tire-wheel assembly is the product of the tire-to-ground radial force and the friction coefficient which in turn is affected by tire tread material elastic and strength properties as influenced by temperature and prior exposure to thermal and other environmental conditions, the nature and quantity of any contaminating substances, tire inflation pressure and footprint shape, and runway surface texture in addition to tire footprint relative velocity.

When braking system operation is examined within the context of the total vehicle system it is evident that the antiskid control elements must continually adjust brake torque in an attempt to achieve consonance with the other forces acting upon the tire wheel assembly. Since the forces acting upon the tire-wheel assembly are usually quite large compared to tire and wheel inertia, the antiskid system must accomplish brake torque

adjustment very rapidly. Figure 8 shows an oscillograph trace of axle vertical force component and brake torque recorded during landing of an F-111A aircraft on the main runway at Edwards AFB, California under dry conditions. This information was recorded for reasons other than antiskid system evaluation; however, it shows how axle vertical load variations resulting from airplane bouncing triggers antiskid operation as evidenced by brake torque varying in an attempt to follow the braking force potential. The higher frequency component of brake torque oscillation, at approximately 8 HZ, is caused by antiskid operation. It can be observed that each instance of large brake torque reduction corresponds with an instance of reduced axle vertical force. For this stop the pilot applied constant maximum braking during the interval shown. For any type airplane with any type antiskid system, antiskid cycling triggered by a sudden reduction in braking force potential incurred by either changes in tire-to-runway friction coefficient or by changes in radial wheel load can be expected to occur whenever the brake is applied with sufficient intensity.

As previously stated, the frequency and magnitude of the oscillatory braking force produced by antiskid cycling is not independent of braking system effectiveness. To achieve reasonably good braking performance under most conditions an antiskid brake control system should have approximately 10 HZ or greater cyclic frequency potential. Unfortunately, for many (perhaps most) airplanes 10 HZ is very near or above the landing gear fore and aft first mode natural frequency. Provisions must therefore be included within the brake control system to restrict the brake force oscillatory magnitude and/or cyclic frequency in a manner so that structurally damaging load magnification is prevented.

Figure 7 showed that the natural tendency is for the larger magnitude brake force oscillations to have a higher frequency than that for smaller magnitude oscillations. Since most of the antiskid system characteristics which promote achievement of improved braking performance for low braking force potential conditions such as wet runways, also produce higher antiskid cyclic rate potential, any steps taken to enhance braking performance for slippery conditions must be very carefully evaluated with respect to their effects upon dynamic loading whenever circumstances of high brake force potential are encountered. Therefore, the dominant consideration when evaluating total braking system compatibility is assuring that the antiskid induced oscillatory braking force does not have a combination of amplitude and frequency which is structurally detrimental under any condition of airplane usage. It is most often necessary to sacrifice braking system performance under some circumstances to achieve such compatibility.



LANDING GEAR LOADS RECORDED ON F-111A NO. 12  
FLT NO. 62 LANDING

Figure 8 Aircraft Landing Gear Vertical and Horizontal Loads

Antiskid system evaluation is usually performed during the initial design or system development phase for most new aircraft to assure stopping performance objectives can be achieved and to verify no adverse dynamic loading will be produced. These evaluations may be analytical, experimental or a combination of both and most often are performed as laboratory dynamometer tests, hybrid hardware-analog computer analyses and aircraft taxi tests. The analytical evaluation is usually accomplished by utilizing a setup composed of hardware representative of the aircraft components interfaced with an electronic analog computer. The computer is used to solve mathematical equations describing such parameters as aircraft motion, landing gear motion, tire and wheel motion, tire-to-runway friction, aerodynamic forces and brake torque. The actual behavior of a laboratory setup including such components as antiskid electronic circuitry, the brake, hydraulic control valves and interconnecting lines or other devices is measured by suitable instrumentation and fed into the computer to obtain a composite solution. This analysis procedure is used because a complete mathematical computer setup may be considered too expensive or because accurate mathematical descriptions for some components such as the electronic antiskid control circuit are not available. If any actual hardware is used in the computer setup, the analysis must be performed "real time".

While these hybrid hardware-computer analyses serve many useful purposes, several analytical limitations are incurred with a "real time" solution. Some of these analytical limitations are: (a) some significant parameters such as brake torsional displacement, tire circumferential displacement with respect to the wheel and unsprung mass position (position of the wheel, brake and axle suspended between springs representing the tire and shock absorber strut) have very high rates of vibration making their observation and interpretation very difficult. This same problem is encountered when attempting to interpret antiskid operation as recorded during vehicle testing, (b) if actual hardware is used as a part of the computer solution the effects of component characteristic variations cannot be evaluated unless such variations are physically produced. The large expenditure of time and money required to accomplish such evaluation is usually prohibitive, (c) the instrumentation used to interface the hardware with the computer introduces additional variables to an otherwise very complex system.

The above analytical difficulties can be overcome or significantly reduced by employing an all-mathematical approach and operating the analog computer at a reduced time scale or by

using a digital computer. As can be determined from the work accomplished under Contract F33615-70-C-1004 and described in AFFDL-TR-70-128, a major difficulty encountered with the all mathematical analysis approach is the large number and complexity of the mathematical operations result in relatively large computation expense. A part of the analytical refinement accomplished during this program has been directed toward reducing computation expense; however, with respect to total system analysis there are some relatively complex mathematical operations remaining. Depending upon particular circumstances and the type of problem to be solved, useful analytical results can be achieved either with an all-mathematical approach having various degrees of complexity or with the hybrid hardware-analog computer approach.

Laboratory dynamometer test evaluation of antiskid braking system operation provides a relatively low cost and very low risk means for examining many factors relative to system performance and compatibility. The dynamometer test results can be used to establish parameter values for analytical uses or to confirm analytical predictions. Even though dynamometer testing cannot be representative of aircraft operation in some respects, if properly conducted they will establish the limits of a particular equipment's capabilities and provide insight into how the equipment might be changed to achieve a more compatible system. A very advantageous aspect of dynamometer testing is that almost any conceivable parameter can be controlled or at least monitored with relative ease and a particular test can be duplicated if desired. Aircraft taxi or flight tests are needed to confirm that predicted brake system performance and compatibility are actually achieved. However, because of the great difficulties involved in controlling and/or measuring many parameters on an airplane and because of unacceptably high costs and/or high risks involved in producing a controlled demonstration under limiting conditions, it is not generally practical to consider aircraft testing as the only braking system evaluation technique.

Considering the previously described factors which influence antiskid operation whenever contemplating analysis of braking system effectiveness for use in establishing airplane stopping performance, it becomes evident that the random variation of such parameters as runway profile and tire-to-ground friction coefficient makes precise prediction of exact occurrences virtually impossible and impractical. However, since the random variations of many other factors such as brake application speed, wind direction and velocity, pilot brake system operating technique, and runway distance remaining from point of brake

application also significantly influence the relative success which will be achieved during an individual instance of brake system usage, it must be acknowledged that the relatively minor variations in antiskid operation from one instance to the next are not greatly significant. The primary benefits to be derived from analyzing antiskid effects upon airplane stopping performance are: to establish the relative capability of one aircraft type as compared to another for some defined runway condition, to evaluate the relative capabilities of one antiskid system type as compared to another on the same airplane, to evaluate the effects of possible variations in basic airplane configuration and landing gear characteristics upon braking system operation, and to establish braking system component performance requirements which are necessary for achieving some specified stopping performance for a particular aircraft type. By applying the antiskid evaluation techniques utilized during this program, answers may be provided for such questions as: Is it reasonable to expect that an airplane achieve the same stopping performance on any runway as might have been achieved during official performance demonstrations on the very smooth runway at Edwards AFB, California?, or Is it reasonable to expect the same level of braking system effectiveness from two different type airplanes equipped with the same type antiskid system if the airplanes differ with respect to tire size and landing gear elastic characteristics so as to affect the amount and frequency of load oscillation between the tire footprint and the ground? The answers to such questions can then provide the basis for judging braking system acceptability under particular circumstances and for establishing whether or not some change to the braking system equipment and/or some change in airplane operating procedures ought to be implemented.

Much of the preceeding discussion is recognized to be relatively common knowledge among those who routinely participate in the design, analysis and testing of aircraft braking systems. This discussion has been presented to establish the basis for parameters chosen for consideration and the rationale for the various analytical assumptions employed during this program. It is also hoped that by reviewing some of the fundamental aspects of antiskid operation, those who have not been previously exposed to the subject may be provided some insight into the problem and may thereby be able to achieve greater benefits from applying the antiskid analysis techniques.

#### D. PROBLEM DISCUSSION

A prior program, conducted under U.S. Air Force Contract F33615-70-C-1004 and administered by the Air Force Flight Dynamics Laboratory, resulted in development of an analysis procedure for predicting aircraft antiskid performance and total system compatibility. The results of this prior program are described in Report Number AFFDL-TR-70-128.

The analytical procedures consist of a complete mathematical description of the antiskid system components along with the airplane, other aircraft components and systems related to or influenced by antiskid operation, and the characteristics of the surface upon which the airplane is operating. The mathematical description includes such considerations as landing gear dynamic motion, tire elasticity, brake torque response, antiskid electronic circuitry, brake hydraulic control system dynamics, runway surface profile, and tire-to-runway friction characteristics. Both "On-Off" and "Modulated" antiskid systems are considered. Procedures for quantitative evaluation of the influencing parameters and examples of their usage are also presented. The mathematical description consists of analytical components as follows:

- (1) Brake - Brake torque, hydraulic displacement and inlet flow rate are computed as functions of time considering applied brake pressure, relative velocity between the braking friction surfaces, axial elasticity, heat stack inertia, piston position and velocity, and the various friction coefficients (lining, torque tube and wheel splines, piston seals) as functions of velocity.
- (2) Hydraulic System - Hydraulic pressure at the brake, at the antiskid valve inlet and outlet, and at the pilots metering valve is computed as a function of time considering pilot command, system supply pressure, compressibility and inertia of the actuation media, line flow resistance and elasticity, variable flow areas within the pilots metering valve and antiskid valve as functions of spool position, and volume of the various containment vessels (lines, valve bodies, brake housing).
- (3) Airplane and Landing Gear - The position and velocity of the airplane and the landing gear elements with respect to the airplane are computed with respect to time considering forces from the wheel and brake, aerodynamic forces, runway profile, shock strut elasticity and damping, shock strut position, aircraft inertia, and control surface position.

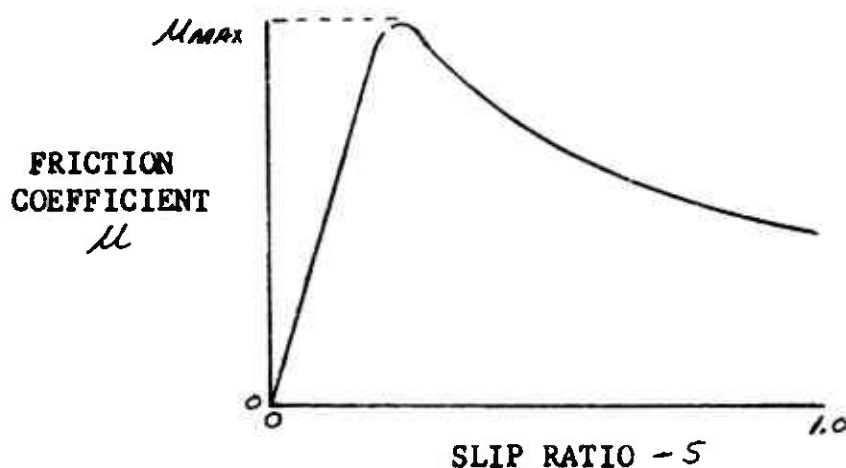
- (4) Wheel and Tire - The forces between the wheel-tire assembly and the airplane and between the wheel-tire assembly and the runway are computed with respect to time considering tire-to-runway friction coefficient as a function of relative velocity and runway surface condition including hydroplaning effects, tire radial and circumferential deformation and its rate, applied brake torque and axle velocity.
- (5) Wheel Speed Sensor - Antiskid control circuit input signal is computed as a function of time considering wheel angular velocity and characteristics of the antiskid wheel speed sensor device.
- (6) Antiskid Control Circuit - Antiskid valve voltage is computed as a function of time considering the input signal from the wheel speed sensor and the control circuit characteristics (the dynamic behavior of the various circuit elements is described).
- (7) Antiskid Control Valve - Antiskid control valve spool position is computed as a function of time considering the applied valve voltage from the control circuit, first stage pressure response characteristics, and inlet, outlet and return port pressure.
- (8) Control Surface Position - Horizontal tail position is computed as a function of time considering pilot command, stability augmentation system characteristics, and airplane pitch rate.
- (9) Runway Surface Profile - Runway surface profile is defined as a function of the airplane's longitudinal displacement.

The analytical prediction procedure is implemented by combining the individual analytical components to obtain a total system composite solution. An electronic computer is used to produce a simultaneous solution of all mathematical equations. The mathematical descriptions previously developed with corrections and refinements resulting from work accomplished during this program are contained in Appendix A herein. To permit confident and useful employment of the analytical procedure a controlled physical demonstration to show its validity and to assure all significant parameters are included and properly accounted for should be performed, and simplification and refinement should be accomplished wherever possible to reduce complexity and consequent

computation expense. During the course of this program the second factor above became the major consideration in that only a very small fraction of the analytical effort planned could be accomplished.

As with the analysis of any physical phenomena the degree of complexity incurred with an analysis of antiskid operation is related to the degree of solution precision which is being attempted. At the onset of the analytical effort it was recognized that if any significant improvement in the analysis of antiskid compatibility was to be accomplished, some greater than usual analytical complexity would be required because the influence of such high frequency oscillations as brake squeal and tire tread circumferential displacement was to be accounted for. It was hoped that some way could be found to combine these complex analytical elements needed for compatibility evaluation with simpler analytical elements as are more appropriate for evaluating airplane stopping performance. Unfortunately, efforts expended toward accomplishing this goal have not produced very successful results. The following discussion describing various possible mathematical treatments of tire-to-ground friction illustrates the analytical dissonance between a procedure best suited for evaluating antiskid compatibility and a much less complex treatment suitable for airplane stopping performance evaluation.

A very important aspect of antiskid brake control system analysis is the mathematical treatment of the relationship between tire-to-runway friction force and the amount of tire-to-runway slippage. This mathematical treatment is influenced by budgetary considerations, computer setup and computer capabilities. For a real time analog computer setup the usual procedure is to define the friction coefficient between the tire and runway surface as a function of wheel slip ratio as shown in Figure 9(a). In this case, the amount of tire slippage is expressed as a fraction of the axles horizontal velocity. Figure 9(b) shows an alternate procedure where friction coefficient is expressed as a function of slip velocity. Figure 10 shows how these functions are used to compute the brake force and the brake force is then used in the computation of wheel slippage. Both of the above can give fairly good analytical results when evaluating braking system performance but do not produce computer operation which correlates very well with the effects of antiskid operation as recorded during vehicle tests.



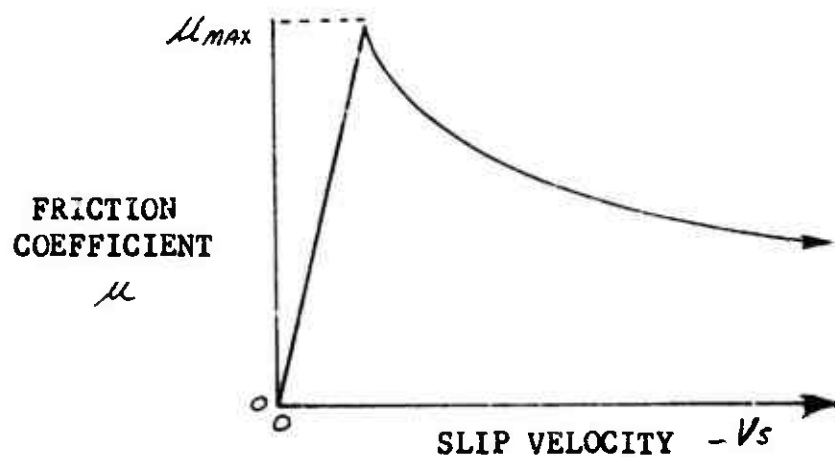
$$S = 1 - \frac{\dot{\Theta}_w R_e}{\dot{X}_A}$$

$\dot{\Theta}_w =$  TIRE ANGULAR VELOCITY

$\dot{X}_A =$  TRANSLATIONAL VELOCITY OF TIRE  
ROTATIONAL AXIS (AXLE) RELATIVE  
TO THE GROUND

$R_e =$  TIRE UNBRAKED ROLLING RADIUS

(a) FRICTION COEFFICIENT - SLIP RATIO FUNCTION



$$V_s = \dot{X}_A - \dot{\Theta}_w R_e$$

(b) FRICTION COEFFICIENT - SLIP VELOCITY FUNCTION

Figure 9 Tire Friction Coefficient Functions

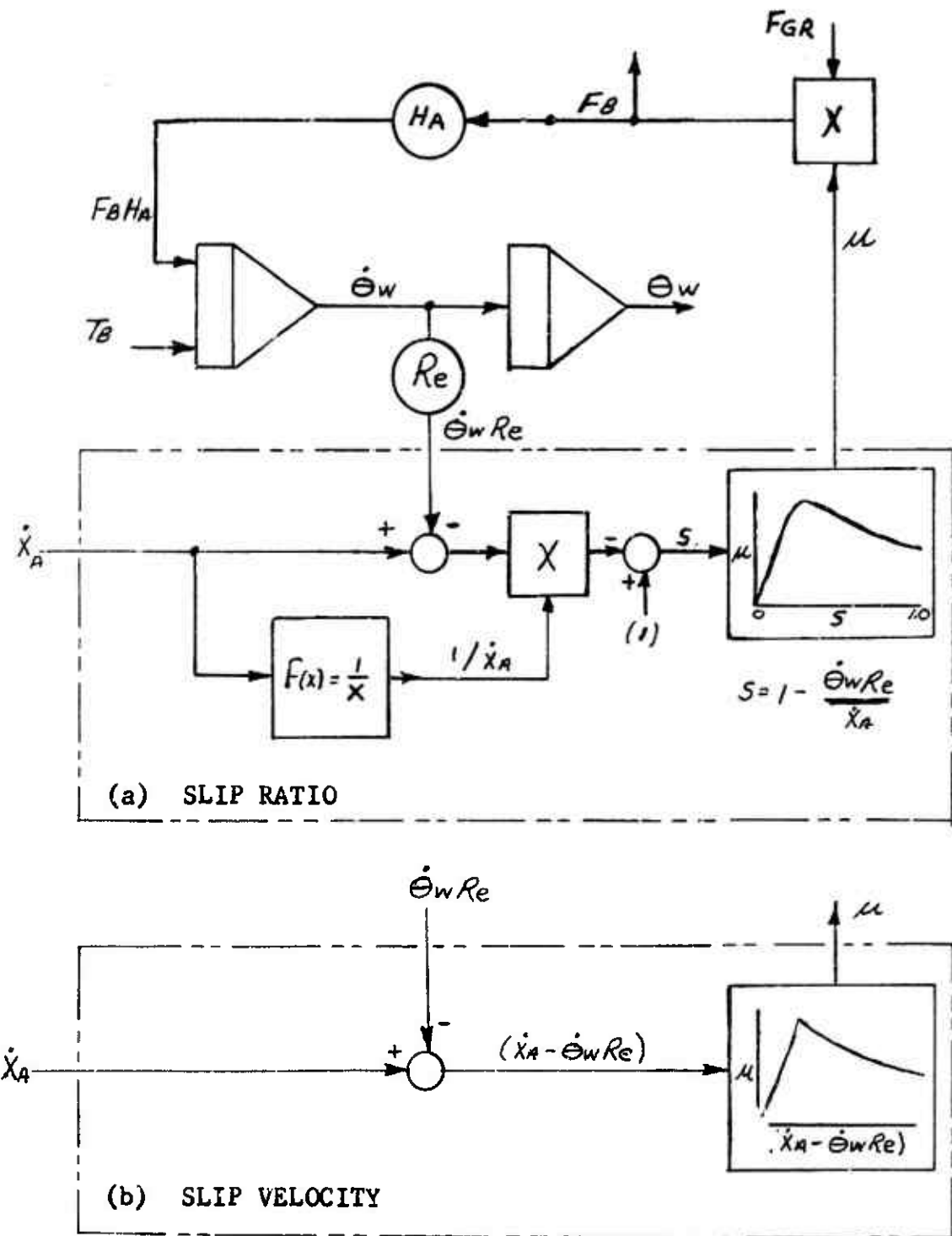


Figure 10 Tire Friction Computation

As described in Reference 17, a critical examination of the above mathematical treatment of the relationship between tire-to-runway friction force and tire-to-runway slippage will reveal that in the stable positive slope region of the friction force-slippage relationship the amount of apparent slippage is the result of the braking force and tire elastic deformation, not the cause of some value of friction coefficient being in existence, and that in the unstable negative slope region of the friction force-slippage relationship the amount of friction force decay is a function of the tire footprint actual slippage not some percentage of the axle velocity. Consequently, the characteristics of the friction coefficient-slip ratio function, if used, must be established relatively arbitrarily because of the very large variations which must be approximated over a wide range of conditions. It is not uncommon to set the initial slope of the friction coefficient-slip ratio function to be compatible with computer capabilities rather than attempt to simulate the tire elastic properties as would be more realistic.

Considering the above, using the analytical convenient slip ratio-friction coefficient technique cannot produce truly credible analytical results. Using the friction coefficient-slip velocity approach is capable of more believable analytical results if the function can be adequately defined. The mathematical treatment of the brake force-tire slippage phenomenon described in Appendix A herein better represents actual physical occurrences. This procedure is to account for the tire tread torsion and translational deformation relative to the wheel when computing footprint velocity relative to the runway. However, because of the tire treads' very high acceleration, a real time analog computer or relatively long integration time step digital computer solution is not practically achievable. Using the tire mathematical model described in Appendix A along with the definition of tire properties from Reference 1 allows the examination of such effects as tire size and inflation pressure upon braking system compatibility. These effects can be of considerable significance for the case of small high pressure tires.

There are other analytical elements such as brake torque computation and hydraulic valve operation where there are similar differences between the type of mathematical treatment which is best suited for compatibility analysis as compared with performance evaluation. It has been concluded that a single analysis procedure is not likely to ever be formulated which will be capable of general usage for all antiskid analysis tasks in an

economically feasible fashion. Accordingly, an alternate more simplified analysis procedure has been formulated. The analytical techniques of the simplified procedure are intended to be primarily used for performance evaluation. However, some compatibility aspects of antiskid operation can be analyzed.

## SECTION II

### VERIFICATION TESTING

The initial step toward verifying, correlating and refining the previously developed aircraft antiskid performance and total system compatibility analysis procedures was to conduct a controlled physical demonstration of total braking system operation. This demonstration consisted of a number of braked stops performed on a laboratory brake test dynamometer using a test set-up including an aircraft landing gear assembly to support the tire, wheel and brake, the brake actuation hydraulic system, and an antiskid system. During these braked stops various forces, hydraulic pressure and displacements describing the landing gear dynamic behavior, antiskid and hydraulic brake control systems' operation and braking performance were recorded so that this information could be compared with the corresponding information predicted by the analytical procedures for the same circumstances. The controlled demonstration was intended to show the effects upon braking performance and total system compatibility which result from varying such total system characteristics as:

- (1) Hydraulic flow restriction at various points in the brake actuation system
- (2) Tire radial and torsional stiffness
- (3) Antiskid control characteristic
- (4) Landing gear fore and aft natural frequency
- (5) Tire-to-runway braking force potential.

#### A. TOTAL SYSTEM TEST INSTALLATION

The total system test installation consisted of:

- (1) A support fixture equipped with a movable carriage simulating the aircraft landing gear attachment points. A carriage loading and control system was provided so that the landing gear could be landed on the 192 inch diameter flywheel of the inertia brake test dynamometer located in the AFFDL Landing Gear Test Facility, Building 31, Area B, Wright Patterson Air Force Base, Ohio.

- (2) One F-111 main landing gear tire-wheel-brake assembly installed on the necessary F-111 landing gear structural components so as to complete an installation the same as that for the aircraft left main wheel.
- (3) A mockup of the F-111 hydraulic brake actuation and control system including pilot's metering valve, accumulator, lines and fittings.
- (4) An antiskid control system including wheel speed sensor, control circuit and antiskid valve.
- (5) Instrumentation equipment as required to measure and record dynamometer flywheel speed and distance, braked wheel speed, hydraulic pressure at the brake and at the antiskid valve inlet, brake torque, radial and tangential forces between the tire and dynamometer flywheel, and electrical signal at the antiskid control valve. The instrumentation consisted of:
  - (a) Electrical resistance strain gage pressure transducers with appropriate excitation power supply and resistance measuring electronic circuitry (CEC System D) to measure hydraulic pressure at the brake and at the antiskid valve inlet. The accuracy of the pressure measurements was within  $\pm 25$  psig.
  - (b) The output from the antiskid wheel speed sensor (a D.C. tachometer) was used to measure braked wheel speed. The speed was determined within 2 percent by using the tachometer calibration curve and an electronic D.C. voltmeter (same as described in (e) for antiskid valve electrical signal).
  - (c) A light beam type electronic pulse generator and 200 hole perforated disc with appropriate electronic circuitry was used to measure dynamometer flywheel speed and distance. Distance measurement within  $\pm .25$  ft. and velocity measurement within  $\pm 1.5$  miles per hour was accomplished with an electronic counter and by the oscillograph.
  - (d) Electrical resistance strain gages installed on the axle were used to measure the radial and tangential forces between the tire and dynamometer flywheel and brake torque. CEC System D excitation power supply

and resistance measuring electronic circuitry were used for strain gage output recording. The axle was calibrated using a calibration fixture previously used for flight test load calibration.

- (e) An electronic D.C. voltmeter was used to measure the electrical signal at the antiskid control valve. This voltmeter is the oscillograph galvanometer with appropriate shunt. Voltage measurement was within  $\pm .5$  volts.

Outputs from these measuring devices were recorded with respect to time on a CEC direct writing oscillograph and on magnetic tape.

Instrumentation calibration was accomplished by accepted laboratory practice with respect to standards traceable to the National Bureau of Standards.

During the course of the testing alternate equipment items such as different size tires, different antiskid control circuits and different hydraulic flow restrictors were assembled into the total system installation as appropriate to produce the desired overall system configuration for individual test conditions. The total system test installation is shown on Figures 11, 12, 13, 14, 15 and 16. Figure 17 shows two views of the 192 inch diameter inertia brake test dynamometer located in the AFFDL Landing Gear Test Facility prior to installation of the total system test support fixture. These two views correspond to those shown on Figure 11 and Figure 12 after the total system test support fixture was installed.

The total system test support fixture was designed and fabricated at the Fort Worth Operation of General Dynamics Convair Aerospace Division in Fort Worth, Texas. After assembly the support fixture was structurally proof tested at Fort Worth, Texas and then disassembled, shipped to Wright-Patterson Air Force Base, Ohio and installed in the AFFDL Landing Gear Test Facility. The support fixture has 28.0 inches carriage stroke and will accommodate a landing gear having up to 50.0 inches tire diameter. The movable carriage weighs approximately 15000 pounds and with the initially installed size actuator powered by the existing 1500 psi hydraulic system test loadings over the range of 0 - 30,000 pounds applied radially on the dynamometer flywheel can be accomplished. The support fixture structural capacity is 50,000 pounds and by increasing the size or number of load actuators or by increasing the capacity of the

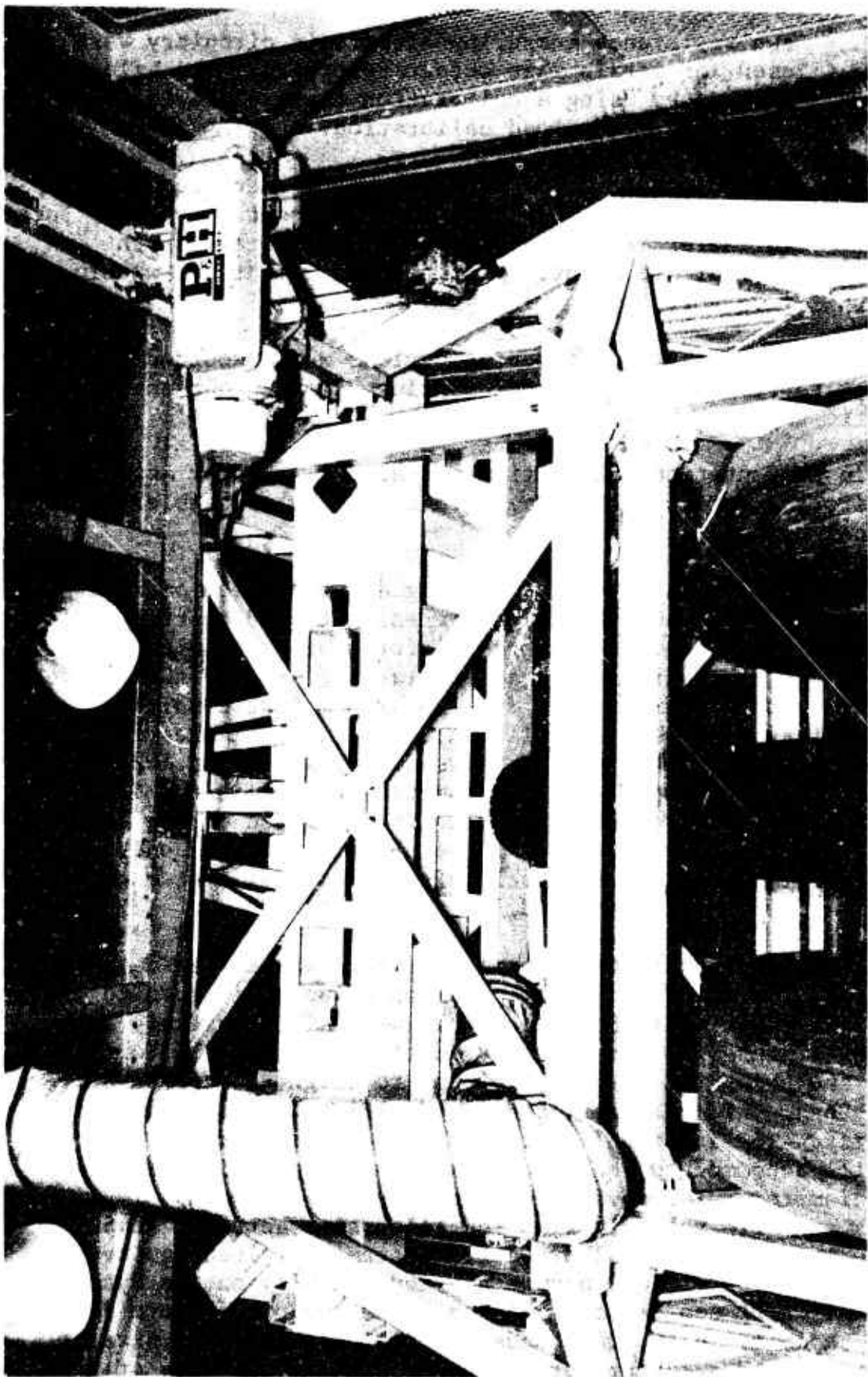


Figure 11 Total System Test Installation - Landing Gear and Support Fixture  
Viewed Looking North Inside Dynamometer Cage

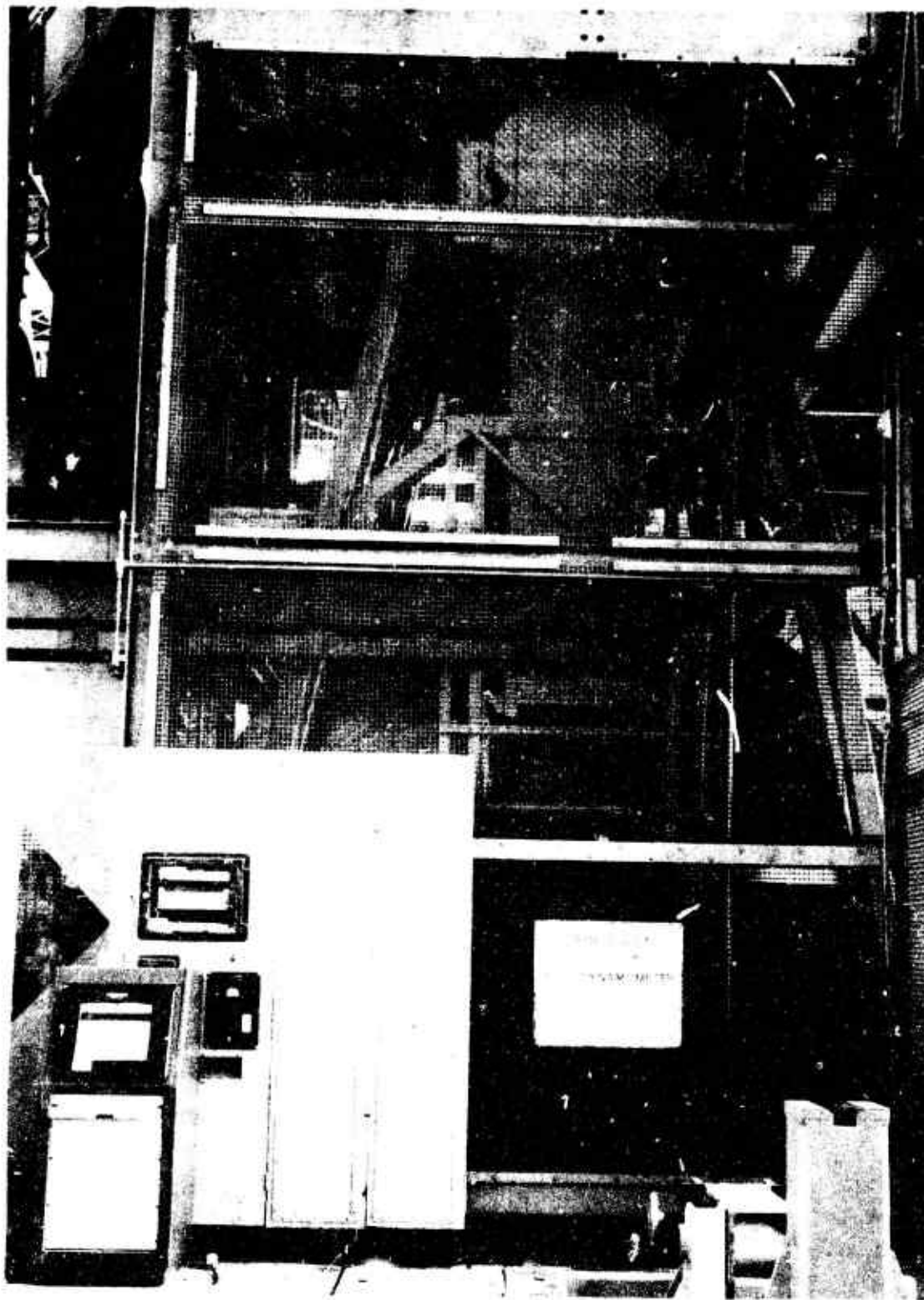


Figure 12 Total System Test Installation Support Fixture  
Viewed Looking East from Outside Dynamometer Cage

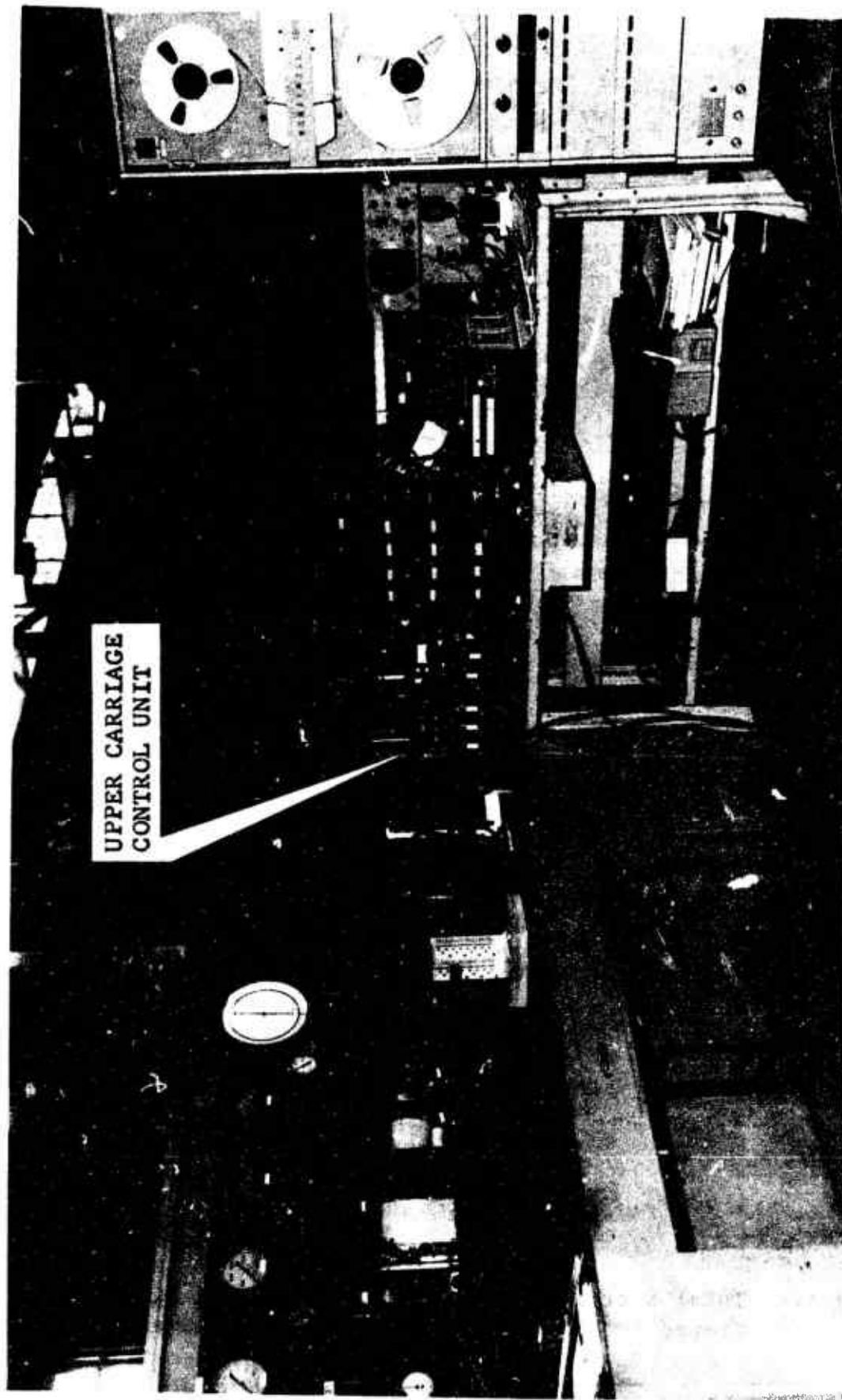


Figure 13 Total System Test Installation - Dynamometer Control Console,  
Upper Carriage Control Unit and Data Recording Equipment

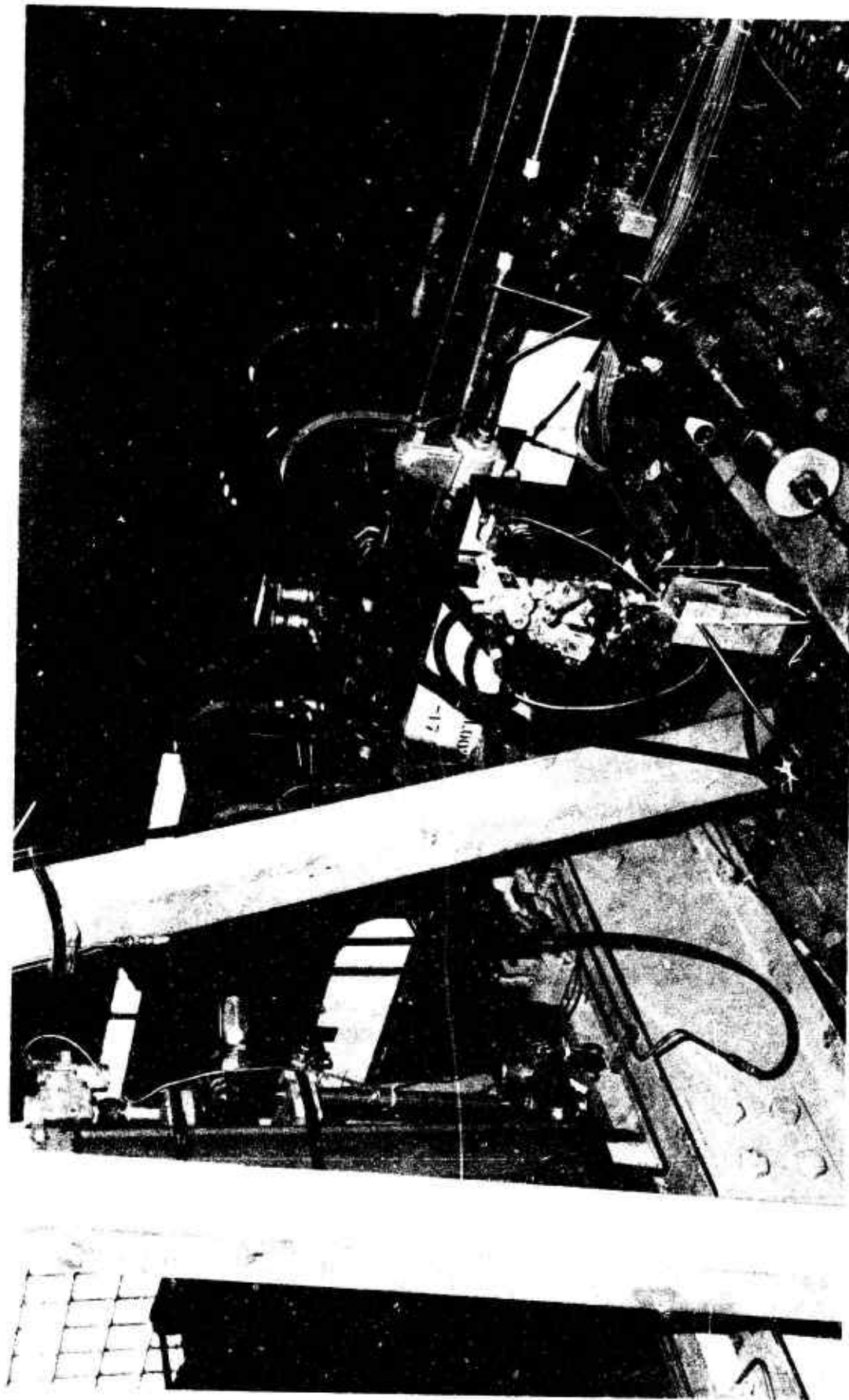


Figure 14 Total System Test Installation - Aircraft Brake Metering Valve and Accumulator with Upper Carriage Loading System Components Viewed from Top of Dynamometer Cage

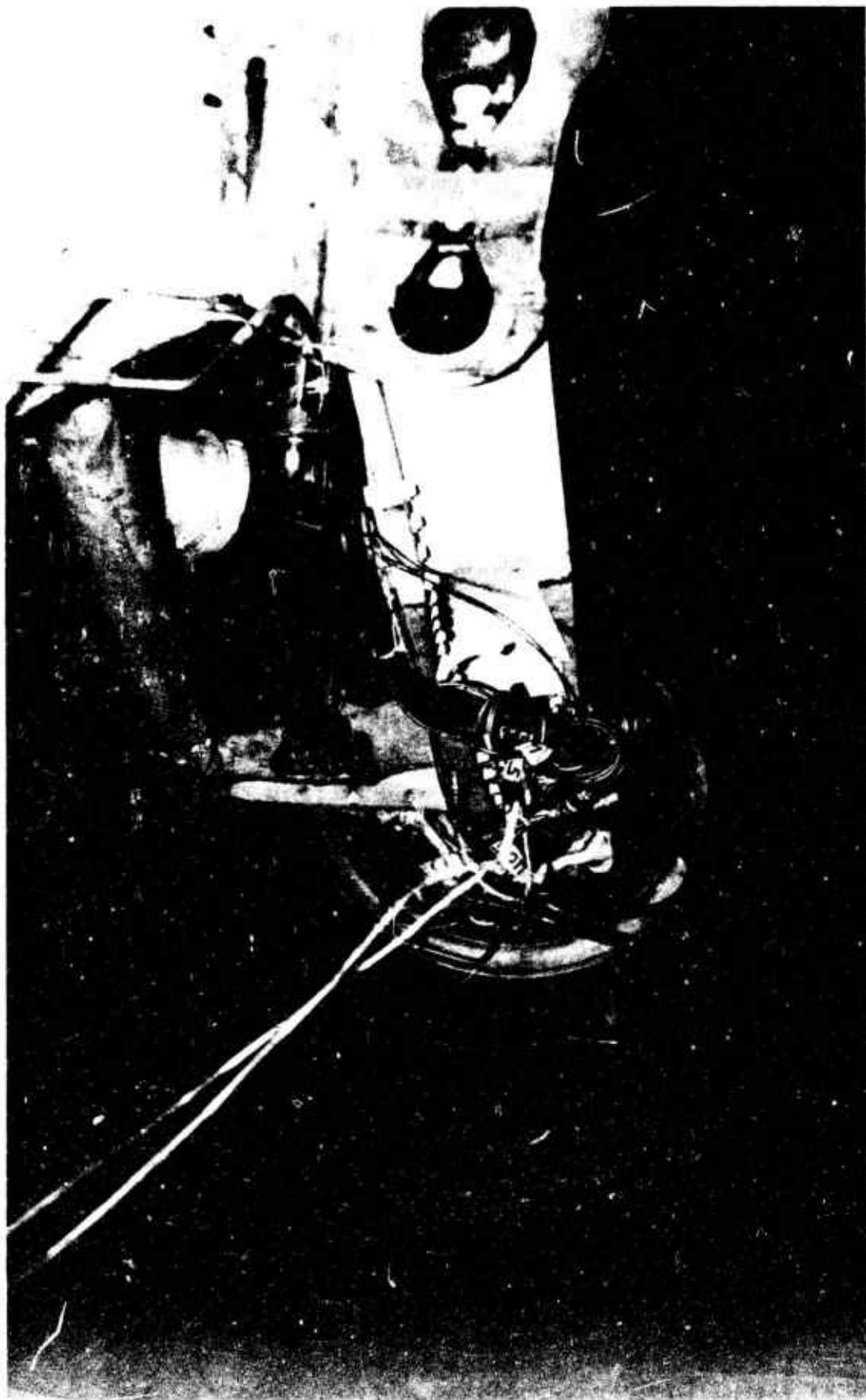


Figure 15 Total System Test Installation - F-111 Main Landing Gear Left Wheel  
Installed Over Dynamometer Flywheel - Viewed Looking Outboard and  
Forward

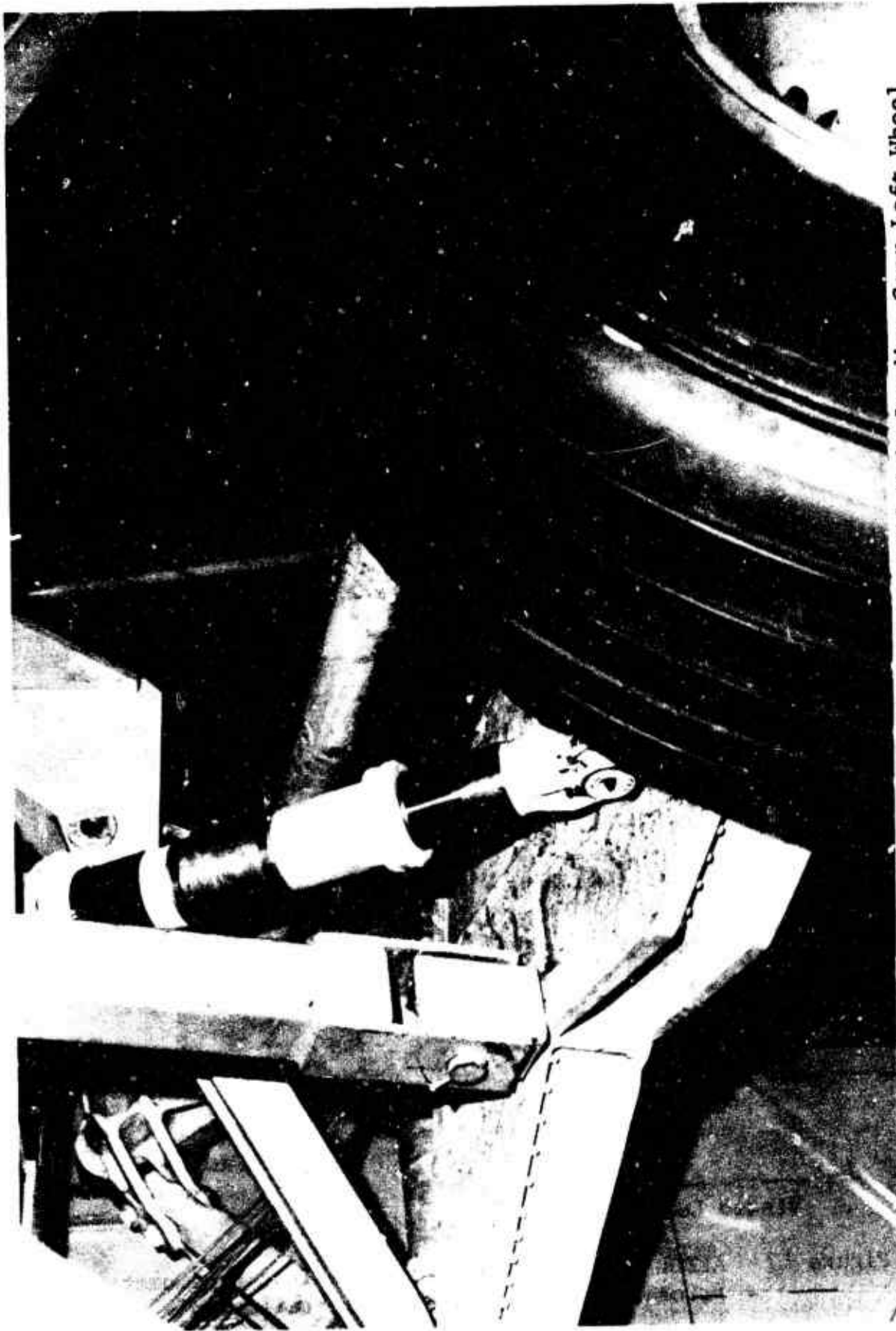
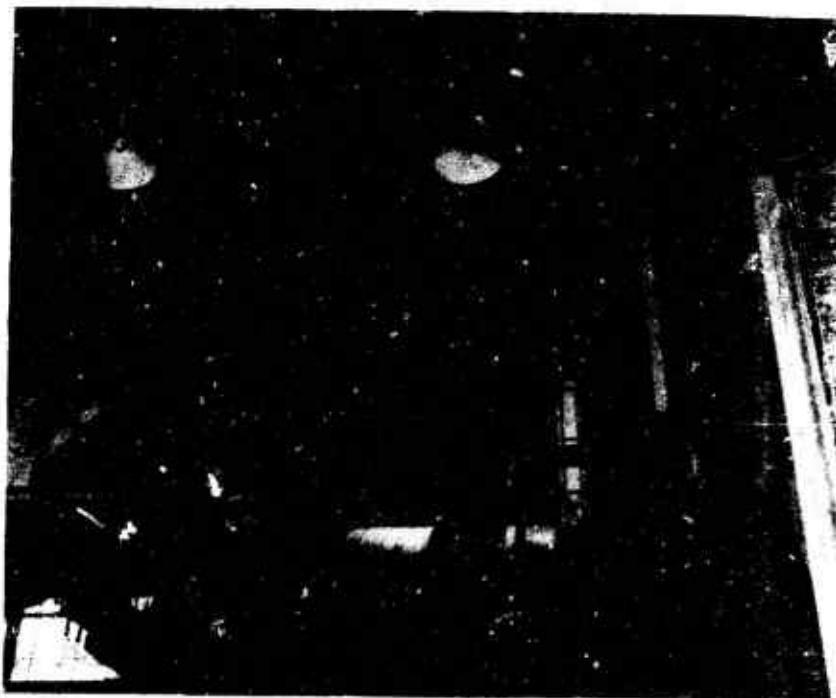
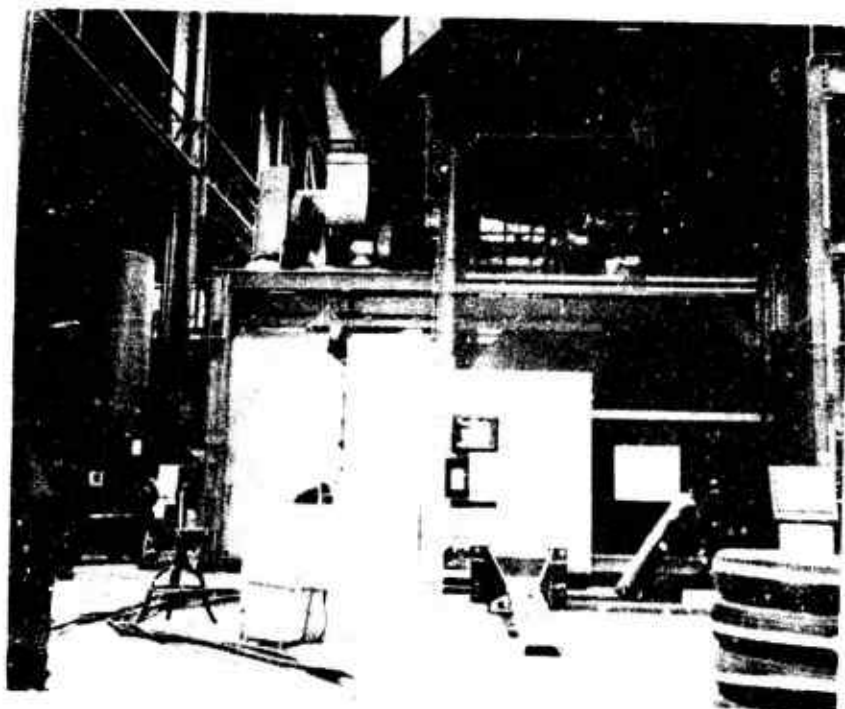


Figure 16 Total System Test Installation - F-111 Main Landing Gear Left Wheel Installed Over Dynamometer Flywheel - Viewed Looking Inboard and Aft



Viewed Looking North From Inside of Cage



Viewed Looking East From Outside of Cage

Figure 17 AFFDL 192 Inch Diameter Brake Test Dynamometer  
Prior to Total System Test Installation

existing hydraulic system test loadings up to 50,000 pounds can be accomplished. Figure 18 shows the support fixture while being subjected to proof loading for the side load design condition and Figure 19 shows the fixture set up to apply proof loading for the landing design condition. Because the support fixture is not structurally symmetrical for loading applied in the plane of the flywheel, both landing and braking design proof loads were applied in each direction (i.e., as installed, horizontal loads acting both North and South). Because of support fixture symmetry in the plane of the flywheel shaft, proof loading for the side load condition was applied in the direction of horizontal load acting West only. The proof loadings applied are: for the landing design condition, 142,000 pounds (1.5 times the resultant of 75,000 pounds vertical combined with 57,750 pounds horizontal in a plane 19.0 inches above the flywheel), for the braking design condition 117,000 pounds (1.5 times the resultant of 50,000 pounds vertical combined with 60,000 pound horizontal in a plane tangent to the flywheel), and for the side load design condition (drift landing) 144,000 pounds which is 1.5 times the resultant of 75,000 pounds vertical combined with 60,000 pounds horizontal and in a plane tangent to the flywheel.

The support fixture carriage loading and control system consists of an electrohydraulic servo actuator in combination with a solid state electronic amplifier/comparator unit. The test fixture control unit as shown in Figure 13 allows the operator to lock or unlock the overhead carriage, command landing or unlanding, control the amount of landing load applied, apply or release the brake, bleed the carriage load hydraulic equipment and implement emergency unlanding.

#### B. TEST CONDITIONS AND PROCEDURES

The testing was accomplished by performing braked stops with a combination of different equipment configurations and different applied loading as listed in Table 1. The various equipment configurations listed are:

- (1) Antiskid System - The antiskid systems used during the tests consisted of a production F-111 wheel speed sensor (Goodyear Part Number 9542613) and antiskid control valve (Goodyear Part Number 9550255) connected with one of the following antiskid control circuits:

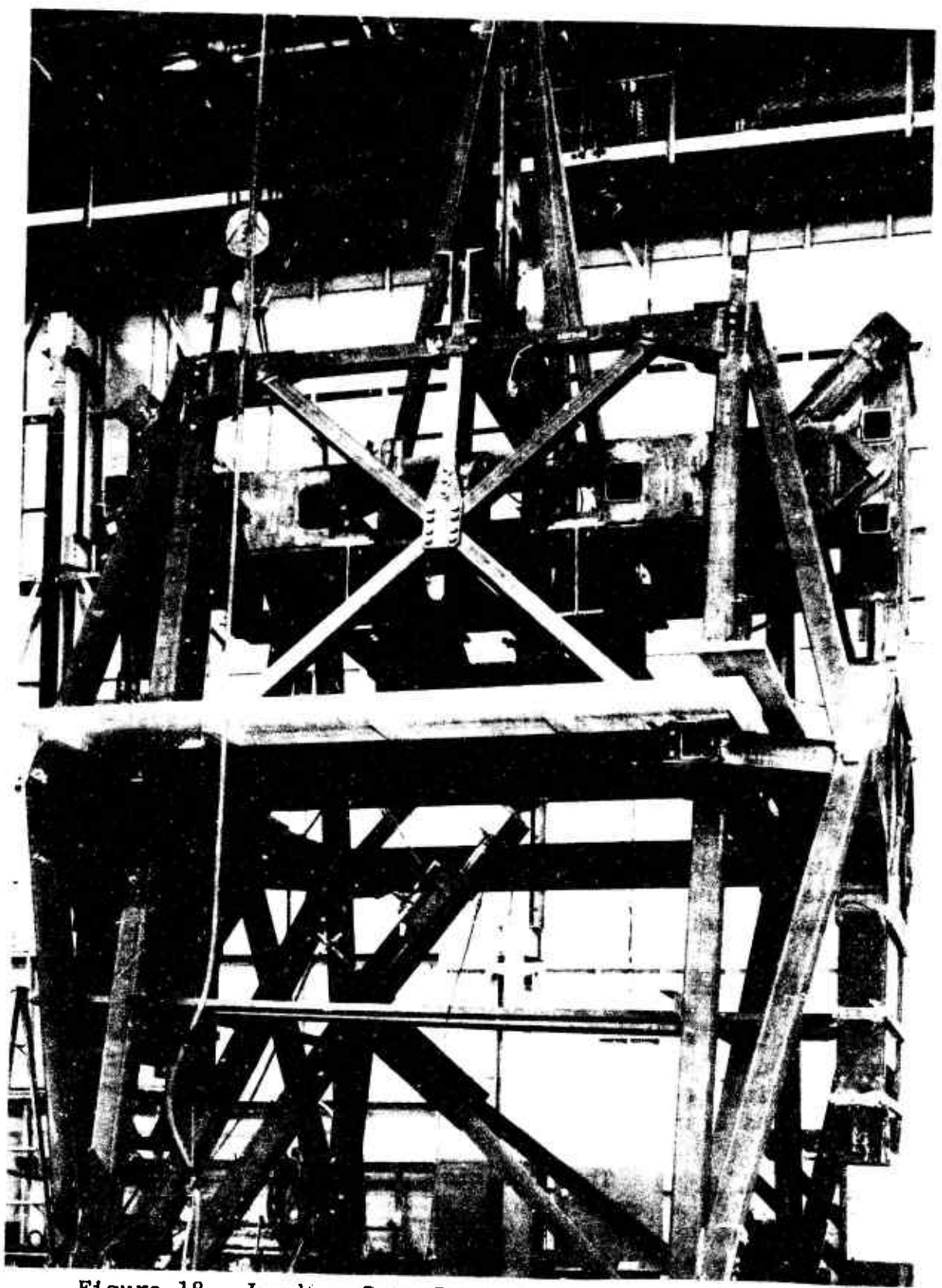


Figure 18 Landing Gear Support Fixture Structural  
Proof Test for Side Load Condition

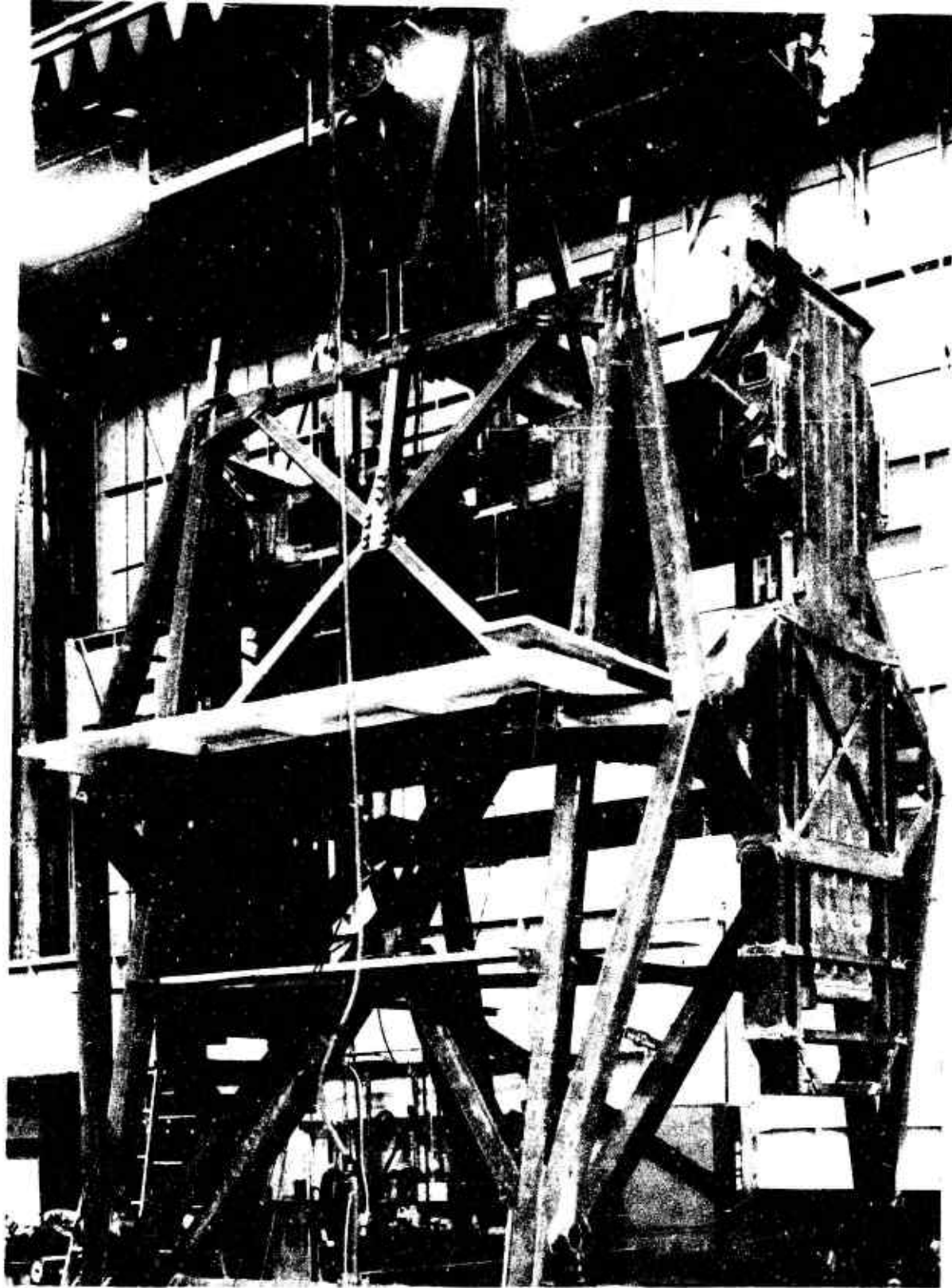


Figure 19    Landing Gear Support Fixture Structural  
Proof Test For Landing Load Condition

**Table 1    Test Condition Summary**

COND. NO.	ANTISKID SYSTEM	TIRE SIZE	TIRE AND SHOCK STRUT INFLATION	HYD. CONFIG.	APPLIED VERTICAL LOAD
1	ON-OFF-A	47 X 18	150-A	A	17,000
2	ON-OFF-A	47 X 18	150-A	A	13,000
3	ON-OFF-A	47 X 18	150-A	A	9,000
4	ON-OFF-A	47 X 18	150-A	A	5,000
5	ON-OFF-A	47 X 18	50-A	A	5,000
6	ON-OFF-A	47 X 18	50-A	A	13,000
7	ON-OFF-A	42 X 13	200-A	A	17,000
8	ON-OFF-A	42 X 13	200-A	A	13,000
9	ON-OFF-A	42 X 13	200-A	A	9,000
10	ON-OFF-A	42 X 13	200-A	A	5,000
11	ON-OFF-A	42 X 13	200-A	B	5,000
12	ON-OFF-A	42 X 13	200-A	B	13,000
13	ON-OFF-A	42 X 13	200-A	C	5,000
14	ON-OFF-A	42 X 13	200-A	C	13,000
15	ON-OFF-A	42 X 13	200-A	D	5,000
16	ON-OFF-A	42 X 13	200-A	D	13,000
17	ON-OFF-A	42 X 13	200-B	C	17,000
18	ON-OFF-A	42 X 13	200-B	C	13,000
19	ON-OFF-A	42 X 13	200-B	C	9,000
20	ON-OFF-A	42 X 13	200-B	C	5,000
21	ON-OFF-B	42 X 13	200-A	C	13,000
22	ON-OFF-B	42 X 13	200-A	C	5,000
23	ON-OFF-B	47 X 18	150-A	C	13,000
24	ON-OFF-B	47 X 18	150-A	C	5,000
25	MOD-A	47 X 18	150-A	C	13,000
26	MOD-A	47 X 18	150-A	C	5,000
27	MOD-A	47 X 18	150-B	A	13,000
28	MOD-A	47 X 18	50-A	A	5,000
29	MOD-A	47 X 18	150-A	A	17,000
30	MOD-A	47 X 18	150-A	A	13,000
31	MOD-A	47 X 18	150-A	A	9,000
32	MOD-A	47 X 18	150-A	A	5,000
33	MOD-A	42 X 13	200-A	A	17,000
34	MOD-A	42 X 13	200-A	A	13,000
35	MOD-A	42 X 13	200-A	A	9,000
36	MOD-A	42 X 13	200-A	A	5,000

- (a) ON-OFF-A antiskid control circuit was a bread board version of the production F-104 and B-58 circuit except that an amplifier was added to the input in an attempt to achieve compatibility with the F-111 wheel speed sensor and to account for the difference in tire size.
  - (b) ON-OFF-B antiskid control circuit was the same as ON-OFF-A except the skid detection threshold and skid recovery signal settings were adjusted to achieve better stopping performance for the condition where high braking force potential exists.
  - (c) MOD-A antiskid control circuit was the production F-111 circuit with a modification of a resistance value in the modulating section. This modification was to facilitate the computation of analytically predicted performance and should have had negligible effect upon antiskid operation.
- (2) Tire Size - The following two different size tire and wheel assemblies are physically interchangeable on the F-111 axle and fit with the F-111A brake assembly. The difference in weight of these two tire and wheel assemblies was expected to produce a preceivable change in landing gear fore and aft natural frequency.
- (a) 47 X 18-18 size 26 ply rating tire mounted on a F-111A wheel assembly (B.F. Goodrich Part No. 3-1156-7) - This is the production F-111A equipment.
  - (b) 42 X 13-18 size 28 ply rating tire mounted on a F-111B wheel (B.F. Goodrich Part No. 3-1155-5).
- (3) Hydraulic Configuration - The hydraulic brake actuation and control system used for these tests was a mockup of the production F-111 system with the following alterations:
- (a) Hydraulic Configuration A was the production configuration with no alteration except that a single long hose was used in place of a combination of hard line and two short hoses between the metering valve and the landing gear.
  - (b) Hydraulic Configuration B was the production system modified by installing a moderate hydraulic flow restriction (.060 inch diameter orifices) between the antiskid valve and the brake.

- (c) Hydraulic Configuration C was the production system modified by installing a moderate hydraulic flow restriction (.070 inch diameter orifices) between the pilot's metering valve and the antiskid valve.
  - (d) Hydraulic Configuration D was the production system modified by installing a very high hydraulic flow restriction (.035 inch diameter orifices) between the pilot's metering valve and the antiskid valve.
- (4) Tire and Shock Strut Inflation Conditions - The test run conditions listed in Table I include variations in the total system configuration with respect to the shock strut and tire inflation pressures. The shock strut inflation pressure condition A is equivalent to that used on the F-111 and is sufficiently high to keep the shock struts upper stage fully extended. In the upper stage fully extended position and with the vertical loads associated with landing gross weights, shock strut stroking does not occur because there is insufficient compressive force to overcome the extending load. In this case the tire absorbs all of the airplane's vertical motion with respect to the ground and fairly large tire load variations result. Shock strut inflation pressure condition B is a lower pressure as is required to allow the upper stage to be compressed enough to produce two inches axle travel from the upper stage fully extended position when the test load is applied statically. This shock strut inflation condition would allow some of the vertical position variation in the aircraft's landing gear attachment to be absorbed by shock strut stroking as would occur with a conventional single stage strut arrangement. In this case the variation in tire loads should have been reduced. Even though these tests were performed with a laboratory set up where large vertical load variations should not occur the elastic deflection of the load carriage was expected to produce some variation of vertical load.

Different tire inflation pressure conditions were imposed to achieve changes in tire radial and torsional stiffness. The higher pressures were those which are usually used on the airplane (no flywheel correction applied) and the lower pressures were those which will produce approximately the same deflection for the test load imposed as is experienced on the airplane.

On Table 1 the tire and shock strut inflation condition is indicated by the tire inflation pressure in psig and the shock strut inflation condition letter as described above.

Since these tests were performed to produce information to be used for verification of the analytical prediction procedure, the test conditions were formulated to be compatible with the analytical procedure. The achievement of good (or even acceptable) braking performance was not expected for some test conditions. The reason for using the On-Off type antiskid control circuit for the majority of the test conditions was that the analytical prediction for On-Off operation was believed to be more economical than for the modulated control circuit operation. The objectives for the individual test conditions were:

- Test conditions number 1, 2, 3 and 4 were to examine the variation in braking system performance which results from variations in tire-to-runway braking force potential.
- Test conditions number 5 and 6 were to examine the effects of tire stiffness. The results of these test runs will be compared to conditions 2 and 4.
- Test conditions number 7, 8, 9 and 10 were to examine the effects of changing the landing gear fore and aft natural frequency.
- Test conditions number 11, 12, 13, 14, 15 and 16 were to examine the effects of variations in hydraulic system flow restrictions.
- Test conditions number 17, 18, 19 and 20 were to examine the effects of the landing gear's vertical compliance as influenced by shock strut characteristic.
- Test conditions number 21, 22, 23 and 24 were to examine the effects of changing the control circuit's operating characteristic.
- Test conditions number 25 and 26 were to determine the effects of varying the hydraulic system restriction in conjunction with modulated antiskid circuit operation.
- Run condition 27 was to determine the effects of the landing gear's vertical compliance in conjunction with modulated antiskid circuit operation.

- Test run condition 28 was to determine the effects of tire stiffness in conjunction with modulated antiskid circuit operation.
- Test conditions number 29, 30, 31 and 32 were to determine the variation in braking system performance with modulated antiskid circuitry resulting from variations in tire-to-runway braking force potential.
- Test conditions number 33, 34, 35 and 36 were to determine the effects of increased landing gear fore and aft natural frequency along with variations in tire-to-runway braking force potential with modulated antiskid system operation.

For all test conditions the dynamometer flywheel inertial equivalent was 10,147 pounds, the brake application speed was 135 mph and brake release speed was 10 mph. The resultant kinetic energy absorption was 6.15 million foot pounds as compared with 18 million foot pounds F-111A brake 45 stop energy capacity. This low energy condition was used for economy in that brake wear was minimized, test runs could be conducted more frequently because long brake cooling periods were avoided, and the computation expense required to analyze a complete test run was reduced. Each test run was performed as follows:

- The applicable total system installation test configuration was installed in the test set-up and the antiskid control circuit was functionally checked. The applicable landing load was set on the carriage load control system.
- The flywheel was accelerated to approximately 140 mph peripheral speed and the wheel was landed with the applicable applied load. When 135 mph flywheel speed was reached the brake was applied by positioning the aircraft pilot's metering valve for 1600 psi steady state output pressure. Prior to landing the instrumentation and recording equipment was started to record the applicable parameters during the test.
- When the flywheel speed had been reduced to 10 mph, the brake was released so that the aircraft wheel was allowed to coast. At approximately 2 mph flywheel speed the aircraft wheel was unlanded. The dynamometer flywheel was not brought to a complete stop because significant antiskid operation does not occur below 10 mph locked wheel detection speed and because repeated high torque low speed usage causes excessive brake wear and lining damage.

### C. TEST RESULTS

Since this testing was performed for verification of the analytical prediction procedure, the criteria for evaluating the relative success or failure of an individual test run is established by the degree of agreement between actual occurrences and the analytically predicted occurrences. The nature of the testing was such that the test results could be evaluated by direct observation of the oscillograph traces showing the recorded data. Items which were evaluated are:

- Landing gear fore and aft load magnitude and oscillation frequency.
- The character and magnitude of braked wheel speed variation throughout individual antiskid cycles.
- Relative braking effectiveness as indicated by stopping distance and dynamometer flywheel deceleration rate.
- The ability of the antiskid system to prevent skids when conditions of low tire-to-runway friction potential are encountered.
- The overall compatibility between the various elements within the total system. For instance, was the hydraulic brake line flow restriction excessive such that satisfactory tire skid prevention or the achievement of satisfactory stopping performance was inhibited.

Test runs were performed for all of the 36 test conditions listed in Table 1 and the test data was recorded as intended. Figure 20 shows an oscillograph record for test condition No. 29 with a reduced time scale. This oscillograph is typical of the other test conditions except for length. As can be observed the antiskid system operated reasonably well.

In most respects practically all of the test results except for those from test condition No. 29 were unsatisfactory in that the circumstances of the test runs were beyond the bounds of the circumstances for which the analysis procedures were intended to represent. The primary difficulty was that the On-Off antiskid circuit operation was totally unsatisfactory and not representative of any type antiskid system which might ever be attempted to be used on an airplane. Unsatisfactory On-Off antiskid operation was caused by the wheel speed signal being severely

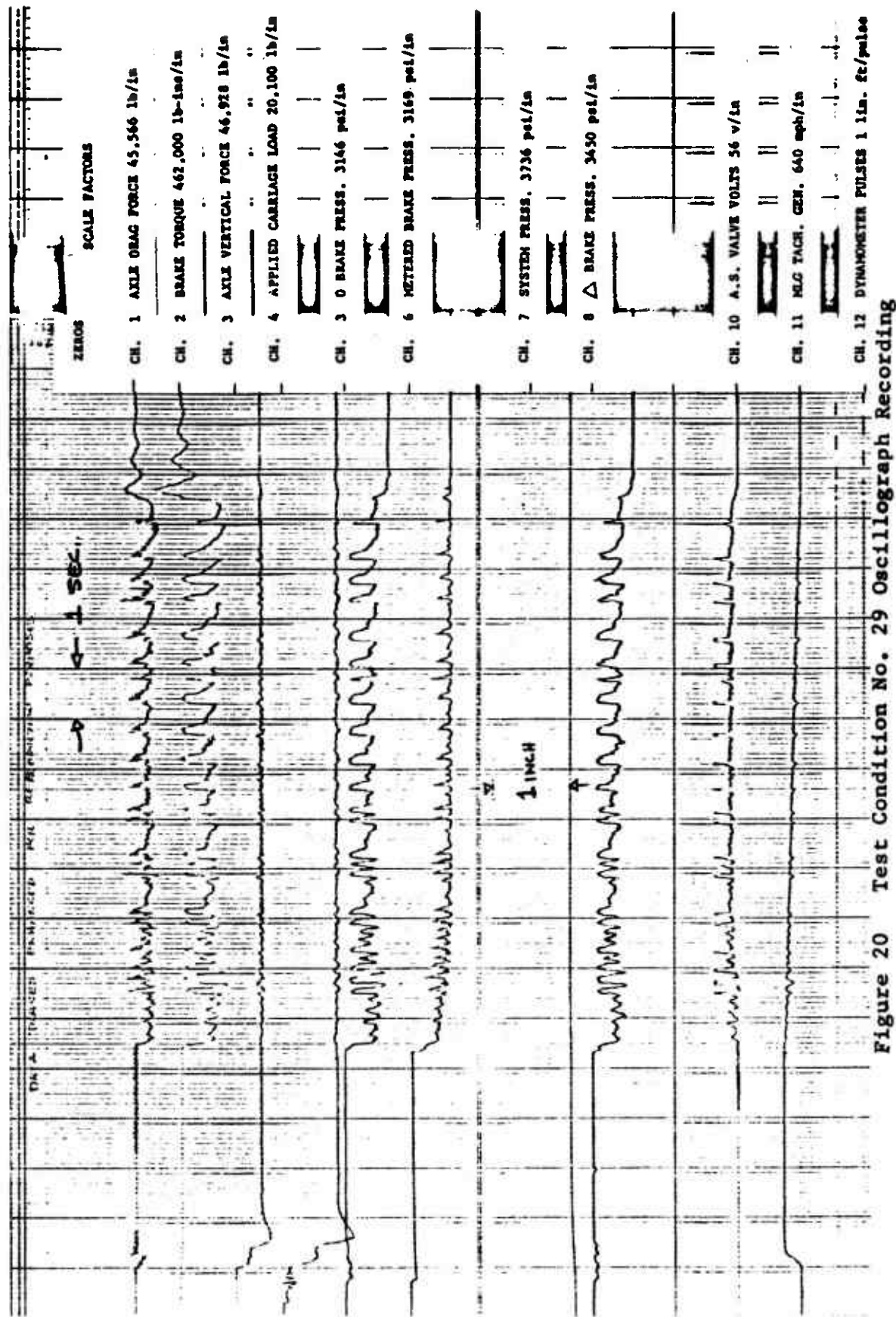


Figure 20 Test Condition No. 29 Oscillograph Recording

distorted by the amplifier which was intended for adapting the F-111 wheel speed sensor to provide the proper input to the F-104 type electronic circuit. The existence of the problem was recognized at the time the tests were being conducted; however, the means for prompt resolution was not available. Testing was continued because the degree of wheel speed signal distortion was not believed to be as great as it was later determined to be. When the magnitude of the problem was identified there was insufficient remaining time with which to implement suitable corrective action and repeat the test runs.

As a result of the unsatisfactory On-Off antiskid operation, a large number of severe tire skids occurred. These tire skids caused the tread compound to become reverted. Even though the flywheel surface was cleaned between test runs, the reverted tire tread compound contaminated the flywheel surface during the first few wheel revolutions such that tire-to-flywheel friction coefficient was much less than that which is usually available and which was planned for. Since the test runs for conditions using the modulated antiskid control circuit were performed such that they were interspersed with the tests using On-Off antiskid circuit, the results of these tests were adversely affected by the abnormal tire tread condition. This problem could have been avoided if additional tires had been available for replacement or if the tests had been performed so that those using modulated antiskid circuit had been performed first.

Observation of the oscillograph records during the course of the test revealed brake pressure increase and decrease was occurring at a rate less than that which had been expected. The test setup was inspected for possible unplanned excessive restriction in the hydraulic lines from the brake to the antiskid and brake metering valves and the antiskid valve was changed on one occasion; however, no cause for apparent high restriction could be found. This effect did not cause any significant difficulty with antiskid operation during testing but does cause an analytical problem as discussed in Section IV.

## SECTION III

### ANALYSIS REFINEMENT

Early in this program it was realized that if any appreciable amount of test data correlation was to be accomplished it would be necessary to devise some way to reduce analytical complexity because of the prohibitive computation expense which would otherwise be incurred. This problem was previously discussed in Section I herein. To permit evaluation of such effects as brake chatter and squeal, the tread circumferential and radial displacement with respect to the wheel, and hydraulic system resonant pressure surges, the analysis procedures as previously formulated contain a number of second order differential equations describing phenomena having very high oscillatory frequencies, some well above 100 HZ. Provisions for these effects were included because there have been instances where they have been the cause of braking system incompatibility problems. In addition, the examination of tire tread displacement with respect to the wheel provides the only known means of adequately explaining a tire's braking force versus apparent slippage relationship.

As a first step toward analytical refinement the antiskid valve mathematical model was revised as described in Section 7 of Appendix A. Additional damping was added between the tire tread and the wheel and the tire-to-ground friction coefficient versus slip velocity function was modified as described in Section 4 of Appendix A. These simplifications were helpful but did not significantly reduce computation expense. It is evident that there are infinitely many minor variations of the mathematical models formulated and that the useful analytical tool whereby "high gain" second order differential equations are replaced with first order equations could be employed in many more instances than it has. However, by these means establishing the simplest possible composite solution which could be useful requires a great deal of time consuming experimentation. To overcome this problem it was decided to revert to the more usual antiskid analytical techniques and formulate a simplified analysis procedure. For the following simplified mathematical description all of the elements previously described separately, except for the wheel speed sensor and antiskid control circuit, are combined into a single simplified model representing a brake test dynamometer type setup. This simplified model is essentially the same as that which would be (and has been) used on an analog computer operating at "real time" with actual aircraft antiskid control circuit hardware. For this case such high frequency

second order equations as those for axle torsional displacement, tire tread displacement relative to the wheel, brake disc axial displacement and hydraulic valve spool displacement are not included. There is also a significant difference in the treatment of the tire-to-ground friction force for this model in that the friction coefficient versus footprint relative slip velocity function has been modified to have a relatively moderate slope through zero as shown in Figure 24. This modification is required to represent the elastic displacement of the tire tread relative to the wheel which is not being computed. The same format as used in Appendix A is used.

#### A. MATHEMATICAL DESCRIPTION

Each major element of the system is described separately as in Appendix A even though all elements are combined into a single system.

##### Hydraulic System

The hydraulic system supplies brake actuation pressure,  $P_B$ , and consists of a pressure source, the antiskid valve flow control spool, the brake actuation cylinder and interconnecting piping as shown in Figure 21. As described in Appendix A hydraulic flow is established by the product of a pressure function  $\phi$  and a flow coefficient function  $A_{cv}$  as follows.

$$(1) \quad \phi(X, Y) = \text{SIGN}(X - Y) \sqrt{|X - Y|}$$

$$(2) \quad A_{cv}(X) = A_{cvo} \quad \text{IF } X \geq S_{cvo}$$

$$= \text{MAX} \{ A_{cvL}, X(A_{cvo}/S_{cvo}) \} \quad \text{IF } X < S_{cvo}$$

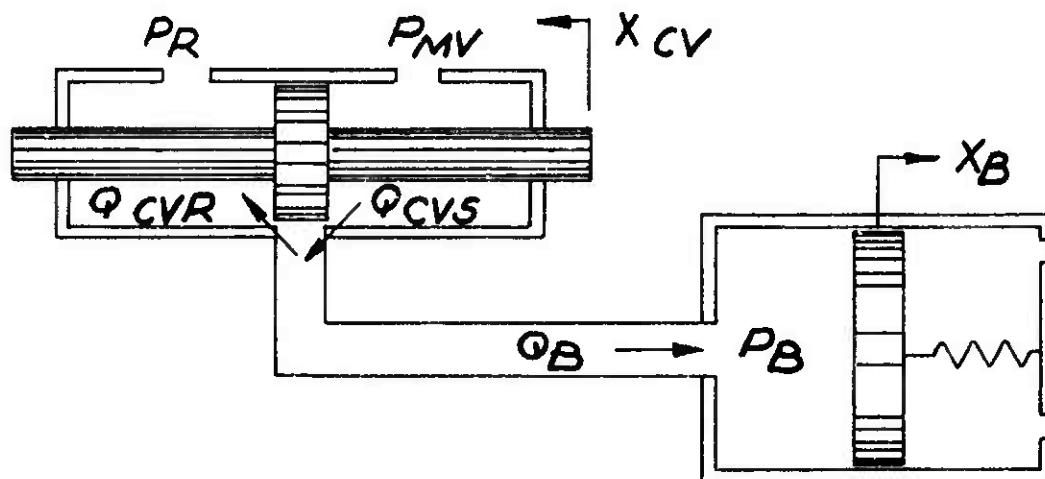


Figure 21 Simplified Brake Hydraulic System Schematic

The pressure source is the pilot's metering valve output having pressure  $P_{MV}$ . As the pilot applies the brakes, the metering valve output pressure increases from reservoir pressure,  $P_R$ , to the command pressure value,  $P_{CP}$ , as a function of time in accordance with equation (3).

$$(3) \quad P_{MV} = T(P_{CP} - P_R) / T_{CP} + P_R \quad \text{IF } 0 \leq T \leq T_{CP} \\ = P_{CP} \quad \text{IF } T > T_{CP}$$

The antiskid valve flow control spool position,  $X_{CV}$ , establishes the brake application or brake release flow coefficients,  $A_{CVS}$  and  $A_{CVR}$  respectively, according to equations (4) and (5).

$$(4) \quad A_{CVS} = A_{CVS0} \quad \text{IF } (X_{CV} - S_{CL}) \geq S_{CV0} \\ = \max\{A_{CVL}, (X_{CV} - S_{CL})(A_{CVS0}/S_{CV0})\} \quad \text{IF } (X_{CV} - S_{CL}) < S_{CV0}$$

$$(5) \quad A_{CVR} = A_{CVR0} \quad \text{IF } (-S_{CL} - X_{CV}) \geq S_{CV0} \\ = \max\{A_{CVL}, (-S_{CL} - X_{CV})(A_{CVR0}/S_{CV0})\} \quad \text{IF } (-S_{CL} - X_{CV}) < S_{CV0}$$

The flow thru the antiskid valve flow control spool is then given by equations (6), (7) and (8).

$$(6) \quad Q_{CVS} = A_{CVS} \phi < P_{MV}, P_B >$$

$$(7) \quad Q_{CVR} = A_{CVR} \phi < P_B, P_R >$$

$$(8) \quad Q_B = Q_{CVS} - Q_{CVR}$$

If the brake actuation piston area per line is  $A_{BPS}$ , then the piston velocity,  $\dot{X}_B$ , is given by equation (9).

$$(9) \quad \dot{X}_B = Q_B / A_{BPS}$$

The brake actuation pressure is established from the brake pressure volume characteristic as described by equation (10).

$$(10) \quad P_B = \begin{cases} C_{BPL} X_B + P_{B0} & \text{IF } X_B \leq 0 \\ C_{BPU} X_B + P_{B0} & \text{IF } X_B > 0 \end{cases}$$

The value for piston displacement  $X_B$  is established by integrating  $\dot{X}_B$  from equation (9).

### Antiskid Control Valve

The antiskid control valve mathematical description consists of the equations establishing the flow control spool position,  $X_{CV}$ , as a function of the valve's characteristics and the input control signal,  $E_V$ , as follows:

$$(11) \quad X_{SC} = C_{SCVR} E_V$$

$$(12) \quad R_{SC} = \begin{cases} 1.0 & \text{IF } X_{SC} \leq X_{SCM} \\ (X_{SCR} - X_{SC}) / (X_{SCR} - X_{SCM}) & \text{IF } X_{SCM} < X_{SC} < X_{SCR} \\ 0.0 & \text{IF } X_{SC} \geq X_{SCR} \end{cases}$$

$$(13) \quad P_{SC} = R_{SC} (P_{MV} - P_R) + P_R + P_{CVB}$$

$$(14) \quad V_{CV} = G_{CV} (P_{SC} - P_B)$$

$$(15) \quad \dot{X}_{CV} = \begin{cases} \min \{ 0, V_{CV} \} & \text{IF } S_{CVA} \leq X_{CV} \\ V_{CV} & \text{IF } S_{CVR} < X_{CV} < S_{CVA} \\ \max \{ 0, V_{CV} \} & \text{IF } X_{CV} \leq S_{CVR} \end{cases}$$

### Brake Torque System

Brake torque is the product of the number of friction surfaces, the normal force between friction surfaces, the friction coefficient between friction surfaces and the normal force radius. The normal force is the product of the effective actuation pressure,  $P_E$ , and the brake piston area,  $A_{BP}$ . The effective pressure is determined from equation (16) as follows:

$$(16) \quad P_E = \max \{ 0, P_B - P_{BDC} - P_{BF} \text{ SIGN}(\dot{X}_B) \}$$

The brake torque,  $T_{BT}$ , is determined by equations (17), (18) and (19) where the friction coefficient is defined as a function of the relative velocity between the friction surfaces,  $V_B$ .  $W_T$  is the wheel angular velocity.

$$(17) \quad V_B = R_{BT} W_T$$

$$(18) \quad \begin{aligned} \mu_B &= \mu_{B1} + \mu_{B2} \text{EXP} < -\alpha_B V_B > & \text{IF } V_B > 0 \\ &= 0 & \text{IF } V_B = 0 \\ &= -\mu_{B1} - \mu_{B2} \text{EXP} < \alpha_B V_B > & \text{IF } V_B < 0 \end{aligned}$$

$$(19) \quad T_{BT} = A_{BP} R_{BT} 2 N_R (P_E) (\mu_B)$$

In the above  $N_R$  is the number of rotors. Since each rotor has a friction surface on each side, the number of friction surfaces is  $2 N_R$ .

#### Wheel and Tire System

Figure 22 shows the wheel and tire system representing a brake test dynamometer setup. The horizontal force,  $F_G$ , on the wheel (from the axle) is given by equation (20).

$$(20) \quad F_G = -C_G \dot{X}_G - D_G \ddot{X}_G$$

If  $T_{BT}$  is the brake torque and  $F_{BT}$  is the friction force at the tire-flywheel interface, the tire and wheel equations of motion for horizontal translation and rotation are:

$$(21) \quad W_G \ddot{X}_G = F_G - F_{BT}$$

$$(22) \quad W_{IT} \dot{W}_T = F_{BT} R_{TO} - T_{BT}$$

The relative velocity between tire tread and the flywheel,  $V_R$ , is given by equation (23).

$$(23) \quad V_R = V_F + \dot{X}_G - R_R W_T$$

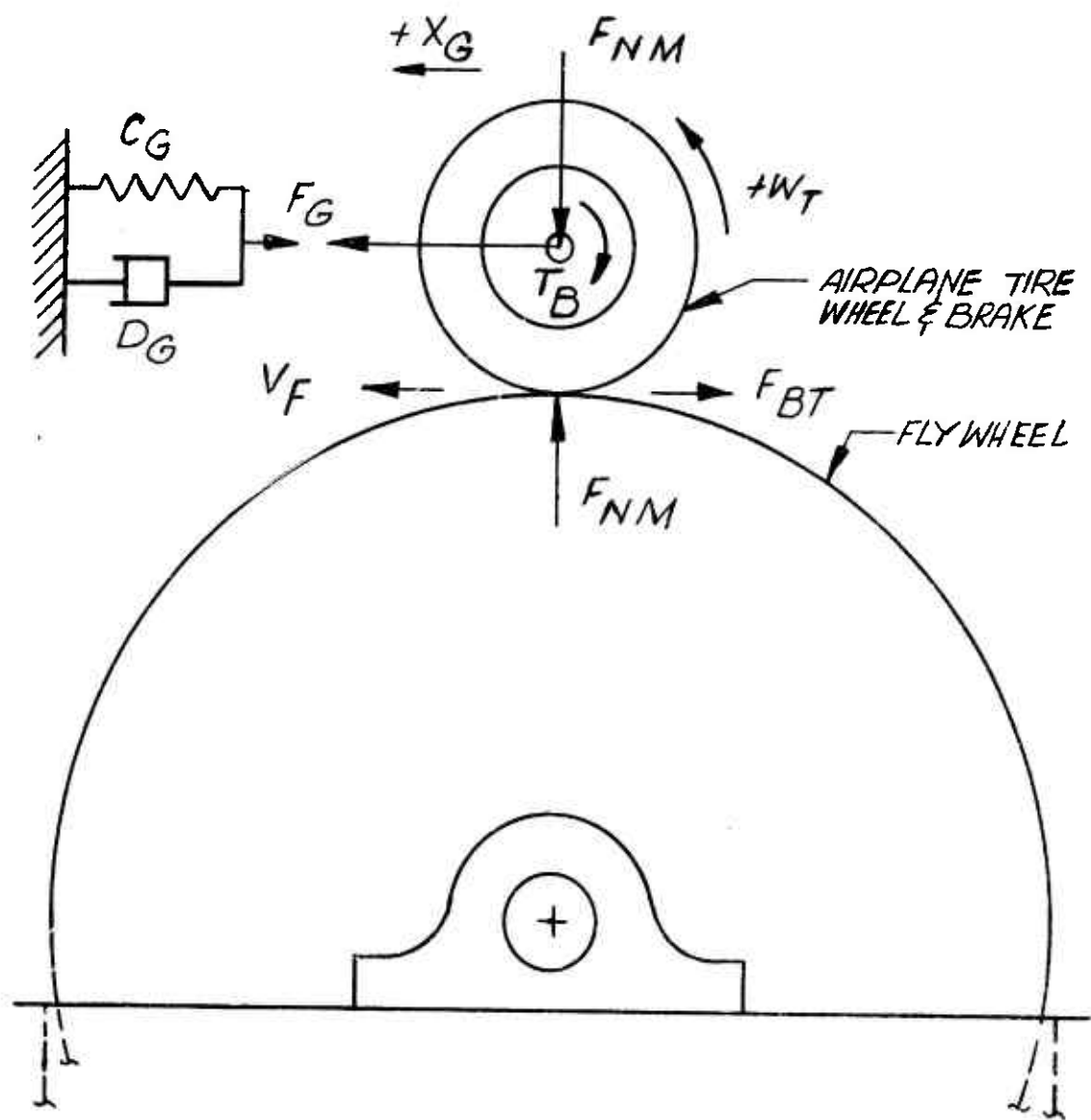


Figure 22 Dynamometer Flywheel Setup

The braking force,  $F_{BT}$ , is established by the tire vertical force,  $F_{Nm}$ , and the tire-to-ground friction coefficient,  $\mu_T$ , by equations (24) and (25).

$$(24) \quad F_{BT} = F_{Nm} \mu_T$$

$$(25) \quad \begin{aligned} \mu_T &= \mu_{T1} + (\mu_{T2} - E_T V_F) \text{EXP} \langle -\alpha (V_R - V_{R0}) \rangle \quad \text{IF } V_R > V_{R0} \\ &= (V_R / V_{R0}) (\mu_{T1} + \mu_{T2} - E_T V_F) \quad \text{IF } -V_{R0} \leq V_R \leq V_{R0} \\ &= -\mu_{T1} - (\mu_{T2} - E_T V_F) \text{EXP} \langle \alpha (V_R + V_{R0}) \rangle \quad \text{IF } V_R < -V_{R0} \end{aligned}$$

The flywheel velocity,  $V_F$ , and flywheel peripheral distance,  $X_F$ , are computed by integrating equations (26) and (27).

$$(26) \quad \dot{V}_F = -F_{BT} / W_F$$

$$(27) \quad \dot{X}_F = V_F / 12$$

Figure 23 shows the Simplified Antiskid Analysis System Equation Flow Diagram.



## B. PARAMETER EVALUATION

The parameters applicable to the simplified antiskid analysis procedure are listed in Table 2. The values for each parameter are that for test condition No. 29 as established by the procedures described in Appendix A for the applicable case except as follows:

The antiskid control valve gain,  $G_{cv}$ , is set at a value such that if the valve spool had constant velocity it would move through its entire travel in 0.010 seconds which is the step input response time of the valve with 1500 psi differential pressure. Therefore,

For .070 inches spool travel in .01 seconds,

$$\dot{X}_{cv} = .07/.01 = 7 \text{ inches per second.}$$

$$G_{cv} = \dot{X}_{cv} / \Delta P = 7/1500 = 0.0047 \text{ in}^3/\text{sec lbf}$$

The positive slope portion of the tire-to-ground friction coefficient function was established from information presented in Reference 1, for a 17.00-20 tire which is about the same size as the 47 X 18 tire used during testing:

From Figure 54 (page 38) of Reference 1:

$$F_x = r K_x S_i \text{ for an axle velocity of approximately } 100 \text{ ft/sec.}$$

Where  $F_x$  = Braking force  
 $r$  = Tire free radius  
 $K_x$  = Tire fore and aft spring rate  
 $S_i$  = slip ratio

$$\text{By definition } S_i = \frac{\text{slip velocity}}{\text{axle velocity}}$$

For a 47 X 18 tire with 13,000 pounds radial load and 150 psi inflation pressure,  $K_x = 6830$  pounds/inch (see Reference 1, page 22, equation 47).

For a 47 X 18 tire  $r = 23.35$  inches

Since  $F_x = \mu F_z = r K_x S_1$  ,

$$\mu = \frac{r K_x S_1}{F_z} = \frac{(23.35)(6830) S_1}{13000}$$

$$\text{OR } \mu = 12.22 S_1 = 12.22 \frac{\text{SLIP VELOCITY}}{\text{AXLE VELOCITY}}$$

From Figure A40 in Appendix A  $\mu_{\text{MAX}} = .496$  for 2400 in/sec aircraft velocity. Use this value even though axle velocity for data from Reference 1 is only 1200 inches/sec.

Let  $V_{RO} =$  slip velocity for  $\mu_{\text{MAX}}$  : Therefore,

$$V_{RO} = \text{Axle Velocity} \left( \frac{\mu_{\text{MAX}}}{12.22} \right)$$

$$V_{RO} = 1200 \left( \frac{.496}{12.22} \right)$$

$$V_{RO} = 48.7 \text{ inches/sec}$$

Figure 24 shows the resultant tire friction coefficient versus slip velocity function.

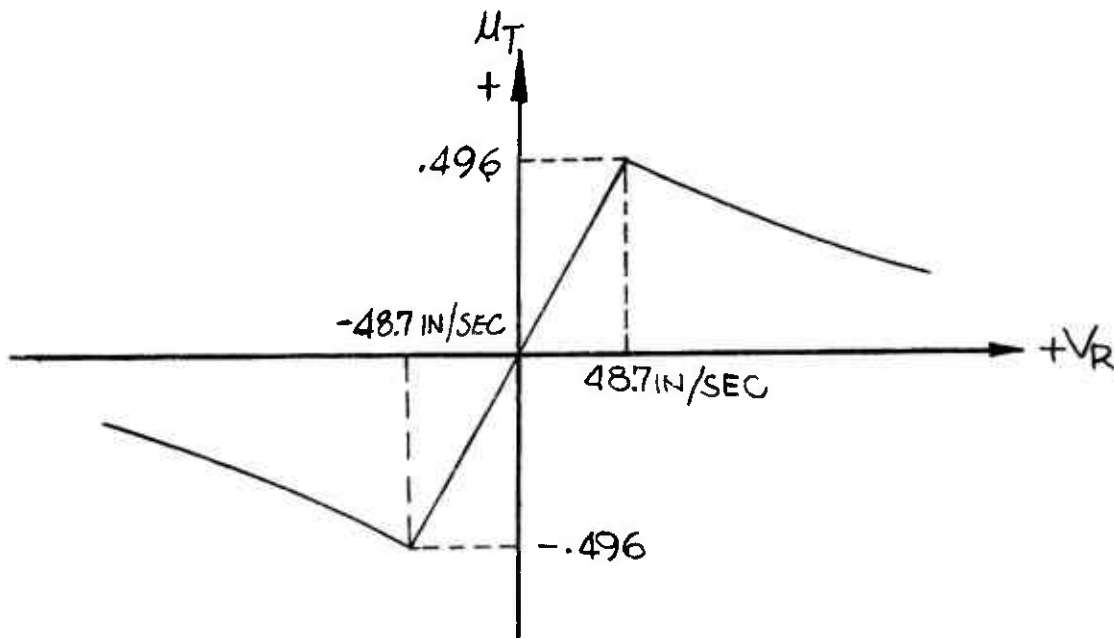


Figure 24 Tire-To-Ground Friction Coefficient Versus Relative Velocity

Table 2 Simplified Antiskid Analysis System Parameters (Sheet 1 of 4)

SYMBOL	TYPE	VALUE	UNITS	DESCRIPTION
$\alpha$	C	$0.25 \times 10^{-2}$	SEC/INCH	Tire Friction Parameter
$\alpha_B$	C	$0.30 \times 10^{-1}$	SEC/INCH	Brake Lining Friction Parameter
$A_{BP}$	C	$0.133 \times 10^2$	INCHES <sup>2</sup>	Piston Area per Brake
$A_{BPS}$	C	$0.665 \times 10$	INCHES <sup>2</sup>	Piston Area per Control Valve
$A_{CV(x)}$	F			Control Valve Flow Coefficient Function
$A_{CVL}$	C	0.0	IN <sup>4</sup> /SEC LBF <sup>1/2</sup>	Control Valve Leakage Flow Coefficient
$A_{CVR}$	V		IN <sup>4</sup> /SEC LBF <sup>1/2</sup>	Control Valve Return Flow Coefficient
$A_{CVS}$	V		IN <sup>4</sup> /SEC LBF <sup>1/2</sup>	Control Valve Supply Flow Coefficient
$A_{CVRO}$	C	$0.72 \times 10$	IN <sup>4</sup> /SEC LBF <sup>1/2</sup>	Control Valve Return Full Flow Coefficient
$A_{CVSO}$	C	0.34	IN <sup>4</sup> /SEC LBF <sup>1/2</sup>	Control Valve Supply Full Flow Coefficient
$C_{BPL}$	C	$0.665 \times 10^3$	PSI/INCH	Control Valve Supply Full Flow Coefficient
$C_{BPU}$	C	$0.4725 \times 10^5$	PSI/INCH	Brake P-V Slope (Discs not in contact)
$C_G$	C	$0.353 \times 10^5$	LBF/INCH	Brake P-V Slope (Discs in contact)
$C_{SCVR}$	C	$0.12 \times 10$	INCHES/VOLT	Fore and Aft Spring Rate at Axle
$D_G$	C	$0.234 \times 10^2$	LBF/SEC/INCH	Control Valve Input Coefficient
$E_V$	C		VOLTS	Fore and Aft Damping Coefficient at Axle
$E_T$	V(I)			Antiskid Valve Volts
$F_G$	C	$0.65 \times 10^{-4}$	DIMENSIONLESS	Tire Friction Velocity Correction Coefficient
$F_{BT}$	V		POUNDS	Fore and Aft Force at Axle
$F_{NM}$	V		POUNDS	Friction Force Between Tire and Ground
$G_{CV}$	C	$.130 \times 10^5$	POUNDS	Vertical Force on Tire from Ground
$d(x, y)$	C	$.47 \times 10^{-2}$	IN <sup>3</sup> /SEC LBF	Control Valve Gain
$P_B$	F			Hydraulic Pressure Function
$P_{B0}$	V	$.180 \times 10^3$	PSI	Brake Cylinder Pressure
$P_{BR}$	C	$.130 \times 10^3$	PSI	Brake Cylinder Pressure at Time Zero
$P_{BDC}$	C	$.200 \times 10^3$	PSI	Brake Return Spring Preload Pressure
$P_E$	C		PSI	Brake Disc Contact Pressure
$P_{MV}$	V		PSI	Effective Pressure for Brake Torque
$P_{CP}$	C	$0.160 \times 10^4$	PSI	Metering Valve Output Pressure
				Pilots Command Brake Pressure

Table 2 Simplified Antiskid Analysis System Parameters (Sheet 2 of 4)

SYMBOL	TYPE	VALUE	UNITS	DESCRIPTION
$P_{CVB}$	C	$0.25 \times 10^2$	PSI	Control Valve Bias Pressure
$P_{FB}$	C	$0.219 \times 10^2$	PSI	Brake Piston Friction Hysteresis
$P_{SC}$	V		PSI	Antiskid Control Pressure
$P_R$	C	0.0	PSI	Hydraulic System Reservoir Pressure
$Q_B$	V		$IN^3/SEC$	Hydraulic Flow into the Brake
$Q_{CVR}$	V		$IN^3/SEC$	Hydraulic Flow thru Antiskid Valve to Return
$Q_{CVS}$	V		$IN^3/SEC$	Hydraulic Flow thru Antiskid Valve from Supply
$R_{BT}$	C	$0.625 \times 10$	INCHES	Brake Piston Torque Producing Radius
$R_R$	C	$0.228 \times 10^2$	INCHES	Tire Effective Rolling Radius
$R_{SC}$	V		DIMENSIONLESS	Control Valve Regulating Function
$R_{TO}$	C	$0.2173 \times 10^2$	INCHES	Height of Axle Above Ground
$S_{CL}$	C	$0.50 \times 10^{-2}$	INCHES	Control Valve Overlap
$S_{CV0}$	C	$0.30 \times 10^{-1}$	INCHES	Control Valve Full Open Spool Travel
$S_{CVA}$	C	$0.35 \times 10^{-1}$	INCHES	Control Valve Max Application Travel
$S_{CVR}$	C	$-0.35 \times 10^{-1}$	INCHES	Control Valve Max Release Travel
$T_{BT}$	V		INCH LBF	Brake Torque
$T$	V(I)		SECONDS	Time
$T_{CP}$	C	0.10	SECONDS	Time to Reach Max Command Pressure
$M_B$	V		DIMENSIONLESS	Brake Lining Friction Coefficient
$M_{B1}$	C	0.15	DIMENSIONLESS	Brake Lining Friction Parameter
$M_{B2}$	C	0.10	DIMENSIONLESS	Brake Lining Friction Parameter
$M_T$	V		DIMENSIONLESS	Tire-to-Ground Friction Coefficient
$M_{T1}$	C	0.20	DIMENSIONLESS	Tire Friction Parameter
$M_{T2}$	C	0.45	DIMENSIONLESS	Tire Friction Parameter
$V_B$	V		INCHES/SEC	Brake Lining Velocity
$V_{CV}$	V		INCHES/SEC	Control Valve Spool Velocity
$V_F$	V		INCHES/SEC	Flywheel Peripheral Velocity
$V_{F0}$	C	$.240 \times 10^4$	INCHES/SEC	Flywheel Peripheral Velocity at Time Zero
$\dot{V}_F$	V		INCHES/SEC <sup>2</sup>	Flywheel Peripheral Acceleration

Table 2 Simplified Antiskid Analysis System Parameters

(Sheet 3 of 4)

SYMBOL	TYPE	VALUE	UNITS	DESCRIPTION
$\dot{V}_F$	c	0.0	$\text{INCHES/SEC}^2$	Flywheel Peripheral Acceleration at Time Zero
$\dot{V}_R$	v		$\text{INCHES/SEC}$	Relative Velocity Between Tire Footprint & Ground
$\dot{V}_R$	c	$0.487 \times 10^2$	$\text{INCHES/SEC}$	Tire Friction vs Velocity Parameter
$W_G$	c	$0.155 \times 10$	$\text{LBF SEC}^2/\text{IN}$	Wheel, Tire, Brake & Supporting Structure Mass
$W_{IT}$	c	$0.163 \times 10^3$	$\text{LBF IN SEC}^2$	Tire, Wheel & Brake Rotor Moment of Inertia
$W_T$	v(o)		$\text{RAD/SEC}$	Tire & Wheel Angular Velocity
$W_{TO}$	c	$0.1053 \times 10^3$	$\text{RAD/SEC}$	Tire & Wheel Angular Velocity at Time Zero
$\dot{W}_T$	v		$\text{RAD/SEC}^2$	Tire & Wheel Angular Acceleration
$\dot{W}_{TO}$	c	0.0	$\text{RAD/SEC}^2$	Tire & Wheel Angular Acceleration at Time Zero
$X_B$	v		$\text{INCHES}$	Brake Piston Position
$X_{B0}$	c	0.0	$\text{INCHES}$	Brake Piston Position at Time Zero
$\dot{X}_B$	v		$\text{INCHES/SEC}$	Brake Piston Velocity
$\dot{X}_{B0}$	c	0.0	$\text{INCHES/SEC}$	Brake Piston Velocity at Time Zero
$X_{BR}$	c	$0.275 \times 10^{-2}$	$\text{INCHES}$	Brake Piston Position for Full Release
$X_{BDC}$	c	0.1078	$\text{INCHES}$	Brake Piston Position at Disc Contact
$\dot{X}_{CV}$	v		$\text{INCHES}$	Control Valve Spool Position
$\dot{X}_{CV0}$	c	$+35 \times 10^{-1}$	$\text{INCHES}$	Control Valve Spool Position at Time Zero
$\dot{X}_{CV}$	v		$\text{INCHES/SEC}$	Control Valve Spool Velocity
$\dot{X}_{CV0}$	c	0.0	$\text{INCHES/SEC}$	Control Valve Spool Velocity at Time Zero
$X_F$	v(o)		$\text{FEET}$	Flywheel Peripheral Distance
$X_{SC}$	v		$\text{INCHES}$	Control Valve Pressure Regulation Parameter
$X_{SCM}$	c		$\text{INCHES}$	Value of $X_{SC}$ for Maximum Regulation
$X_{SCR}$	c		$\text{INCHES}$	Value of $X_{SC}$ for Zero Regulation
$X_G$	v		$\text{INCHES}$	Axle Horizontal Position
$X_{G0}$	c	0.0	$\text{INCHES}$	Axle Horizontal Position at Time Zero
$\dot{X}_G$	v		$\text{IN/SEC}$	Axle Horizontal Velocity
$\dot{X}_{G0}$	c	0.0	$\text{IN/SEC}$	Axle Horizontal Velocity at Time Zero
$\ddot{X}_G$	v		$\text{IN/SEC}^2$	Axle Horizontal Acceleration
$\ddot{X}_{G0}$	c	0.0	$\text{IN/SEC}^2$	Axle Horizontal Acceleration at Time Zero

Table 2 Simplified Antiskid Analysis System Parameters (Sheet 4 of 4)

SYMBOL	TYPE	VALUE	UNITS	DESCRIPTION
WF	C	26.29	$\text{LBF-SEC}^2/\text{IN}$	Flywheel Mass
NR	C	7.0	DIMENSIONLESS	Number of Brake Rotors
V <sub>MIN</sub>	C	160.0	INCHES/SEC	Flywheel Peripheral Velocity for Terminating Problem
$\dot{X}_{F0}$	C	200.0	FEET/SEC	Flywheel Peripheral Velocity at Time Zero
$\ddot{X}_F$	V		FEET/SEC	Flywheel Peripheral Velocity
X <sub>F0</sub>	C	0.0	FEET	Flywheel Peripheral Distance at Time Zero

in addition to formulating the simplified analysis procedure, some minor corrections have been made to the On-Off and modulated antiskid control circuit mathematical models as shown in Section 6 of Appendix A. For the On-Off circuit equation (N2) was not previously separately identified. Since Diode D2 is in the current path it is necessary to consider current AD2 separately so that its value can be limited to positive values only.

For the modulated antiskid circuit a minor modification of the computation sequence was required to place the proper limits on current  $AEQ2$ . For circuit conditions 3, 4, 7, 8, 11 and 12 where the valve drive amplifier is operating in the amplification mode, an upper current limit is necessary to represent the saturated condition. With the revised computation sequence, the value of  $AEQ2$ , once established and properly limited, is used for computing VB and  $Ac4$ . Previously, the equation for  $AEQ2$  was substituted into the equations for VB and  $Ac4$  so that all three parameters were computed from the instantaneous capacitor voltages.

## TEST DATA CORRELATION

Test data correlation was accomplished by comparing the analytical predictions for test condition number 29 with the test results. Figure 25 shows an expanded time scale oscillograph record of the first two seconds of the test for condition number 29. The variations of brake cylinder pressure, horizontal and vertical force on the axle, brake torque, braked wheel speed, and antiskid valve voltage are shown with respect to time. Two brake cylinder pressures, identified by " $\Delta$ " and " $\circ$ ", are shown because the F-111 brake has two independent sets of actuation cylinders and each set is controlled by separate metering valve and antiskid valve elements. Figure 26 shows the variation of the same or comparable quantities as predicted from the simplified analysis procedure for the first second of the stop. For the analytically generated information only one cylinder pressure is shown and the axle drag is shown in deflection units instead of force units. The information shown on Figure 26 was obtained from an electronic digital computer solution of simplified analysis procedure mathematical equations described in Section III combined with the Option 2 wheel speed sensor and modulated antiskid control circuit mathematical models from Sections 5 and 6 of Appendix A. The digital computer input data is shown on Table 3 and the computer program listing is in Appendix B.

A comparison between the test results shown on Figure 25 and the analytical predictions shown on Figure 26 reveals the following:

- ° The antiskid cyclic frequency is much higher for the Analytical prediction than was obtained in the test
- ° The brake pressure change rate in the test was much lower than analytically predicted
- ° The modulating antiskid circuit elements are not operating for the analytical prediction and were operating during the test.

It is believed that these differences are caused by both analytical and test difficulties. As was previously mentioned in Section II the brake pressure change rates were observed to be much lower than expected. Figure 27 shows part of an oscillograph record from an aircraft test performed by the Air

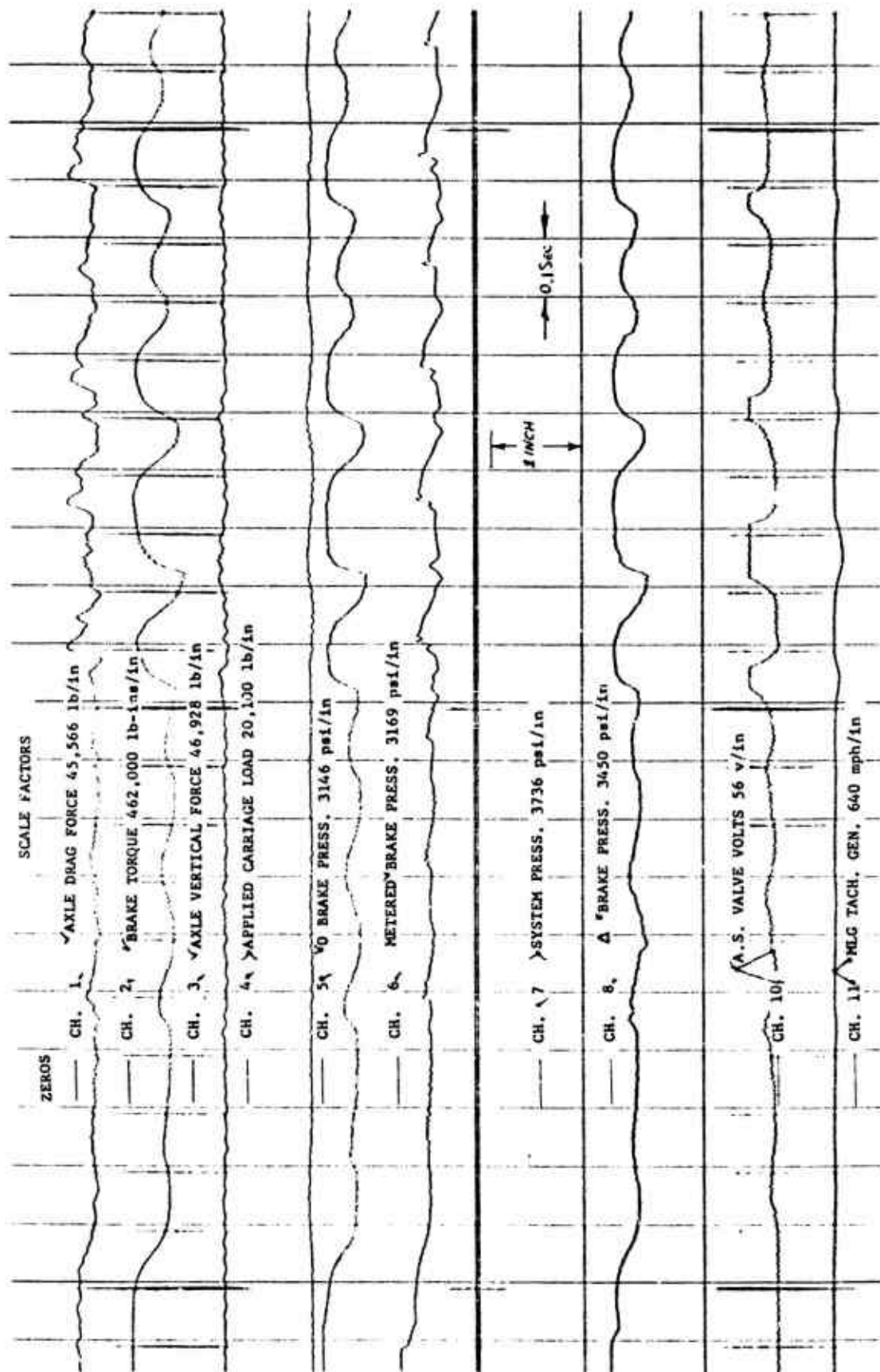


Figure 25 Expanded Time Scale Oscillograph Record of Test Condition No. 29

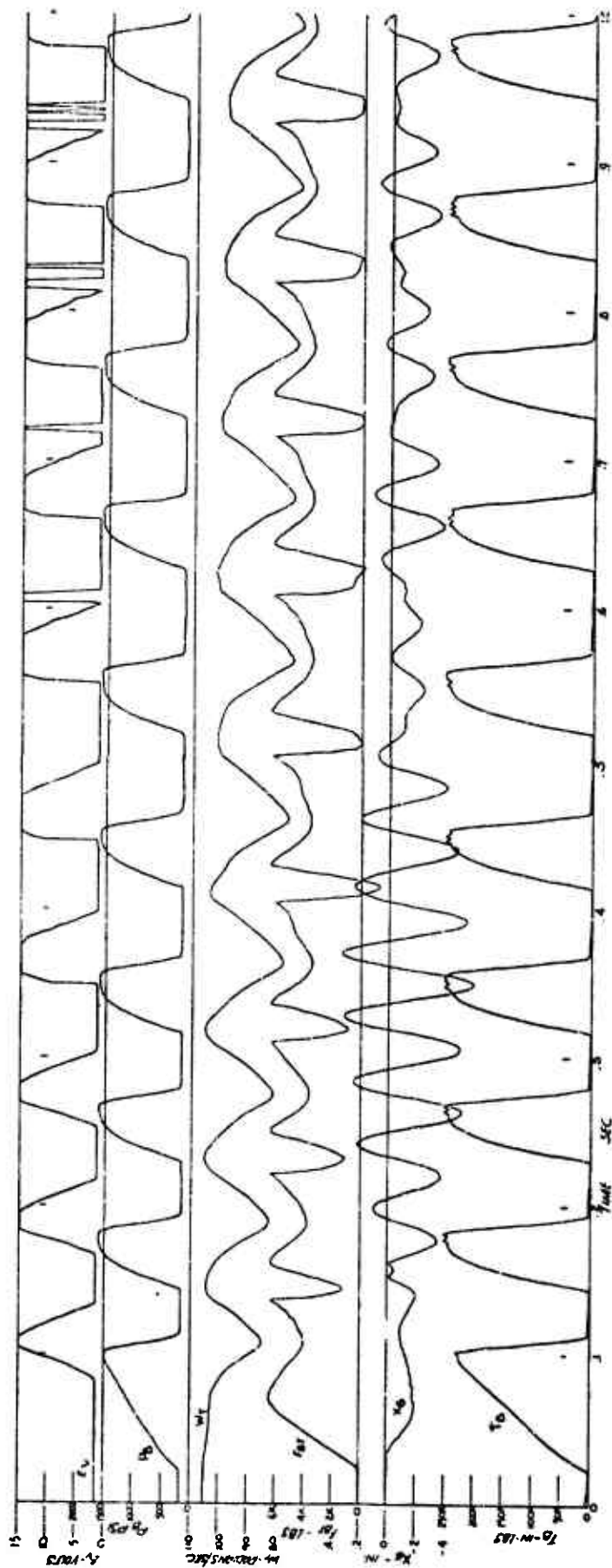


Figure 26 Analytically Predicted Antiskid Operation

Table 3 Computer Input Data for Test - Analysis Correlation

GENERAL DYNAMICS  
6600 PROCEDURE A1C

CONVAIR AEROSPACE DIVISION  
PROBLEM 46343-22

FORT WORTH OPERATION  
26/08/73 PAGE 0301

copy.

INPUT DATA

TIME BETWEEN STEPS= .2000E-03      SYSTEM RUN TIME = .1000E+01      CHECKOUT AbA MICROFILM OPT= 1

INTERNAL PRINT INTERVAL = .1000E-02      SYSTEM PRINT INTERVAL = .1000E-02

ACVRO = .7200E+00      ACVSO = .3400E+00      PCVB = .2500E+02      VMIN = .1600E+03      NR = 7

SIMPLIFIED BRAKE CONTROL

ALPHA= .2500E-02      ALPHB= .3000E-01      ABP= .1330E+02      ABPS= .6650E+01      ACR= 0.      ACVO= 0.

ACVL= 0.      CBPL= .6650E+03      CBPU= .4725E+05      CC= .3530E+05      CSCVR= .1200E+01      DC= .2340E+02

ET= .6500E-04      FNME= .1300E+05      GOV= .4700E-02      P80= .1800E+03      PCP= .1600E+04      PF8= .2190E+02

FR= 0.      R8T= .6250E+01      RR= .2240E+02      RTD= .2173E+02      SCL= .5000E-02      SCVO= .3000E-01

SCVA= .3500E-01      SCVR= -.3500E-01      TCP= .1000E+00      UB1= .1500E+00      UB2= .1000E+00      UT1= .2000E+00

UT2= .4500E+00      VF= .2400E+04      VR0= .4870E+02      WG= .1550E+01      WTO= .1053E+03      WIT= .1630E+03

XCV0= .3500E-01      XSCM= .3600E+01      XSCR= .1440E+02      X80= 0.      XCO= 0.      XDG0= 0.

XFD= 0.      XFO0= .2000E+03

OPTION 2

WHEEL SPEED SENSOR

CMCC= .1147E+00      ESN= 0.      ES= .1210E+02

CONTROLLER

CM= .2300E+00      C404= .2476E+04      C435= .1060E+00      C406= .6600E+02      C449= .1A63E-05      C450= .4740E-06

C407= .1510E+01      C446= .1825E-05      C447= .1000E-08      C448= .4650E-06      C458= -.1710E-04      C459= .5200E-04

C451= .1000E-04      C452= -.1570E-05      C456= .3400E-04      C457= .2700E-07      C527= .4650E-06      C528= .4740E-06

C460= .2700E-07      C461= .1325E-04      C462= -.8340E-04      C526= .1825E-05      C533= .1325E-04      C534= .5720E-04

C529= .1960E-05      C530= .1567E-05      C531= .3400E-04      C532= -.1710E-04      C569= .5200E-04      C570= .1400E-07

C535= .6240E-04      C566= .1400E-07      C567= -.1710E-04      C568= .1325E-04      C578= .4740E-06      C579= .1860E-05

C571= .8340E-04      C575= .1325E-05      C576= .1000E-08      C577= .4650E-06      C608= .3700E+05      C609= .3030E+07

C580= .1000E-03      C581= -.1570E-05      C605= .7250E-05      C606= .2920E+02      C614= .3600E+02      C615= .3520E+03

C604= .1610E-04      C611= .2220E+06      C612= .9010E+00      C613= .5190E-05      C620= .1000E-02      C621= .6000E-03

C616= .9200E+00      C617= .3760E-05      C618= .1000E-04      C619= .7700E-05      C802= .4290E-05      C803= .5362E+03

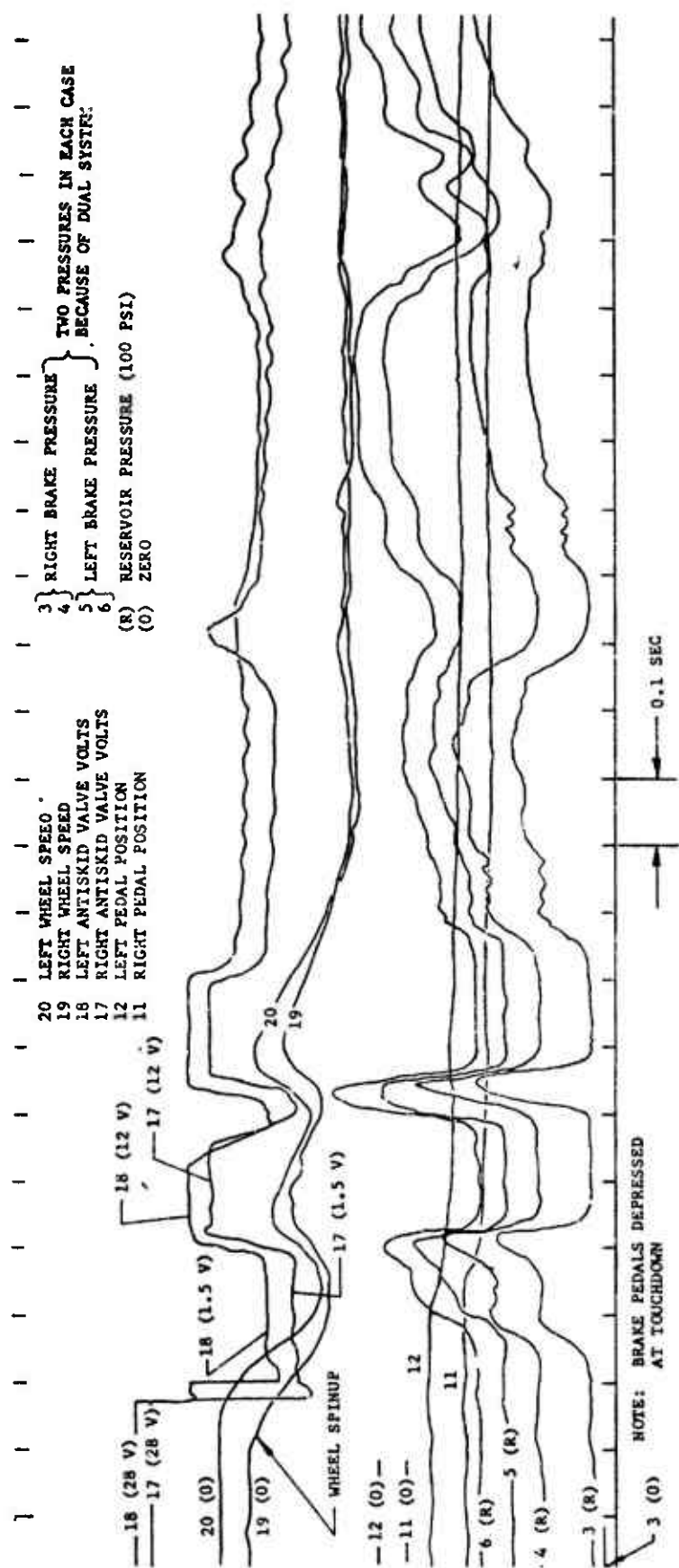
C622= .2460E-03      C623= .5930E-03      C800= .9940E+00      C801= .9167E+04      C808= .2228E+03      C809= .4530E-04

C804= .1091E-03      C805= .5520E-03      C806= .2166E+03      C807= -.2304E-03      VC2= 0.      VC3= 0.

C810= .1754E-03      C811= .9300E-01      C812= -.1501E-03      VC1= .1208E+02      VC4D= 0.      VC4E= .1510E+01

VC4= 0.      VC10= 0.      VC20= 0.      VC3C= 0.

70



F-111A No. 9  
EDWARDS AFB TEST

Figure 27 Antiskid Operation Recorded During Aircraft Landing

Force at Edwards Air Force Base, California. Many pertinent occurrences are shown on this record one of which is the brake pressure change rates. Records such as this were the basis for the pressure change rates expected during the testing phase of this program. It can be seen that for high rate valve voltage changes, the brake pressure changes on the airplane at about the same rate as was analytically predicted rather than as experienced during laboratory testing. To achieve agreement between analytical prediction and laboratory test result, the analytical parameters describing hydraulic flow restriction need to be modified to describe the laboratory test set-up. This could be done either by measuring the flow restriction in the laboratory (which should have been accomplished) or by trial and error experimentation with the analytical procedure. Neither has been accomplished. The differences in hydraulic flow restriction between the analytical prediction and the laboratory test set-up are primarily responsible for the different antiskid cyclic rates.

The failure of the analytical procedures to predict the operational characteristics of the antiskid control circuit modulating elements seems to be caused by two problems. The first is that for some undetermined reason, the computer program is not computing the same influence of capacitor C2 voltage upon antiskid valve voltage as a static check of the equations would indicate. The voltage of capacitor C2 controls the valve amplifier bias. Efforts toward finding the cause of this problem have not been successful. The second and most significant problem from an analytical viewpoint is that the "gain" for equations defining the current, AC2, which is charging capacitor C2, is so high that even with the .0002 second integration time step used, very large overshoots in capacitor C2 voltage occur. For this circumstance the valve amplifier bias is much too large which in turn causes the valve voltage to be too high. It is believed that the second difficulty is obscuring the cause of the first.

A related similar problem involving excessively high negative values of current AC4 was recognized prior to testing. Based on some experimental work accomplished by the Antiskid Engineering Department of the Goodyear Aerospace Corp., the value of R12, as shown on Figure A51 in Appendix A, was increased to limit the value of AC4 to an amount which could be analytically accommodated with a reasonable integration time step. This change in resistance value was previously mentioned in Section II. It is evident that a similar change could be implemented with regard to the excessively high positive values of current AC2.

The analytical difficulty experienced with the computation of antiskid control circuit parameter AC2, or any other parameter within the total system, should be recognized as typical of problems frequently encountered while attempting to mathematically analyze antiskid operation. For each instance a decision must be made to determine how the goals, toward which the analytical effort is directed, can be best accomplished either by implementing an appropriate simplifying mathematical technique so that a "brute force" solution is obtained, or by requiring some change be made to the equipment being evaluated. This decision is usually influenced by such factors as the analyst's experience, degree of prior equipment usage, cost of implementing the hardware change, consequence of enduring the problem, and the relative timing within the aircraft program when the problem is identified.

The specific analytical problem encountered during this program, wherein the equations for computing control circuit parameter AC2 have coefficients which necessitate an extremely small integration time step for obtaining a digital computer solution, could be resolved by any one of several ways. The practical significance of this analytical difficulty is that it indicates that the modulating circuit elements are susceptible to high frequency disturbances. If the problem is associated with circumstances where the absence of high frequency disturbance, such as brake squeal, can be assured, the best solution to the problem is to add a small resistance to current AC2 flow path so that its computation does not upset the whole analysis. For a case where the absence of high frequency disturbance cannot be assured it would be prudent to actually modify the antiskid circuit to reduce the "gain" on current AC2. For this second instance, the analytical difficulty is the definition of a real problem. It can be expected that similar situations regarding brake torque or hydraulic pressure computations may occur.

For the F-111 type Goodyear modulated antiskid circuit, the modulating elements susceptibility to high frequency disturbance is a very marginal situation in that actual occurrence of any indication of this effect during aircraft operation is extremely rare; however, such indication has occasionally occurred. When the digital computer solution was attempted with a 0.001 second integration time step, antiskid circuit operation was totally inhibited by capacitor C2 voltage overshoots. With the .0002 second time step computer solution, as shown on Figure 26, the valve signal "noise" during the last few cycles indicates that

the same inhibition is about to occur. If such analytical result had been available at the time this circuit was being formulated, it is very probable that some suitable corrective action would have been incorporated.

A significant aspect of the analytical procedures used for the test data correlation is type of computation equipment which was utilized. The digital computer solution using discrete time step integration will help identify some real incompatibilities within the brake system. However, the appearances of these incompatibilities may be exaggerated if the integration time step is not fairly small. The experience of this program is that, in general, the necessity for using an integration time step shorter than .0002 seconds to avoid computation difficulties indicates a situation where real incompatibility exists.

## SECTION V

### FLUIDIC CONTROLLED PNEUMATIC BRAKE ACTUATION SYSTEM DESIGN STUDY

Research studies have been conducted at Convair Aerospace and elsewhere to evaluate the application of fluidic control elements to aircraft wheel brake antiskid control systems. The results of the studies indicate that there is good potential for achieving more dependable braking system operation if a fluidic controlled brake actuation system is used instead of the more conventional hydraulic actuation system. The areas of primary improvement are reduced fire hazard and more constant antiskid control operation over a wide temperature range. For the case of modern carbon disc brakes which are operated at extremely high temperature, the fire hazard associated with hydraulic actuation is particularly significant. As an initial step in the evaluation of a fluidic controlled pneumatic braking system, antiskid brake control system components which are physically and functionally suitable for airplane usage have been designed. By having performed such detail design it is possible to establish the effects, if any, upon the other aircraft systems and components which might be required if the fluidic controlled pneumatic brake actuation system were installed. Such consideration is also necessary during the design of the components.

Figure 28 shows a block diagram of a fluidic controlled pneumatic braking system incorporating a modulated antiskid feature. For laboratory test evaluation the 3000 psi stored nitrogen pressure supply would be used. An aircraft installation might use either a stored nitrogen supply or a high pressure compressor combined with a smaller storage capacity.

Figure 29 shows a modulator type fluidic wheel speed sensor unit which is physically interchangeable with the F-111 D.C. electrical tachometer. The sensor consists of two-proximity sensors excited by a wheel driven slotted cup. The output of the sensors, a frequency signal, is the input to a frequency-to-analog converter module. The converter wheel speed signal is filtered and amplified to produce a linear analog output signal that is linearly proportional to wheel speed. The circuit diagram of the fluidic wheel speed sensor is shown on Figure 30.

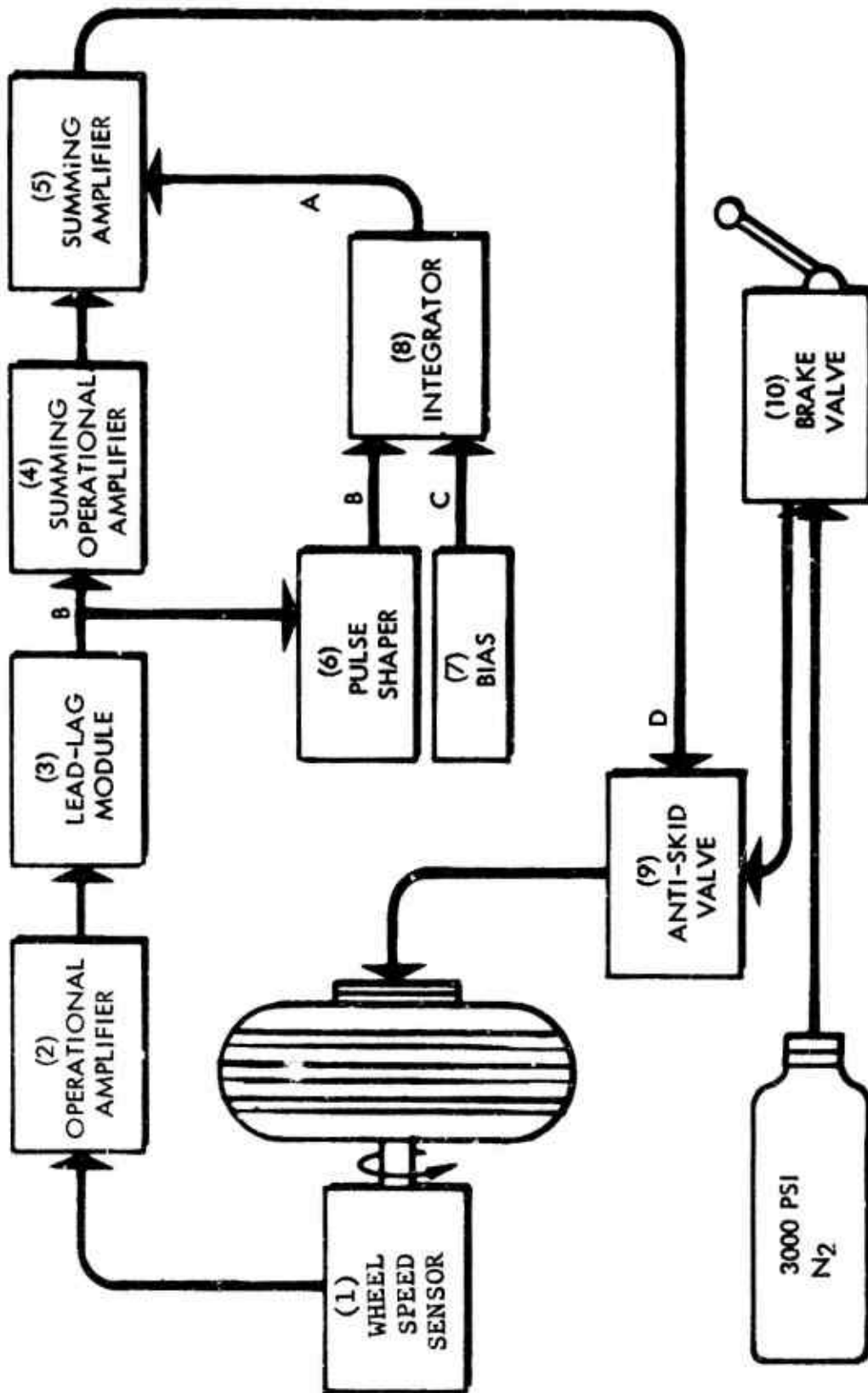


Figure 28 Fluidic Controlled Pneumatic Braking System

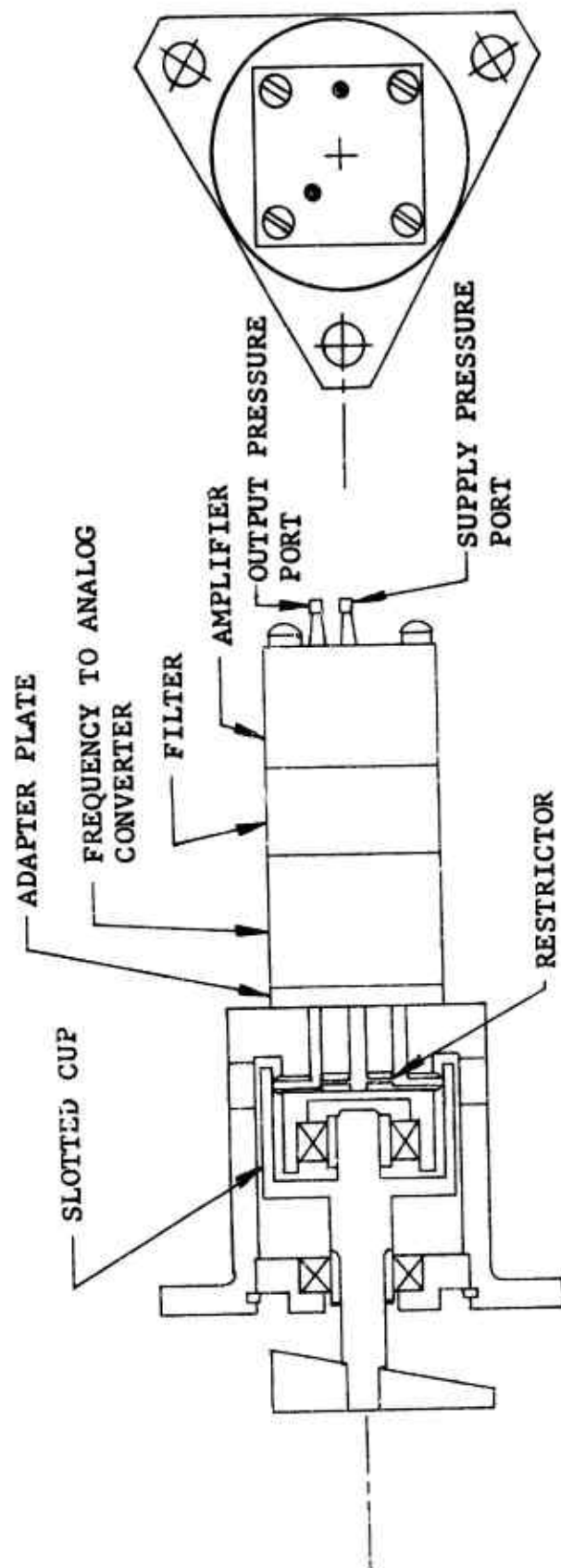


Figure 29 Fluidic Wheel Speed Sensor

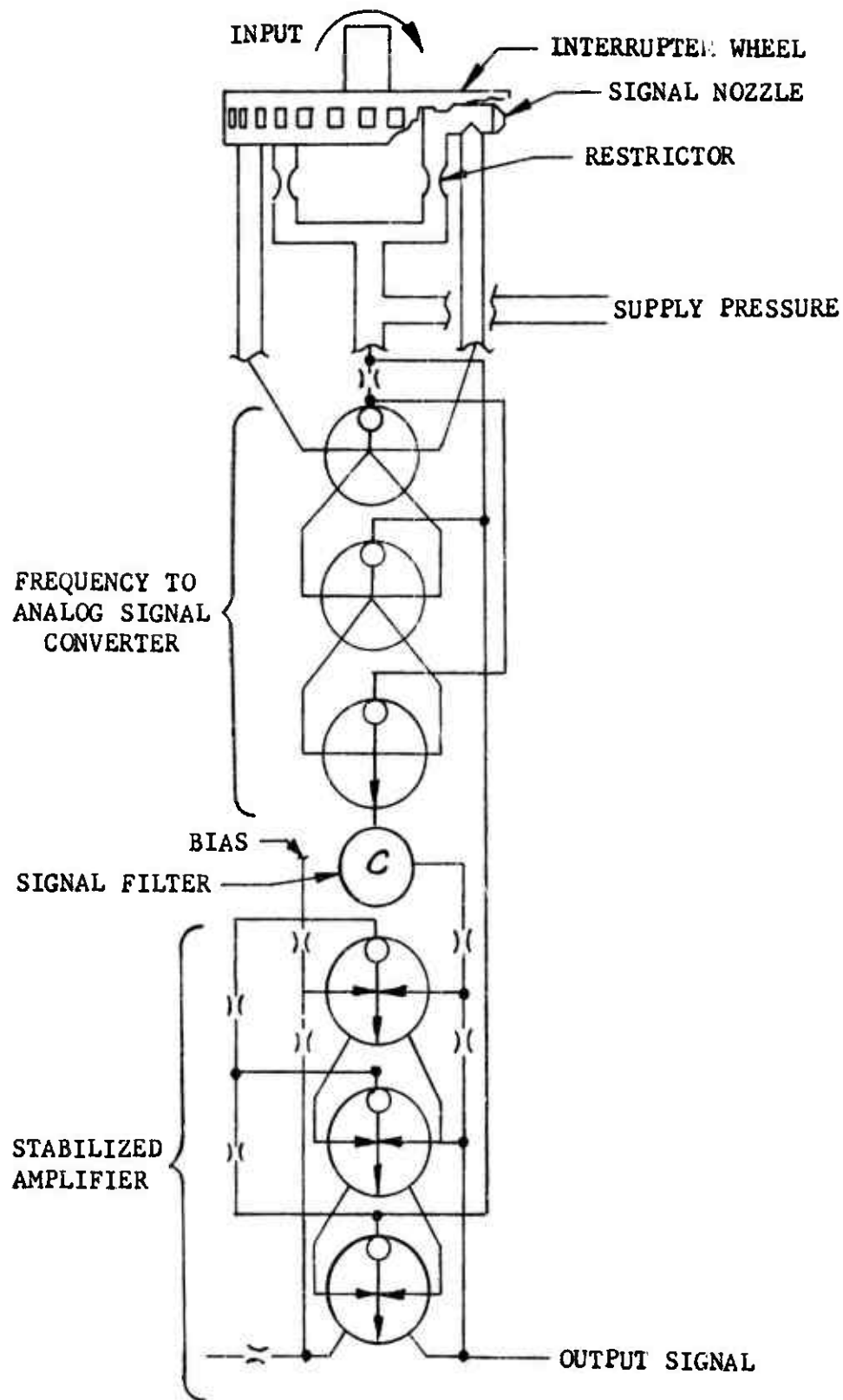
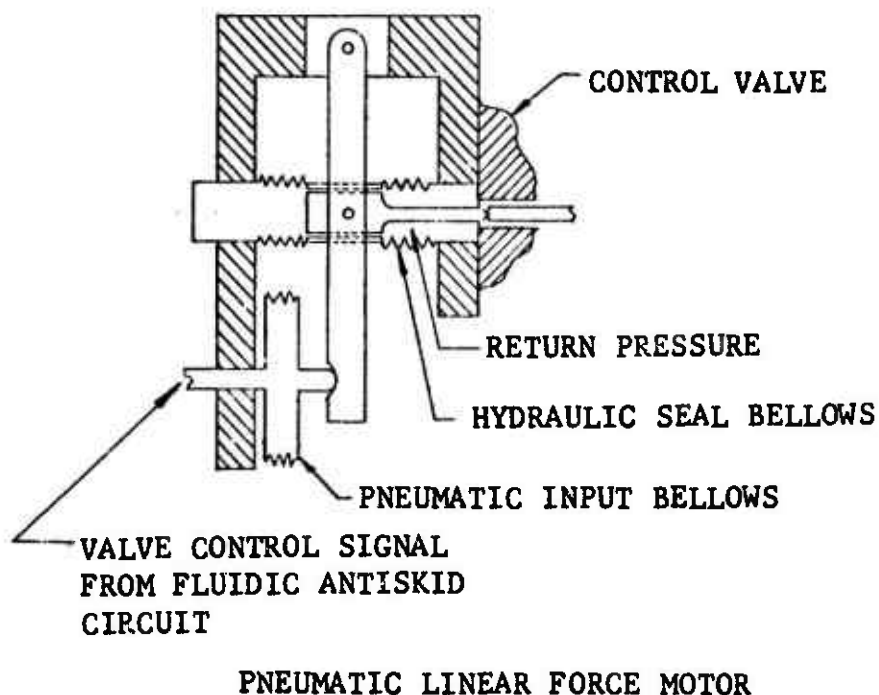
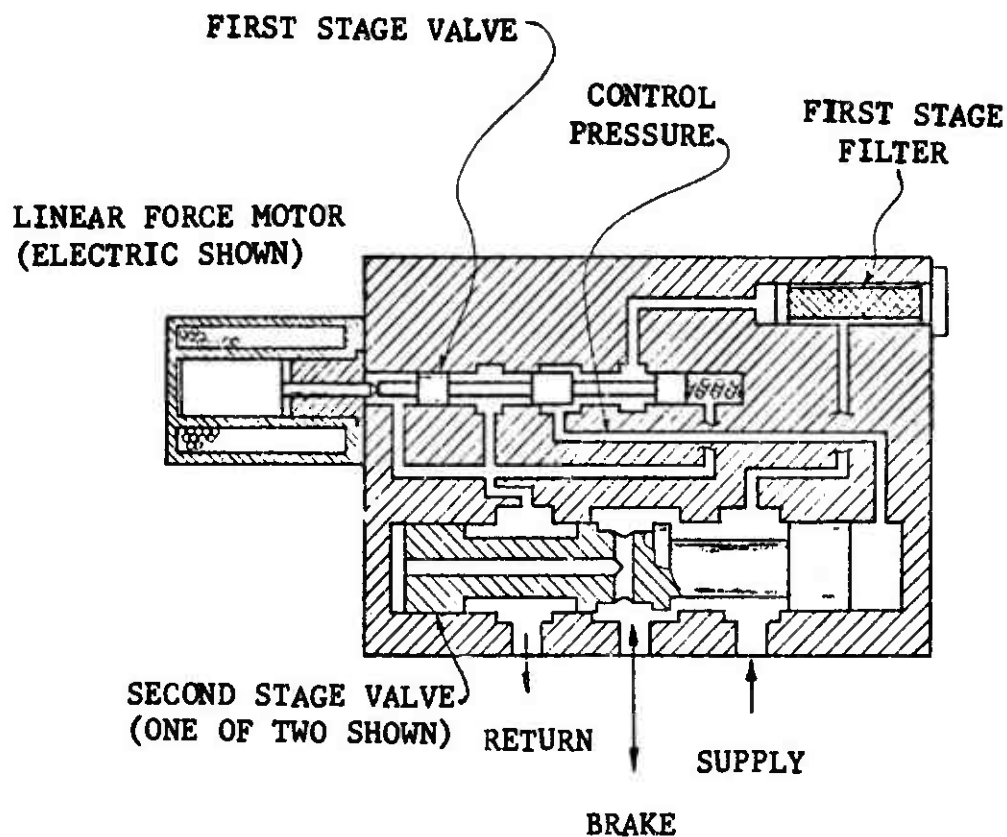


Figure 30 Fluidic Wheel Speed Sensor Schematic/Circuit Diagram

Figure 31 is a schematic showing how a F-111 hydraulic antiskid valve would be modified for pneumatic actuation by a pressure signal from a fluidic control circuit. To permit pneumatic actuation the electric linear force motor is replaced by a pressure bellows type linear force motor. For a limited evaluation test the hydraulic valve could be used for pneumatic pressure control if proper lubrication provisions are employed. For sustained pneumatic application the valve spool materials and perhaps a noninterflow poppet type second stage would be required; however, such a valve would have the same basic size, weight and cost as the hydraulic valve.

Since the fluidic control system will operate by relatively low level pneumatic pressure signals, it is necessary that all the control elements be physically located in close proximity to each other and the valve be located as close to the brake as is practical. The exact physical arrangement of the control circuit elements needs to be tailored to each application. The control circuit consists of items 2 thru 8 as shown on Figure 28. Item 2 is an operational amplifier providing gain and signal stability for the wheel speed sensor input to the lead-lag module. The lead-lag module, Item 3, is used for differentiating the wheel speed signal to produce a wheel acceleration signal. Item 4 is a variable gain operational amplifier for gain and impedance matching. A multi-input amplifier, identified as Item 5, is used for summing acceleration and bias circuit signals. The bias control circuit consists of Items 6, 7 and 8. The pulse shaper accepts an acceleration input signal and generates an output pulse of constant amplitude and adjustable time duration whenever the acceleration reaches a threshold value. The bias input consists of a linear restrictor. Integration is performed by a delayed (R-C) positive feedback circuit. These fluidic control circuit elements for one wheel can be packaged in a volume about two times as great as that for the equivalent electronic circuit elements - a space 3 x 3 x 4 inches. However, for many aircraft such as the F-111, these fluid elements could be installed inside the axle in a space not suitable for the electronic circuit elements or much of anything else.

The cost of a single set of fluidic components for laboratory evaluation is about four times as great as the production electric system; however, in comparable quantities the fluidic units would be approximately the same price and the electric units based on current catalog prices for fluidic elements. A major advantage of the fluidic system components is their ability to withstand intense vibration and high temperature. From this brief design study it has been concluded that fluidic control of a pneumatic brake actuation system can be practically accomplished.



PNEUMATIC LINEAR FORCE MOTOR

Figure 31 Adaption of an Electrical Antiskid Valve for Pneumatic Actuation

## REFERENCES

1. Smiley, Robert F. and Horne, Walter B. Mechanical Properties of Pneumatic Tires with Special Reference to Modern Aircraft Tires. NASA TR R-64.
2. Leland, T. J. W. and Taylor, G. R. Effects of Tread Wear on the Wet Runway Braking Effectiveness of Aircraft Tires. J. Aircraft Vol. 2 No. 2, March - April 1965.
3. Horne, W. B. and Leland, T. J. W. Influence of Tire Tread Pattern and Runway Surface Condition of Braking Friction and Rolling Resistance of a Modern Aircraft Tire. NASA TN D-1376.
4. Parker O-Ring Handbook, Parker Seal Company, Culver City, California, Cleveland, Ohio. Catalog 5700, June 1957
5. Daugherty, R. L. and Ingersoll, A. C. Fluid Mechanics McGraw-Hill 1954.
6. Blackburn, J. F., Reethof, G., and Shearer, J. L. Fluid Power Control. The M. I. T. Press 1960.
7. Lee, L. T. A Graphical Compilation of Damping Properties of Both Metallic and New Metallic Materials. AFML-TR-66-169. May 1966.
8. Ungar, E. E. and Hatch, D. K. High Damping Materials Prod. Eng. Vol. 32, No. 16, pp. 44-56, April 17, 1961.
9. Campbell, James E. Investigation of the Fundamental Characteristics of High Performance Hydraulic Systems, USAF Technical Report No. 5997, June 1950 ATI No. 91966.
10. Tanner, J. A. and Batterson, S. A. An Experimental Study of the Elastic Properties of Several Aircraft Tires During the Application of Braking Loads. Langley Working Paper 592. May 6, 1968.
11. Morris, J. G. Three Track Elevation Profiles Measured at Two United States Government Installations. NASA TN D-5545.

## REFERENCES

(Continued)

12. Thomson, W. T. Mechanical Vibrations. Prentice-Hall, Inc. 1953.
13. Technical Manual No. T. O. 4BA8-22-3, Overhaul Instructions with Illustrated Parts Breakdown, Skid Control Box Part No. 9543941 (Goodyear)
14. Transistor Circuit Design, Engineering Staff of Texas Instruments, Inc., Edited by Joseph A. Walston and John R. Miller, McGraw-Hill Book Co. 1963
15. Riddle, Robert L. and Ristenbatt, Marlin P. Transistor Physics and Circuits. Prentice Hall 1958.
16. Nanavati, Rajendra P. An Introduction to Semiconductor Electronics, McGraw-Hill Book Company 1963.
17. Batterson, Sidney A. A Study of the Dynamics of Airplane Braking Systems as Affected by Tire Elasticity and Brake Response. NASA TN D-3081

## APPENDIX A

### MATHEMATICAL MODELS

The analysis of antiskid operation is conducted using a modular approach whereby the problem is divided into several component parts, each having inputs and outputs defined so that the outputs from one or more components are provided as inputs to other components. By combining all the analytical components, a composite simultaneous solution is obtained. This Appendix lists analytical models formulated to mathematically describe the following aircraft components or systems (the computer program subroutine identification is given within parentheses after each item):

1. Brake Assembly  
(Brake System)
2. Brake Actuation Hydraulic System  
(Hydraulic System)
3. Vehicle and Wheel Structural Support  
(Airplane System)
4. Wheel and Tire  
(Wheel and Tire System)
5. Antiskid Wheel Speed Sensor  
(Wheel Speed Sensor)
6. Antiskid Control Circuit  
(Antiskid Control Circuit)
7. Antiskid Control Valve  
(Antiskid Control Valve)
8. Aerodynamic Control Surface Positioning System  
(Horizontal Tail Control)
9. Runway Profile  
(Runway System)

These component mathematical models are the same as those initially developed under Air Force Contract F33615-70-C-1004 as described in Report No. AFFDL-TR-70-128 except for corrections or modifications which have been incorporated as a result of analytical refinement conducted during this program. The analytical components are combined into composite solutions for three cases: 1. A laboratory inertia dynamometer set-up, 2. An airplane having three degrees of freedom (i.e., longitudinal and vertical translation and pitch rotation), 3. An airplane having six degrees of freedom (i.e., longitudinal, vertical and lateral translation and pitch, roll and yaw rotation). For the case of the

laboratory dynamometer set-up, two versions of the composite solution are provided. The first is the same as that previously described in Report No. AFFDL-TR-70-128 which utilizes the same analytical components as the airplane solutions and the second is a simplified solution combining all the analytical components with minimal mathematical complexity and is described in report Section III.

Alternate mathematical models have been formulated for some of the analytical components. These alternate mathematical models are listed in the applicable sections alphabetically and are provided for instances where they are needed to describe more than one type of equipment which might be used such as antiskid control circuits, where there are analytical benefits to be gained by utilizing a less complex mathematical model for circumstances where a more complex model is not required, or where modifications are needed for their proper application within the various composite solutions.

#### Format and Convention Usage

The presentation of the analytical component mathematical models follows a common format insofar as practical. The section describing each analytical component begins with an introductory explanation of its function or its characteristics relevant to antiskid operation. Following this introduction is the main body of the discussion under the heading, "A. Mathematical Description," containing the derivation of the equations that describe the system dynamically. This section is concluded with an equation flow diagram showing the relationship among the various system equations. A final discussion follows under the heading, "B. Parameter Evaluation," which sets forth methods of determining the values of the constants appearing in the system equations. The system presentation closes with a "Table of Parameters" which lists all of the system variables and constants.

The flow diagram which appears at the end of Section A is provided principally as an aid in the preparation of the digital computer program which solves the system equations. This flow diagram could also be used for an analog solution. The following conventions apply as to the usage of the flow diagrams: The triangles outside the enclosing phantom line denote variables which are used as inputs and outputs to other systems. The numbered rectangles refer to equations within the system. As an example, in Figure A3 the rectangle

numbered 9 indicates that  $T_{BT}$  is a function of  $u_B$  and  $F_B$  and that the equation that gives the exact relationship is equation 1.9. No constants are shown in these diagrams. The triangles denoting integrators do not always contain an equation number. If the input to an integrator is  $\dot{X}_P$  and its output is  $X_P$ , then the equation is implied. Thus, as in Figure A64, if the input to an integrator is  $R_4$  and the output is  $u_{R4}$ , then the equation  $u_{R4} = \int R_4 dt$ , or equivalently,  $\dot{u}_{R4} = R_4$ , is implied. Because of the size of the six degree airplane system, the flow diagram in Figure A32 is slightly different. Its use is strictly limited to the digital program generation. It says that all equations within one block must be written before proceeding to the next block. Thus, the first variables to be solved for are  $\dot{Z}_{SN}$ ,  $Z_{SN}$ ,  $\dot{Y}_{DLN}$ , ...,  $S_{ML}$ . After this  $F_{VN}$ ,  $F_{LN}$ , ...,  $\dot{Z}_{GLR}$  are solved for. After this  $\dot{X}_{AXL}$ ,  $X_{AXL}$ , ...,  $F_{NN}$  etc.

The "Table of Parameters" is a listing of all variables and constants found in the equations of that system. Each variable is identified by its symbol, description, units, and "Type." The "Type" is listed as v, v(i), and v(o) depending on whether the variable is only used within the system, is received as an input from another system, or is an output to another system. Each constant is identified by its symbol, units, description, "type," and value. The "type" for each constant is always "c" and its value is that used with the F-111 antiskid system.

Table A1 lists the mathematical conventions utilized throughout this study.

Table A1 Explanation of Mathematical Convention

Convention	Description
$\dot{x}$	A dot over a variable denotes differentiation with respect to time.
Computer Notation	All variables are expressed in a form to harmonize with Fortran character utilization. Thus a variable $w_{TE}$ would appear as WTE. Also, in general, the following practice is adhered to. If $x_{TT}$ is a variable, then XTT is its Fortran form. The symbol for $\dot{x}_{TT}$ is XTTD. The symbol for $\ddot{x}_{TT}$ is XTDD. The initial condition is denoted by adding 0 (zero). Thus $\dot{x}_{TT}$ at time = 0 is denoted by XTDO.
$Z_{GD}(\alpha)$	The brackets "<>" are used exclusively to denote the position of a function argument. The script $\alpha$ is used to denote an arbitrary variable. The parentheses "( )" are normally used to denote multiplication.
$ T_{BT} $	Placing a parameter symbol between two vertical bars denotes the absolute value of the parameter. The absolute value of a signed number N is defined as N when N is positive and as -N when N is negative. For example: $ 3  = 3$ and $ -3  = 3$ .
$\text{MIN} \{x_1, x_2, \dots, x_N, C_i\}$ <p style="text-align: center;">OR</p> $\text{MAX} \{x_1, x_2, \dots, x_N, C_i\}$	The braces preceded by "MIN" or "MAX" denote the value of the least (or largest) of the constant or the parameters enclosed within the braces.

Three different total system mathematical models have been formulated to perform antiskid analysis. The first model which is referred to as the flywheel system represents an antiskid system installed on a wheel and brake which are mounted on a dynamometer. The second system, referred to as the three degree system, represents an antiskid system installed on a wheel and brake mounted on a rigid airplane which is allowed three degrees of freedom (longitudinal translation down the runway, translation vertically, and pitch rotation). The third system, referred to as the six degree system, represents a rigid airplane having all six degrees of freedom and equipped with a conventional single wheeled main landing gear incorporating independent antiskid control of each brake. All of these systems are created utilizing the models described in Section III. The basic reason for utilizing three models is economics. The six degree system takes at least twice as long to run as the flywheel system and not all antiskid system parameters require the sophistication of the six degree system. However, it might be necessary to check certain effects under the most comprehensive circumstances.

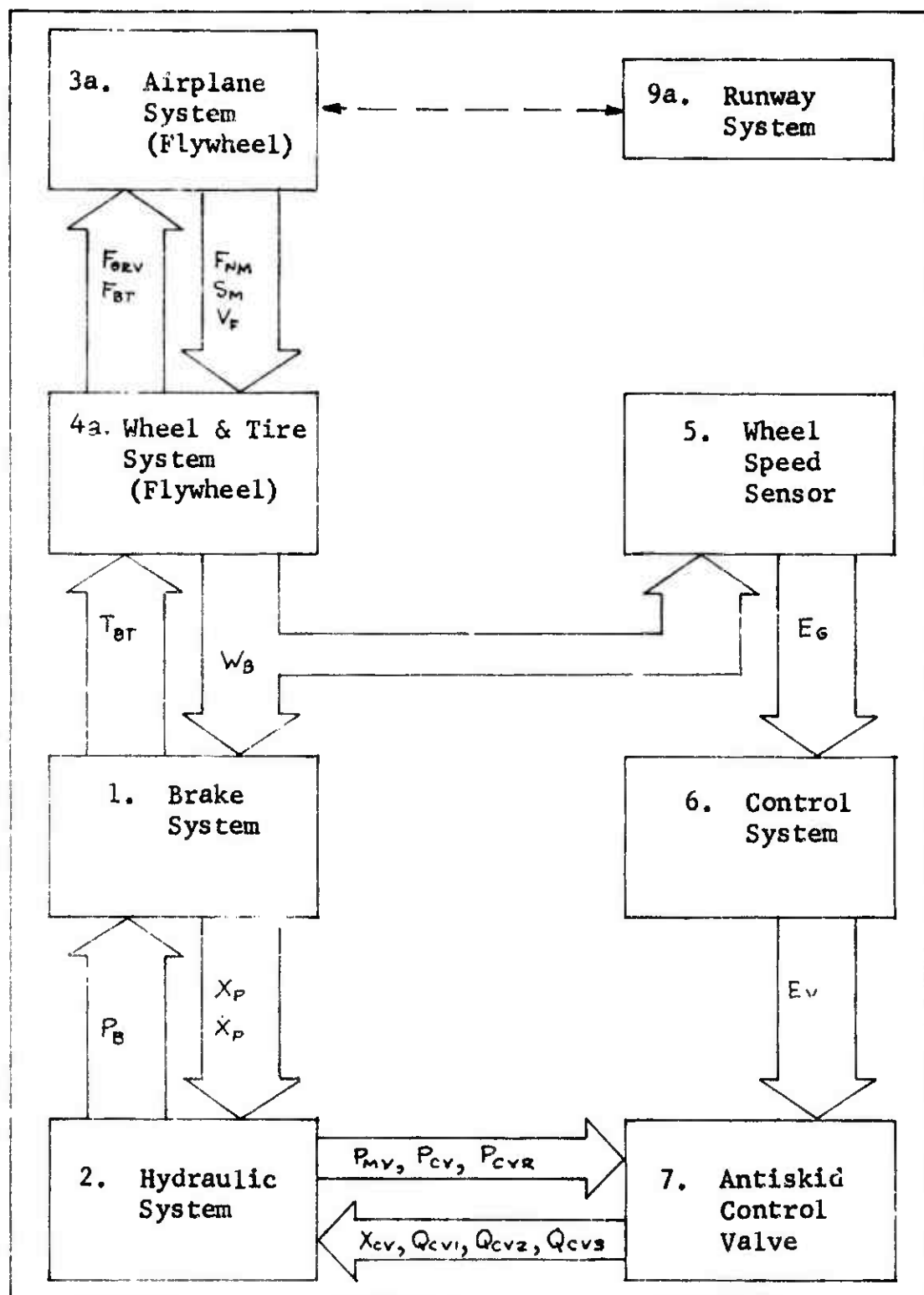
The "Basic Control System" is made of the following elements:

1. Brake System
2. Hydraulic System
3. Wheel Speed Sensor
4. Control System
5. Antiskid Control Valve

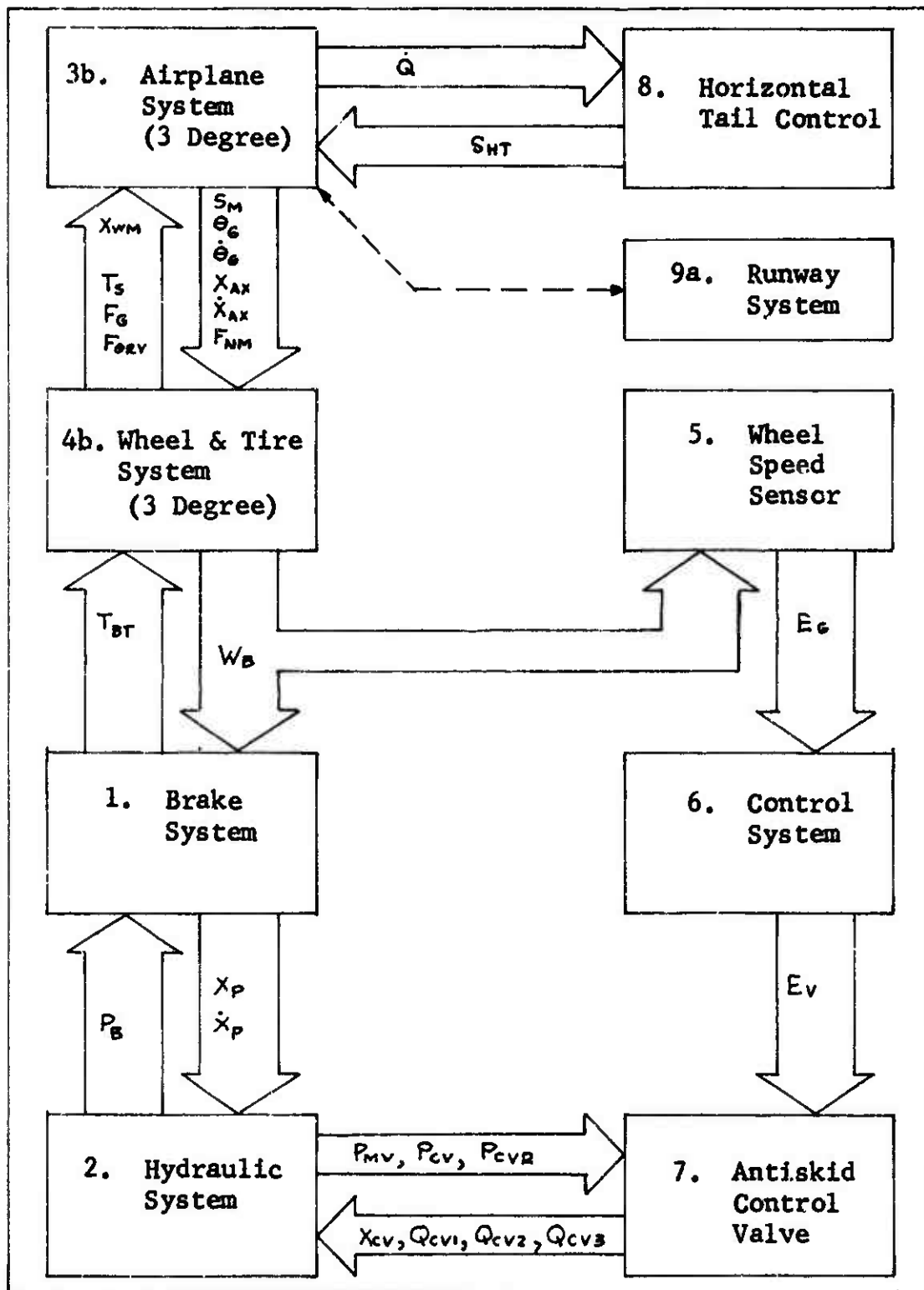
To form the flywheel system, the "Basic Control System" is combined with the 3a. Airplane System (Flywheel), 4a. Wheel and Tire System (Flywheel), and the 9a. Runway System. To form the three degree system, the "Basic Control System" is combined with the 3b. Airplane System (3 Degree), 4b. Wheel and Tire System (3 Degree), 8. Horizontal Tail Control System, and 9a. Runway System. The six degree system incorporates two separate "Basic Control Systems" and two separate 4c. Wheel and Tire Systems. These are combined with a 3c. Airplane System (6 Degree) which utilizes the

8. Horizontal Tail Control and 9c. Runway System (6 Degree). When utilizing the "Basic Control Systems" with the six degree system, the variables communicating with the airplane model are reidentified to correspond to the right or left side of the airplane. Thus,  $X_{AXR}$  is  $X_{AX}$  in the right side and  $X_{AXL}$  is  $X_{AX}$  in the left side.

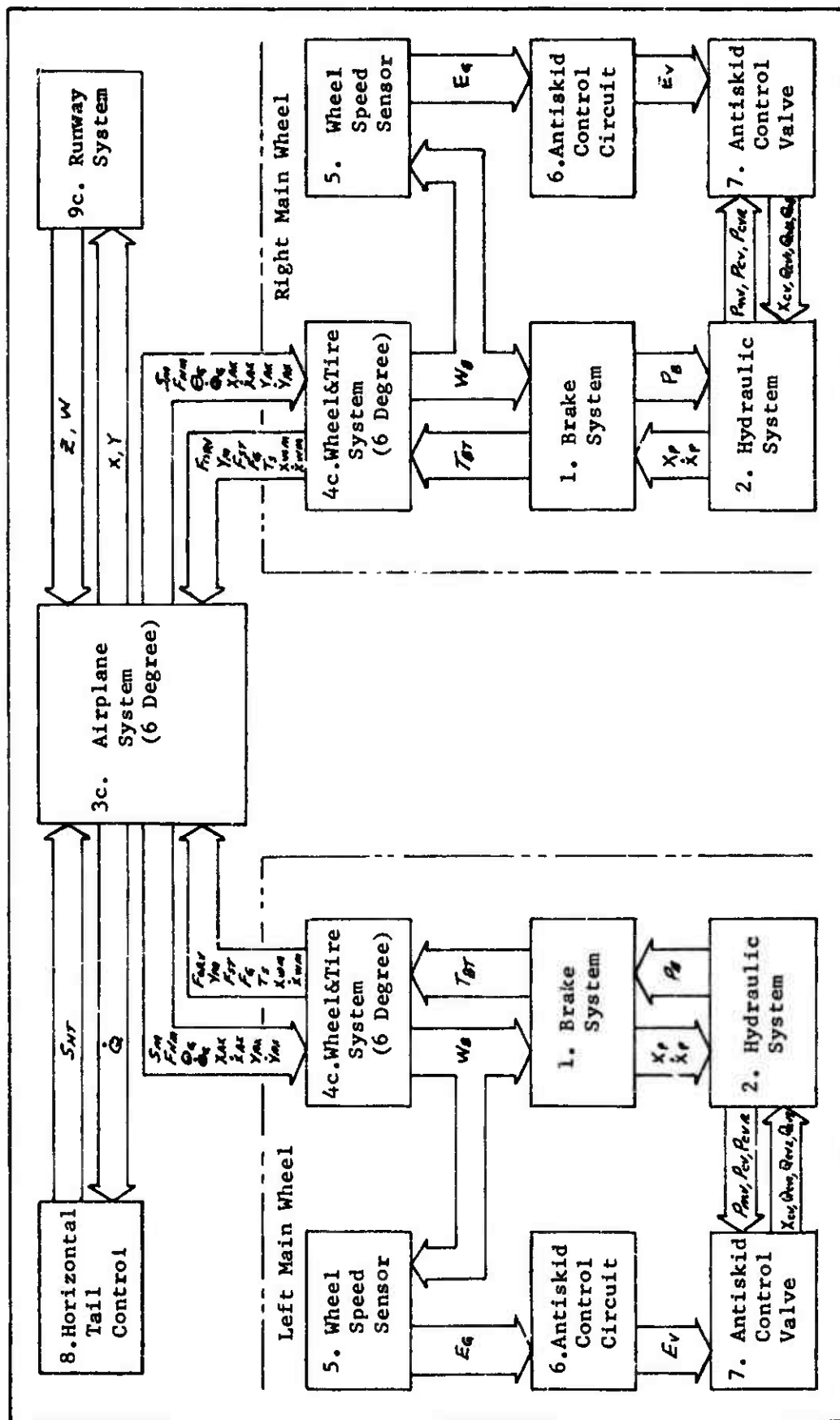
The high degree of modularity used in this analysis is desirable for three reasons. The first reason is that it is easy to combine the component models together to form different types of overall systems. This is true not only from modeling considerations but especially from programming aspects. As an example, the only basic change required to accommodate a twin or tandem gear would be to remodel the strut in the airplane system. The second reason for modularity is the difficulty in being completely general. Should a component arise which is not described by the existing models, it is easy to create a new program for the new model without having to modify the operation of other systems. Thus, from the programming point of view, to incorporate a new wheel speed sensor for example, the new model program can fall back on the existing read, write, and logic statements of the existing wheel speed model. The input and output variables of the new component model are automatically incorporated properly into the overall computational procedure, unless some new variables are defined. The following flow diagrams show the relationships between the various elements in the composite solutions.



Flywheel System Composite Solution Flow Diagram



Three Degree System Composite Solution Flow Diagram



Six Degree System Composite Solution Flow Diagram

## 1. BRAKE ASSEMBLY

The conventional airplane brake consists of a series of discs which are alternately stators and rotors. The stators are restrained from rotating about the axle by splines or keyways. The rotors are similarly connected to the wheel and hence rotate with the wheel and tire. The brake torque is produced by axially compressing the disc stack; usually by hydraulically actuated pistons. Many brakes use return springs to release the brake stack against the return pressure of the hydraulic system. The amount of dynamic torque which is produced by the brake at any instant is the product of the friction force between the rubbing surfaces and the radial distance between the friction force and the axis of wheel rotation. The friction force is the product of the normal force between the rubbing surfaces and the friction coefficient. A more simple mathematical treatment of the brake is a part of the simplified Antiskid Analysis Procedure.

### A. Mathematical Description

In this analysis  $X_p$  will denote the brake piston linear displacement. The pistons, rotors, and stators are treated as a single mass system in the axial mode ( $X_p$  direction). The forces acting on the brake mass in the axial mode are:

- a. Brake actuation force: equals (brake pressure) x (piston area)
- b. Force due to axial restraint
- c. Keyway friction force
- d. Brake piston seal friction force
- e. Brake return spring force
- f. Brake piston bottoming force

Figure A1 shows the brake system and the forces acting in the axial mode. Each of the axial forces is established as follows:

#### a. Brake Actuation Force

The brake actuation pressure  $P_0$  is received as an input from the hydraulic system. The brake actuation force is given by  $P_0 A_{0p}$ , where  $A_{0p}$  is the total brake piston area.

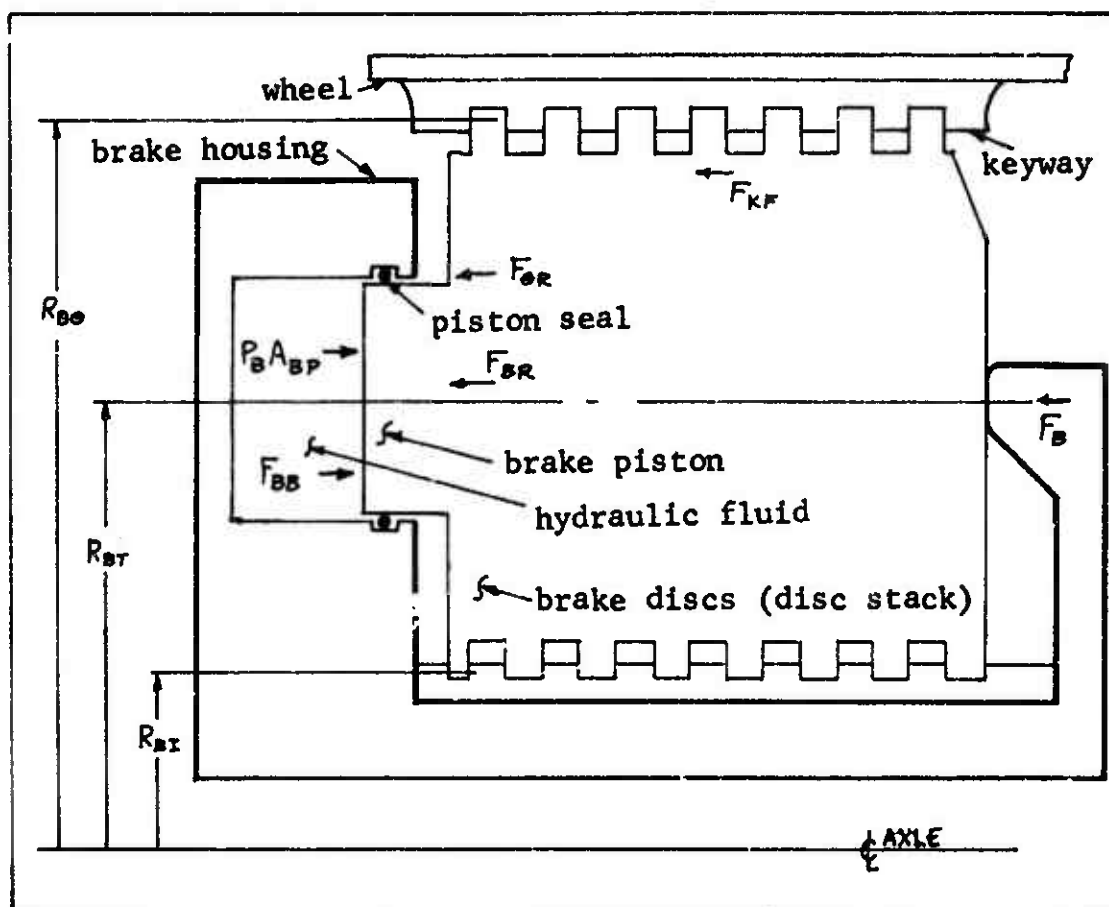


Figure A1 Forces Acting on the Brake Discs

### b. Force due to Axial Restraint

The axial restraining force reflects the elasticity in the brake discs, the back plate, and the piston housing and is a function of their cumulative displacements. A way to derive this characteristic is from a curve of brake volumetric displacement vs. brake pressure. This characteristic does not include friction or return spring effects.

Let  $F_B$  denote the force due to axial restraint. And be defined by

$$(1.1) \quad F_B = F_{B1} + F_{B2}$$

$$(1.2) \quad F_{B1} = \begin{cases} C_{B1} (X_P - S_{B1}) + D_{B1} \dot{X}_P & \text{IF } X_P \geq S_{B1} \\ 0 & \text{IF } X_P < S_{B1} \end{cases}$$

$$(1.3) \quad F_{B2} = \begin{cases} C_{B2} (X_P - S_{B2}) + D_{B2} \dot{X}_P & \text{IF } X_P \geq S_{B2} \\ 0 & \text{IF } X_P < S_{B2} \end{cases}$$

### c. Keyway Friction Force

Let the keyway friction characteristic be defined by a function,  $G_F$ , as shown in Figure A2 and expressed mathematically as:

$$(1.4) \quad G_F = \begin{cases} 1.0 & \text{IF } \dot{X}_P \geq V_{FS} \\ G_{FM} + (1 - G_{FM}) \dot{X}_P / V_{FS} & \text{IF } V_{FS} > \dot{X}_P > 0 \\ 0.0 & \text{IF } \dot{X}_P = 0 \\ -G_{FM} + (1 - G_{FM}) \dot{X}_P / V_{FS} & \text{IF } 0 > \dot{X}_P > -V_{FS} \\ -1.0 & \text{IF } -V_{FS} \geq \dot{X}_P \end{cases}$$

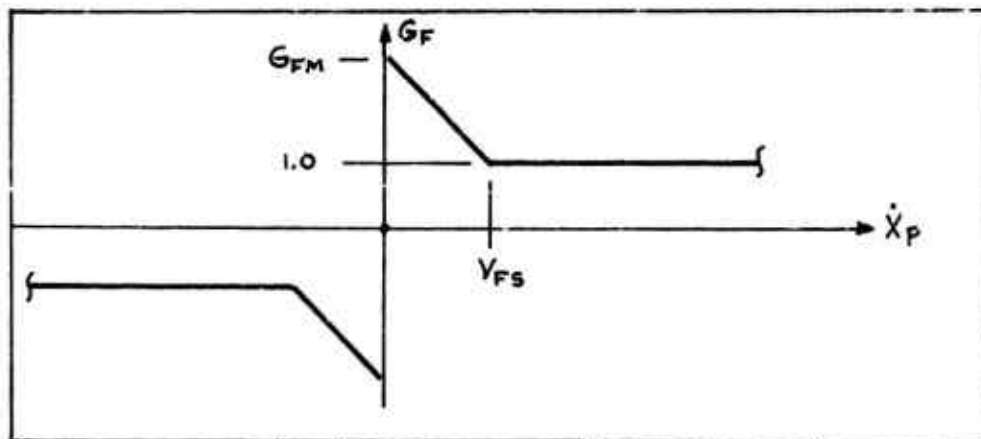


Figure A2 Keyway Friction Characteristic

The brake torque,  $T_{BT}$ , is transferred to the wheel and tire through the rotor keyways. Torque,  $T_{BT}$ , is also transmitted to the axle. The major portion is transmitted through the stator keyways. The remaining portion of the torque is transmitted as piston side loading which results from friction between the pistons and the pressure plate. Let  $100 H_{B1}$  denote the percentage of brake torque transferred through the stator keyways and let  $100 H_{B2}$  denote the percentage of torque transferred through the pistons. Naturally,  $H_{B1} + H_{B2} = 1$ . The normal force on the stator keys is thus  $H_{B1}|T_{BT}|/R_{B1}$ , while the normal force on the rotor keys is  $|T_{BT}|/R_{B2}$ . The total keyway friction force is then given by

$$(1.5) \quad F_{KF} = |T_{BT}| G_F \mu_K (H_{B1}/R_{B1} + 1/R_{B2})$$

d. Brake Piston Seal Force

Let  $F_{OR}$  denote the seal friction force. Then

$$(1.6) \quad F_{OR} = G_F (H_{OFC} + H_{OFP} P_B + |T_{BT}| \mu_{rp} H_{B2}/R_{BT})$$

### e. Brake Return Spring Force

The piston return force  $F_{BR}$  is given by

$$(1.7) \quad F_{BR} = F_{BR0} + C_{BR} X_P$$

### f. Brake Piston Bottoming Force

In the brake released condition, an axial force is developed between the pistons and housing to balance return spring preload. This piston bottoming force is defined as:

$$(1.8) \quad F_{BB} = \begin{cases} -C_{BB}(X_P - S_{BB}) - D_{BB}\dot{X}_P & \text{FOR } X_P \leq S_{BB} \\ 0 & \text{FOR } X_P > S_{BB} \end{cases}$$

This concludes the discussion of the axial brake forces.

Let  $R_{NR}$  be the number of rotors. Let  $W_B$  be the relative angular velocity between the rotors and stators as received from the wheel and tire system. The brake torque  $T_{BT}$  is then given by

$$(1.9) \quad T_{BT} = 2R_{NR} F_B R_{BT} \mu_B$$

Where  $\mu_B$  is:

$$(1.10) \quad \mu_B = \begin{cases} \mu_{B1} + \mu_{B2} e^{-\alpha_B V_B} & \text{IF } V_B > 0 \\ 0 & \text{IF } V_B = 0 \\ -\mu_{B1} - \mu_{B2} e^{+\alpha_B V_B} & \text{IF } V_B < 0 \end{cases}$$

Where  $V_B$  is:

$$(1.11) \quad V_B = R_{BT} W_B$$

Summing the forces in the axial direction yields:

$$(1.12) \quad W_{BE} \ddot{X}_P = P_B R_{BP} - F_B - F_{KF} - F_{BR} - F_{BR} + F_{BB}$$

In Equation (1.12)  $W_{BE}$  is the brake mass which experiences axial motion. Generally,  $W_{BE}$  is the brake heat sink mass. Figure A3 shows the relationship of the brake system equations. Table A2 lists the system parameters.

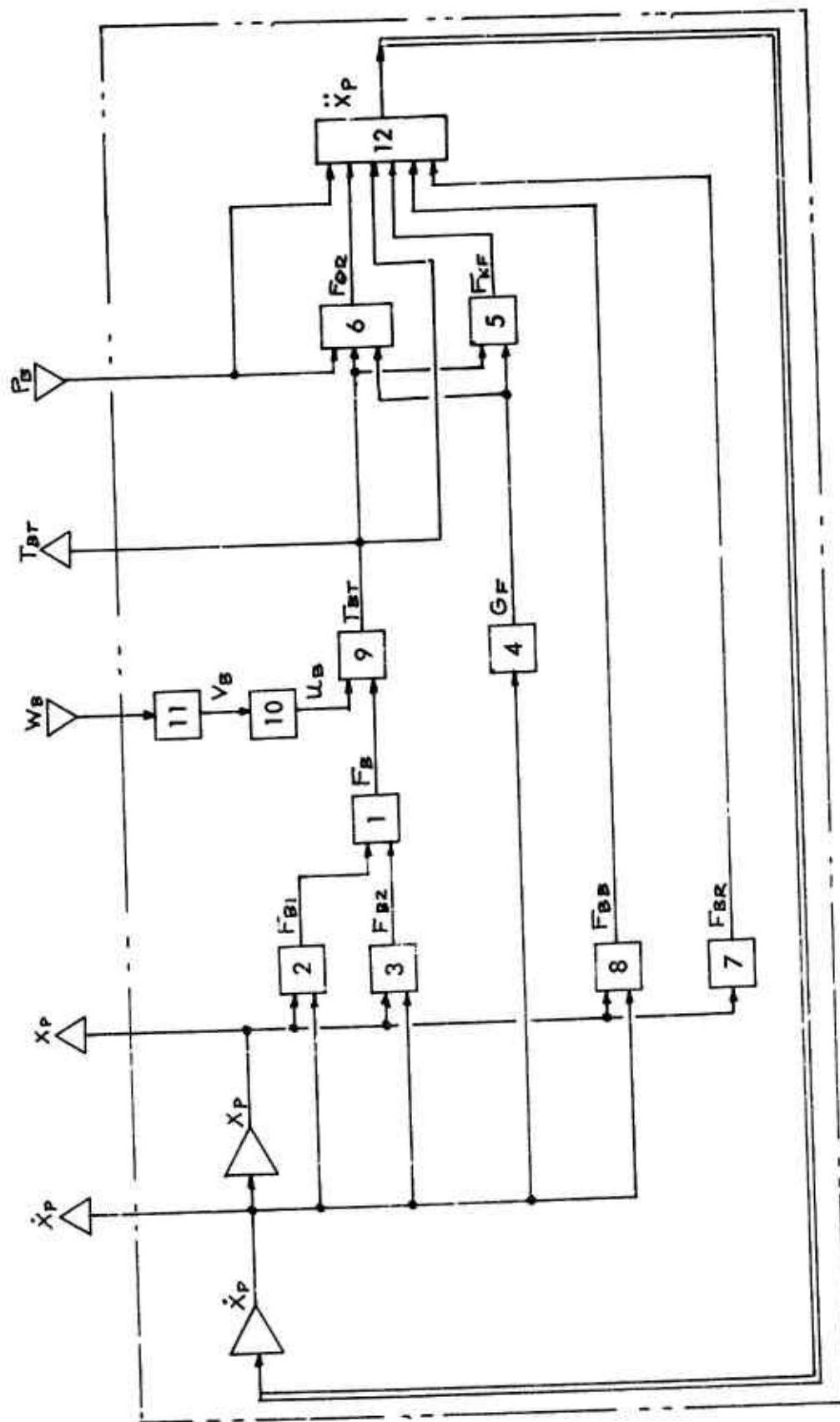


Figure A3 Brake Assembly Equation Flow Diagram

## B. Parameter Evaluation

Figure A4 shows a plot of brake piston displacement as a function of brake application pressure for a new brake.

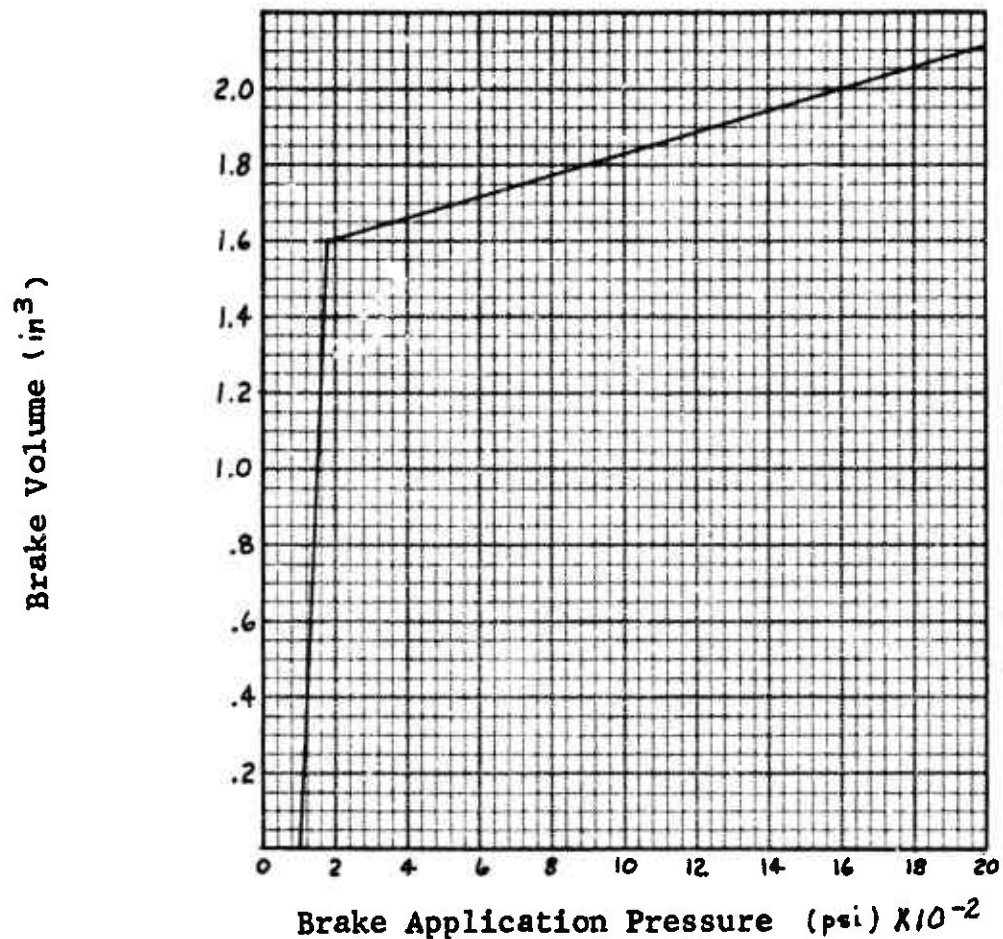


Figure A4 Brake Pressure Volume Characteristic

Assuming that no frictional effects are present,  $C_{BR}$  and  $C_{BI}$  can be derived as follows: Since the initial slope is due to spring return force only, then

$$(1.13) C_{BR} = \left( \frac{\Delta P}{\Delta V} \right) A_{BP}^2 = \left( \frac{80}{1.6} \right) (13.3)^2 = 8850 \text{ lb/in}$$

From the other slope on the curve,

$$(1.14) C_{BI} = \left( \frac{\Delta P}{\Delta V} \right) A_{BP}^2 = \left( \frac{1420}{.4} \right) (13.3)^2 - 8850 = 6.20 \times 10^5 \text{ lb/in}$$

For a new brake  $C_{BZ} = 0$ .

Assuming that the discs all move together, since the heat sink weight is 138 LBM, then  $W_{BF} = 138/386 = .358$  LBF SEC<sup>2</sup>/IN. The natural frequency is then  $\omega_n = \sqrt{K/M}$   
 OR  $\omega_n = \sqrt{(6.2 \times 10^5)/(1.358)} = 1315$  RAD/SEC  
 Assuming that  $\eta = .01$  (see page 117),

$$(1.15) \quad D_{B1} = \frac{\eta C_{B1}}{\omega_n} = \frac{(.01)(6.2 \times 10^5)}{(1315)} = 4.71 \text{ lbf sec/in}$$

It is assumed that  $X_p = 0$  when the brake pressure is 100 psi. Thus

$$(1.16) \quad F_{BP0} = A_{BP} P_0 = (13.3)(100) = 1330 \text{ lbf}$$

Since the brake piston displacement is 1.55 IN<sup>3</sup> before the brake discs come into contact, then  $S_{B1} = 1.55/13.3 = .1165$  in.

Since the F-111 brake has 8 stators with 14 rubbing surfaces,  $H_{B1}$  cannot be greater than 1/14. A conservatively high value of  $H_{B1} = .05$  has been assumed and it follows that  $H_{B2} = .95$ .

The brake piston seals are equivalent to MS28775-219. The seal friction force is established using the procedures described in Reference 4. The seal sliding friction force is a function of rubber compound hardness, amount of installed compression, length of rubbing surface, seal groove projected area and applied hydraulic pressure. For the MS28775-219 size seal having 10 percent installed compression and 70 degree Shore A hardness the sliding friction force is 2.88 lbf plus 0.02 lbf per psi applied pressure per seal. There are 10 pistons in the brake housing; therefore,

$$(1.17) \quad H_{OFC} = (10)(2.88) = 28.8 \text{ lbf}$$

$$(1.18) \quad H_{OFP} = (10)(0.02) = 0.20 \text{ lbf/psi}$$

Conservatively high values for the friction coefficients  $\mu_K$  and  $\mu_{KP}$  are estimated as  $\mu_K = .15$  and  $\mu_{KP} = .10$ .  $G_{FM}$  is estimated to be 1.50.

Values for the following brake dimensional characteristics are then from the appropriate brake component drawings:

$R_{BI} = 4.40$  IN,  $R_{BT} = 6.25$  IN, and  $R_{BD} = 8.25$  IN.

Observations of braking stops indicate that for an average F-111 brake lining,

$$u_{B1} = .15$$

$$u_{B2} = .10$$

$$\alpha_B = .03 \text{ SEC/IN}$$

Table A2 Brake Assembly Parameters (Sheet 1 of 2)

SYMBOL	TYPE	VALUE	UNITS	DESCRIPTION
$A_{BP}$	C	13.3	IN	Piston area per brake
$\alpha_B$	C	0.03	SEC/IN	Brake lining friction parameter
$C_{B1}$	C	$6.2 \times 10^5$	LB/IN	} Brake Disc spring rate characteristic
$C_{B2}$	C	0.0	LB/IN	
$C_{BP}$	C	$1.0 \times 10^5$	LB/IN	Bottoming spring rate
$C_{BR}$	C	8950.	LB/IN	Return spring rate
$D_{B1}$	C	4.71	LB SEC/IN	} Brake Disc damping coeff.
$D_{B2}$	C	0.0	LB SEC/IN	
$D_{BB}$	C	400.	LB SEC/IN	Bottoming damping coeff.
$F_B$	V		LB	Force between brake plates
$F_{B1}$	V		LB	} $F_B = F_{B1} + F_{B2}$
$F_{B2}$	V		LB	
$F_{BS}$	V		LB	Bottoming Force
$F_{BR}$	V		LB	Return Force
$F_{BRO}$	C	1330.	LB	Return force when $X_p = 0$
$F_{KF}$	V		LB	Keyway friction force
$F_{OR}$	V		lb	"O-ring" friction force
$G_f$	V			Friction breakout function to
$G_{FM}$	C	1.50	Dimensionless	Ratio of breakout friction to running friction
$H_{B1}$	C	0.05	Dimensionless	Fraction of brake torque removed by stator keys
$H_{B2}$	C	0.95	Dimensionless	Fraction of brake torque removed thru pistons
$H_{BFC}$	C	28.8	LB	} O-ring friction
$H_{BFP}$	C	0.20	LB/PSI	

Table A2 Brake Assembly Parameters (Sheet 2 of 2)

SYMBOL	TYPE	VALUE	UNITS	DESCRIPTION
$P_b$	v (1)		LB/IN	Brake pressure
$R_{s1}$	c	4.40	IN	Radius to center of press on stator key
$R_{se}$	c	8.25	IN	Radius to center of press on rotor key
$R_{sr}$	c	6.25	IN	Radius to piston centers
$R_{nr}$	c	7	Dimensionless	Number of rotors
$S_{b1}$	c	.1165	IN	Displacement of piston to engage $C_{s1}$
				Spring Rate
$S_{b2}$	c	0.0	IN	Displacement of piston to engage $C_{s2}$
				Spring Rate
$S_{sb}$	c	0.0	IN	Value of $X_p$ when bottoming occurs
$T_{sr}$	v (0)		IN LB	Brake torque
$U_s$	v		Dimensionless	Brake lining friction coeff.
$U_{s1}$	c	0.15	Dimensionless	Brake lining friction characteristic
$U_{s2}$	c	0.10	Dimensionless	Friction coeff. of keyways (running)
$U_k$	c	0.15	Dimensionless	Friction coeff. between pistons and walls (running)
$U_{kp}$	c	0.10	Dimensionless	Velocity of brake lining
$V_b$	v		IN/SEC	Friction breakout parameter
$V_{fs}$	c	0.10	IN/SEC	Rotational speed between stators and rotors
$W_b$	v (1)		RAD/SEC	Brake mass
$W_{bc}$	c	0.358	LB SEC /IN	Brake piston displacement
$X_p$	v (0)		IN	Brake piston displacement when $t = 0$
$X_{p0}$	c	0.0	IN	Brake piston displacement
$\dot{X}_p$	v (0)		IN/SEC	Brake piston velocity
$\dot{X}_{p0}$	c	0.0	IN/SEC	Brake piston velocity when $t = 0$
$\ddot{X}_p$	v		IN/SEC	Brake piston accel.

## 2. BRAKE ACTUATION HYDRAULIC SYSTEM

The hydraulic system is the brake actuation power source and is made up of the four components as shown in Figure A5 : the pilot's metering valve, the antiskid control valve, the control line, and the brake piston housing. The pilot's metering valve is a pressure regulator, usually having a mechanical input, which has a steady state output pressure ( $P_{mv}$ ) at a level commanded by the pilot ( $P_{com}$ ). The antiskid valve is a pressure regulator which has a steady state output as dictated by the antiskid control device. For a modulated antiskid system, the control valve is a variable pressure servo type regulator and for an ON-OFF antiskid system the control valve is an ON-OFF valve. The control line is simply the fluid transmission line or containment vessel connecting the control valve to the brake housing. The brake housing is a collection of cylinders and pistons which act to compress the brake discs. From a hydraulic system aspect, the control valve is a variable area orifice, where the orifice area is a function of spool position. The control valve spool position is received as an input from computations described in a section devoted to the operation of the control valve.

In the description of the brake actuation system, there are two principal effects which should be accounted for. The first is the time lag which exists between the control valve output pressure ( $P_{cv}$ ) and the actual brake pressure ( $P_b$ ). This lag is caused by the fluid's resistance to flow due to inertia and friction and by the brake pressure's dependence upon fluid volume within the pressure cavity. The second effect is the instantaneous brake pressure intensity as influenced by fluid inertia and the combined elasticity of the fluid and the pressure cavity. Rapid valve operation can cause pressure overshoot and oscillation due to "water hammer" effects. This overshoot can cause excessive brake torque and may interfere with proper control valve operation. The pilot's metering valve pressure drop and response characteristics are included in the actuating system description so that these effects upon antiskid operation can be examined. To allow for a variety of brake actuation systems which might be encountered, provision is made to accommodate both hydraulic and pneumatic actuation media. The line connecting the control valve and the brake can be treated as a separate fluid cavity or the effects of its volume may be lumped with the brake as would be appropriate for a short line.

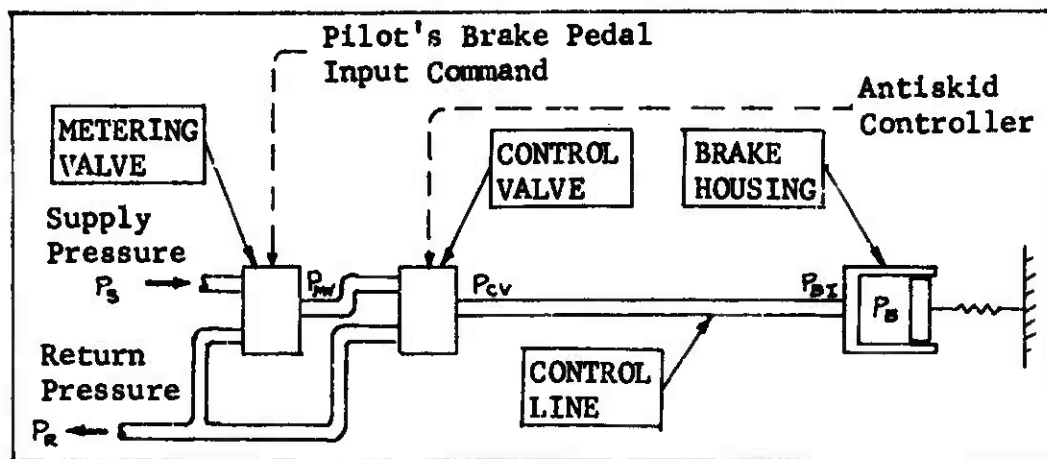


Figure A5 Hydraulic System Components

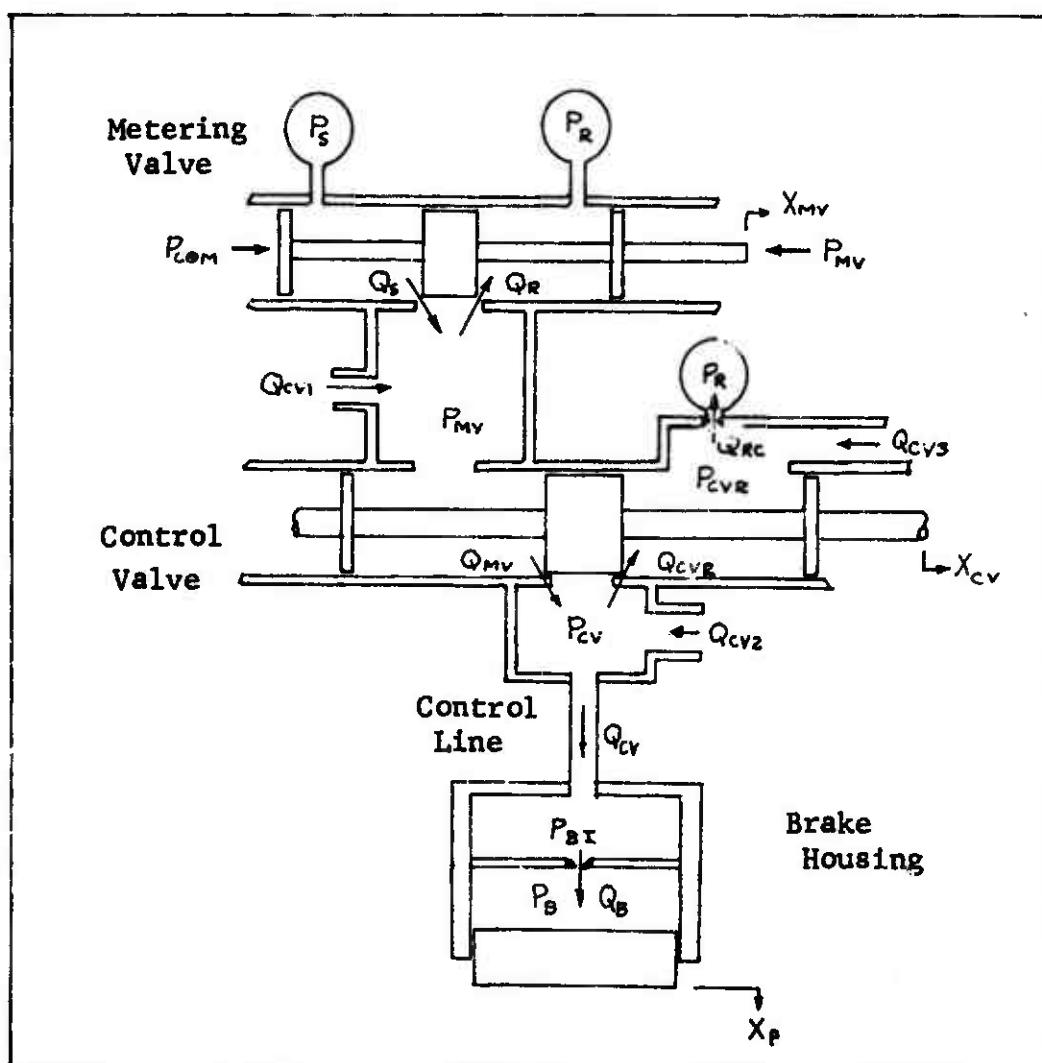


Figure A6 Hydraulic System Schematic for Options 1, 2 and 3

# A. Mathematical Description (Options 1, 2 and 3)

Figure A6 is a schematic of the brake hydraulic system. The analytical procedures of References 5 and 6 are utilized to mathematically describe the system.

Let  $P_{COM}$  denote the brake pressure which is commanded by the pilot and define  $P_{COM}$  such that it increases from a minimum value,  $P_R$ , (reservoir pressure) to the desired steady state value  $P_{CP}$ , as a linear function of time over an interval,  $T_{CP}$ , as follows:

$$(2.1) \quad P_{COM} = \begin{cases} T(P_{CP} - P_R)/T_{CP} + P_R & \text{IF } 0 \leq T \leq T_{CP} \\ P_{CP} & \text{IF } T_{CP} < T \end{cases}$$

The metering valve attempts to maintain  $P_{MV}$  at the level of  $P_{COM}$ . The metering valve spool displacement  $X_{MV}$  is defined by equations (2.2) and (2.3).

$$(2.2) \quad V_{MV} = G_{mv} (P_{COM} - P_{MV})$$

$$(2.3) \quad \dot{X}_{MV} = \begin{cases} \min \{ 0, V_{MV} \} & \text{IF } S_{MVU} \leq X_{MV} \\ V_{MV} & \text{IF } S_{MVL} < X_{MV} < S_{MVU} \\ \max \{ 0, V_{MV} \} & \text{IF } X_{MV} \leq S_{MVL} \end{cases}$$

Let  $\phi\langle X, Y \rangle$  be a function defined as follows:

(a) For hydraulic fluid

$$(2.4) \quad \phi\langle X, Y \rangle = \text{SIGN}(X - Y) \sqrt{|X - Y|}$$

(b) For compressible pneumatic fluids

$$(2.5) \quad \text{IF } X > Y \text{ and } X \geq Y/R_{CRIT} \quad \text{WHERE } R_{CRIT} = \left[ \frac{2}{(\gamma_a + 1)} \right]^{\frac{\gamma_a}{\gamma_a - 1}}$$

$$\phi\langle X, Y \rangle = X \left[ 1 - (R_{CRIT})^{\frac{\gamma_a - 1}{\gamma_a}} \right]^{1/2} / \left[ (R_{CRIT})^{\gamma_a} \right]$$

IF  $X \geq Y$  and  $X \leq Y/R_{CRIT}$

$$\phi\langle X, Y \rangle = X \left[ 1 - \left( \frac{1}{X} \right)^{\frac{\gamma_a - 1}{\gamma_a}} \right]^{1/2} / \left( \frac{1}{X} \right)^{\gamma_a}$$

IF  $Y \geq X$  and  $Y \leq X/R_{CRIT}$

$$\phi\langle X, Y \rangle = -\phi\langle Y, X \rangle$$

IF  $Y > X$  and  $Y \geq X/R_{CRIT}$

$$\phi\langle X, Y \rangle = -\phi\langle Y, X \rangle$$

Let  $A_{MV}(x)$  be defined by:

$$(2.6) A_{MV}(x) = \begin{cases} A_{MVO} & \text{if } x \geq S_{MVO} \\ \max\{A_{MVL}, x A_{MVO}/S_{MVO}\} & \text{if } x < S_{MVO} \end{cases}$$

Let  $A_{MVS}$  and  $A_{MVR}$  be defined by:

$$(2.7) A_{MVS} = A_{MV}(X_{MV})$$

$$(2.8) A_{MVR} = A_{MV}(-X_{MV})$$

Then

$$(2.9) Q_S = A_{MVS} \phi(P_S, P_{MV})$$

$$(2.10) Q_R = A_{MVR} \phi(P_{MV}, P_R)$$

Let  $V_{MVV}$  be the fluid volume from the output of the metering valve up to the input of the control valve.

Then

$$(2.11) \dot{P}_{MV} = (B_{MV}/V_{MVV})(Q_S - Q_R - Q_{MV} + Q_{CV1})$$

Let  $A_{CV}(x)$  be defined by:

$$(2.12) A_{CV}(x) = \begin{cases} A_{CVO} & \text{if } x \geq S_{CVO} \\ \max\{A_{CVL}, x A_{CVO}/S_{CVO}\} & \text{if } x < S_{CVO} \end{cases}$$

Let  $A_{CVS}$  and  $A_{CVR}$  be defined by

$$(2.13) A_{CVS} = A_{CV}(X_{CV} - S_{CL})$$

$$(2.14) A_{CVR} = A_{CV}(-S_{CL} - X_{CV})$$

Then

$$(2.15) Q_{MV} = A_{CVS} \phi(P_{MV}, P_{CV})$$

$$(2.16) Q_{CVR} = A_{CVR} \phi(P_{CV}, P_{CVR})$$

$$(2.17) \dot{P}_{CVR} = (B_{CVR}/V_{CVR})(Q_{CVR} - Q_{RC} + Q_{CV3})$$

$$(2.18) Q_{RC} = A_{RC} \phi(P_{CVR}, P_R)$$

The volume of the cavity occupied by the brake actuation media is established by equation (2.19) as follows:

$$(2.19) \quad V_B = V_{B0} + A_{BPS} \dot{X}_P$$

Three options for the control line mathematical description are provided to cover a variety of circumstances which may be encountered. The third option is representative of a typical aircraft installation and is used in analyzing the F-111 system.

The first option is for a control line with hydraulic fluid considering volume effects only. This option will not predict "water hammer" but is satisfactory for many cases, particularly for the case of a short control line 50 inches or less in length. The following equations describe the first option:

$$(2.20a) \quad Q_{CV} = Q_{MV} - Q_{CVR} + Q_{CV2}$$

$$(2.21a) \quad \dot{P}_{CV} = (B_B/V_B) (Q_{CV} - A_{BPS} \dot{X}_P)$$

$$(2.22a) \quad P_{BI} = P_{CV}$$

$$(2.23a) \quad P_B = P_{BI}$$

$$(2.24a) \quad Q_B = Q_{CV}$$

The following equations are applicable to the second option for the control line using compressible pneumatic fluid.

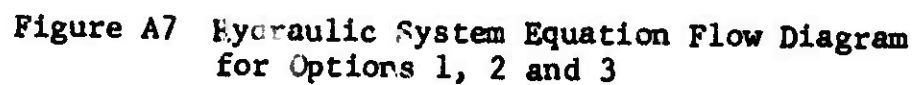
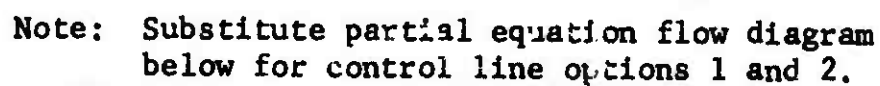
$$(2.20b) \quad Q_{CV} = Q_{MV} - Q_{CVR} + Q_{CV2}$$

$$(2.21b) \quad \dot{P}_{CV} = (B_B/V_B) (Q_{CV} - P_{CV} A_{BPS} \dot{X}_P / B_B)$$

$$(2.22b) \quad P_{BI} = P_{CV}$$

$$(2.23b) \quad P_B = P_{BI}$$

$$(2.24b) \quad Q_B = Q_{CV}$$



The third option is for a control line with hydraulic fluid where both volume and inertial effects are considered and is described by the following equations:

$$(2.20c) \quad \dot{Q}_{CV} = (A_{BL}/R_{HO}S_{BL})(P_{CV} - P_{BI} - D_{RBL}Q_{CV} - D_{TBL}Q_{CV}/Q_{CV})$$

$$(2.21c) \quad \dot{P}_{CV} = (B_{BL}/V_{BL})(Q_{MV} - Q_{CVR} - Q_{CV} + Q_{CV2})$$

$$(2.22c) \quad \dot{P}_{BI} = (B_{BL}/V_{BL})(Q_{CV} - Q_B)$$

$$(2.23c) \quad Q_B = A_{BO} \phi(P_{BI}, P_B)$$

$$(2.24c) \quad \dot{P}_B = (B_B/V_B)(Q_B - A_{BPS}\dot{x}_P)$$

An Option 4 Hydraulic System is described to provide a simplified mathematical description of the hydraulic system which does not account for metering valve transient spool movement. For this model the metering valve is assumed to be full open for hydraulic flow to the brake and fully closed for hydraulic flow from the brake. Hydraulic flow direction and amount is established by control valve spool position as shown schematically in Figure A8. In addition the brake piston velocity is defined as the brake hydraulic flow rate divided by the piston area so that the hydraulic volume is the integral of the flow. Option 4 hydraulic system mathematical description is developed as follows:

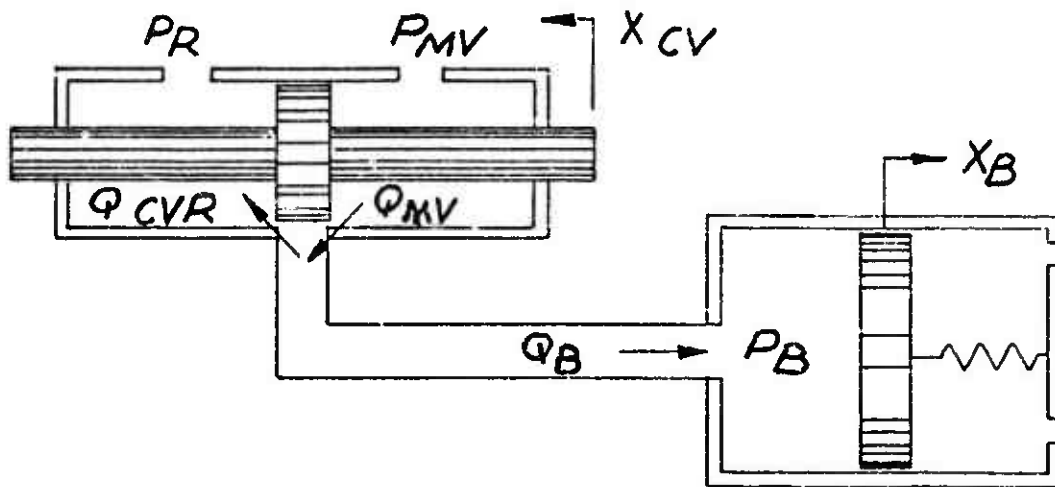


Figure A8 Option 4 Hydraulic System Schematic

Let  $P_{CP}$  denote the brake pressure which is commanded by the pilot. Let  $P_{MV}$ , metering valve output pressure increase from a minimum value,  $P_R$ , (reservoir pressure) to the desired steady state pressure,  $P_{COM}$ , as a linear function of time over an interval,  $T_{CP}$ , as follows:

$$(2.1d) \quad P_{MV} = T(P_{CP} - P_R) / T_{CP} + P_R \quad \text{IF } 0 \leq T \leq T_{CP} \\ = P_{CP} \quad \text{IF } T > T_{CP}$$

Let the brake pressure,  $P_B$ , be a function of brake fluid volume as follows:

$$(2.2d) \quad P_B = P_{B1} + P_{B2}$$

$$(2.3d) \quad P_{B1} = P_{BR1} + C_{BV1} V_B \quad \text{IF } 0 \leq V_B \leq V_{BC} \\ = 0 \quad \text{IF } V_B > V_{BC}$$

$$(2.4d) \quad P_{B2} = P_{BR2} + C_{BV2} V_B \quad \text{IF } V_{BC} < V_B \\ = 0 \quad \text{IF } 0 \leq V_B \leq V_{BC}$$

Let the control valve flow area for brake application,  $A_{CVS}$ , be defined as a function of spool relative position:

$$(2.5d) \quad A_{CVS} = A_{CVS0} \quad \text{IF } X_{CV} \geq S_{CV0} \\ \max \{ A_{CVL}, X_{CV} (A_{CVS0}) / S_{CV0} \} \quad \text{IF } X_{CV} < S_{CV0}$$

In a similar way, let the control valve flow area for brake release,  $A_{CVR}$ , be defined as follows:

$$(2.6d) \quad A_{CVR} = A_{CVR0} \quad \text{IF } X_{CV} \leq -S_{CV0} \\ \min \{ A_{CVL}, X_{CV} (A_{CVR0}) / S_{CV0} \} \quad \text{IF } X_{CV} > -S_{CV0}$$

Then:

$$(2.7d) \quad Q_{mv} = A_{cvS} \phi < P_{mv}, P_B >$$

$$(2.8d) \quad Q_{cVR} = A_{cVR} \phi < P_B, P_R >$$

Where the function  $\phi$  is as previously defined by equation (2.4)

$$(2.9d) \quad Q_B = Q_{mv} - Q_{cVR}$$

$$(2.10d) \quad V_B = \int Q_B$$

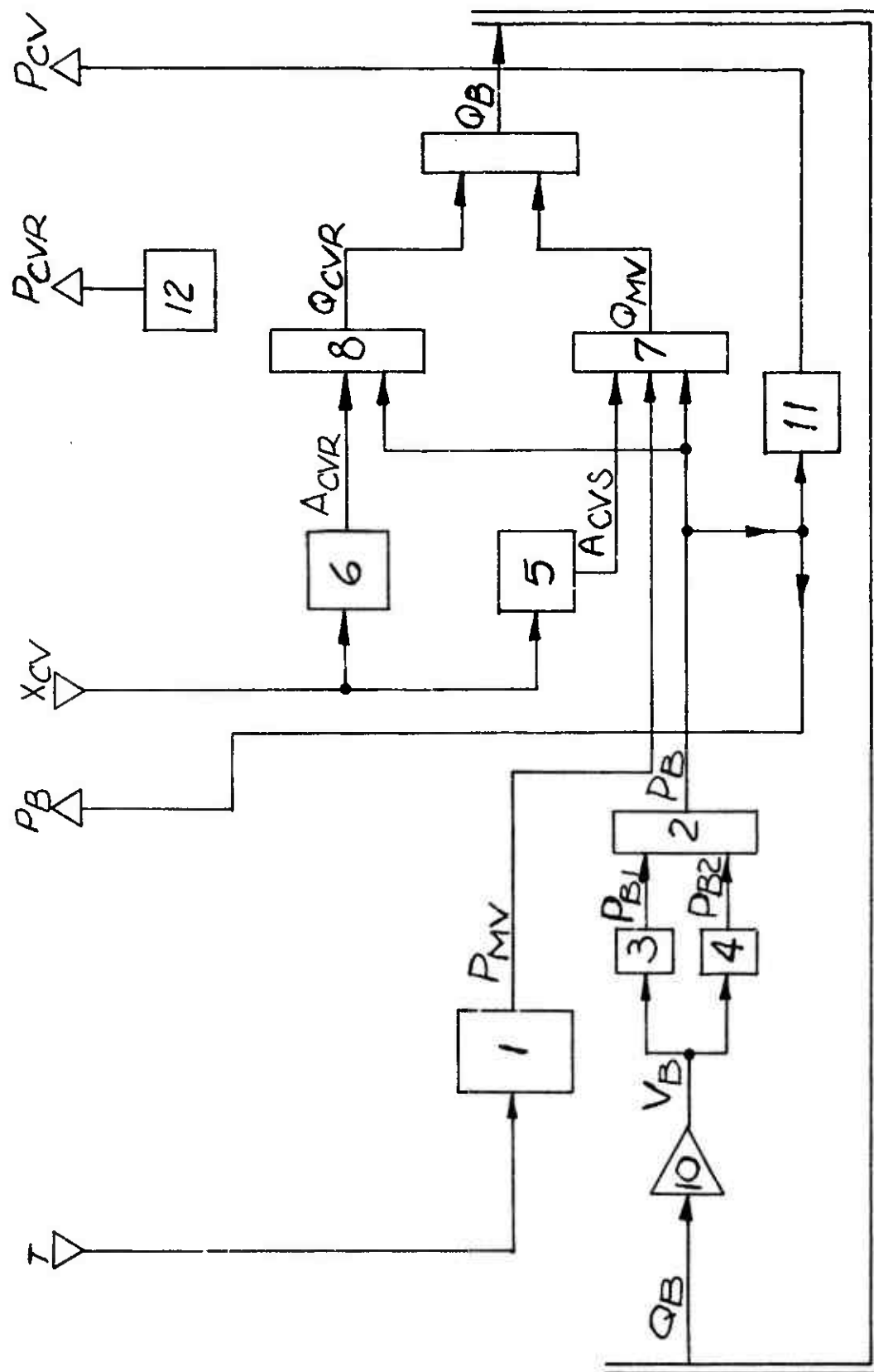
For compatibility with the other hydraulic system options as they interface with other systems:

$$(2.11d) \quad P_{cv} = P_B$$

$$(2.12d) \quad P_{cVR} = P_R$$

Figure A9 shows the Option 4 Hydraulic System Equation flow diagram.

In this study the brake system hydraulic supply pressure,  $P_S$ , is treated as a constant. If  $P_S$  varies significantly due to operation of other aircraft hydraulic system equipment, this variable pressure defined as a function of time may be used.



## B. Parameter Evaluation

For this study the third optional control line description as applied to the F-111 is of primary interest. For this case MIL-H-5606 hydraulic fluid is used. The hydraulic fluid properties for a mean temperature of 100°F and 1500 psi are:

- (1) Adiabatic bulk modulus:  $\beta = 248,000$  psi
- (2) Density:  $\rho = .781 \times 10^{-4}$  LBF SEC<sup>2</sup>/IN<sup>4</sup>
- (3) Kinematic viscosity:  $\nu = .0267$  IN<sup>2</sup>/SEC

The system supply pressure is 3000 psi and the return pressure is 100 psi. Initially, all flows are zero and all pressures except the supply pressure are at 100 psi. The pilot's input command pressure  $P_{COM}$  is also 100 psi. The pilot's input  $P_{COM}$  will go from 100 to 1500 psi in 0.2 seconds. Thus  $T_{CP} = 0.2$  sec and  $P_{CP} = 1500$  psi.

### Metering Valve

When the metering valve spool is centered, the flow area is essentially zero for both the return and supply lines. In this spool position  $X_{mv} = 0.0$ . From equation (2.3) the spool is constrained to stay between  $S_{mvl}$  and  $S_{mvu}$ .

For the metering valve,  $S_{mvl} = -.06$  in and  $S_{mvu} = .06$  in. However, when  $X_{mv}$  is at  $+.05$ , the valve area has reached its maximum for the flow  $Q_s$ . When  $X_{mv} = -.05$ , the area is maximum for the return flow  $Q_R$ . Thus  $S_{mvo} = .05$ . By actual measurement, with the valve full open (area =  $A_{mvo}$ ) at 100° F, the flow is 9.23 in<sup>3</sup>/sec. at 200 psi  $\Delta P$ . Thus from (2.9) or (2.10),

$$(2.25) \quad A_{mvo} = Q / \sqrt{\Delta P} = 9.23 / \sqrt{200} = .653 \text{ IN}^4/(\text{sec})(\text{lbf})^{1/2}$$

In the F-111 system, the metering valve is situated next to the control valve so that the volume  $V_{MV}$  is quite small.  $V_{MV}$  was calculated from the valve drawing as being about  $1.0 \text{ in}^3$ . Also, the valve body is considered to be much stiffer than the hydraulic fluid so that the effective bulk modulus is the fluid modulus. Thus,  $B_M = 248,000 \text{ psi}$ .  $G_{MV}$  was estimated from analog studies to be about .05.

### Control Valve

For the control valve,  $X_{cv} = 0.0$  when the spool is centered. At this point the flow area is zero so that  $A_{cvL} = 0.0$ . The flow area remains zero for  $-.005 \leq X_{cv} \leq .005$ . Thus the valve has an overlap of .005 in. and  $S_{CL} = .005$ . An additional movement of .030 in. produces full area so  $S_{cv0} = .030$ . By actual measurement at this position at  $100^\circ\text{F}$ , the flow is  $7.7 \text{ in}^3/\text{sec}$ . at  $50 \text{ psi } \Delta P$ . Thus

$$(2.26) \quad A_{cv0} = Q/\sqrt{\Delta P} = 7.7/\sqrt{50} = 1.090 \text{ in}^4/(\text{sec})(\text{lbf})^{1/2}$$

The following values are estimates of the return characteristics of the control valve:  $V_{cVR} = 2.0 \text{ in}^3$ ,  $B_{cVR} = 248,000 \text{ psi}$ ,  $A_{RC} = 1.0 \text{ in}^4/(\text{sec})(\text{lbf})^{1/2}$ .

### Control Line

The control line is  $1/4$  inch outside diameter steel tubing having  $0.14$  inch wall thickness and internal cross sectional area,  $A_{BL}$ , equal to  $.0386 \text{ in}^2$ . Because of the thin wall, the tube elasticity greatly reduces the bulk modulus. The equivalent bulk modulus,  $B_e$ , may be calculated from

$$(2.27) \quad B_e = B \left( \frac{1}{\left(\frac{B}{E}\right)\left(\frac{D}{t}\right) + 1} \right)$$

Where       $B$  = Fluid bulk modulus  
               $E$  = Young's modulus of tube material  
               $D$  = Mean tube diameter  
               $t$  = Tube wall thickness

Thus

$$(2.28) B_{BL} = \frac{248000}{\frac{(1.248 \times 10^6)(.236)}{(30 \times 10^6)(.014)} + 1} = 217,700 \text{ PSI}$$

The control/line length,  $S_{BL}$ , is 191 inches with various types of flow restrictors according to the following table.

Table A3 Control Line Restrictions

Description	"K" Value*	Number n	nk
An815-4J Union	.54	1	.54
AN832-4J Union	.54	1	.54
AN821-4J Elbow (90°)	1.23	4	4.92
AN837-4J Elbow (45°)	.89	1	.89
90° Tube Bend	.01	12	.12
90° Hose Fitting	1.25	1	<u>1.25</u>
Total			8.26

\* $\Delta h = KV^2/2g$  Where  $V$  is the velocity in the line.

The "K" values in Table A3 were derived from information contained in Reference 5.

Equation (2.20c) is the result of summing forces on the mass of fluid in the control line. The friction losses are depicted by a turbulent flow loss  $D_{TBL} Q_{cv}^2$  and a laminar flow loss  $D_{LBL} Q_{cv}$ . It is assumed that all the turbulent flow losses come from elbows, etc., which are listed in Table 3. The loss due to the line itself is considered to be always laminar. This assumption of laminar flow for

the line is justified for two reasons: (1) the loss in the line is small compared to other losses in the system; (2) the flow is normally laminar anyway (Reynolds Number is less than 6000 for the F-111 system).

For the turbulent losses

$$\begin{aligned} (2.29) \quad \Delta P &= \rho g \Delta h \\ &= K \rho v^2 / 2 \\ &= (K \rho / 2 A^2) Q^2 \end{aligned}$$

Thus

$$\begin{aligned} (2.30) \quad D_{TBL} &= \frac{K \rho}{2 (A_{BL})^2} \\ &= \frac{(8.26)(.781 \times 10^{-4})}{2 (.0386)^2} \\ &= .216 \text{ lbf sec}^2 / \text{IN}^2 \end{aligned}$$

For laminar losses, at temperatures normally encountered, the "oscillatory" friction is higher than the steady state friction. See Reference 9. The pressure loss can be written as

$$(2.31) \quad \Delta P = R_L (L/A^2) Q$$

For the steady state case as shown in Reference 6,

$$(2.32) \quad R_L = 8 \pi \rho \nu$$

In Figure 10 values for this theoretical steady state  $R_L$  are compared over a range of temperatures to values from Reference 9 which were experimentally established for oscillatory flow. Since the hydraulic flow in the brake control line associated with antiskid operation is transitory, the laminar flow resistance base on experimental measurements for oscillatory flow is used.

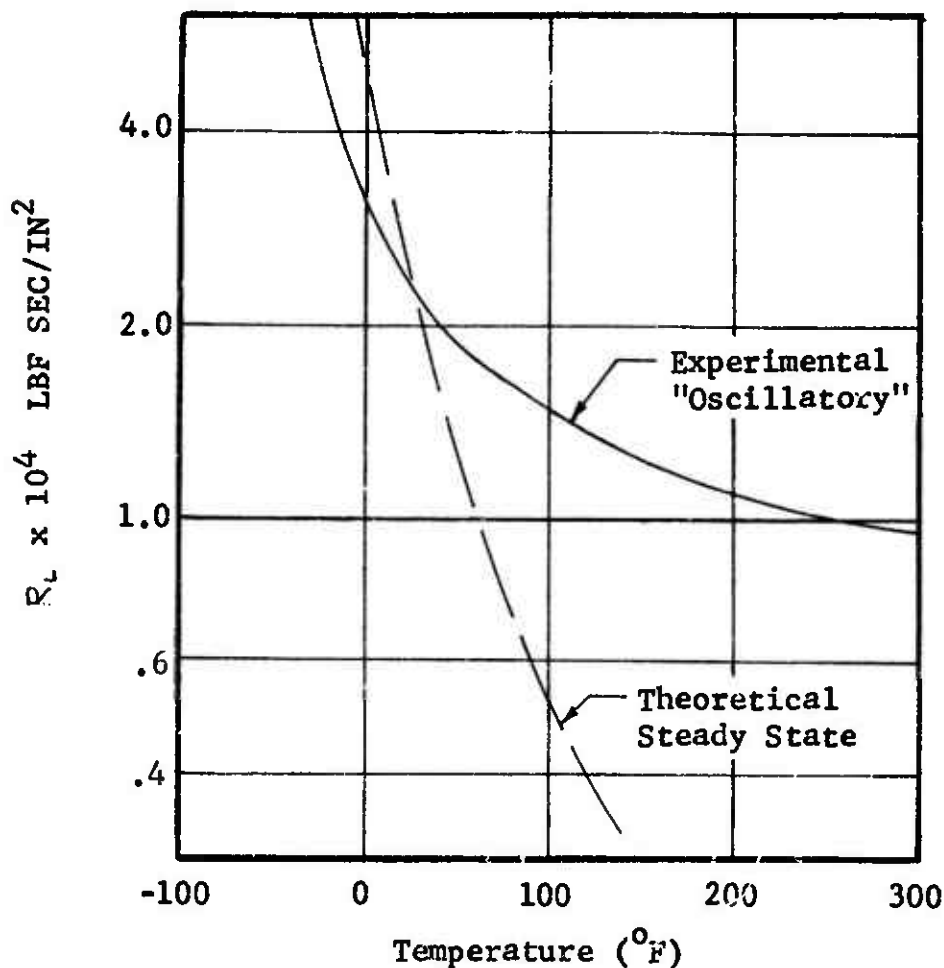


Figure A10 Hydraulic Fluid Damping Characteristic

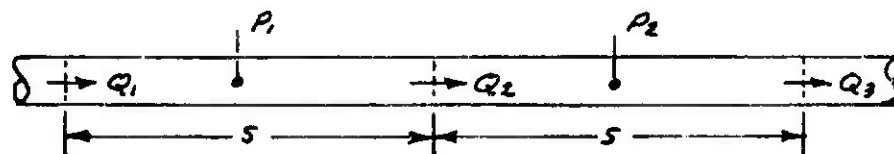
From Figure A10 at 100°F  $R_L$  for the experimental oscillatory case is  $1.5 \times 10^{-4}$  LBF SEC/IN<sup>2</sup>

Therefore:

$$\begin{aligned}
 (2.33) \quad D_{RBL} &= \frac{(R_L)(S_{BL})}{(A_{BL})^2} = \frac{(1.5 \times 10^{-4})(191)}{(.0386)^2} \\
 &= 19.22 \text{ lbf sec/in}^5
 \end{aligned}$$

When a "lumped parameter" type analysis as described by equations (2.20c), (2.21c) and (2.22c) is used for the control line the resulting natural frequency is somewhat lower than the actual line, if the actual line volume,  $V_{BL}$ , is used. The value of  $V_{BL}$  is adjusted as follows to achieve the correct natural frequency for the "lumped parameter" description.

Consider hydraulic fluid flowing through a line with cross sectional area,  $A$ , and divided into segments having equal length,  $S$ , as shown below.



If each segment is treated as a separate pressure vessel having volume,  $V$ , with a flow in and a flow out, and if equations of the form of (2.20c) (2.21c) and (2.22c) are written for these pressure vessels, neglecting friction, the following expressions are obtained:

$$(2.34) \quad \dot{Q}_2 = (A/\rho S)(P_1 - P_2)$$

$$(2.35) \quad \dot{P}_1 = (B/V)(Q_1 - Q_2)$$

$$(2.36) \quad \dot{P}_2 = (B/V)(Q_2 - Q_3)$$

By substituting equations (2.35) and (2.36) into equation (2.34) differentiated once with respect to time the following differential equation is formed:

$$(2.37) \quad \ddot{Q}_2 = (A/\rho S)(B/V) [(Q_1 - Q_2) - (Q_2 - Q_3)]$$

or

$$(2.38) \quad \ddot{Q}_2 + 2(AB/\rho SV) Q_2 = (AB/\rho SV)(Q_1 + Q_3)$$

Equation (2.38) establishes that the natural frequency of each line segment is:

$$(2.39) \quad f_n = \frac{1}{2\pi} \sqrt{\frac{2AB}{\rho SV}} \quad \text{cps}$$

However, vibration theory considering distributed mass and elasticity establishes the speed of sound,  $C$ , in the line as:

$$(2.40) \quad C = \sqrt{B/\rho} \quad \text{in/sec}$$

For fundamental mode oscillation in a closed end tube having length,  $S$ , the natural period,  $T_c$ , is:

$$(2.41) \quad T_c = 2S/c \quad \text{SEC}$$

Therefore, the natural frequency,  $g_n$ , of an actual tube segment is:

$$(2.42) \quad g_n = 1/T_c = (1/2S) \sqrt{B/\rho} \quad \text{CPS}$$

By equating the two expressions for natural frequency, equations (2.39) and (2.42), the volume of the line segment which will have the same natural frequency as the actual is established as:

$$(2.43) \quad V = 2AS/\pi^2$$

Thus,

$$(2.44) \quad V_{BL} = \frac{2}{\pi^2} A_{BL} S_{BL} = \frac{(2)(.0386)(191)}{\pi^2} = 1.495 \text{ IN}^3$$

### Brake Housing

The brake housing has ten pistons of  $1.33 \text{ in}^2$  area each. Since the number of pistons serviced by one control line is five, then  $A_{gps} = 5(1.33) = 6.65 \text{ in}^2$ . The fluid volume in the brake housing with the pistons bottomed ( $X_p = 0$ ) is  $8.00 \text{ in}^3$ . Thus  $V_{B0} = 4.00 \text{ in}^3$  or one-half the total volume. The orifice coefficient  $A_{B0}$  was estimated to be about  $2.0 \text{ IN}^4/\text{SEC lbf}^{1/2}$ .

### Optional Systems

The option 1 system neglects the line inertial effects. The parameters have the same value as the corresponding parameters for the option 3 system, except that  $V_{B0}$  should include any line volume. Thus, for the F-111 system, with the option 1 system,  $V_{B0} = 4.00 + .0386(191) = 11.36 \text{ IN}^3$ .

The option 2 description is used for systems with compressible pneumatic fluid. The appropriate parameters will be evaluated for nitrogen at  $100^\circ\text{F}$  as the fluid media and isothermal processes are assumed except for orifice flow calculations. While the heat transfer characteristics of the brake system components have not been rigorously evaluated, the usual component installation is such that assuming isothermal processes is valid. The mathematical description of the brake actuation control system using compressible pneumatic fluid is written using equations of the same general form as for those describing the hydraulic system, thereby minimizing the

the number of equations and enhancing computation flexibility. Utilizing the hydraulic equations when pneumatic fluid is used requires that the appropriate parameters be expressed in suitable mathematically equivalent terms. Consider the characteristic equation of state for a perfect gas:

$$(2.45) \quad P = \frac{MRT}{V}$$

And the definition:

$$(2.46) \quad \frac{dP}{dt} = \frac{\partial P}{\partial m} \frac{dm}{dt} + \frac{\partial P}{\partial V} \frac{dV}{dt} + \frac{\partial P}{\partial T} \frac{dT}{dt}$$

For the assumed isothermal process, substitution of equation (2.45) into equation (2.46) gives:

$$(2.47) \quad \dot{P} = \left(\frac{RT}{V}\right) \dot{m} - \left(\frac{RT}{V}\right) \frac{m}{V} \dot{V}$$

For those cases, such as for the metering valve and control valve pressure cavities, where the volume is not changing,  $\dot{V}$  is zero and equation (2.47) reduces to:

$$(2.48) \quad \dot{P} = \left(\frac{RT}{V}\right) \dot{m}$$

For hydraulic fluid,  $\dot{P}$  is described by equations having the form of equation (2.49) below. (See equation (2.11) for instance.)

$$(2.49) \quad \dot{P} = \left(\frac{\beta}{V}\right) Q$$

Noting the similarity between equation (2.48) and equation (2.49) it is obvious that if  $RT$  is used in place of  $\beta$  and if  $\dot{m}$  is used in place of  $Q$ , the "Hydraulic" equations can be used for computing performance of a system using pneumatic fluid. Thus,  $\beta_B = \beta_{cVR} = \beta_{mv} = RT$ .

For nitrogen  $R = 662.4 \text{ in lbF/lbm}^\circ\text{F}$  and at  $100^\circ\text{F}$   
 $RT = (662.4)(460 + 100) = 371 \times 10^6 \text{ in lbF/lbm.}$

Since  $P/RT = M/V$ , equation (2.47) can be written as

$$(2.50) \quad \dot{P} = \left(\frac{RT}{V}\right) \left[ \dot{m} - \left(\frac{P}{RT}\right) \dot{V} \right]$$

Equation (2.21b) is obtained by substituting  $\beta_B$  for  $RT$ ,  $A_{BPS} \dot{X}_P$  for  $\dot{V}$ , and  $Q$  for  $\dot{m}$  in equation (2.50), thereby accounting for the change in brake volume caused by piston movement.

Equation (2.51) below, from Reference 6, describes the mass flow rate of a gas from a container having high pressure,  $P_H$ , through an orifice of area,  $A_o$ , to a container having

low pressure,  $P_L$  .

$$(2.51) \quad \dot{m} = \left( \frac{C_o A_o}{R} \sqrt{\frac{2GC_p}{T}} \right) P_H \left( \frac{P_H}{P_L} \right)^{1/2} \sqrt{1 - \left( \frac{P_H}{P_L} \right)^{\frac{\gamma-1}{\gamma}}}$$

Equation (2.52) below, from Reference 6, describes the volumetric flow rate of hydraulic fluid through an orifice under similar circumstances.

$$(2.52) \quad Q = C_o A_o \left( \sqrt{2/\rho} \right) \sqrt{P_H - P_L}$$

Both equations (2.51) and (2.52) can be written in the form  $Q = A_F \phi(P_H, P_L)$  where  $\phi(P_H, P_L)$  is a flow function as defined by equations (2.4) and (2.5) for the appropriate circumstances and where  $A_F$  is a flow coefficient accounting for orifice and fluid properties. For the case of hydraulic fluids a value of  $C_o \sqrt{2/\rho} = 103.5 \text{ in}^2/\text{lbF}^{1/2} \text{ sec}$  has been established by experience as being representative of an average orifice (i.e.,  $C_o \approx 0.65$ ). The metering valve flow coefficient,  $A_{mvo}$ , previously computed is  $0.653 \text{ in}^4/\text{sec lbF}^{1/2}$ ; therefore, the apparent actual orifice area,  $A_o$ , for the metering valve is  $A_o = 0.653/103.5 = .63 \times 10^{-2} \text{ in}^2$  .

For the case of the pneumatic system with nitrogen at  $100^\circ\text{F}$  as the working fluid and using  $C_p = 2300 \text{ in lbF/lbm}^\circ\text{F}$ , and  $R = 662.4 \text{ in lbF/lbm}^\circ\text{F}$ :

$$\begin{aligned} (2.53) \quad A_{mvo} &= \frac{C_o A_o}{R} \sqrt{\frac{2GC_p}{T}} \\ &= \frac{(.8)(.63 \times 10^{-2})}{662.4} \sqrt{\frac{(12)(386)(2300)}{560}} \\ &= 0.43 \times 10^{-3} \text{ lbm in}^2/\text{lbF sec} \end{aligned}$$

Using the same procedure establishes that:

$$A_{cvo} = 0.716 \times 10^{-3} \text{ lbm in}^2/\text{lbF sec}$$

$$A_{rc} = 0.658 \times 10^{-3} \text{ lbm in}^2/\text{lbF sec}$$

Table A4 lists the parameters for Hydraulic System Options 1, 2 and 3. The parameters which apply for the Option 4 Hydraulic System are listed in Table A5.

Table A4 Option 1, 2 and 3 Hydraulic System Parameters (Sheet 1 of 5)

SYMBOL	TYPE	VALUE	UNITS	OP*			DESCRIPTION
				1	2	3	
$A_{BL}$	c	.0386	$IN^2$			X	Cross sectional area of brake control line
$A_{B\theta}$	c	2.00	$IN^4/SEC LBF^{\frac{1}{2}}$			X	Brake housing orifice coefficient
$A_{BPS}$	c	6.65	$IN^2$	X	X	X	Brake piston area (per brake line)
$A_{CV} \langle x \rangle$	f			X	X	X	Control valve flow area function
$A_{CVL}$	c	0.00	$IN^4/SEC LBF^{\frac{1}{2}}$	X	X	X	Control valve leakage flow coeff.
$A_{CVO}$	c	0.00	$LBM IN^2/LBF SEC$				
$A_{CVR}$	v	1.09	$IN^4/SEC LBF^{\frac{1}{2}}$	X	X	X	Control valve full open flow coeff.
$A_{CVS}$	v	.716X10 <sup>-3</sup>	$LBM IN^2/LBF SEC$	X	X	X	Control valve return flow coeff.
$A_{MV} \langle x \rangle$	f			X	X	X	Control valve supply coeff.
$A_{MVL}$	c	0.00	$IN^4/SEC LBF^{\frac{1}{2}}$	X	X	X	Metering valve flow area function.
$A_{MVO}$	c	0.00	$LBM IN^2/SEC LBF$	X	X	X	Metering valve leakage coeff.
$A_{MVO}$	c	.653	$IN^4/SEC LBF^{\frac{1}{2}}$	X	X	X	Metering valve full open flow coeff.
$A_{MVR}$	v	.429X10 <sup>-3</sup>	$LBM IN^2/SEC LBF$	X	X	X	Metering valve return flow coeff.
$A_{MVS}$	v		$IN^4/SEC LBF^{\frac{1}{2}}$	X	X	X	Metering valve supply flow coeff.
$A_{RC}$	c	1.00	$IN^4/SEC LBF^{\frac{1}{2}}$	X	X	X	Control valve return line restriction.
$B_B$	c	.658X10 <sup>-3</sup>	$LBM IN^2/LBF SEC$	X	X	X	Bulk modulus within the brake housing.
	c	.248X10 <sup>6</sup>	$LBF/IN^2$	X	X	X	
	c	.371X10 <sup>6</sup>	$IN LBF/LBM$	X	X	X	Temp X gas constant.

\*See notes on Sheet 5

Table A4 Option 1, 2 and 3 Hydraulic System Parameters (Sheet 2 of 5)

SYMBOL	TYPE	VALUE	UNITS	OP*			DESCRIPTION
				1	2	3	
B <sub>SL</sub>	c	.218 X 10 <sup>6</sup>	LBF/IN <sup>2</sup>				Fluid bulk modulus in control line.
B <sub>cvr</sub>	c	.248 X 10 <sup>6</sup>	LBF/IN <sup>2</sup>	X			Fluid bulk modulus in return of control V.
	c	.371 X 10 <sup>6</sup>	IN LBF/LBM		X		Temp. X gas constant, Cont Valve Return Cavity
B <sub>mv</sub>	c	.248 X 10 <sup>6</sup>	LBF/IN <sup>2</sup>	X			Bulk modulus at MV outlet
	c	.371 X 10 <sup>6</sup>	IN LBF/LBM		X		Temp X gas constant, metering valve outlet
D <sub>REL</sub>	c	19.22	LBF SEC/IN <sup>5</sup>			X	Laminar line loss coeff.
D <sub>TAL</sub>	c	.216	LBF SEC <sup>2</sup> /IN <sup>8</sup>			X	Turbulent line loss coeff.
G <sub>MV</sub>	c	.05	IN <sup>3</sup> /SEC LBF	X		X	Metering valve gain
	c	.05	IN <sup>3</sup> /SEC LBF		X		
Y <sub>a</sub>	c	1.40	Dimensionless			X	Ratio of specific heats $\gamma_a = (c_p/c_v)$
P <sub>B</sub>	v(o)		LBF/IN <sup>2</sup>	X	X	X	Brake Pressure
P <sub>eo</sub>	c	100	LBF/IN <sup>2</sup>		X	X	Brake pressure at time = 0.
	v		LBF/IN <sup>2</sup>	X			
P <sub>B</sub>	v		LBF/IN <sup>2</sup> SEC		X		Time derivative of brake press.
P <sub>BI</sub>	v		LBF/IN <sup>2</sup>	X	X	X	Press. at brake inlet.
P <sub>Bo</sub>	c	100	LBF/IN <sup>2</sup>		X	X	Brake inlet press at time = 0.
	v		LBF/IN <sup>2</sup>	X			
P <sub>BI</sub>	v		LBF/IN <sup>2</sup> SEC		X		Brake inlet press time derivative
P <sub>com</sub>	v	1500	LBF/IN <sup>2</sup>	X	X	X	Pilot's command press.
P <sub>cp</sub>	c		LBF/IN <sup>2</sup>	X	X	X	Steady state command press.
P <sub>cv</sub>	v(o)		LBF/IN <sup>2</sup>	X	X	X	Control valve output press.
P <sub>cvo</sub>	c	100	LBF/IN <sup>2</sup>		X	X	Control valve press at time = 0.
	c	14.7	LBF/IN <sup>2</sup>	X			
P <sub>cv</sub>	v		LBF/IN <sup>2</sup> SEC		X	X	Derivative of control valve press.

Table A4 Option 1, 2 and 3 Hydraulic System Parameters (Sheet 3 of 5)

SYMBOL	TYPE	VALUE	UNITS	OP			DESCRIPTION
				1	2	3	
$P_{CVR}$	v(o)	100	$LBF/IN^2$	X	X	X	Return press in cont. valve.
$P_{Cvro}$	c	14.7	$LBF/IN^2$	X	X	X	Cont valve ret press time 0
$\dot{P}_{CVR}$	v		$LBF/IN^2$	X	X	X	Derivative of cont VA press ret
$\phi(x,y)$	f		$LBF/IN^2$	X	X	X	Flow function
$P_{MV}$	v(o)	100	$LBF/IN^2$	X	X	X	Metering valve output press.
$P_{MVO}$	c	14.7	$LBF/IN^2$	X	X	X	Metering valve press at time = 0.
$\dot{P}_{MV}$	v		$LBF/IN^2$	X	X	X	Time derivative of MV press
$P_R$	c	100	$LBF/IN^2$	X	X	X	Return pressure
$P_S$	c	14.7	$LBF/IN^2$	X	X	X	System supply pressure.
$Q_B$	c	3000	$IN^3/SEC$	X	X	X	Flow into brake (per line)
$Q_{CV}$	v		$LBM/SEC$	X	X	X	Flow out of control valve
$Q_{CVO}$	c	0.0	$IN^3/SEC$	X	X	X	Control valve flow at time = 0
$\dot{Q}_{CV}$	v		$LBM/SEC$	X	X	X	Time derivative cont VA flow
$Q_{CV1}$	v(i)		$IN^3/SEC$	X	X	X	Feedback flows from control valve.
$Q_{CV2}$	v(i)		$LBM/SEC$	X	X	X	
$Q_{CV3}$	v(i)		$IN^3/SEC$	X	X	X	

Table A4 Option 1, 2 and 3 Hydraulic System Parameters (Sheet 4 of 5)

SYMBOL	TYPE	VALUE	UNITS	OP			DESCRIPTION
				1	2	3	
$Q_{CVR}$	V		IN <sup>3</sup> /SEC	X		X	Return flow in control valve
$Q_{MV}$	V		LBM/SEC	X	X		Metering valve flow
$Q_R$	V		IN <sup>3</sup> /SEC		X		Return flow from metering valve
$Q_{RC}$	V		LBM/SEC	X	X	X	Return flow from control valve
$Q_S$	V		IN <sup>3</sup> /SEC	X	X	X	Flow into system
$R_{CRIT}$	C		LBM/SEC		X		Critical pressure ratio
$R_{HO}$	C	$\#$	Dimensionless		X		Fluid density
$S_{BL}$	C	$.781 \times 10^{-4}$	LBF SEC <sup>2</sup> /IN <sup>4</sup>	X		X	Control line length
$S_{CL}$	C	191.0	IN	X	X	X	Control valve overlap
$S_{CVO}$	C	.005	IN	X	X	X	Spool distance from full closed to full open (C.V)
$S_{MVL}$	C	.030	IN	X	X	X	Min. Neg. spool travel (met. valve)
$S_{MVO}$	C	-.060	IN	X	X	X	Spool travel from full closed to full open (met. valve)
$S_{MVU}$	C	.050	IN	X	X	X	Max. Pos. Spool travel (met. valve)
$T$	C	.060	SEC	X	X	X	Time
$T_{CP}$	V(i)	.200	SEC	X	X	X	Time for $P_{com} = P_{cp}$
$V_B$	C		IN <sup>3</sup>	X	X	X	Brake fluid volume (per line)
$V_{BO}$	V	4.00	IN <sup>3</sup>	X	X	X	Brake fluid volume when $X_p = 0$
$V_{BL}$	C	1.495	IN <sup>3</sup>	X	X	X	Corrected line volume

$\#$  Calculate from  $\gamma_o$ , see Equation (2.5)

Table A4 Option 1, 2 and 3 Hydraulic System Parameters (Sheet 5 of 5)

SYMBOL	TYPE	VALUE	UNITS	OP*			DESCRIPTION
				1	2	3	
$V_{CVR}$	C	2.00	IN <sup>3</sup>	X	X	X	Control valve return volume.
$V_{MV}$	V		IN/SEC	X	X	X	Metering valve control variable.
$V_{MIV}$	C	1.00	IN <sup>3</sup>	X	X	X	Volume between metering & control valve.
$X_{CV}$	V(i)		IN	X	X	X	Control valve spool position.
$X_{MV}$	V		IN	X	X	X	Metering valve spool position.
$X_{MVO}$	C	0.0	IN	X	X	X	Metering valve spool position at time=0
$\dot{X}_{MV}$	V		IN/SEC	X	X	X	Metering valve spool velocity.
$X_P$	V(i)		IN	X	X	X	Brake piston displacement
$\dot{X}_P$	V(i)		IN/SEC	X	X	X	Brake piston velocity

\*An x denotes application in option 1, 2, or 3 as explained on page 35-37.

- Option 1 Brake actuation system using hydraulic fluid where the control line description considers volume effects only.
- Option 2 Brake actuation system using compressible pneumatic fluid.
- Option 3 Brake actuation system using hydraulic fluid where the control line description considers both volume and inertia effects.

Table 4.5 Option 4 Hydraulic System Parameters (Sheet 1 of 2)

SYMBOL	TYPE	VALUE	UNITS	DESCRIPTION
ACVR	v		IN <sup>4</sup> /SEC LBF <sup>1/2</sup>	Hydraulic flow coefficient, control valve return
ACVRO	c	1.09	IN <sup>4</sup> /SEC LBF <sup>1/2</sup>	Hydraulic flow coeff, control valve return, full open to return
ACVS	v		IN <sup>4</sup> /SEC LBF <sup>1/2</sup>	Hydraulic flow coeff, control valve supply
ACVSO	c	1.09	IN <sup>4</sup> /SEC LBF <sup>1/2</sup>	Hydraulic flow coeff, control valve supply, full open to supply
ACVL	c	0	IN <sup>4</sup> /SEC LBF <sup>1/2</sup>	Hydraulic flow coeff, Control valve null position
CBVI	c	50	LBF/IN <sup>5</sup>	Brake pressure - Volume coefficient - Before disc contact
CBVZ	c	3550	LBF/IN <sup>5</sup>	Brake pressure - Volume coefficient - After disc contact
PCP	-		LBF/IN <sup>2</sup>	Pilot command brake pressure
PCV	v(o)	1500	LBF/IN <sup>2</sup>	Control valve output pressure
PCVR	v(o)		LBF/IN <sup>2</sup>	Return pressure in control valve
PR	c	100	LBF/IN <sup>2</sup>	Reservoir pressure
PB	v(o)		LBF/IN <sup>2</sup>	Brake pressure
PBR1	c	100	LBF/IN <sup>2</sup>	Brake bias pressure before disc contact
PBR2	c	-5480	LBF/IN <sup>2</sup>	Brake bias pressure after disc contact
PBI	v		LBF/IN <sup>2</sup>	Brake pressure before disc contact
PB2	v		LBF/IN <sup>2</sup>	Brake pressure after disc contact
QMV	v		IN <sup>3</sup> /SEC	Hydraulic flow rate out of metering valve
QCVR	v		IN <sup>3</sup> /SEC	Hydraulic flow rate from control valve to return
QB	v		IN <sup>3</sup> /SEC	Hydraulic flow rate into brake
SCVO	c	0.030	IN	Position of control valve spool for max flow

Table A5 Option 4 Hydraulic System Parameters (Sheet 2 of 2)

SYMBOL	TYPE	VALUE	UNITS	DESCRIPTION
$T$	v(l)		SEC	Time for $P_{mv} = P_{cp}$
$T_{CP}$	c	0.1	SEC	Control Valve Spool position
$X_{CV}$	v(l)		IN <sup>3</sup>	Brake hydraulic volume
$V_B$	v	0	IN <sup>3</sup>	Brake hydraulic volume at time zero
$V_{BO}$	c		IN <sup>3</sup>	Metering valve output pressure
$P_{mv}$	v		LBF/IN <sup>2</sup>	Brake volume at disc contact
$V_{BC}$	c	1.6	IN <sup>3</sup>	

### 3a VEHICLE AND WHEEL STRUCTURAL SUPPORT (FLYWHEEL)

Figure A11 shows the model for the airplane system as it might be simulated with a dynamometer flywheel set-up. The mass  $W_A$  is supported by the tire and is determined by the percentage of the airplane weight carried on one main gear. The mass  $W_{AR}$  represents some part of the airplane structure which could vibrate in sympathy with certain ground discontinuities such as wing mounted fuel tanks or armament. The forces  $F_{LO}$  and  $F_{AL}$  act on  $W_A$  because of gravity and aerodynamic lift, respectively.

#### A. Mathematical Description

The shock strut stroke is denoted by  $Z_{sm}$ . This stroke is determined by  $Z$  and  $Z_{wm}$ .

$$(3a.1) \quad Z_{sm} = Z_{wm} - Z + S_m G_L$$

$$(3a.2) \quad \dot{Z}_{sm} = \dot{Z}_{wm} - \dot{Z}$$

The shock strut force  $F_{vm}$  is given by equation (3a.3)

$$(3a.3) \quad F_{vm} = F_{vms} \langle Z_{sm} \rangle + D_{vm} \dot{Z}_{sm} + A_{vm} \langle Z_{sm} \rangle \dot{Z}_{sm} |\dot{Z}_{sm}| + D_{vmc} G_m \langle \ddot{Z}_{sm} \rangle$$

Where

$$G_m \langle X \rangle = \begin{aligned} &+1.0 && \text{FOR } X > 0 \\ &= 0 && \text{FOR } X = 0 \\ &= -1.0 && \text{FOR } X < 0 \end{aligned}$$

Let  $Z_{go}$  and  $Z_{gop}$  denote the height and slope of the ground (or flywheel surface). Let  $S_m$  denote the tire deflection. Then  $S_m$  and  $\dot{S}_m$  are determined by

$$(3a.4) \quad S_m = \max \{ 0.0, Z_{go} \langle X_F \rangle - Z_{wm} + R_{OT} \}$$

$$(3a.5) \quad \dot{S}_m = Z_{gop} \langle X_F \rangle V_F - \dot{Z}_{wm}$$

The force  $F_{NM}$  acting vertically upward on the tire is then given by

$$(3a.6) \quad F_{NM} = S_m (C_{MT} + D_{MT} \dot{S}_m)$$

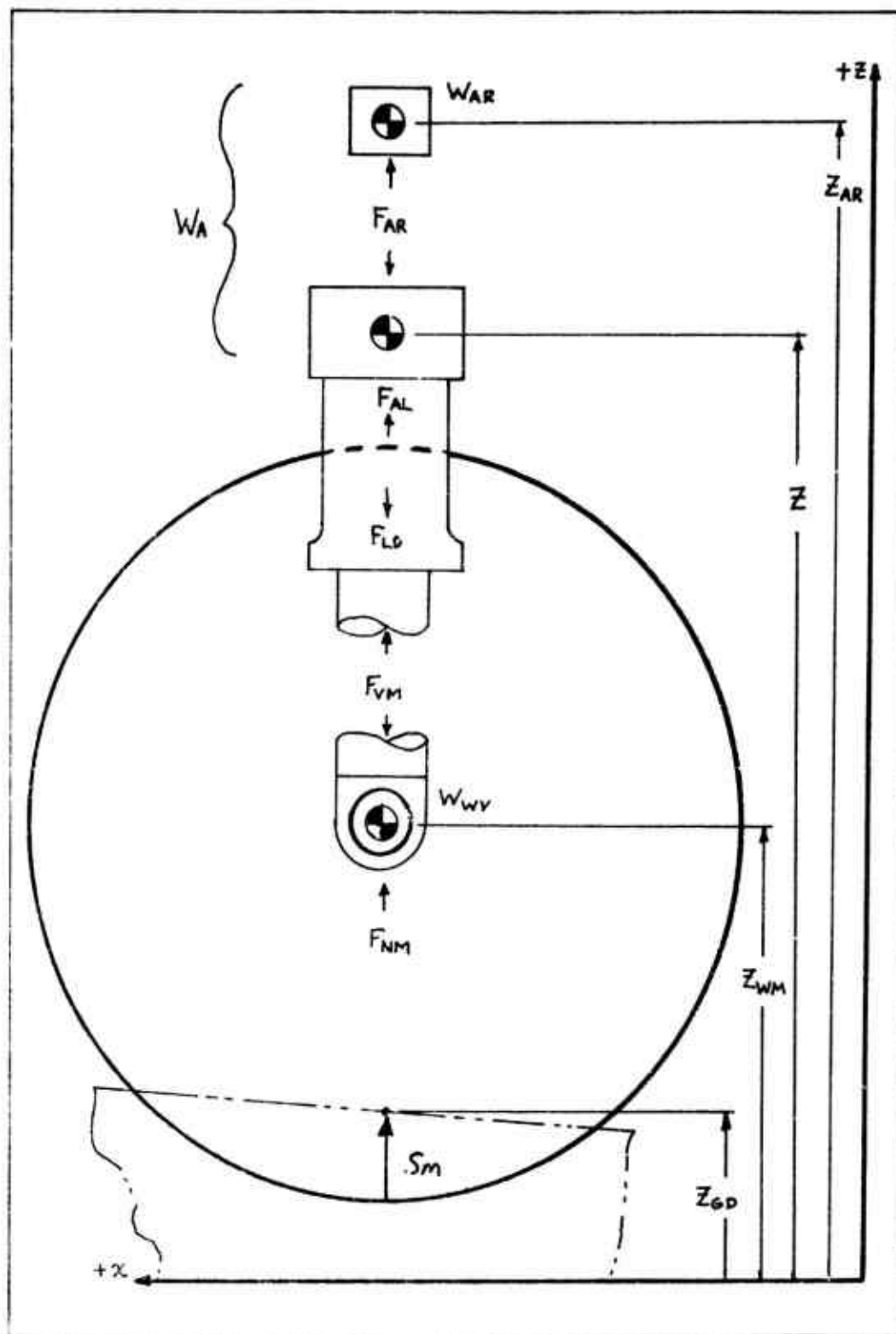


Figure A1 Flywheel System Model

Summing forces in the vertical direction on the unsprung mass  $W_{WV}$ , there follows:

$$(3a.7) \quad W_{WV} \ddot{Z}_{WM} = F_{NM} - F_{VM} + F_{ORV}$$

Where  $F_{ORV}$  is the tire unbalance force.

For the mass  $W_{AR}$ , summing forces vertically gives:

$$(3a.8) \quad W_{AR} \ddot{Z}_{AR} = F_{AR}$$

$$(3a.9) \quad F_{AR} = C_{AR} (Z - Z_{AR}) + D_{AR} (\dot{Z} - \dot{Z}_{AR})$$

The aerodynamic lift and drag forces  $F_{AL}$  and  $F_{AD}$  are defined as follows:

$$(3a.10) \quad F_{AL} = C_{AL} V_F^2$$

$$(3a.11) \quad F_{AD} = C_{AD} V_F^2$$

The equation which determines  $Z$  is given as

$$(3a.12) \quad (W_A - W_{AR}) \ddot{Z} = F_{VM} + F_{AL} - F_{LD} - F_{AR}$$

The equation for the flywheel velocity is given by

$$(3a.13) \quad W_{AT} \dot{V}_F = F_{TH} - F_{AD} - 2 F_{BT}$$

Where  $F_{TH}$  is a force equivalent to engine thrust and  $W_{AT}$  is the airplane mass. The aircraft's longitudinal displacement is established by

$$(3a.14) \quad X_F = \int V_F dt + X_{F0}$$

The equation flow diagram for the airplane system (flywheel) is shown on Figure A12.

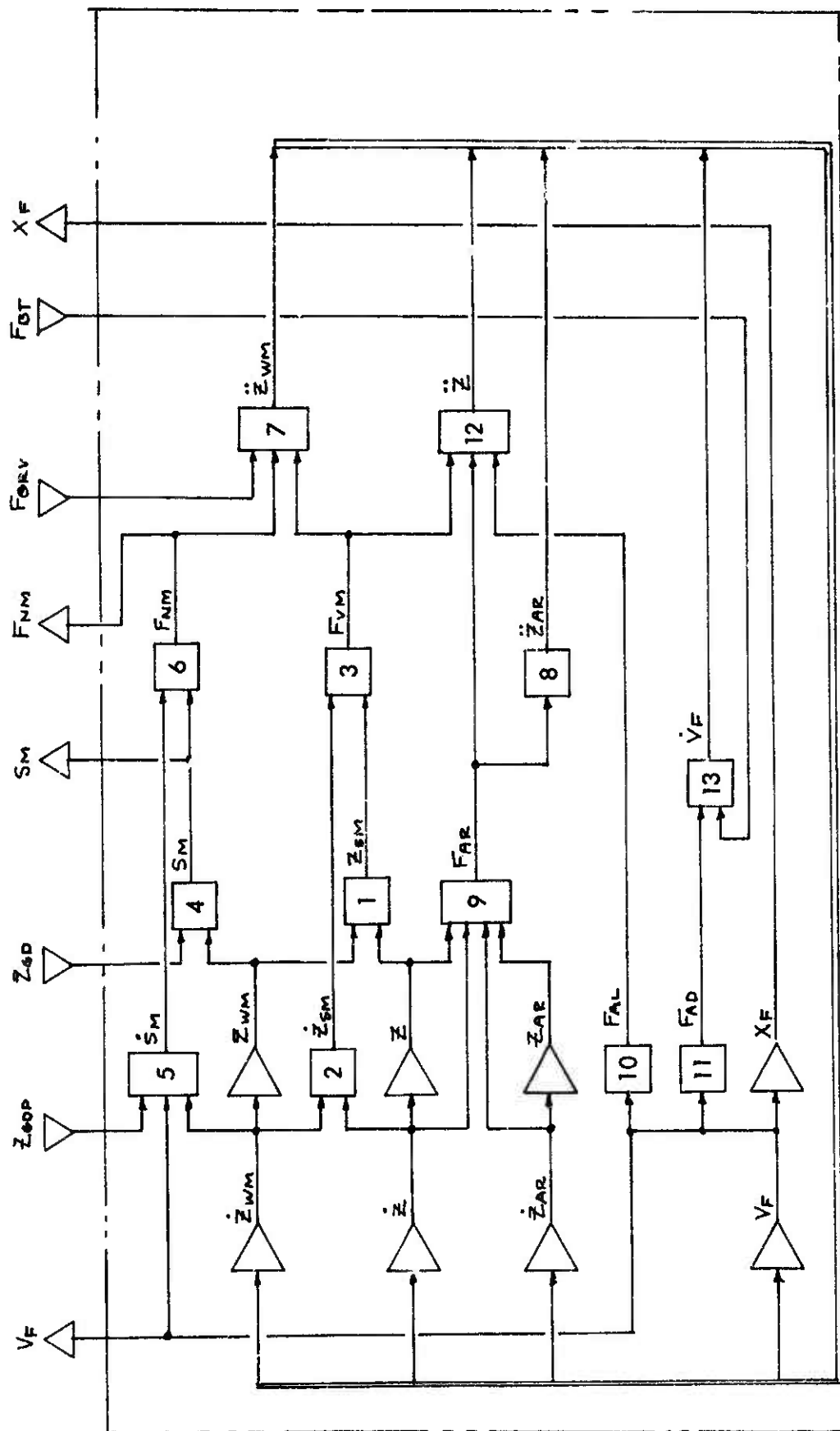


Figure A 12 Airplane System (Flywheel) Equation Flow Diagram

## B. Parameter Evaluation

### Shock Strut Characteristics

Figures A13 and A14 show the main gear load and damping characteristics for one gear.

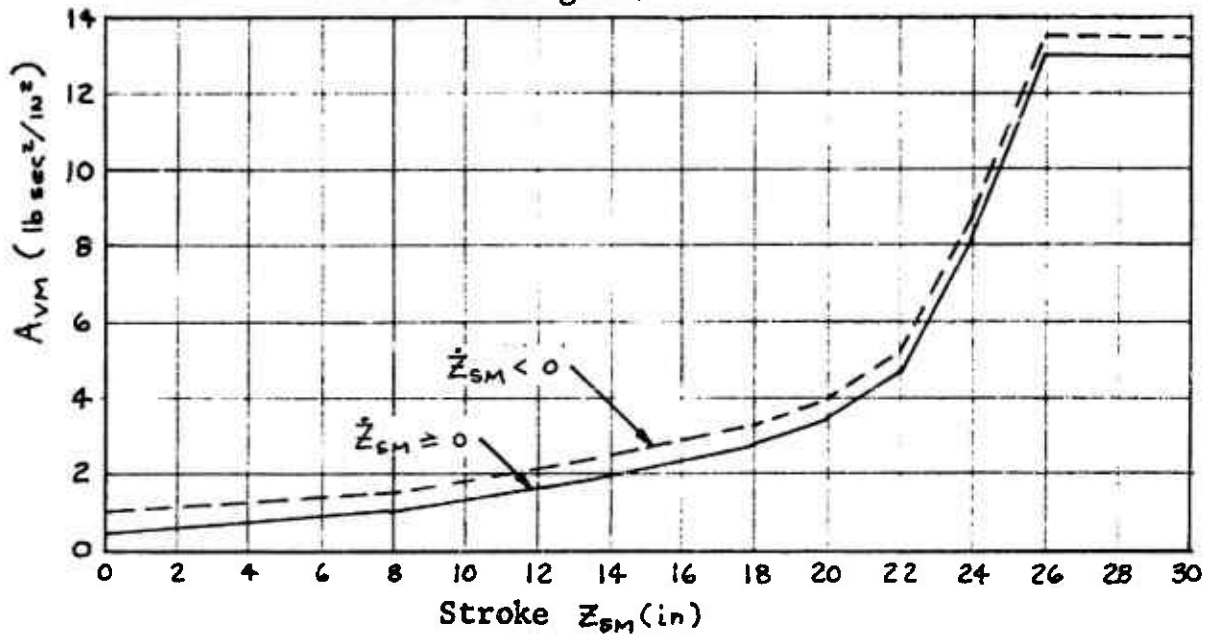


Figure A13 Main Gear Damping Curve

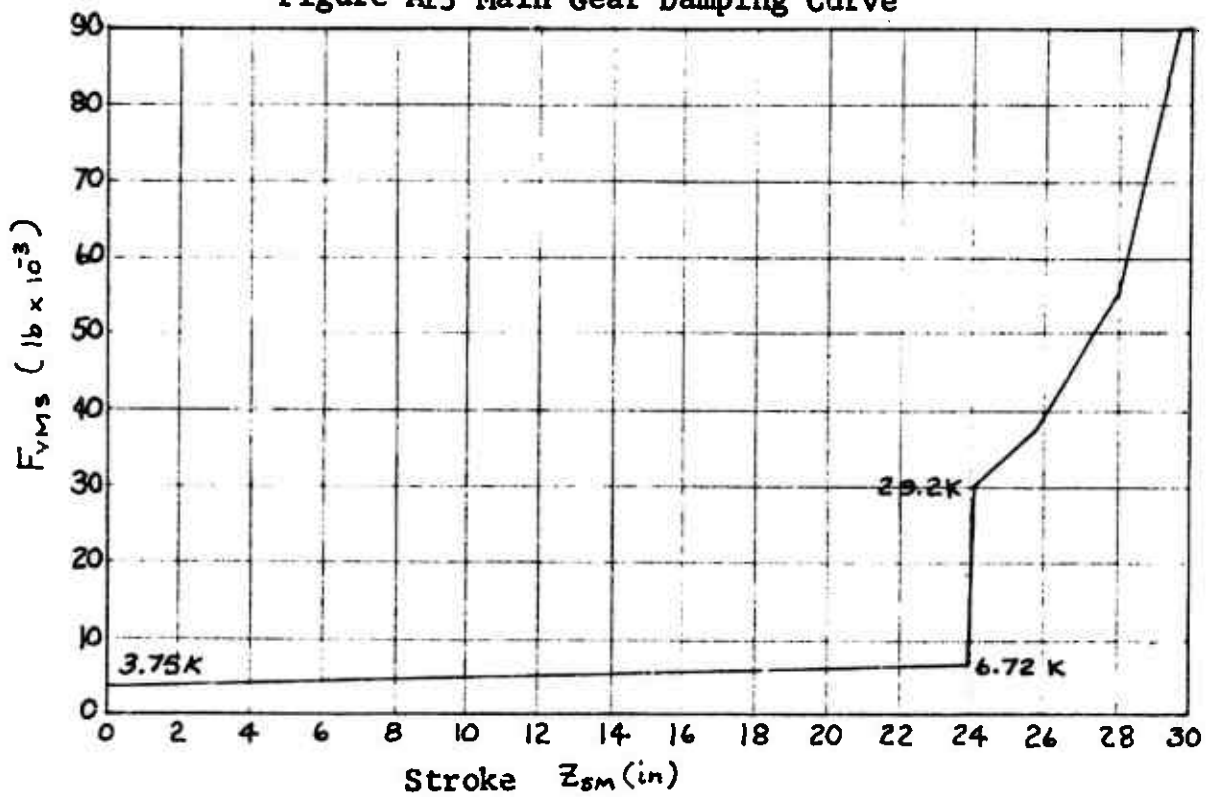


Figure A14 Main Gear Air Load Curve

### Vertical Tire Characteristics

In equation (3a.6) it has been assumed that the tire loading characteristic is given by an equation of the form

$$(3a.15) \quad F = S(C + D\dot{S})$$

Let the following terms be defined for a tire:

$F_R$  = Rated load

$P_R$  = Rated pressure

$S_R$  = Rated deflection

If  $P$  is the actual pressure, then obviously the tire spring rate,  $C$ , is

$$(3a.16) \quad C = \left(\frac{P}{P_R}\right) \left(\frac{F_R}{S_R}\right)$$

From reference 1 (Equation 132) the damping force,  $F_D$ , is established as:

$$(3a.17) \quad F_D = \left(\frac{\eta C}{\omega}\right) \dot{S}$$

It is assumed that the damping force is related to the undamped natural frequency at rated conditions. The undamped natural frequency,  $\omega$ , is established as:

$$(3a.18) \quad \omega = \sqrt{\frac{K}{M}} = \sqrt{\frac{F_R G}{S_R F_R}} = \sqrt{\frac{G}{S_R}}$$

Where  $G = 386 \text{ IN/SEC}^2$ . Also from Equations 137 and 138 of Reference 1:

$$(3a.19) \quad \eta = 2 \eta_R / [1 + (P/P_R)]$$

Where  $\eta_R = 0.1$ .

The main landing gear shock strut linear damping coefficient,  $D_{VM}$ , is set equal to zero for the example problem.

The unsprung mass,  $W_{wv}$ , experiencing vertical motion is 6.44 lbm. Thus,  $W_{wv} = (644)/386 = 1.667 \text{ lbf sec}^2/\text{in}$ .

As previously assumed in Equation (3a.15),  $F_0 = 50\dot{S}$   
Equating the two expressions for  $F_0$  at rated deflection

$$(3a.20) \quad \frac{\eta C}{\omega} = S_R D$$

Or

$$(3a.21) \quad D = \frac{\eta C}{\omega S_R} = \frac{\eta F_R}{(S_R)^2} \left( \frac{P}{P_R} \right) \sqrt{\frac{S_R}{G}}$$

For the 47 x 18 - 18 26 ply rating F-111 main tire,  
 $P = P_R = 150$  psi

$F_R = 38,100$  lb. and  $S_R = 4.00$  IN.

Thus

$$(3a.22) \quad C_{MT} = \left( \frac{P}{P_R} \right) \left( \frac{F_R}{S_R} \right) = \frac{(150)(38100)}{(150)(4.00)} = 9530 \text{ lbf/IN}$$

$$(3a.23) \quad D_{MT} = \left( \frac{P}{P_R} \right) \left( \frac{\eta F_R}{S_R^2} \right) \sqrt{\frac{S_R}{G}}$$

$$= \frac{(150)(.1)(38100)}{(150)(4.00)^2} \sqrt{\frac{4.0}{386}} = 24.24 \text{ lbf sec/IN}^2$$

#### Aircraft Characteristics

For the example problem, an airplane weight of 57,000 lb. is used. The static vertical load on one main gear is 25,200 lbs. so that

$$(3a.24) \quad W_A = 25,200/G = 65.0 \text{ lbf sec}^2/\text{IN}.$$

For a velocity of  $V_F = 2400$  IN/SEC and a representative tire-to-runway braking coefficient of .45 at the main wheel, the tire load is 21,400 lbs. Thus  $F_{L0} = 21,400$  lb.

The total aircraft mass is  $W_{AT} = 57000/G = 147.8 \text{ lbf sec}^2/\text{IN}.$

The mass  $W_{AR}$  is used to simulate some airplane resonant effect. For illustrative purposes, it is assumed that  $W_{AR} = 1000 \text{ LBM} = 2.59 \text{ LBF SEC}^2/\text{IN}$  and has a natural frequency of 12 cps. Therefore, since  $\omega = 2\pi(12) = 75.4 \text{ rad/sec}$  and  $k = m\omega^2$ ,

$$(3a.25) C_{AR} = \omega^2 W_{AR} = (75.4)^2 (2.59) = 14,720 \text{ lb/in}$$

Using 3 percent critical damping gives

$$(3a.26) D_{AR} = (.03) 2 \sqrt{C_{AR} W_{AR}} = \\ = (.03) 2 \sqrt{(14,720)(2.59)} = 11.72 \text{ lb sec/in}$$

The initial conditions are calculated for equilibrium. At time = 0, let  $X_F = 0$  so that  $Z_{GD} \langle X_F \rangle = 0$  since  $Z_{GD} \langle 0 \rangle$  is always 0. Let  $V_{FO} = 1200 \text{ IN/SEC}$  and assume that  $C_{AL} = C_{AD} = 0$

From equation (3a.6),

$$(3a.27) S_m = F_{NM} / C_{MT} = 26000 / 9530 = 2.73 \text{ in}$$

From equation (3a.4),

$$(3a.28) Z_{WMO} = (0 - 2.73 + 23.98) = 20.59 \text{ in}$$

From figure A14 when  $F_{VMS} = 26000 \text{ lb.}$ ,

$Z_{SM} = 23.98 \text{ in}$  and from equation (3a.1),

$$(3a.29) Z_0 = Z_{WMO} - Z_{SM} + S_m g_L = 20.59 - 23.98 + 83.41 = 80.0 \text{ in.}$$

Also  $Z_{ARO} = Z_0 = 80.0 \text{ in.}$

For the example problem the effects of aerodynamic forces are not included in the flywheel simulation; therefore,  $C_{AD} = 0.0$  and  $C_{AL} = 0.0$ .

The unsprung mass moving vertically,  $W_{WV}$ , is the same as  $W_{GW}$  described in the Section 4a Wheel and Tire System (Flywheel) for horizontal motion. Therefore,  $W_{WV} = 1.60 \text{ lbf sec}^2/\text{in.}$

The average engine idle thrust is 1000 lbf. Therefore,  $F_{TM} = 1000 \text{ lbf.}$

Table A6 Vehicle and Wheel Structural Support (Flywheel) Parameters  
(Sheet 1 of 3)

SYMBOL	TYPE	VALUE	UNITS	DESCRIPTION
A <sub>VM</sub>	V*		lb sec <sup>2</sup> /in <sup>2</sup>	Shock strut damping characteristic.
C <sub>AD</sub>	C	0.0	lb sec <sup>2</sup> /in <sup>2</sup>	Aerodynamic drag coefficient.
C <sub>AL</sub>	C	0.0	lb sec <sup>2</sup> /in <sup>2</sup>	Aerodynamic lift coefficient.
C <sub>AR</sub>	C	14,720	lb/in	Spring rate associated with mass W <sub>AR</sub>
C <sub>MT</sub>	C	9530	lb/in	Tire vertical spring rate
D <sub>AR</sub>	C	11.72	lb sec/in	Damping coeff. associated with mass W <sub>AR</sub>
D <sub>MT</sub>	C	38.8	lb sec/in <sup>2</sup>	WAR Tire damping coefficient
D <sub>VM</sub>	C	0.0	lb sec/in	Shock strut linear damping coeff.
F <sub>AD</sub>	V		lb	Aerodynamic drag force on airplane.
F <sub>AL</sub>	V		lb	Aerodynamic lift force on airplane
F <sub>AR</sub>	V		lb	Force associated with mass WAR
F <sub>BT</sub>	V(i)		lb	Braking force
F <sub>LD</sub>	C	21,400	lb	Static force on tire
F <sub>oev</sub>	V(i)		lb	Tire unbalance force (vertical)
F <sub>NM</sub>	V(o)		lb	Tire normal force
F <sub>TH</sub>	C	1000	lb	Engine thrust
F <sub>VM</sub>	V		lb	Shock strut force
F <sub>VMS</sub>	V**		lb	Shock strut force with $\dot{Z}_{SM} = 0$
S <sub>M</sub>	V(o)		in	Tire deflection
S <sub>M</sub>	V		in/sec	Rate of tire deflection
V <sub>F</sub>	V		in/sec	Flywheel velocity
V <sub>F0</sub>	C	2400	in/sec	Flywheel velocity at time = 0

\*point plot input see Figure 13  
\*\*point plot input see Figure 14

Table A6 Vehicle and Wheel Structural Support (Flywheel) Parameters  
(Sheet 2 of 3)

SYMBOL	TYPE	VALUE	UNITS	DESCRIPTION
$W_A$	C	65.0	lb sec <sup>2</sup> /in	Airplane mass carried on main gear.
$W_{AR}$	C	2.59	lb sec <sup>2</sup> /in	Mass of airplane substructure.
$W_{AT}$	C	147.8	lb sec <sup>2</sup> /in	Total airplane mass
$W_{WV}$	C	1.667	lb sec <sup>2</sup> /in	Unsprung mass
$X_F$	V(0)		in	Flywheel surface distance traveled.
$X_{FO}$	C	0.0	in	Flywheel distance at time = 0.
$Z$	V		in	Vertical location of equivalent apl. mass C.G.
$Z_0$	C	80.0	in	Vertical location of equivalent mass at time = 0
$\dot{Z}$	V		in/sec	Velocity of apl. mass
$\dot{Z}_0$	C	0.0	in/sec	Velocity of apl mass at time = 0
$\ddot{Z}$	V		in/sec <sup>2</sup>	Acceleration of apl mass
$Z_{AR}$	V		in	Auxiliary mass location
$Z_{AR0}$	C	80.0	in	Auxiliary mass location at time = 0
$\dot{Z}_{AR}$	V		in/sec	Auxiliary mass velocity
$\dot{Z}_{AR0}$	C	0.0	in/sec	Auxiliary mass velocity at time = 0
$\ddot{Z}_{AR}$	V		in/sec <sup>2</sup>	Auxiliary mass acceleration
$Z_{GD}$	V(i)		in.	Ground height
$Z_{GDP}$	V(i)		in/in	Ground slope
$Z_{SM}$	V		in	Shock Strut Stroke
$\dot{Z}_{SM}$	V		in/sec	Shock strut stroke velocity

Table A6 Vehicle and Wheel Structural Support (Flywheel) Parameters  
(Sheet 3 of 3)

SYMBOL	TYPE	VALUE	UNITS	DESCRIPTION
$Z_{WM}$	V		in	Axle location (vertical)
$Z_{WMO}$	C	20.59	in	Axle location at time = 0
$\dot{Z}_{WM}$	V		in/sec	Axle velocity (vertical)
$\dot{Z}_{WMO}$	C	0.0	in/sec	Axle location at time = 0
$\ddot{Z}_{WM}$	V		in/sec <sup>2</sup>	Axle acceleration
$D_{VMC}$	C	200	Lb	Coulomb friction coeff
$G_m(x)$	F			Coulomb friction function
$R_{OT}$	C	23.32	in	Undelected tire radius*
$S_{MCL}$	C	83.41	in	Fully extended shock strut length
$\dot{V}_F$	V		in/sec <sup>2</sup>	Flywheel acceleration
$\dot{V}_{F0}$	C	7.0	in/sec <sup>2</sup>	Flywheel acceleration at time zero

\*Same as for tire and wheel system

3b. VEHICLE AND WHEEL STRUCTURAL SUPPORT (3 DEGREE AIRPLANE SYSTEM)

The three degree airplane system is built around a rigid body airplane which is allowed to move vertically, horizontally (parallel to the runway centerline), and rotationally in the pitch mode. This model provides for the interaction of the anti-skid system with those effects which are related to airplane pitch. This includes such pitch effects as change in the aerodynamic lift, drag, and moment due to change in wing angle of attack, change in the aerodynamic lift, drag, and moment due to changes in elevator deflection as dictated by the stability augmentation system (pitch mode), change in tire loading due to braking pitch moment, and the effect of ground slope and roughness as reacted through both the main and nose gears.

A. Mathematical Description

Figure A15 shows the three coordinates which describe the airplane position relative to reference points on the earth's surface.

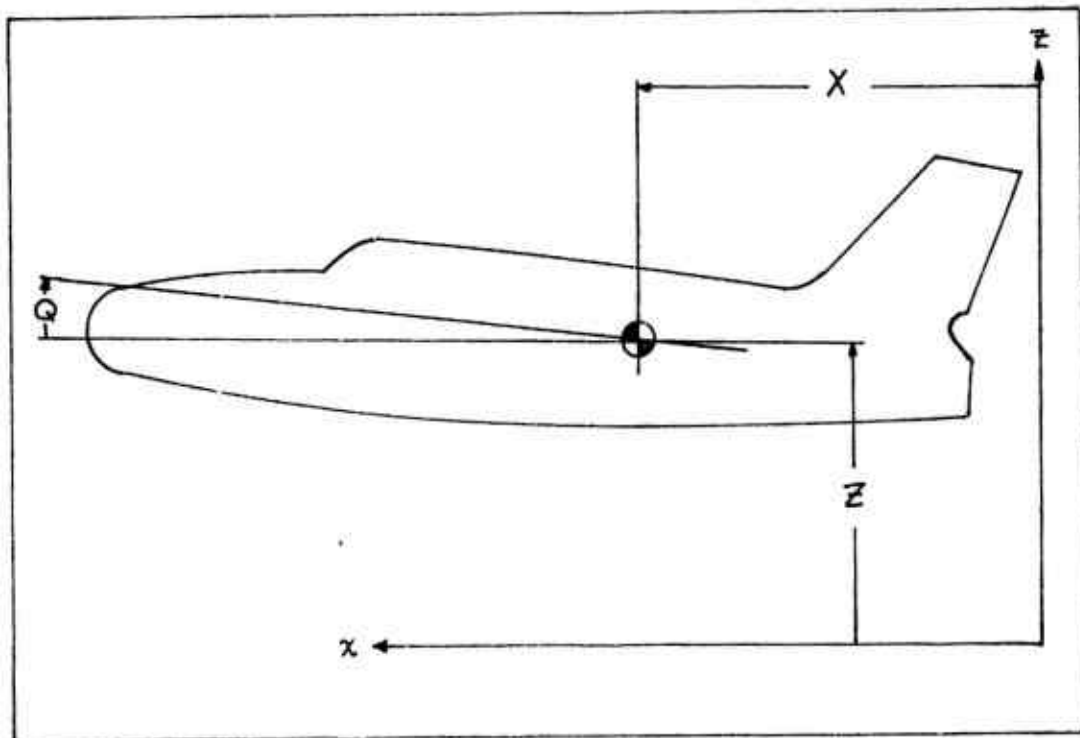


Figure A15 Airplane Coordinates

Figure A16 shows the gear extended dimensions as measured in the airplane's water line-fuselage station reference system.

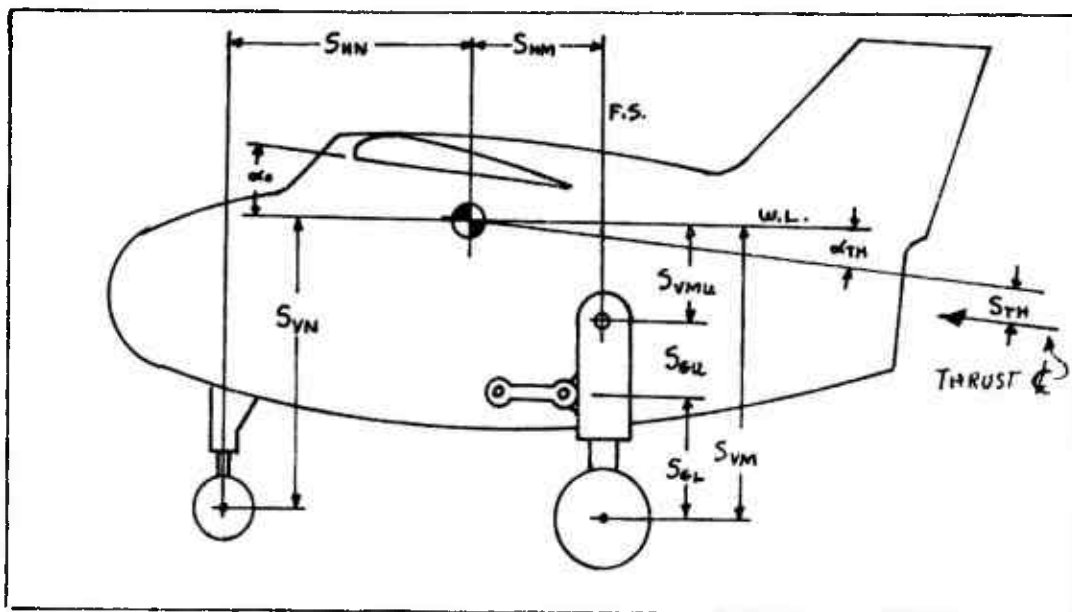


Figure A16 Airplane Geometry

Let  $Z_{GD}(x)$  denote the runway profile height and let  $\dot{Z}_{GD}(x)$  denote the runway profile slope.

#### Nose Gear

Let  $Z_{SN}$  and  $\dot{Z}_{SN}$  denote the nose strut stroke and stroke velocity. From Figure A17,  $Z_{SN}$  and  $\dot{Z}_{SN}$  are given by

$$(3b.1) \quad Z_{SN} = Z_{WN} + S_{VN} - Z - S_{HN} Q$$

$$(3b.2) \quad \dot{Z}_{SN} = \dot{Z}_{WN} - \dot{Z} - S_{HN} \dot{Q}$$

The nose gear shock strut force is then given by

$$(3b.3) \quad F_{VN} = F_{VNS}(Z_{SN}) + D_{NN} \dot{Z}_{SN} + A_{VN}(Z_{SN}) \dot{Z}_{SN} |\dot{Z}_{SN}|$$

$F_{NN}$ , the normal ground force at the nose gear is given by

$$(3b.4) \quad F_{NN} = S_N (C_{NT} + D_{NT} \dot{S}_N)$$

where  $S_N$  is the nose tire deflection.  $S_N$  and  $\dot{S}_N$  are given by:

$$(3b.5) S_N = \max \{ 0.0, Z_{GD} \langle X_{WN} \rangle + R_{OTN} - Z_{WN} \}$$

$$(3b.6) \dot{S}_N = Z_{GDP} \langle X_{WN} \rangle \dot{X}_{WN} - \dot{Z}_{WN}$$

Summing vertical forces on the nose wheel,

$$(3b.7) W_{WN} \ddot{Z}_{WN} = F_{NN} - F_{VN}$$

$$(3b.8) F_{DN} = U_{RRN} F_{NN}$$

### Main Gear

Let  $Z_{SM}$  and  $\dot{Z}_{SM}$  denote the main gear stroke and stroke velocity:

$$(3b.9) Z_{SM} = Z_{WM} - Z + S_{VM} + S_{HM} Q$$

$$(3b.10) \dot{Z}_{SM} = \dot{Z}_{WM} - \dot{Z} + S_{HM} \dot{Q}$$

The main gear shock strut force is given by:

$$(3b.11) F_{VM} = F_{VMS} \langle Z_{SM} \rangle + D_{VM} \dot{Z}_{SM} + A_{VM} \langle Z_{SM} \rangle \dot{Z}_{SM} |\dot{Z}_{SM}| + O_{VMC} G_m \langle \dot{Z}_{SM} \rangle$$

Let  $S_M$  denote the main gear tire deflection. Then the tire normal force is given by:

$$(3b.12) F_{NM} = S_M (C_{MT} + D_{MT} \dot{S}_M)$$

$$(3b.13) S_M = \max \{ 0.0, Z_{GD} \langle X_{AX} \rangle + R_{OTM} - Z_{WM} \}$$

$$(3b.14) \dot{S}_M = Z_{GDP} \langle X_{AX} \rangle \dot{X}_{AX} - \dot{Z}_{WM}$$

Summing vertical forces on the main wheel, where  $F_{ORV}$  is the vertical component of the tire unbalance force,

$$(3b.15) W_{WM} \ddot{Z}_{WM} = F_{NM} - F_{VM} + F_{ORV}$$

Figure A18 shows the model of the main gear. With the assumption that the gear weight is much less than the air-plane weight (that is,  $W_u \ll W_A$ ), it follows that:

$$(3b.16) W_u S_{Gu}^2 \ddot{\Theta}_G = F_u S_{Gu} - F_G (S_{Gu} + Z_{GL}) - T_S$$

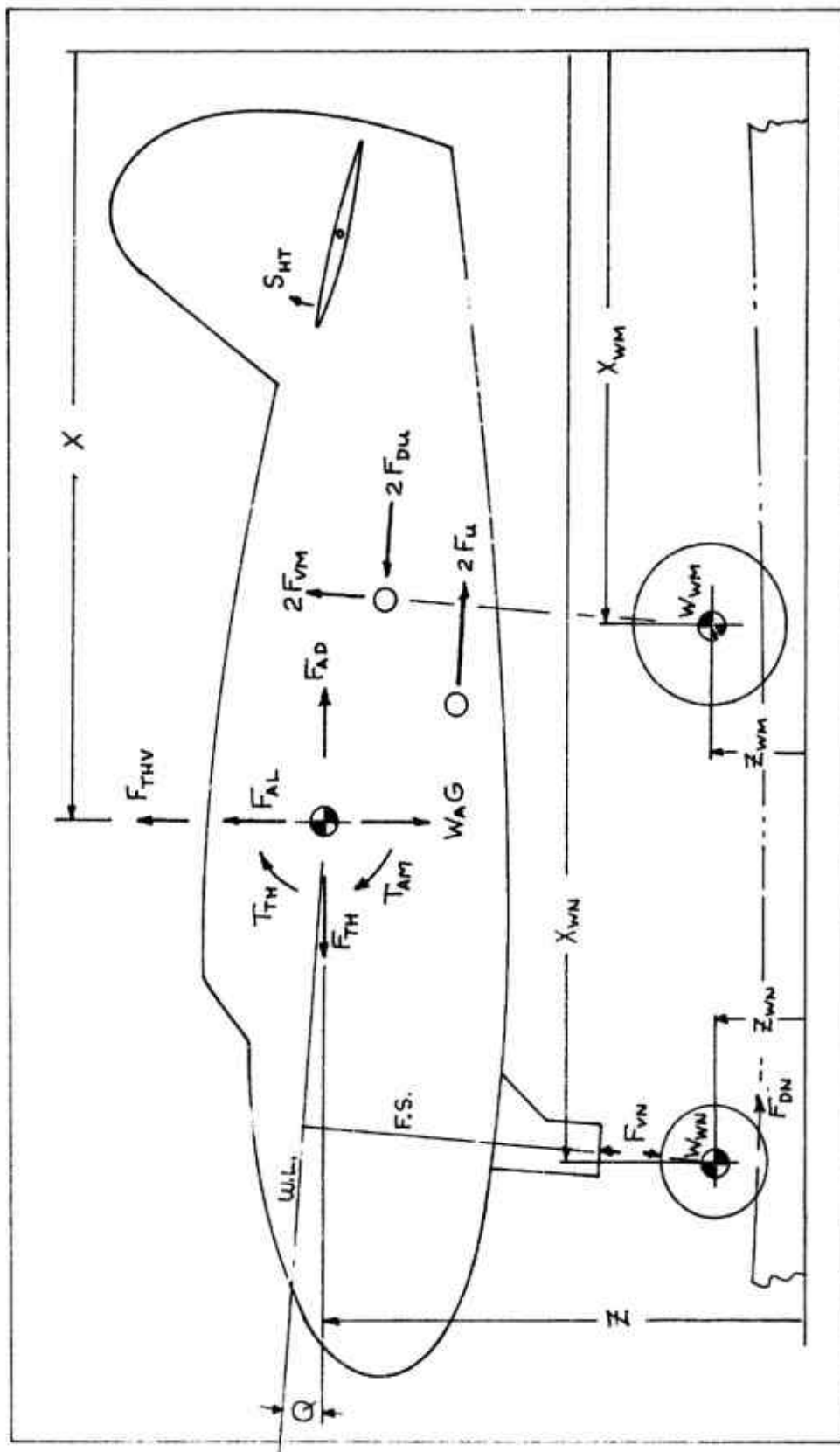


Figure A17 Airplane Dynamics

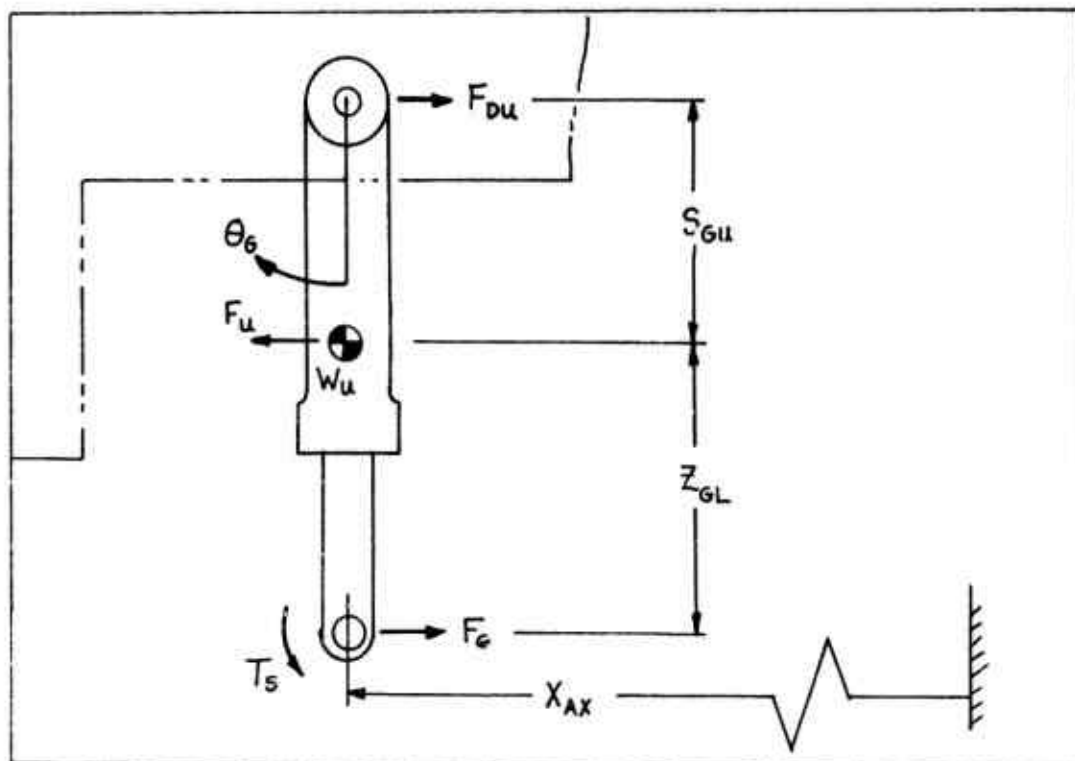


Figure A18 Main Strut Model

where  $Z_{GL}$  is determined by:

$$(3b.17) \quad Z_{GL} = S_{GL} - Z_{SM}$$

$F_{Du}$  can then be computed by summing moments about the CG,

$$(3b.18) \quad F_{Du} = (F_G Z_{GL} + T_s) / S_{Gu}$$

where

$$(3b.19) \quad F_u = S_{Gu} (C_u (Q - \theta_G) + D_u (\dot{Q} - \dot{\theta}_G))$$

$T_s$  and  $F_G$  are outputs from the tire and wheel system. The horizontal axle reference location is denoted by  $X_{Ax}$ .  $X_{Ax}$  is given by:

$$(3b.20) \quad X_{Ax} = X - S_{HM} + (S_{Gu} + Z_{GL}) \theta_G$$

$$(3b.21) \quad \dot{X}_{Ax} = \dot{X} + (S_{Gu} + Z_{GL}) \dot{\theta}_G$$

## Thrust

Referring to Figures A16 and A17, if  $F_{TH}$  is the thrust, then

$$(3b.22) F_{THV} = F_{TH} (\alpha_{TH} + Q)$$

$$(3b.23) T_{TH} = S_{TH} F_{TH}$$

## Aerodynamics

The dynamic Air Force  $Q_A$  is given by:

$$(3b.24) Q_A = \dot{X}^2 A_{REF} R_{HA} / 288.0$$

The aerodynamic lift, drag, and moment are then given by:

$$(3b.25) F_{AL} = C_{AL} Q_A$$

$$(3b.26) F_{AD} = C_{AD} Q_A$$

$$(3b.27) T_{AM} = C_{AM} Q_A$$

If  $\alpha_w$  denotes the wing angle of attack relative to the air, then:

$$(3b.28) \alpha_w = \alpha_o + (180/\pi)(Q - \dot{Z}/\dot{X})$$

Let  $S_{HT}$  denote the horizontal tail deflection. Then the aerodynamic coefficients are given by:

$$(3b.29) C_{AL} = G_{AL} + B_{AL} \alpha_w + E_{AL} S_{HT}$$

$$(3b.30) C_{AD} = G_{AD} + B_{AD} \alpha_w + E_{AD} S_{HT}$$

$$(3b.31) C_{AM} = G_{AM} + B_{AM} \alpha_w + E_{AM} S_{HT}$$

## Dynamics

Referring to Figure A17,

$$(3b.32) W_A \ddot{Z} = F_{AL} + F_{THV} - W_A G + 2F_{VM} + F_{VN}$$

$$(3b.33) W_A \ddot{X} = F_{TH} - F_{AD} + 2F_{DU} - 2F_U - F_{DN}$$

$$(3b.34) W_{IQ} \ddot{Q} = F_{VN} S_{HN} - 2F_{VM} S_{HM} + 2F_{DU} S_{VMU} + T_{TH} + T_{AM} - 2F_U (S_{GU} + S_{VMU}) - F_{DN} (Z - Z_{GD} \langle X_{WN} \rangle)$$



where

$$(3b.35) \quad X_{WN} = X + S_{HN} + S_{VN} Q$$

$$(3b.36) \quad \dot{X}_{WN} = \dot{X} + S_{VN} \dot{Q}$$

Figure A19 shows the system flow diagram.

## B. PARAMETER EVALUATION

### Shock Strut Characteristics

Figures A20 and A21 show the nose gear load and damping characteristics.

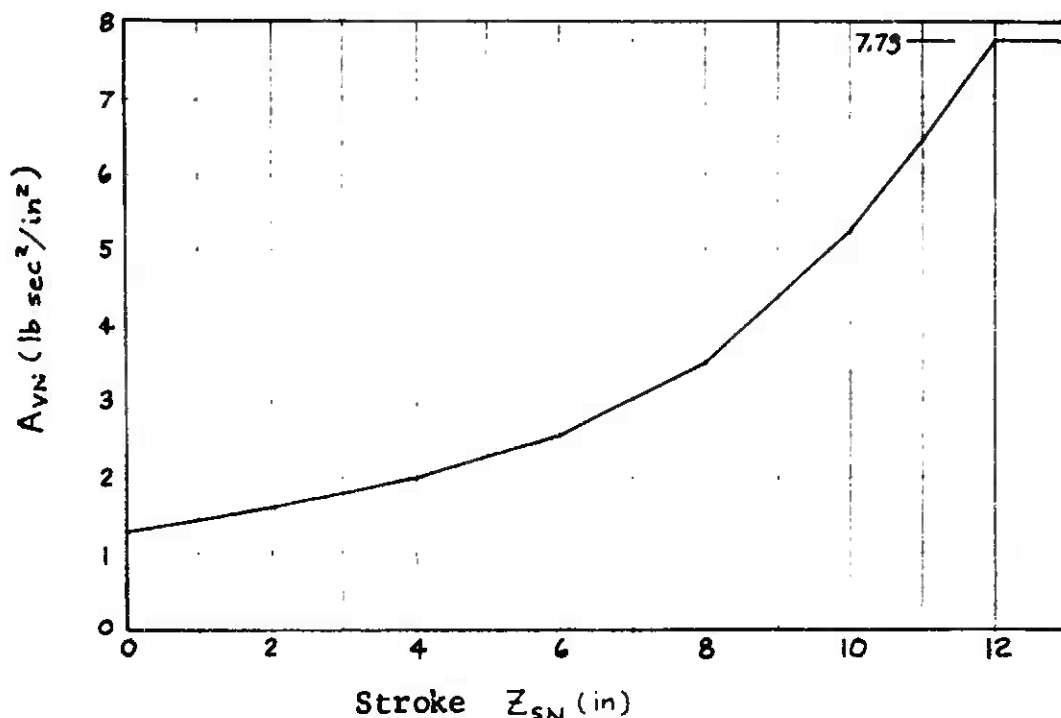


Figure A20 Nose Gear Damping Curve

### Nose Tire Characteristics

See also page 135 of the flywheel system. The 22 x 6.6-10 16-ply rating nose tire has a rating of 9150 lbs. at 190 psi. The deflection is 1.50 inches. The operating pressure is 190 psi. Since these are two nose tires,

$$(3b.37) \quad C_{NT} = \left( \frac{P}{P_R} \right) \frac{F_R}{S_R} = \left( \frac{190}{190} \right) \frac{(2)(9150)}{(1.50)} = 12,200 \text{ lb/in}$$

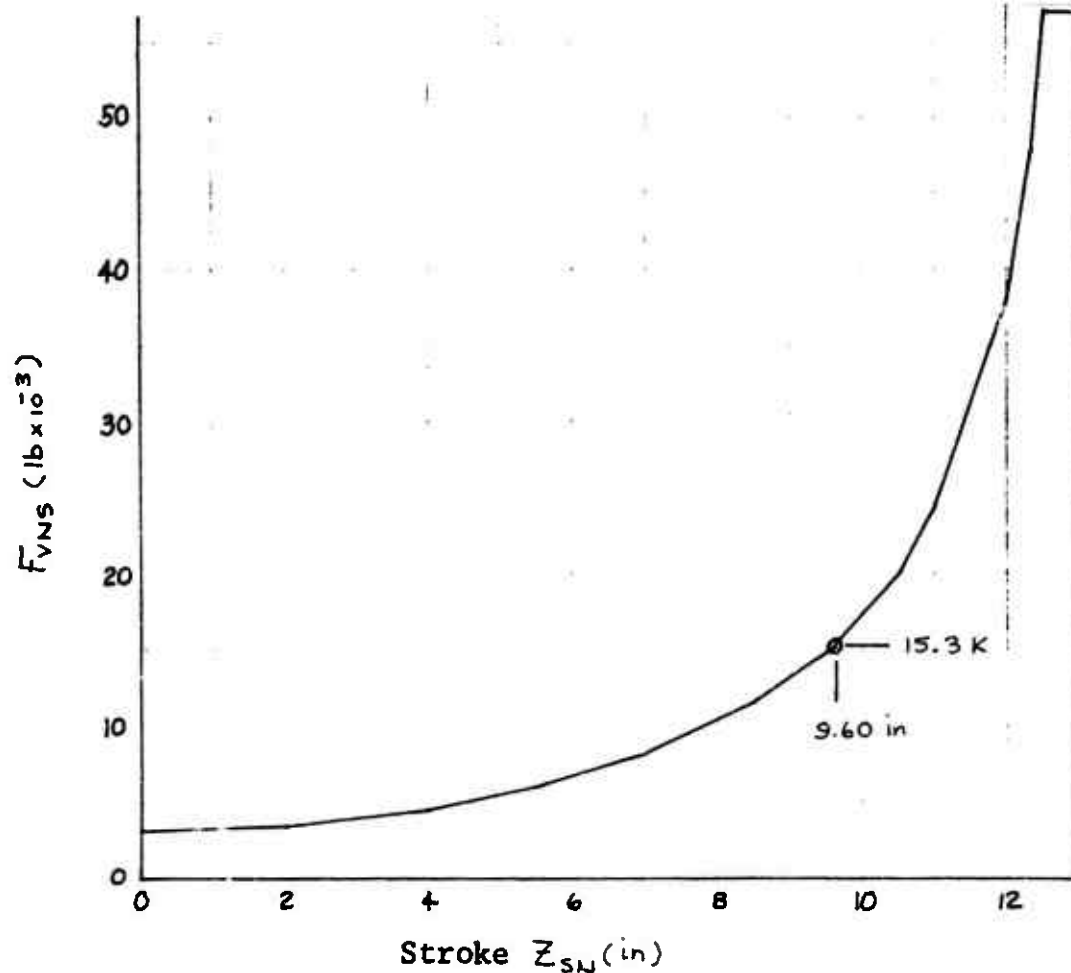


Figure A21 Nose Gear Air Load Curve

Since  $\eta = 0.1$ ,

$$\begin{aligned}
 (3b.38) \ C_{NT} &= \frac{\eta F_R}{S_R^2} \left( \frac{P}{P_R} \right) \sqrt{\frac{S_R}{G}} \\
 &= \frac{(0.1)(2)(9150)}{(1.50)^2} \left( \frac{190}{190} \right) \sqrt{\frac{1.50}{386}} = 50.6 \frac{\text{lb sec}}{\text{in}^2}
 \end{aligned}$$

The nose tire rolling resistance coefficient is  $U_{RRN} = .020$  and the unsprung nose tire mass (mass of tires, wheels, axle, and lower shock strut) is  $W_{WN} = 175/386 = .453 \text{ LBF SEC}^2/\text{IN}$ . The nose tire undeflected radius,  $R_{0TN}$ , is 10.8 in.

#### Main Tire Characteristics

The main tire undeflected radius,  $R_{0TM}$ , is 23.32 inches. The other main tire characteristics are computed as shown on page 134.

## Main Gear Characteristics

The F-111 main gear spring rate parameters were computed from load-deflection data recorded during structural testing and correlated with data from jig drop tests and from flight tests.

Figure A22 shows the model which has the same form as that described in equations (3b.16) through (3b.21) and in the wheel and tire system. The rotational spring rate of one main gear about its pivot is  $26 \times 10^6$  in lb/rad.

The remaining values are calculated (at static position) as:

$$(3b.39) \quad \left\{ \begin{array}{l} S_{Gu} = 21.0 \text{ in} \\ W_u = 279 \text{ lbm} = .723 \text{ lb sec}^2/\text{in} \\ W_{Gw} = W_{wm} = 644 \text{ lbm} = 1.667 \text{ lb sec}^2/\text{in} \\ C_G = 200,000 \text{ lb/in} \end{array} \right.$$

Thus from figure 22,  $C_u$  is given by

$$(3b.40) \quad C_u = C_{u(ROT)} / S_{Gu}^2 = 26 \times 10^6 / 21^2 = 59,000 \text{ lb/in}$$

The first mode natural frequency of the model is 21.84 cps. Assuming that  $\eta$  is .054 (about 3% critical), then evaluating the damping at  $\omega = (2\pi)(21.84) = 137.5 \text{ rad/sec}$  there follows:

$$(3b.41) \quad D_G = \frac{\eta C_G}{\omega} = \frac{(.054)(200,000)}{(137.5)} = 78.6 \frac{\text{lb sec}}{\text{in}}$$

$$(3b.42) \quad D_U = \frac{\eta C_u}{\omega} = \frac{(.054)(59,000)}{(137.5)} = 23.2 \frac{\text{lb sec}}{\text{in}}$$

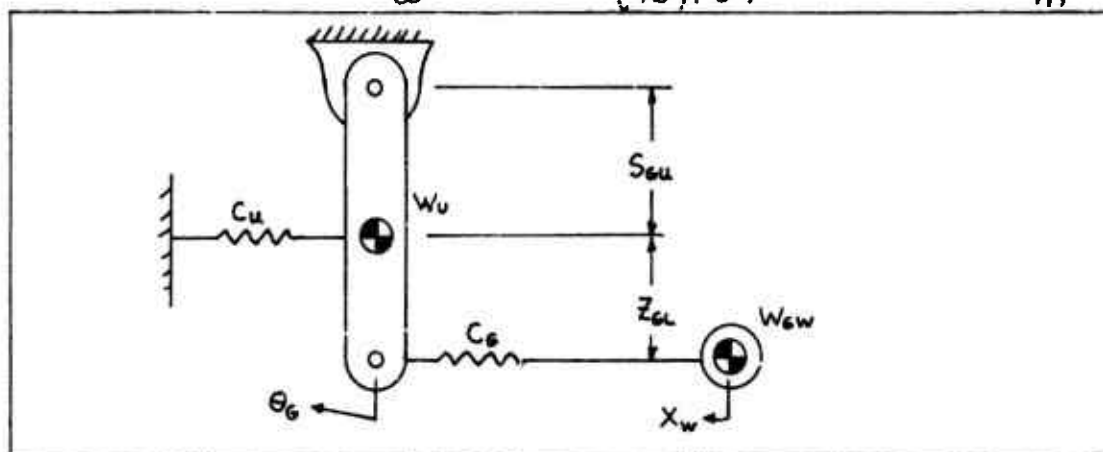


Figure A22 Main Gear Strut and Wheel Model

### Aerodynamic Data

For finding the aerodynamic data, the F-111A is landing with flaps at  $34^\circ$ , wings swept to  $26^\circ$ , and spoilers applied. An equilibrium airplane condition of  $\alpha_w = 2^\circ$  and  $S_{HT} = -5^\circ$  is assumed. For these conditions,

$$(3b.43) \quad C_L = 0.13 \quad \frac{\partial C_L}{\partial \alpha_w} = .128 \text{ deg}^{-1} \quad \frac{\partial C_L}{\partial S_{HT}} = .022 \text{ deg}^{-1}$$

$$(3b.44) \quad C_D = .258 \quad \frac{\partial C_D}{\partial \alpha_w} = .000 \text{ deg}^{-1} \quad \frac{\partial C_D}{\partial S_{HT}} = -.0036 \text{ deg}^{-1}$$

$$(3b.45) \quad C_{MA} = 0.00 \quad \frac{\partial C_{MA}}{\partial \alpha_w} = -.025 \text{ deg}^{-1} \quad \frac{\partial C_{MA}}{\partial S_{HT}} = -.0352 \text{ deg}^{-1}$$

The aerodynamic reference point is F.S. 526.8, WL 197.2. Assuming the airplane C.G. at F.S. 519.0, WL 180.0, if  $\Delta x$  and  $\Delta y$  are given by:

$$(3b.46) \quad \Delta x = FSA - FSCG = 526.8 - 519.0 = 7.8 \text{ inches}$$

$$(3b.47) \quad \Delta y = WLA - WLCG = 197.2 - 180.0 = 17.2 \text{ inches}$$

Then if  $\bar{C} = 108.5$  inches is the length of the M.A.C., then  $C_m \bar{C}$  at the airplane C.G. is given by:

$$(3b.48) \quad C_m \bar{C} = C_{MA} \bar{C} - C_L \Delta x + C_D \Delta y \\ = (0.0)(108.5) - (0.13)(7.8) + (.258)(17.2) = 34.24 \text{ inches}$$

Also,

$$(3b.49) \quad \frac{\partial C_m \bar{C}}{\partial \alpha_w} = \frac{\partial C_{MA} \bar{C}}{\partial \alpha_w} - \frac{\partial C_L}{\partial \alpha_w} \Delta x + \frac{\partial C_D}{\partial \alpha_w} \Delta y \\ = (-.025)(108.5) - (.128)(7.8) + (0.0)(17.2) = -.371$$

$$(3b.50) \quad \frac{\partial C_m \bar{C}}{\partial S_{HT}} = \frac{\partial C_{MA} \bar{C}}{\partial S_{HT}} - \frac{\partial C_L}{\partial S_{HT}} \Delta x + \frac{\partial C_D}{\partial S_{HT}} \Delta y \\ = (-.0352)(108.5) - (.022)(7.8) - (.0036)(17.2) = -3.759$$

Thus from equations (3b.29), (3b.30), and (3b.31),

$$(3b.51) \begin{cases} C_{AL} = C_L = 0.13 \\ B_{AL} = (\partial C_L / \partial \alpha_w) = .128 \text{ deg}^{-1} \\ E_{AL} = (\partial C_L / \partial S_{HT}) = .022 \text{ deg}^{-1} \end{cases}$$

$$(3b.52) \begin{cases} C_{AD} = C_D = .258 \\ B_{AD} = (\partial C_D / \partial \alpha_w) = 0.0 \text{ deg}^{-1} \\ E_{AD} = (\partial C_D / \partial S_{HT}) = -.0036 \text{ deg}^{-1} \end{cases}$$

$$(3b.53) \begin{cases} C_{AM} = C_{m\bar{c}} = 3.424 \text{ in} \\ B_{AM} = (\partial C_{m\bar{c}} / \partial \alpha_w) = -.371 \text{ in/deg} \\ E_{AM} = (\partial C_{m\bar{c}} / \partial S_{HT}) = -3.759 \text{ in/deg} \end{cases}$$

(3b.54)

$$(3b.55) \begin{aligned} G_{AL} &= C_{AL} - B_{AL} \alpha_w - E_{AL} S_{HT} \\ &= .013 - (.128)(2) - (.022)(-5.0) = -.016 \end{aligned}$$

$$\begin{aligned} G_{AD} &= C_{AD} - B_{AD} \alpha_w - E_{AD} S_{HT} \\ &= .258 - (0.0)(2) - (-.0036)(-5) = .240 \end{aligned}$$

$$(3b.56) \begin{aligned} G_{AM} &= C_{AM} - B_{AM} \alpha_w - E_{AM} S_{HT} \\ &= 3.424 - (-.371)(2) - (-3.759)(-5) = 2.286 \text{ IN} \end{aligned}$$

### Initial Conditions

Assume that at time = 0.0 seconds the airplane velocity is 2400 in/sec =  $\dot{x}_0$ . The airplane is shown in Figure 23 with brakes off.

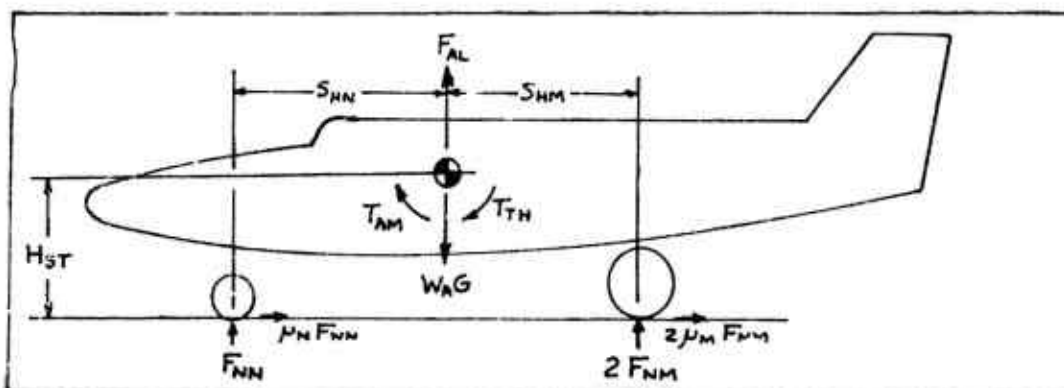


Figure A23 Airplane Initial Equilibrium Forces

Assume that  $\alpha_w = 3^\circ$  and  $S_{HT} = -5^\circ$ , then from equations (3b.29) (3b.30) and (3b.31), there follows:

$$(3b.57) C_{AL} = (-.016) + (.128)(3) + (.022)(-5) = 0.222$$

$$(3b.58) C_{AM} = (2.286) + (-.371)(3) + (-3.759)(-5) = 19.973$$

Since  $S_{HN} = 258.9$ ,  $S_{HM} = 32.6$  inches,  $T_{TH} = 20,000$  in/lb., and if the estimated value for  $H_{ST}$  is 97.2 inches, then

$$(3b.59) F_{NM} = \left( \frac{(T_{TH} + T_{AM}) + (S_{HN} - H_{ST}\mu_N)(WAG - F_{AL})}{(S_{HN} + S_{HM}) + H_{ST}(\mu_M - \mu_N)} \right) \frac{1}{2}$$

Now from equations (3b.24), (3b.25), and (3b.26),

$$(3b.60) Q_A = (2400)^2(525)(.00238)/288 = 25000 \text{ lb}$$

$$(3b.61) F_{AL} = (.222)(25000) = 5500 \text{ lb}$$

$$(3b.62) T_{AM} = (19.973)(25000) = 499,300 \text{ in lb}$$

Thus,

$$(3b.63) F_{NM} = \frac{1}{2} \left( \frac{(499,300) + (257)(57000 - 5500)}{(295.1) + (97.2)(0)} \right)$$

So

$$(3b.64) F_{NM} = 22988 \text{ lb}$$

and

$$\begin{aligned} (3b.65) F_{NN} &= WAG - F_{AL} - 2F_{NM} \\ &= 57000 - 5500 - 2(22988) = 5524 \text{ lb} \end{aligned}$$

Assume that when time = 0 that  $X_{WM} = 0.0$  inches, then  $Z_{GD}\langle X_{WN} \rangle = 0.0$ . Then  $X_{WN} = 295.1$  inches so that  $Z_{GD}\langle X_{WN} \rangle = (9.676 - 9.703)12 = -.32$  inches. Refer to the runway system for values of  $Z_{GD}$ . From equation (3b.12):

$$(3b.66) S_M = (22988)/(9530) = 2.41 \text{ in}$$

Thus from equation (3b.13)

$$(3b.67) \quad Z_{WMO} = 23.32 - 2.41 = 20.91 \text{ in}$$

From Figure A14 in the flywheel system, if  $F_{VMS} = 22,950$  lbs, then  $Z_{SM} = 24.00$  inches. Now, from equation (3b.4)

$$(3b.68) \quad S_N = (5524)/(12,200) = .46 \text{ in}$$

From equation (3b.5), there follows:

$$(3b.69) \quad Z_{WNO} = (-.32) + (10.80) - (.46) = 10.02 \text{ in}$$

Also, from Figure 21, if  $F_{VNS} = 5,600$  lbs. then:  $Z_{SN} = 5 \text{ in}$

Rearranging equations (3b.1) and (3b.9)

$$(3b.70) \quad Z_O + S_{HN} Q_O = S_{VN} + Z_{WNO} - Z_{SN}$$

$$(3b.71) \quad Z_O - S_{HM} Q_O = S_{VM} + Z_{WMO} - Z_{SM}$$

Solving these two equations,

$$(3b.72) \quad Q_O = .0329 \text{ RADIANS}$$

$$(3b.73) \quad Z_O = 82.36 \text{ in}$$

Finally,

$$(3b.74) \quad X_O = X_{WMO} + S_{HM} = 36.20 \text{ in}$$

$$(3b.75) \quad \Theta_{GO} = Q_O = .0329 \text{ RADIANS}$$

The values of the following parameters as listed in Table A7 are established by the airplane's dimensional and mass characteristics:  $\alpha_o$ ,  $\alpha_{TH}$ ,  $A_{REF}$ ,  $S_{CL}$ ,  $S_{HM}$ ,  $S_{HN}$ ,  $S_{VM}$ ,  $S_{VN}$ ,  $S_{GU}$ ,  $S_{TH}$ ,  $W_A$ ,  $W_{IQ}$ , and  $S_{VMU}$ .

For the example problem the density of air at standard conditions, sea level and  $59.6^\circ\text{F}$ , is assumed. Thus,  
 $R_{HA} = .00238 \text{ Slugs / Ft}^3$

The shock strut linear damping coefficients,  $D_{VN}$  for the nose gear and  $D_{VM}$  for the main gear, are set equal to zero for the example problem.

Table A7 3 Degree Airplane System Parameters (Sheet 1 of 5)

SYMBOL	TYPE	VALUE	UNITS	DESCRIPTION
$\alpha_0$	C	1.00	deg	Wing Angle of Incidence
$\alpha_{TH}$	C	-.052	rad	Angle between Thrust $\vec{C}$ and W.L.
$\alpha_W$	V		deg	Wing Angle of Attack
A <sub>REF</sub>	C	525	ft <sup>2</sup>	Wing Ref. Area
A <sub>VN</sub>	V*		lb sec <sup>2</sup> /in <sup>2</sup>	M.G. Shock Strut Damping Characteristic
A <sub>VN</sub>	V*		lb sec <sup>2</sup> /in <sup>2</sup>	N.G. Shock Strut Damping Characteristic
B <sub>AD</sub>	C	0.0	deg <sup>-1</sup>	Aero Drag Parameter
B <sub>AL</sub>	C	.128	deg <sup>-1</sup>	Aero Lift Parameter
B <sub>AM</sub>	C	-.371	in/deg	Aero Moment Parameter
C <sub>AD</sub>	V		-	Aero Drag Coefficient
C <sub>AL</sub>	V		-	Aero Lift Coefficient
C <sub>AM</sub>	V		in	Aero Moment Coefficient
C <sub>MT</sub>	C	9530	lb/in	M.G. Tire Vertical Spring Rate
C <sub>NT</sub>	C	12,200	lb/in	N.G. Tire(s) Vertical Spring Rate
C <sub>U</sub>	C	59,000	lb/in	Drag Brace - Strut Spring Rate
D <sub>MT</sub>	C	38.8	lb sec/in <sup>2</sup>	M.G. Tire Vertical Damping Coeff.
D <sub>NT</sub>	C	50.6	lb sec/in <sup>2</sup>	N.G. Tire Vertical Damping Coeff.
D <sub>U</sub>	C	23.2	lb sec/in	Drag Brace - Strut Damping Coeff.
D <sub>VM</sub>	C	0.0	lb sec/in	M.G. Strut Damping Coefficient
D <sub>VN</sub>	C	0.0	lb sec/in	N.G. Strut Damping Coefficient
E <sub>AD</sub>	C	-.0036	deg <sup>-1</sup>	Aero Drag Coefficient
E <sub>AL</sub>	C	.022	deg <sup>-1</sup>	Aero Lift Coefficient
E <sub>AM</sub>	C	-3.75 s	in/deg	Aero Moment Coefficient
F <sub>AD</sub>	V		lb	Aero Drag
F <sub>AL</sub>	V		lb	Aero Lift
F <sub>DN</sub>	V		lb	Nose Tire Drag
F <sub>DU</sub>	V		lb	Horizontal Load at M.G. Pivot

\* Point Plot Input

Table A7 3 Degree Airplane System Parameters (Sheet 2 of 5)

SYMBOL	TYPE	VALUE	UNITS	DESCRIPTION
$F_G$	V(I)		lb	Horizontal Load on M.G. Axle
$F_{NM}$	V(O)		lb	M.G. Tire Normal Load
$F_{NN}$	V		lb	N.G. Tire Normal Load
$F_{TH}$	C	1000	lb	Engine Thrust
$F_{THV}$	V		lb	Vertical Component of Engine Thrust
$F_u$	V		lb	Load in Fictitious Drag Brace
$F_{VM}$	V		lb	Shock Strut Loag (M.G.)
$F_{VMS}^*$	V		lb	Shock Strut Air Load (M.G.)
$F_{VN}^*$	V		lb	Shock Strut Air Load (N.G.)
$F_{VNS}^*$	V		lb	Shock Strut Air Load (N.G.)
$G$	C	386	in/sec <sup>2</sup>	Gravitational Constant
$G_{AD}$	C	.240	-	Aero Drag Parameter
$G_{AL}$	C	-.016	-	Aero Lift Parameter
$G_{AM}$	C	2.286	in	Aero Moment Parameter
$\Theta_G$	V(O)		rad	M.G. Rotation from Vertical
$\dot{\Theta}_{G0}$	C	.0329	rad	$\Theta_G$ at Time = 0 Sec.
$\ddot{\Theta}_G$	V(O)		rad/sec	Angular Velocity of Main Gear Strut
$\dot{\Theta}_{G0}$	C	0.0	rad/sec	$\ddot{\Theta}_G$ at Time = 0 Sec.
$\ddot{\Theta}_G$	V		rad/sec <sup>2</sup>	Angular Acceleration of Main Gear Strut
$F_{\theta v}$	V(I)		lb	Tire Vertical Unbalance
$Q$	V		rad	Angle of APL W.L. to Horizontal (Pitch)
$Q_0$	C	.0329	rad	Q at Time = 0.0 Sec.
$\dot{Q}_0$	V(O)		rad/sec	APL Pitch Rate
$\ddot{Q}_0$	C	0.0	rad/sec	APL Pitch Rate at Time = 0.0 Sec.

\* Point Plot Input

Table A7 3 Degree Airplane System Parameters (Sheet 3 of 5)

SYMBOL	TYPE	VALUE	UNITS	DESCRIPTION
$\dot{Q}$	V		rad/sec <sup>2</sup>	APL Pitch Acceleration
Q <sub>A</sub>	V		lb	Aerodynamic Pressure x AREF
R <sub>HA</sub>	C	.00238	slug/ft <sup>3</sup>	Air Density
R <sub>OTM</sub>	C	23.32	in	M.G. Tire Undelected Radius
R <sub>OTN</sub>	C	10.80	in	N.G. Tire Undelected Radius
S <sub>GL</sub>	C	93.61	in	*
S <sub>GU</sub>	C	20.0	in	*
S <sub>HM</sub>	C	49.0	in	*
S <sub>HN</sub>	C	222.4	in	*
S <sub>HT</sub>	V(I)		deg	Horizontal Tail Deflection
S <sub>M</sub>	V(O)		in	M.G. Tire Deflection
S <sub>M</sub>	V		in/sec	M.G. Tire Deflection Rate
S <sub>MU</sub>	C	34.875	in	*
S <sub>N</sub>	V		in	N.G. Tire Deflection
S <sub>N</sub>	V		in	N.G. Tire Deflection Rate
S <sub>VM</sub>	C	84.24	in/sec	*
S <sub>VN</sub>	C	85.4	in	*
S <sub>TH</sub>	C	20.00	in	*
T <sub>AM</sub>	V		lb	Aero Moment
T <sub>S</sub>	V		in lb	Moment on M.G. Axle
T <sub>TH</sub>	V(I)		in lb	Moment at C.C. due to Thrust
U <sub>ERN</sub>	C	20,000	in lb	N.G. Tire Rolling Resistance
	C	.020	—	Coefficient
W <sub>A</sub>	C	147.6	lb sec <sup>2</sup> /in	APL Mass
W <sub>IQ</sub>	C	3.66 x 10 <sup>6</sup>	lb sec <sup>2</sup> in	APL Pitch Moment of Inertia About C.G.
W <sub>U</sub>	C	.723	lb sec <sup>2</sup> /in	M.G. Upper Strut Mass
W <sub>WM</sub>	C	1.667	lb sec <sup>2</sup> /in	M.G. Unsprung Mass

\* See Figure A16

Table A7 3 Degree Airplane System Parameters (Sheet 4 of 5)

SYMBOL	TYPE	VALUE	UNITS	DESCRIPTION
$W_{WN}$	C	-453	lb sec <sup>2</sup> /in	N.G. Unsprung Mass
$X$	V		in	Horizontal C.G. Location of APL
$X_0$	C	36.20	in	C.G. Location at Time = 0
$\dot{X}$	V		in/sec	APL Velocity
$\ddot{X}_0$	C	2400	in/sec <sup>2</sup>	APL Velocity at Time = 0
$\ddot{X}$	V		in/sec <sup>2</sup>	APL Acceleration
$X_{AX}$	V(O)		in	M.G. Axle (Undeflected) Location
$\dot{X}_{AX}$	V(O)		in/sec	M.G. Axle Velocity (Undeflected)
$X_{WA}$	V(I)		in	M.G. Axle Location (Horizontal)
$\dot{X}_{WM}$	V(I)		in/sec	M.G. Axle Velocity
$X_{WN}$	V		in	N.G. Axle Location (Horizontal)
$\dot{X}_{WN}$	V		in/sec	N.G. Axle Velocity
$Z$	V		in	Vertical Location of APL C.G.
$Z_0$	C	82.36	in	Vertical Location of APL C.G. at Time = 0
$\dot{Z}$	V		in/sec	APL Vertical Velocity
$\ddot{Z}_0$	C	0.0	in/sec <sup>2</sup>	APL Vertical Velocity at Time = 0
$\ddot{Z}$	V		in/sec <sup>2</sup>	APL Vertical Acceleration
$Z_{60}$	V(I)		in	Runway Contour Height
$Z_{60P}$	V(I)		in/in	Runway Contour Slope
$Z_{6L}$	V		in	Distance from Mass $W_u$ to Strut Axle
$Z_{SM}$	V		in	M.G. Stroke
$\dot{Z}_{SM}$	V		in/sec	M.G. Stroke Velocity
$Z_{SN}$	V		in	N.G. Stroke
$\dot{Z}_{SN}$	V		in/sec	N.G. Stroke Velocity

Table A7 3 Degree Airplane System Parameters

(Sheet 5 of 5)

SYMBOL	TYPE	VALUE	UNITS	DESCRIPTION
$\ddot{Z}_{WN}$	V		$IN/SEC^2$	M.G. Axle Vertical Acceleration
$\dot{Z}_{WN}$	V		$IN$	N.G. Axle Height
$\ddot{Z}_{WNO}$	C	10.02	$IN$	N.G. Axle Height at Time = 0
$\dot{Z}_{WN}$	V		$IN/SEC$	N.G. Axle Vertical Velocity
$\dot{Z}_{WNO}$	C	0.0	$IN/SEC$	N.G. Axle Vertical Velocity at Time = 0
$\ddot{Z}_{WN}$	V		$IN/SEC^2$	N.G. Axle Vertical Acceleration
$DVMC$	C	200	$LB$	Coulomb Friction Coefficient
$G_M$	F			Coulomb Friction Function (See Flywheel System)

### 3c. AIRPLANE SYSTEM (6 DEGREE)

The six-degree airplane system is built around a rigid body airplane which is allowed to move vertically and horizontally (both parallel and perpendicular to the runway centerline). Also, the airplane's yaw, pitch, and roll effects are considered. This model considers all the effects found in the three-degree airplane system. The purpose of the six-degree airplane is primarily two-fold: the first is to evaluate the effects of the anti-skid system on the airplane's directional stability; the second is to evaluate any anti-skid system degradation caused by airplane yaw and side drift movement.

For the nose gear, the model considers the tire and strut characteristics in the vertical direction. Also, the nose tire's yawed rooling characteristics are included. The steering loop is closed by providing a "pilot" function which provides an input to the nose tire. The "pilot" function depends on the airplane's yaw angle. The two main gears are treated as two distinct systems except for any structural coupling which may exist between the two. Provisions are made for side wind perturbation and for aerodynamic effects caused by airplane yaw and roll.

#### A. Mathematical Description

Figure A24 shows the six coordinates which describe the airplane position relative to reference points on the earth's surface.

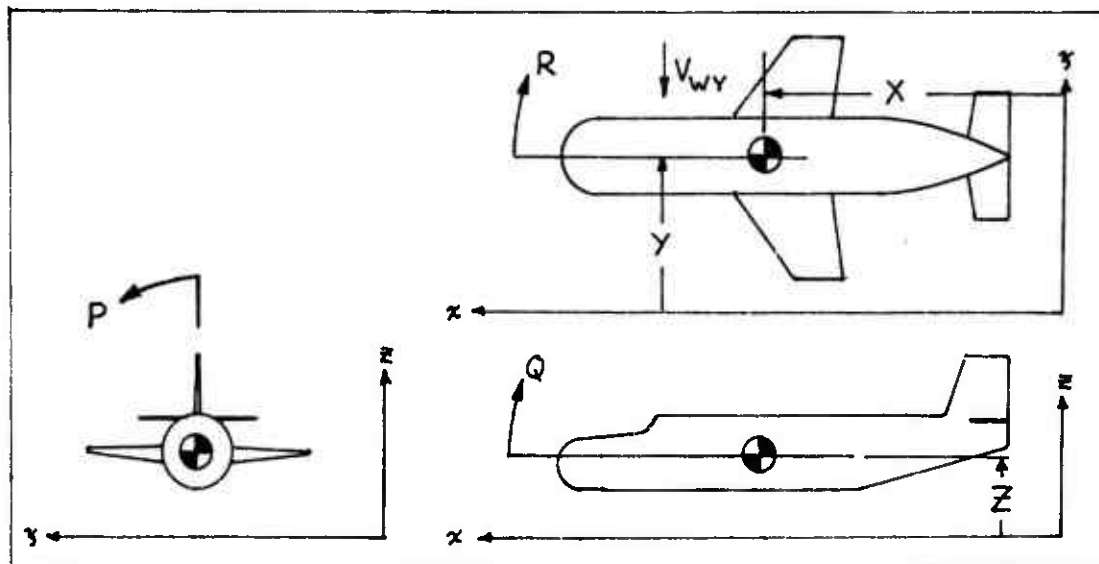


Figure A24 Airplane Coordinates

$V_{wy}$  is a crosswind. The runway is oriented so that its centerline coincides with the x axis for 0 inch runway heights ( $Z_{GD} = 0$ ). This analysis assumes that the pitch (Q) and roll (P) angles are small. Let  $Z_{GD}(x,y)$  denote the runway profile and let  $Z_{GDP}(x,y)$  denote the runway slope ( $Z_{GDP}(x,y) = \partial Z_{GD}(x,y) / \partial x$ ). Figure A25 shows the airplane as measured in the fuselage station-water line reference system.

### Nose Gear

Let  $Z_{SN}$  and  $\dot{Z}_{SN}$  denote the nose gear stroke and stroke velocity. Then we have that:

$$(3c.1) \quad Z_{SN} = Z_{WN} + S_{VN} - Z - S_{HN}Q$$

$$(3c.2) \quad \dot{Z}_{SN} = \dot{Z}_{WN} - \dot{Z} - S_{HN}\dot{Q}$$

The nose gear shock strut force  $F_{VN}$  is then given by:

$$(3c.3) \quad F_{VN} = F_{VNS}(Z_{SN}) + D_{VN}\dot{Z}_{SN} + A_{VN}(Z_{SN})\dot{Z}_{SN}|\dot{Z}_{SN}|$$

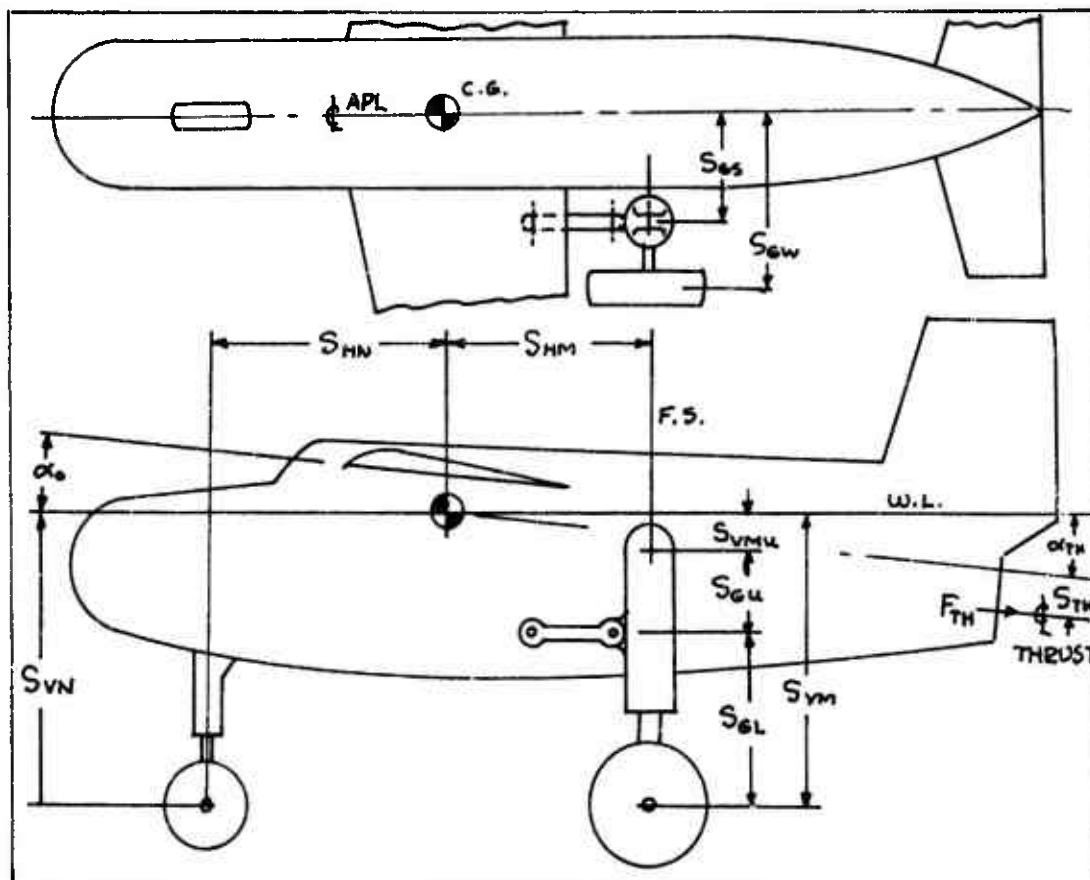


Figure A 25 Airplane Geometry

Figures A26, A27 and A28 show the forces acting on the airplane as seen in the different planes. Let  $F_{LN}$  denote the lateral force on the nose wheel at the axle. Then:

$$(3c.4) \quad W_{WN} \ddot{Y}_N = F_{SNS} - F_{LN}$$

Where  $F_{SNS}$  is the lateral component of the sliding or cornering force of the nose tire. The load  $F_{LN}$  is caused by the nose wheel trying to move laterally relative to the airplane. If this lateral displacement is denoted by  $Y_{DLN}$ , then:

$$(3c.5) \quad F_{LN} = C_{LN} Y_{DLN} + D_{LN} \dot{Y}_{DLN}$$

$$(3c.6) \quad Y_{DLN} = Y_N - Y + (Z + S_{HN}Q)P - S_{HN}R$$

$$(3c.7) \quad \dot{Y}_{DLN} = \dot{Y}_N - \dot{Y} + (Z + S_{HN}Q)\dot{P} + (\dot{Z} + S_{HN}\dot{Q})P - S_{HN}\dot{R}$$

Now  $F_{NN}$  is given by:

$$(3c.8) \quad F_{NN} = S_N (C_{NT} + D_{NT} \dot{S}_N)$$

where

$$(3c.9) \quad S_N = \max \{0.0, Z_{SD} \langle X_{WN}, Y_N \rangle + R_{OTN} - Z_{WN}\}$$

$$(3c.10) \quad \dot{S}_N = Z_{SDP} \langle X_{WN}, Y_N \rangle \dot{X}_{WN} - \dot{Z}_{WN}$$

Summing vertical forces on the nose gear unsprung weight:

$$(3c.11) \quad W_{WN} \ddot{Z}_{WN} = F_{NN} - F_{VN}$$

Assume that the pilot positions the nose wheel with a rate proportional to the airplane yaw angle. Thus:

$$(3c.12) \quad \dot{\Theta}_N = \begin{cases} \min\{0, -G_{PIL} R & \text{if } \Theta_N \geq \Theta_{NMAX} \\ -G_{PIL} R & \text{if } |\Theta_N| < |\Theta_{NMAX}| \\ \max\{0, -G_{PIL} R & \text{if } \Theta_N \leq -\Theta_{NMAX} \end{cases}$$

$\Theta_N$  gives the yaw angle of the nose wheel with respect to the airplane  $\phi$ . The yaw angle of the tire with respect to its direction of motion is given by  $\theta_{YAW}$ .

$$(3c.13) \quad \theta_{YAW} = \Theta_N + R - (\dot{Y}_N / \dot{X}_{WN})$$

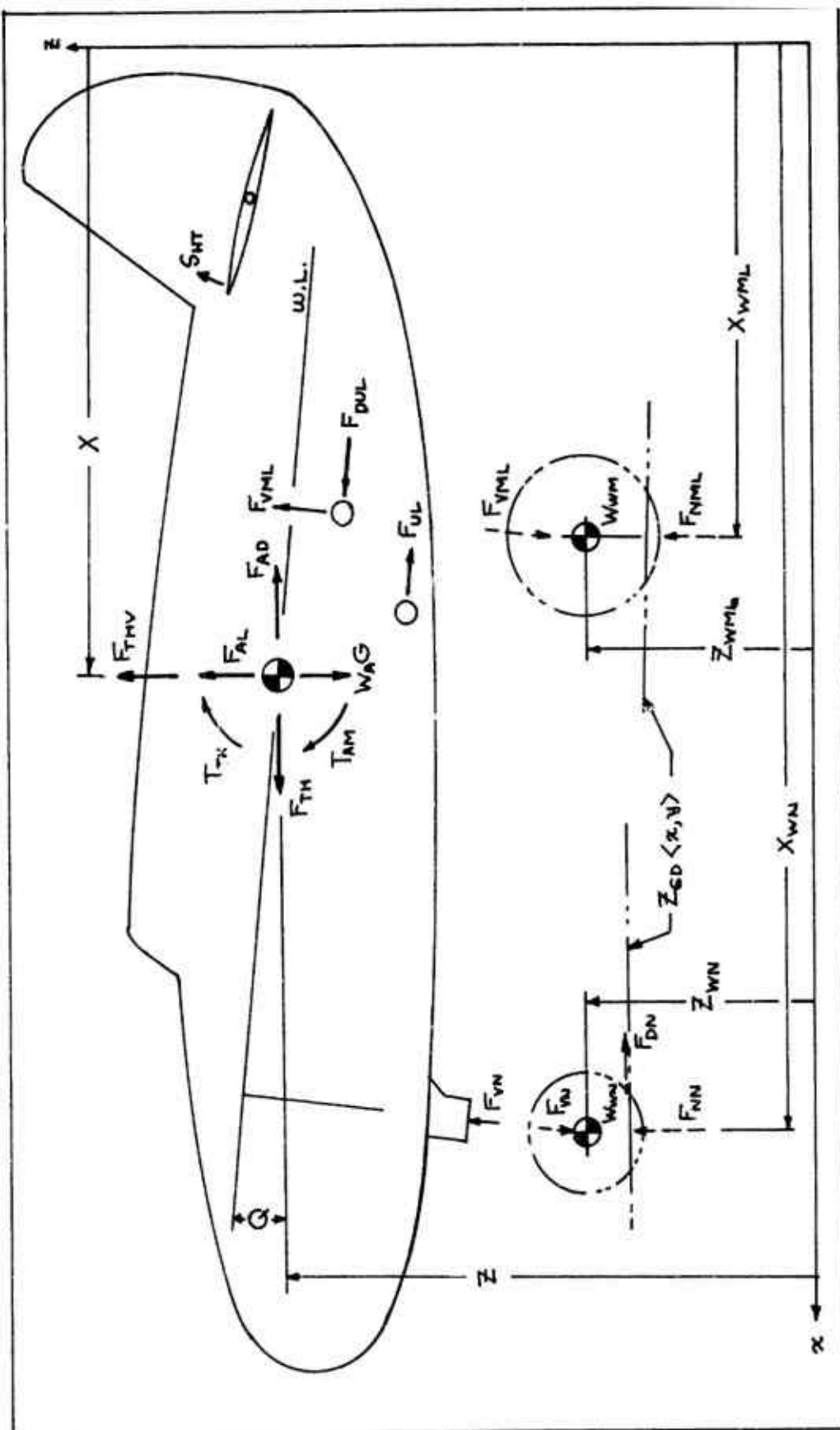
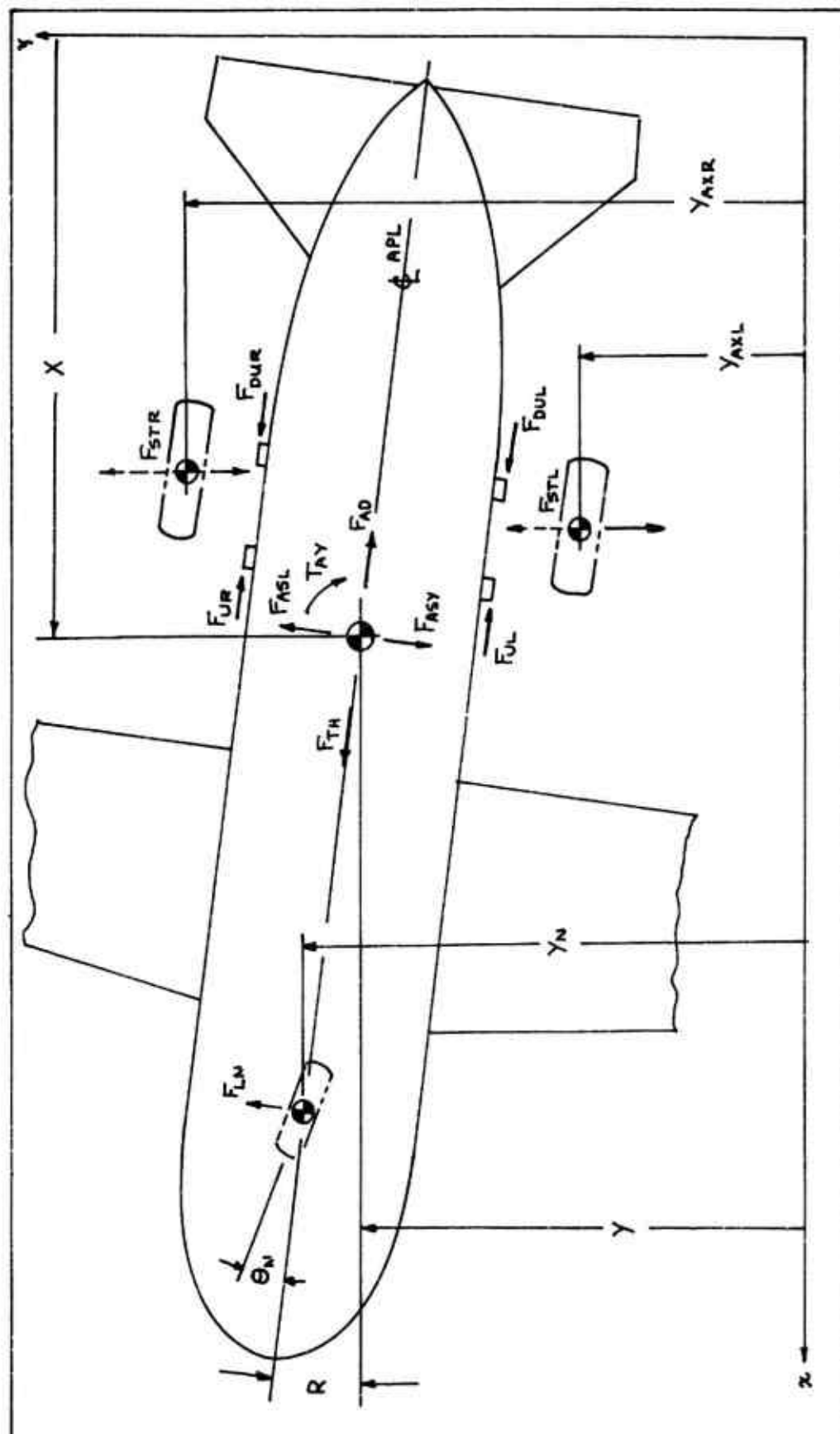


Figure A26 Airplane Dynamics (Pitch)



**Figure A27 Airplane Dynamics (Yaw)**



The steering characteristic is developed from Reference 1 (p. 30). Let  $U_{NTF}$  be the coefficient of friction between the nose tire and the ground. Then the maximum force normal to the tire in the plane of the ground is  $F_{NTF}$  where:

$$(3c.14) F_{NTF} = U_{NTF} F_{NN}$$

Using equation (79) and 80) from Reference 1 :

$$(3c.15) U_{RT} = \begin{cases} P_{WC} \Theta_{YAW} / F_{NTF} & \text{if } F_{NTF} > 0 \\ 0 & \text{if } F_{NTF} \leq 0 \end{cases}$$

$$(3c.16) F_{NCF5} = \begin{cases} F_{NTF} & \text{if } U_{RT} \geq 1.5 \\ F_{NTF} (U_{RT} - 4 U_{RT}^3 / 27) & \text{if } |U_{RT}| < 1.5 \\ -F_{NTF} & \text{if } U_{RT} \leq -1.5 \end{cases}$$

Thus,  $F_{NCF5}$  corresponds to  $F_{\psi, r, e}$  in Reference 1 and  $P_{WC}$  is the cornering power given by:

$$(3c.17) P_{WC} = \begin{cases} C_{P1} S_N - C_{P2} S_N^2 & \text{if } S_N \leq S_{P1} \\ C_{P3} - C_{P4} S_N & \text{if } S_N > S_{P1} \end{cases}$$

The actual normal cornering force  $F_{NCF}$  is not  $F_{NCF5}$ , but lags  $F_{NCF5}$  because of the tire relaxation length. The expression for  $F_{NCF}$  is given by:

$$(3c.18) \dot{F}_{NCF} = (F_{NCF5} - F_{NCF})(\dot{X}_{WN} / S_{YRL})$$

Having obtained  $F_{NCF}$ , then from Figure A29,

$$(3c.19) F_{SWS} = F_{NCF} \cos \langle \Theta_N + R \rangle - U_{RRN} F_{NN} \sin \langle \Theta_N + R \rangle$$

$$(3c.20) F_{DN} = F_{NCF} \sin \langle \Theta_N + R \rangle + U_{RRN} F_{NN} \cos \langle \Theta_N + R \rangle$$

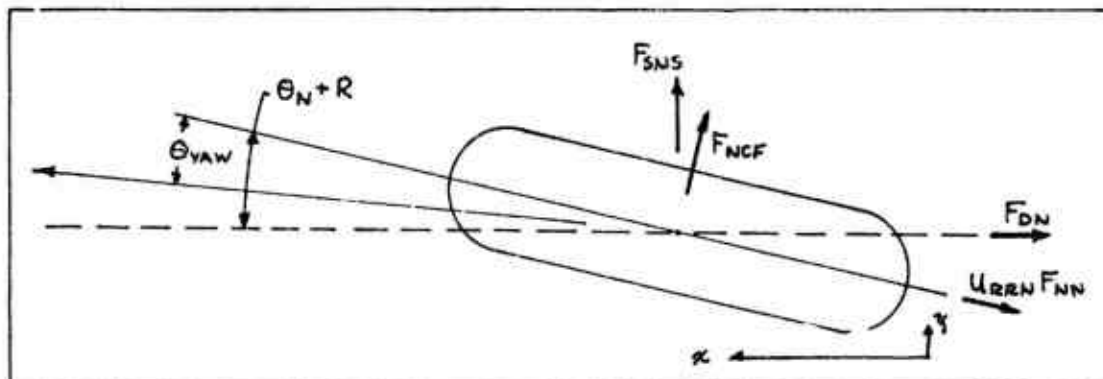


Figure A29 Nose Tire Cornering Force

## Main Gear

Let  $Z_{SM}$  and  $\dot{Z}_{SM}$  denote the stroke and stroke velocity. The additional subscripts L and R refer to the left and right side of the airplane (looking forward).

$$(3c.21) \quad Z_{SMR} = Z_{WMR} - Z + S_{VM} + S_{HM}Q + S_{GW}P$$

$$(3c.22) \quad \dot{Z}_{SMR} = \dot{Z}_{WMR} - \dot{Z} + S_{HM}\dot{Q} + S_{GW}\dot{P}$$

$$(3c.23) \quad Z_{SML} = Z_{WML} - Z + S_{VM} + S_{HM}Q - S_{GW}P$$

$$(3c.24) \quad \dot{Z}_{SML} = \dot{Z}_{WML} - \dot{Z} + S_{HM}\dot{Q} - S_{GW}\dot{P}$$

The main gear shock strut forces are then given by:

$$(3c.25) \quad F_{VMR} = F_{VMS}\langle Z_{SMR} \rangle + D_{VM}\dot{Z}_{SMR} + A_{VM}\langle Z_{SMR} \rangle \dot{Z}_{SMR} |\dot{Z}_{SMR}|$$

$$(3c.26) \quad F_{VML} = F_{VMS}\langle Z_{SML} \rangle + D_{VM}\dot{Z}_{SML} + A_{VM}\langle Z_{SML} \rangle \dot{Z}_{SML} |\dot{Z}_{SML}|$$

Let  $S_M$  denote the main gear tire deflection and let  $F_{NM}$  be the associated load. Thus, in the vertical direction, the relation between the load and tire deflection is given as follows:

$$(3c.27) \quad F_{NMR} = S_{MR} (C_{MT} + D_{MT} \dot{S}_{MR})$$

$$(3c.28) \quad F_{NML} = S_{ML} (C_{MT} + D_{MT} \dot{S}_{ML})$$

$$(3c.29) \quad S_{MR} = \max \{ 0, Z_{GD}\langle X_{WMR}, Y_{MR} \rangle + R_{OTM} - Z_{WMR} \}$$

$$(3c.30) \quad \dot{S}_{MR} = Z_{GDP}\langle X_{WMR}, Y_{MR} \rangle \dot{X}_{WMR} - \dot{Z}_{WMR}$$

$$(3c.31) \quad S_{ML} = \max \{ 0, Z_{GD}\langle X_{WML}, Y_{ML} \rangle + R_{OTM} - Z_{WML} \}$$

$$(3c.32) \quad \dot{S}_{ML} = Z_{GDP}\langle X_{WML}, Y_{ML} \rangle \dot{X}_{WML} - \dot{Z}_{WML}$$

Summing forces in the vertical direction on the main gear wheels,

$$(3c.33) \quad W_{WM} \ddot{Z}_{WMR} = F_{NMR} - F_{VMR} + F_{ORVR}$$

$$(3c.34) \quad W_{WM} \ddot{Z}_{WML} = F_{NML} - F_{VML} + F_{ORVL}$$

Figure A30 shows a side view of the left hand main gear. With the assumption that  $W_k \ll W_A$ ,  $\Theta_{GR}$  and  $\Theta_{GL}$  are described by:

$$(3c.35) W_u S_{GU}^2 \ddot{\theta}_{GR} = S_{GU} F_{UR} + (S_{GU} + Z_{GLR})(F_{TL} - F_{TR} - F_{GR}) - T_{SR}$$

$$(3c.36) W_u S_{GU}^2 \ddot{\theta}_{GL} = S_{GU} F_{UL} + (S_{GU} + Z_{GLL})(F_{TR} - F_{TL} - F_{GL}) - T_{SL}$$

where

$$(3c.37) Z_{GLR} = S_{GL} - Z_{SMR}$$

$$(3c.38) Z_{GLL} = S_{GL} - Z_{SML}$$

The forces  $F_{TR}$  and  $F_{TL}$  are used to impart the correct moment into the gear.

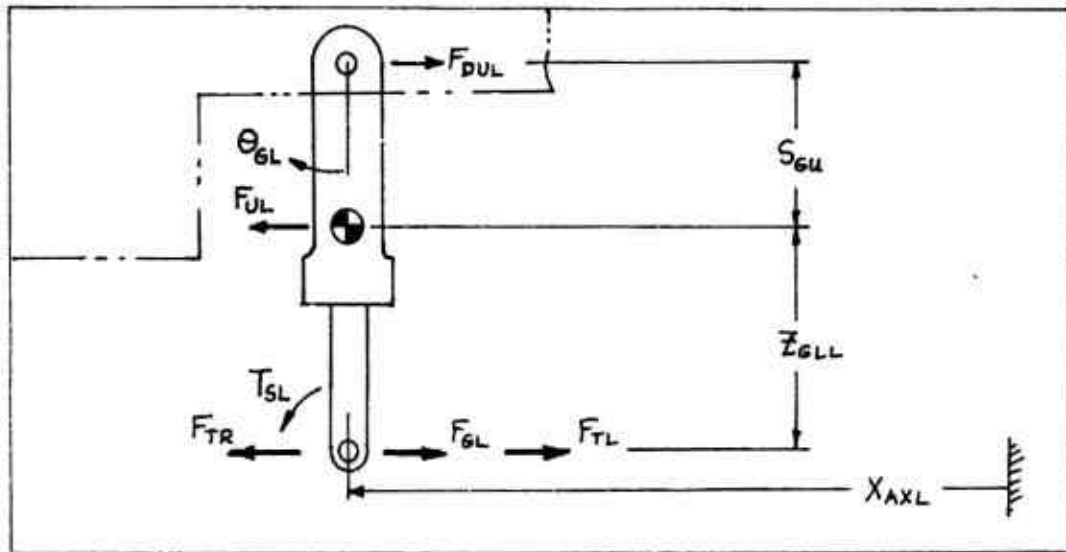


Figure A30 Side View of the Main Gear Strut

The overall gear system model is shown in Figure A31. In order to transmit torque properly, the forces  $F_{TR\theta}$  and  $F_{TL\theta}$  are applied equal and opposite on different sides of the gear. Thus,

$$(3c.39) F_{TR\theta} = F_{GR} (S_{GW} - S_{GS}) / 2 S_{GS}$$

$$(3c.40) F_{TL\theta} = F_{GL} (S_{GW} - S_{GS}) / 2 S_{GS}$$

If it is assumed that 100  $H_A$  percent of this torque is taken directly into the airplane, then 100  $H_G = 100 - 100 H_A$  percent is transmitted through the gear. Thus,

$$(3c.41) F_{TR} = H_G F_{TR\theta}$$

$$(3c.42) F_{TL} = H_G F_{TL\theta}$$

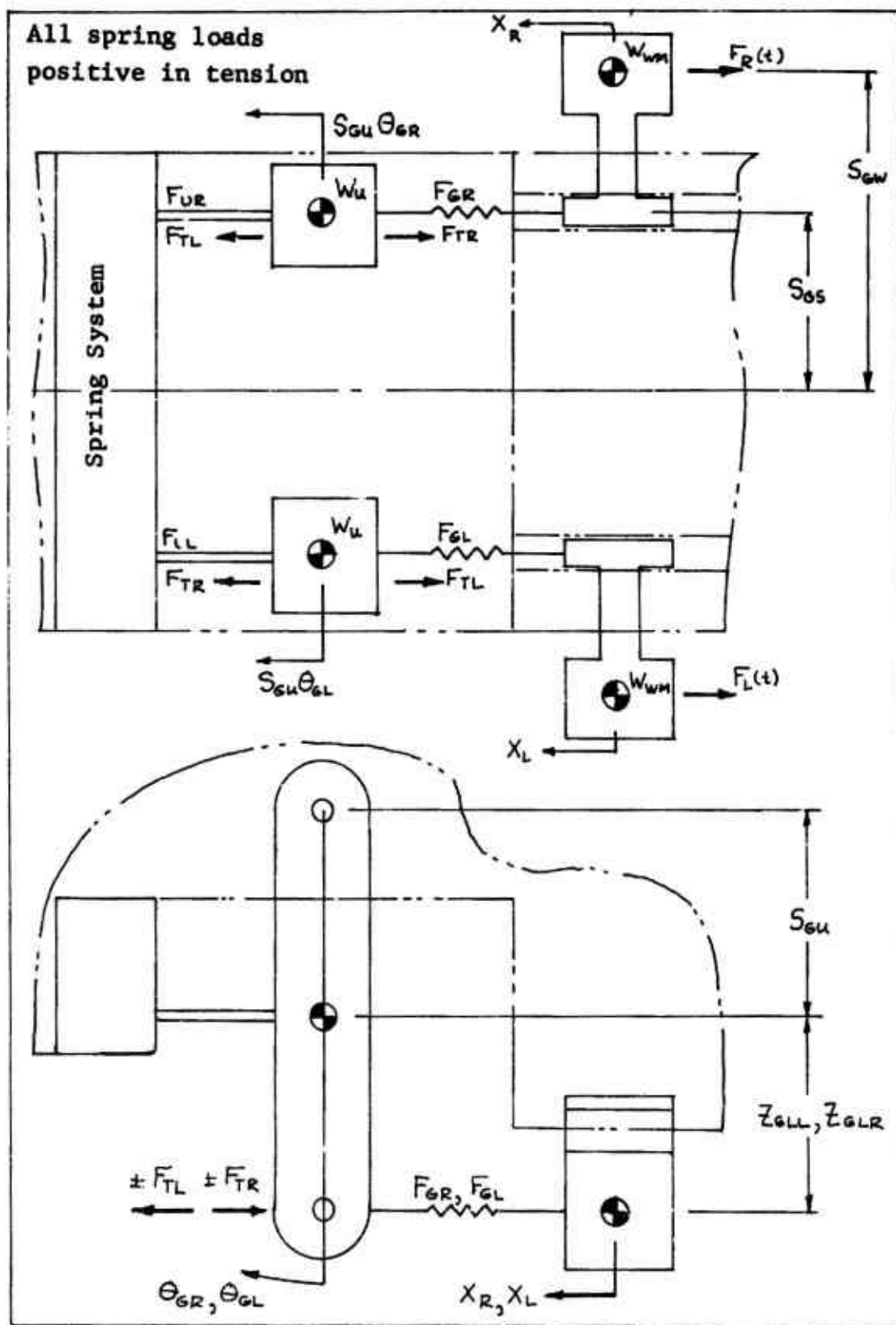


Figure A31 Main Gear Model

Let  $Q_R$  and  $Q_L$  be the difference between the gear rotation and the airplane rotation. That is,

$$(3c.43) \quad Q_R = Q - \theta_{GR}$$

$$(3c.44) \quad Q_L = Q - \theta_{GL}$$

$$(3c.45) \quad \dot{Q}_R = \dot{Q} - \dot{\theta}_{GR}$$

$$(3c.46) \quad \dot{Q}_L = \dot{Q} - \dot{\theta}_{GL}$$

Then we can find constants  $C_{u1}$ ,  $C_{u2}$ ,  $D_{u1}$ , and  $D_{u2}$  such that:

$$(3c.47) \quad F_{UR} = S_{GU}(C_{u1}Q_R - C_{u2}Q_L) + S_{GU}(D_{u1}\dot{Q}_R - D_{u2}\dot{Q}_L)$$

$$(3c.48) \quad F_{UL} = S_{GU}(C_{u1}Q_L - C_{u2}Q_R) + S_{GU}(D_{u1}\dot{Q}_L - D_{u2}\dot{Q}_R)$$

It then follows, assuming negligible strut moment of inertia that:

$$(3.49) \quad F_{DUR} = ((F_{GR} + F_{TR} - F_{TL})\bar{z}_{GLR} + T_{SR}) / S_{GU}$$

$$(3c.50) \quad F_{DUL} = ((F_{GL} + F_{TL} - F_{TR})Z_{GLL} + T_{SL}) / S_{GU}$$

As outputs to the tire and wheel systems we need to compute  $X_{AX}$  and  $Y_{AX}$ .  $X_{AX}$  is shown in Figure 30.  $Y_{AX}$  is assumed to be the undeflected tire footprint position in the y direction.

$$(3c.51) \quad X_{AXL} = X + S_{GW}R + S_{VMU}Q + (S_{GU} + Z_{GLL})\theta_{GL} - S_{HM}$$

$$(3c.52) \quad X_{AXR} = X - S_{GW}R + S_{VMU}Q + (S_{GU} + Z_{GLR})\theta_{GR} - S_{HM}$$

$$(3c.53) \quad \dot{X}_{AXL} = \dot{X} + S_{GW}\dot{R} + S_{VMU}\dot{Q} + (S_{GU} + Z_{GLL})\dot{\theta}_{GL}$$

$$(3c.54) \quad \dot{X}_{AXR} = \dot{X} - S_{GW}\dot{R} + S_{VMU}\dot{Q} + (S_{GU} + Z_{GLR})\dot{\theta}_{GR}$$

$$(3c.55) \quad Y_{AXL} = Y - S_{GW} - (S_{HM} - S_{VMU}Q - (S_{GU} + Z_{GLL})\theta_{GL})R \\ - (S_{VMU} + S_{GU} + Z_{GLL})P$$

$$(3c.56) \quad Y_{AXR} = Y + S_{GW} - (S_{HM} - S_{VMU}Q - (S_{GU} + Z_{GLR})\theta_{GR})R \\ - (S_{VMU} + S_{GU} + Z_{GLR})P$$

$$(3c.57) \quad \dot{Y}_{AXL} = \dot{Y} - (S_{HM} - S_{VMU}Q - (S_{GU} + Z_{GLL})\theta_{GL})\dot{R} \\ + (S_{VMU}\dot{Q} + (S_{GU} + Z_{GLL})\dot{\theta}_{GL})R \\ - (S_{VMU} + S_{GU} + Z_{GLL})\dot{P}$$

$$(3c.58) \dot{Y}_{AXR} = \dot{Y} - (S_{HM} - S_{VMU}Q - (S_{GU} + Z_{GLR})\dot{\Theta}_{GR})\dot{R} \\ + (S_{VMU}\dot{Q} + (S_{GU} + Z_{GLR})\dot{\Theta}_{GR})R \\ - (S_{VMU} + S_{GU} + Z_{GLR})\dot{P}$$

### Engine Thrust

Referring to Figures A26 and A27, if  $F_{TH}$  is the engine thrust, then

$$(3c.59) F_{THV} = F_{TH} (\alpha_{TH} + Q)$$

$$(3c.60) T_{TH} = S_{TH} F_{TH}$$

$$(3c.61) F_{THS} = F_{TH} R$$

### Aerodynamics

The following eight equations apply as in the three-degree model.

$$(3c.62) Q_A = \dot{X}^2 A_{REF} R_{HA} / 288$$

$$(3c.63) F_{AL} = C_{AL} Q_A$$

$$(3c.64) F_{AD} = C_{AD} Q_A$$

$$(3c.65) T_{AM} = C_{AM} Q_A$$

$$(3c.66) \alpha_W = \alpha_0 + (180/\pi)(Q - \dot{Z}/\dot{X})$$

$$(3c.67) C_{AL} = G_{AL} + B_{AL}\alpha_W + E_{AL}S_{HT}$$

$$(3c.68) C_{AD} = G_{AD} + B_{AD}\alpha_W + E_{AD}S_{HT}$$

$$(3c.69) C_{AM} = G_{AM} + B_{AM}\alpha_W + E_{AM}S_{HT}$$

Let  $V_{WV}$  denote the wind gust velocity as shown in Figure A24. If  $\Psi$  and  $\beta$  are defined by:

$$(3c.70) \Psi = (V_{WV} + \dot{Y})/\dot{X}$$

$$(3c.71) \beta = (180/\pi)(\Psi - R)$$

Then  $\beta$  is the angle of sideslip.

Let  $Q_{AT}$  denote the dynamic air pressure (including side wind) multiplied by the reference area. Then:

$$(3c.72) Q_{AT} = ((V_{wy} + \dot{Y})^2 + \dot{X}^2) A_{REF} R_{HA} / 288$$

Then the aerodynamic yaw moment is given by:

$$(3c.73) T_{AY} = C_{AN} / \beta Q_{AT}$$

and the aerodynamic side force is given by:

$$(3c.74) F_{ASY} = C_{AY} / \beta Q_{AT}$$

Finally, an aerodynamic force  $F_{ASL}$  due to a combination of lift and pitch is:

$$(3c.75) F_{ASL} = F_{AL} P$$

Refer to Figure A27 as to the direction of these forces.

### Dynamics

Referring to Figures A26 and A27, summing forces in the x, y, and z direction,

$$(3c.76) W_A \ddot{Z} = F_{AL} + F_{THV} - W_A G + F_{VMR} + F_{VML} + F_{VN}$$

$$(3c.77) W_A \ddot{X} = F_{TH} - F_{AD} + F_{DUR} + F_{DUL} - F_{UR} - F_{UL} - F_{DN}$$

$$(3c.78) W_A \ddot{Y} = F_{THS} - F_{STR} - F_{STL} + F_{LN} + F_{ASL} - F_{ASY}$$

Summing moments about the C.G. we have:

$$(3c.79) W_{IQ} \ddot{Q} = F_{VN} S_{HN} - F_{VMR} S_{HM} - F_{VML} S_{HM} + F_{DUR} S_{VMU} \\ + F_{DUL} S_{VMU} + T_{TH} + T_{AM} - F_{UR} (S_{GU} + S_{VMU}) \\ - F_{UL} (S_{GU} + S_{VMU}) - F_{DN} (Z - Z_{GD} \langle X_{WN} \rangle)$$

$$(3c.80) W_{IR} \ddot{R} = F_{LN} S_{HN} + S_{GS} (F_{UR} - F_{UL} + F_{DUL} - F_{DUR}) + T_{AY} \\ + Z H_A (F_{TRO} - F_{TLO}) S_{GS}$$

$$(3c.81) W_{IP} \ddot{P} = (F_{VML} - F_{VMR}) S_{GW} + F_{ASY} H_{AP} \\ - (Z - Z_{GD} \langle X, Y \rangle) (F_{STR} + F_{STL} + F_{LN})$$

$$(3c.82) X_{WN} = X + S_{HN} + S_{VN} Q$$

$$(3c.83) \dot{X}_{WN} = \dot{X} + S_{VN} \dot{Q}$$



## B. Parameter Evaluation

### Nose Gear Characteristics

Based on a nose gear lateral natural frequency of 12 cps, we have  $\omega_n = 2\pi(12) = 75.5 \text{ RAD/SEC}$ . Since  $W_{WN} = .435$ , then:

$$(3c.84) C_{LN} = W_{WN} \omega_n^2 = .435 (75.5)^2 = 2480 \text{ lb/in}$$

Using  $\eta = .054$  as in the calculation of  $D_\theta$  in the three-degree model,

$$(3c.85) D_{LN} = \eta C_{LN} / \omega_n = (.054)(2480) / 75.5 = 1.78 \text{ lb sec/in}$$

The steering or cornering characteristic parameters are obtained from Reference 1. Based on Figure 44(a) in Reference 1, the value for  $U_{NTF}$  is:

$$(3c.86) U_{NTF} = F_{\psi, r, e(max)} / F_z = 25000 / 45200 = .553$$

Using equation 82 from Reference 1, if  $K = (F + .44 P_R) w^2 = (1.44)(190)(6.6)^2 = 11,920 \text{ lb}$ . then:

$$(3c.87) C_{\phi 1} = 1.2 C_c K / d = (1.2)(57)(11920) / 22 = 37060 \text{ lb/Rad in}$$

$$(3c.88) C_{\phi 2} = 8.8 C_c K / d^2 = (8.8)(57)(11920) / (22)^2 = 12353 \text{ lb/Rad in}^2$$

$$(3c.89) C_{\phi 3} = .0674 C_c K = (.0674)(57)(11920) = 45794 \text{ lb/Rad}$$

$$(3c.90) C_{\phi 4} = .34 C_c K / d = (.34)(57)(11920) / 22 = 10500 \text{ lb/Rad in}$$

$$(3c.91) S_{\phi 1} = .0875 d = (.0875)(22) = 1.925 \text{ in}$$

From Figure 43 in Reference 1 we see that the cornering force lags the yaw angle. Equation 63 in Reference 1 shows that the equation which describes the curves in Figure 43 is given by:

$$(3c.92) F_{y, r} = (1 - e^{-x/L_y}) F_{y, r \max} \langle \Theta_{yaw} \rangle$$

where  $L_y$  is the tire yawed rolling relaxation length. Differentiating this equation, there follows:

$$(3c.93) \frac{dF_{y, r}}{dx} = \frac{e^{-x/L_y}}{L_y} F_{y, r \max} \langle \Theta_{yaw} \rangle$$

Eliminating  $e^{-x/L_y}$  results in:

$$(3c.94) \quad F_{y,r} + L_y \frac{dF_{y,r}}{dx} = F_{y,r \max} \langle \Theta_{yAW} \rangle$$

Equation (3c.18) is obtained by using:

$$(3c.95) \quad \frac{dF_{y,r}}{dx} = \frac{dF_{y,r}}{dt} / \frac{dx}{dt} \approx \frac{\dot{F}_{NCF}}{\dot{X}_{WN}}$$

where it is assumed for large airplane velocities that  $\dot{X}_{WN} = dx/dt$ . We see that the parameter  $S_{yRL}$  is the relaxation length. From Figure 39 of Reference 1, for most conditions,  $S_{yRL}$  is obtained from:

$$(3c.96) \quad S_{yRL} = .6 w (2.8 - .8 P/P_r) \\ = (.6)(6.6)(2.8 - .8) = 7.92 \text{ in}$$

### Main Gear Characteristics

For many airplanes which have a conventional strut arrangement (similar to a B-58) most of the moment about the shock strut  $\phi$  is taken out through the shock strut. In this case equations (3c.41) and (3c.42) would use  $H_G = 0.0$ . In the case of the F-111 gear the opposite result occurs so that  $H_G = 1.0$  and  $H_A = 0.0$ . The following values apply to the F-111 gear:

$$(3c.97) \quad \left\{ \begin{array}{l} W_u = .723 \text{ lb sec}^2/\text{in} \\ W_{WM} = W_{WV} = 1.667 \text{ lb sec}^2/\text{in} \\ S_{Gu} = 21.00 \text{ in} \\ S_{Gw} = 60.00 \text{ in} \\ S_{Gs} = 20.00 \text{ in} \\ H_G = 1.0 \\ H_A = 0.0 \end{array} \right.$$

If loads  $F_R(t) = F_L(t) = F_0$  are applied as shown in figure 31, then because of symmetry, the result will be that  $Q_R = Q_L$ . But then equation (3c.47) says that  $C_{u1} - C_{u2} = F_{UR}/S_{Gu} Q_R$  but  $C_u = F_{UR}/S_{Gu} Q_R$  as shown in the 3 degree model. Thus

$$(3c.98) \quad C_{u1} - C_{u2} = C_u = 59,000 \text{ lb/in}$$

With the main gear at static, if a drag load of 18,000 lb. is applied to the left gear at the ground and -18,000 lb. is applied to the right gear at the ground the observed deflections with  $Q = 0$  are  $Q_L = .0236$  rad and  $Q_R = -.0236$  rad. (Assuming a lateral beam torsional spring rate of  $43.0 \times 10^6$  in lb/rad).

In the equations which describe the gear loading  $T_{SR}$  and  $T_{SL}$  can be chosen as 0 if  $Z_{GLL}$  and  $Z_{GLR}$  are the dimensions to the ground instead of the axle. Thus  $Z_{GL} = Z_{GLL} = Z_{GLR} = 2.2 + 12.9 = 21.4$  in. Equations (3c.35), (3c.36), (3c.39), (3c.40), (3c.41) and (3c.42) can then be combined to give

$$\begin{aligned} (3c.99) \quad F_{UR} - F_{UL} &= \left( \frac{S_{GU} + Z_{GL}}{S_{GU}} \right) (F_{GR} - F_{GL}) \left( 1 + H_G \left( \frac{S_{GW} - S_{GS}}{S_{GS}} \right) \right) \\ &= \left( \frac{21.0 + 21.4}{21.0} \right) (-36000) \left( 1 + \left( \frac{60 - 20}{20} \right) \right) = -212,000 \text{ lb} \end{aligned}$$

Subtracting equation (3c.48) from (3.47) results in

$$(3c.100) \quad F_{UR} - F_{UL} = (C_{u1} + C_{u2}) S_{GU} Q_R - (C_{u1} + C_{u2}) S_{GU} Q_L$$

So that

$$(3c.101) \quad C_{u1} + C_{u2} = \frac{-212000}{(2)(21.0)(-.0236)} = 214,000 \text{ lb/in}$$

Adding and subtracting equations (3c.98) and (3c.101) results in

$$(3c.102) \quad C_{u1} = \frac{59000 + 214000}{2} = 136,500 \text{ lb/in}$$

$$(3c.103) \quad C_{u2} = \frac{214,000 - 59000}{2} = 77,500 \text{ lb/in}$$

At a fore and aft natural frequency of 137.5 rad/sec, the damping coefficients  $D_{u1}$  and  $D_{u2}$  are given as

$$(3c.104) \quad D_{u1} = \eta C_{u1} / \omega = \frac{(.054)(1.36 \times 10^5)}{(137.5)} = 53.4 \text{ lb sec/in}$$

$$(3c.105) \quad D_{u2} = \eta C_{u2} / \omega = \frac{(.054)(.775 \times 10^5)}{(137.5)} = 30.5 \text{ lb sec/in}$$

### Aerodynamic Characteristics

The coefficients for equations (3c.62) thru (3c.69) have been derived in the 3 degree model. For the F-111A in the landing configuration and wings swept to 26 degrees as described in the 3 degree system,  $C_{N\beta} = .0014$  and  $C_{Y\beta} = -.021$ . Then the coefficient  $C_{AY}$  is calculated from

$$(3c.106) \quad C_{AY} = -C_{Y\beta} = .021 \text{ deg}^{-1}$$

Let  $\Delta X = FSA - FSCG$  as in the 3 degree system where  $FSA = 526.8$  and  $FSCG = 519.0$ . Let  $b$  be the wing span. If  $b = 756$  in., then

$$(3c.107) \quad C_{AN} = b C_{N\beta} - \Delta X C_{Y\beta}$$

$$(3c.108) \quad C_{AN} = (756)(.0014) - (7.80)(-.021) = 1.222 \text{ in/deg}$$

### Airplane Characteristics

The parameters listed in Table A8 describing the airplane's dimensional and mass characteristics are those previously derived in the 3 degree model or simply a listing of the appropriate values applicable to the F-111 for which no derivation or computation is required.

Table A8 Airplane System (6 Degree) Parameters (Sheet 1 of 9)

SYMBOL	TYPE	VALUE	UNITS	DESCRIPTION
$\alpha_0$	C	1.00	deg	Wing Angle of Incidence
$\alpha_{TH}$	C	-.052	rad	Angle between Thrust & W.L.
$\alpha_w$	V		deg	Wing Angle of Attack
$A_{REF}$	C	525.0	ft <sup>2</sup>	Wing Reference Area
$A_{VM}$	V*		lb sec <sup>2</sup> /in <sup>2</sup>	M.G. Shock Strut Damping Coeff.
$A_{VN}$	V*		lb sec <sup>2</sup> /in <sup>2</sup>	N.G. Shock Strut Damping Coeff.
$B_{AD}$	C	0.00	deg <sup>-1</sup>	Aero Drag Parameter
$B_{AL}$	C	.128	deg <sup>-1</sup>	Aero Lift Parameter
$B_{AM}$	C	-.371	in/deg	Aero Moment Parameter
$\beta$	V		deg	Angle of Sideslip
$C_{AD}$	V		-	Aero Drag Coefficient
$C_{AL}$	V		-	Aero Lift Coefficient
$C_{AM}$	V		in	Aero Moment Coeff. (Pitch)
$C_{AN}$	C	1.222	in/deg	Aero Moment Coeff. (Yaw)
$C_{AV}$	C	.021	deg <sup>-1</sup>	Aero Side Force Coeff.
$C_{LN}$	C	2480	lb/in	Nose Gear Lateral Spring Rate
$C_{MT}$	C	9530	lb/in	M.G. Tire Vertical Spring Rate
$C_{NT}$	C	12,200	lb/in	N.G. Tire(s) Vertical Spring Rate
$C_{PI}$	C	37,060	lb/rad in	Parameters for $P_{wc}$
$C_{P2}$	C	12,353	lb/rad in <sup>2</sup>	
$C_{P3}$	C	45,794	lb/rad	
$C_{P4}$	C	10,500	lb/rad in	Drag Brace Characteristic Spring Rates
$C_{U1}$	C	$1.365 \times 10^5$	lb/in	
$C_{U2}$	C	$.775 \times 10^5$	lb/in	
$D_{LN}$	C	1.78	lb sec/in	Nose Gear Lateral Damping Coeff.
$D_{MT}$	C	38.8	lb sec/in <sup>2</sup>	M.G. Tire Vertical Damping Coeff.
$D_{NT}$	C	50.6	lb sec/in <sup>2</sup>	N.G. Tire(s) Vertical Damping Coefficient

Table A8 Airplane System (6 Degree) Parameters (Sheet 2 of 9)

SYMBOL	TYPE	VALUE	UNITS	DESCRIPTION
$D_{u1}$	C	53.4	lb sec/in	Drag Brace Characteristic
$D_{u2}$	C	30.5	lb sec/in	Damping Coefficient
$D_{VM}$	C	0.0	lb sec/in	M. G. Shock Strut Linear Damping Coefficient
$D_{VN}$	C	0.0	lb sec/in	N. G. Shock Strut Linear Damping Coefficient
$E_{AD}$	C	-.0036	deg <sup>-1</sup>	Aero Drag Coefficient
$E_{AL}$	C	.022	deg <sup>-1</sup>	Aero Lift Coefficient
$E_{AM}$	C	-3.759	in/deg	Aero Moment Coefficient
$F_{AD}$	V		lb	Aero Drag
$F_{AL}$	V		lb	Aero Lift
$F_{ASL}$	V		lb	Side Force Due to Aero Lift
$F_{ASY}$	V		lb	Side Force Due to Yaw
$F_{DN}$	V		lb	N. G. Rolling Resistance
$F_{DVL}$	V		lb	Horizontal Load at M. G. Pivot
$F_{DUR}$	V		lb	Horizontal Load on M. G. Axle
$F_{GL}$	V(I)		lb	Lateral Nose Gear Load
$F_{GR}$	V(I)		lb	Normal Cornering Force
$F_{LN}$	V		lb	Normal Cornering Force at Time = 0
$F_{NCF}$	V	0.0	lb	Time Derivative of Normal Cornering Force
$F_{NCF0}$	C		lb/sec	Steady State Normal Cornering Force
$\dot{F}_{NCF}$	V		lb	M. G. Tire Normal Load
$F_{NCFs}$	V		lb	
$F_{NML}$	V(o)		lb	
$F_{NMR}$	V(o)		lb	

Table A8 Airplane System (6 Degree) Parameters (Sheet 3 of 9)

SYMBOL	TYPE	VALUE	UNITS	DESCRIPTION
$F_{NN}$	V		lb	N.G. Tire Normal Load
$F_{NTF}$	V		lb	Nose Tire Friction Force
$F_{SNS}$	V		lb	Nose Tire Lateral Force
$F_{STL}$	V(I)		lb	M. G. Lateral Tire Force
$F_{STR}$	V(I)		lb	
$F_{TL}$	V		lb	M. G. Loads for Torque
$F_{TLO}$	V		lb	Takeout Correction
$F_{TR}$	V		lb	
$F_{TKO}$	V		lb	
$F_{TH}$	C	1000.	lb	Engine Thrust
$F_{THV}$	V		lb	Vertical Component of Engine Thrust
$F_{THS}$	V		lb	Side Component of Engine Thrust
$F_{UL}$	V		lb	M. G. Loads in Fictitious Drag Brace
$F_{UR}$	V		lb	M. G. Shock Strut Load
$F_{VML}$	V		lb	
$F_{VMR}$	V		lb	M. G. Shock Strut Air Load Curve
$F_{VMS}$	V*		lb	N. G. Shock Strut Load
$F_{VN}$	V		lb	N. G. Shock Strut Air Load Curve
$F_{VNS}$	V*		lb	Gravitational Constant
G	C	386	in/sec <sup>2</sup>	Aero Drag Parameter
$G_{AD}$	C	.240	-	Aero Lift Parameter
$G_{AL}$	C	-.016	-	Aero Moment (Pitch) Parameter
$G_{AM}$	C	2.286	in	Pilot's Steering Gain
$G_{PIL}$	C	3.0	sec <sup>-1</sup>	Torque Adjustment Parameter
$H_A$	C	0.0	-	$H_A + H_G = 1$
$H_{AP}$	C	0.0	in	Height of Center of Pressure above C. G.

\*Point Plot Input

Table A8 Airplane System (6 Degree) Parameters (Sheet 4 of 9)

SYMBOL	TYPE	VALUE	UNITS	DESCRIPTION
$H_G$	C	1.0	-	Torque Adjustment Parameter
$\Theta_N$	V		rad	Nose Wheel Turn Angle Relative to $A_{PL}\phi$ .
$\Theta_{N0}$	C	0.0	rad	$\Theta_N$ at Time = 0
$\dot{\Theta}_N$	V		rad/sec	$d\Theta_N/dt$
$\Theta_{GR}$	V		rad	M. G. Strut Rotation from Horizontal
$\Theta_{GL}$	V		rad	$\Theta_G$ at Time = 0
$\Theta_{GLO}$	C	.0329	rad	
$\Theta_{GRO}$	C	.0329	rad	
$\dot{\Theta}_{GL}$	V		rad/sec	Angular Velocity of M. G. Strut
$\dot{\Theta}_{GR}$	V		rad/sec	
$\dot{\Theta}_{GLO}$	C	0.0	rad/sec	$\dot{\Theta}_G$ at time = 0
$\dot{\Theta}_{GRO}$	C	0.0	rad/sec	
$\ddot{\Theta}_{GL}$	V		rad/sec <sup>2</sup>	Angular Acceleration of M. G. Strut
$\ddot{\Theta}_{GR}$	V		rad/sec <sup>2</sup>	
$\Theta_{NMAX}$	C	0.7	rad	Maximum Nose Wheel Turning Angle
$\Theta_{YAW}$	V		rad	Nose Wheel Turning Yaw Angle
$\psi$	V		rad	Angle of Relative Wind
$P$	V		rad	Airplane Roll Angle
$P_0$	C	0.0	rad	$P$ at Time = 0
$\dot{P}$	V		rad/sec	Airplane Roll Rate
$\ddot{P}$	V		rad/sec	$\dot{P}$ at Time = 0
$\ddot{P}_0$	C	0.0	rad/sec <sup>2</sup>	Roll Acceleration
$\ddot{P}$	V		rad/sec <sup>2</sup>	
$P_{WC}$	V		lb/rad	Nose Tire Cornering Power
$Q$	V		rad	Airplane Fitch Angle
$Q_0$	C	.0329	rad	$Q$ at Time = 0
$\dot{Q}$	V(o)		rad/sec	Pitch Rate

Table A8 Airplane System (C Degree) Parameters (Sheet 5 of 9)

SYMBOL	TYPE	VALUE	UNITS	DESCRIPTION
$\dot{Q}_0$	C	0.0	rad/sec	Q at Time = 0
$\dot{Q}_A$	V		rad/sec <sup>2</sup>	Pitch Acceleration
$\dot{Q}_{AT}$	V		lb	Aero Press X Aref
$\dot{Q}_L$	V		lb	Aero Press X Aref (Includes Vwy)
$\dot{Q}_L$	V		rad	Angular Position and Velocity
$\dot{Q}_R$	V		rad/sec	of M. G. Relative to the Airplane
$\dot{Q}_R$	V		rad	
$\dot{R}$	V		rad/sec	Airplane Yaw Angle
$\dot{R}_0$	C	0.0	rad	R at Time = 0
$\dot{R}_0$	V		rad/sec	Yaw Rate
$\dot{R}_0$	C	0.0	rad/sec	$\dot{R}$ at Time = 0
$\dot{R}$	V		rad/sec <sup>2</sup>	Yaw Acceleration
$R_{0RM}$	C	23.32	in	M. G. Tire Undelected Radius
$R_{0RN}$	C	10.80	in	N. G. Tire Undelected Radius
$R_{HA}$	C	.00238	slug/ft <sup>3</sup>	Air Density
$S_{GL}$	C	26.50	in	#
$S_{GS}$	C	20.00	in	#
$S_{GU}$	C	21.00	in	#
$S_{GW}$	C	60.00	in	#
$S_{HM}$	C	36.20	in	#
$S_{HN}$	C	258.90	in	#
$S_{HT}$	V(I)		deg	Horizontal Tail Deflection
$S_{MR}$	V(O)		in	M. G. Tire Deflection
$S_{ML}$	V(O)		in	M. G. Tire Deflection Rate
$\dot{S}_{MR}$	V		in/sec	
$\dot{S}_{ML}$	V		in/sec	
$\dot{S}_N$	V		in	N. G. Tire Deflection
$\dot{S}_N$	V		in/sec	N. G. Tire Deflection Rate

# See Figure 25

Table A8 Airplane System (6 Degree) Parameters (Sheet 6 of 9)

SYMBOL	TYPE	VALUE	UNITS	DESCRIPTION
SPI	C	1.925	in	Parameter of Cornering Power Pwc
STH	C	20.00	in	#
SVM	C	84.24	in	#
SVMU	C	36.74	in	#
SVN	C	85.86	in	#
SYRL	C	7.92	in	Nose Tire Relaxation Length (Yaw)
TAM	V		in lb	Aero Pitching Moment
TAY	V		in lb	Aero Yawing Moment
TSL	V(I)		in lb	Moment on M. G. Axle
TSE	V(I)		in lb	
TTH	C	20,000	in lb	
UNTF	C	.553	-	Thrust Moment about C. G.
UREN	C	.02	-	Nose Tire Friction Coefficient
URT	V		-	Nose Tire Rolling Resistance Coefficient
VWY	V*		in/sec	Nose Tire Cornering Parameter Crosswind
WA	C	147.6	lb sec <sup>2</sup> /in	Airplane Mass
WIP	C	$1.465 \times 10^6$	lb sec <sup>2</sup> /in	Roll Moment of Inertia
WDQ	C	$3.66 \times 10^6$	lb sec <sup>2</sup> /in	Pitch Moment of Inertia
WIR	C	$4.93 \times 10^6$	lb sec <sup>2</sup> /in	Yaw Moment of Inertia
WWM	C	1.667	lb sec <sup>2</sup> /in	M. G. Unsprung Mass
WWN	C	.453	lb sec <sup>2</sup> /in	N. G. Unsprung Mass
WU	C	.723	lb sec <sup>2</sup> /in	M. G. Upper Strut Mass
X	V		in	Horizontal Position of APL C.G.
X0	C	36.20	in	X at Time = 0
X	V		in/sec	Airplane Velocity in the x Direction
X0	C		in/sec	Velocity at Time = 0
X	V	2400	in/sec <sup>2</sup>	Airplane Acceleration in the X Direction

\*Point Plot Input

Table A3 Airplane System (6 Degree) Parameters (Sheet 7 of 9)

SYMBOL	TYPE	VALUE	UNITS	DESCRIPTION
$X_{AXL}$	V(O)		in	M.G. Axle Undelected Location ( $x$ Direction)
$\dot{X}_{AXL}$	V(O)		in/sec	M.G. Axle Undelected Velocity ( $x$ Direction)
$X_{WML}$	V(I)		in	{ M.G. Tire Footprint Location and Velocity in the $x$ direction
$\dot{X}_{WML}$	V(I)		in/sec	
$X_{WMR}$	V(I)		in	
$\dot{X}_{WMR}$	V(I)		in/sec	
$X_{WN}$	V		in	{ N.G. Tire Location ( $x$ direction) N.G. Tire Velocity ( $x$ direction) M.G. Undelected Axle Location ( $x$ Direction)
$\dot{X}_{WN}$	V		in/sec	
$X_{AXE}$	V(O)		in	
$\dot{X}_{AXE}$	V(O)		in/sec	
$\gamma$	V		in	M.G. Undelected Axle Velocity ( $x$ Direction)
$\gamma_0$	C	0.0	in	Horizontal C. G. Location ( $\gamma$ Direction)
$\dot{\gamma}$	V		in/sec	$\gamma$ at Time = 0 Airplane C.G. Velocity in $\gamma$ Direction
$\ddot{\gamma}_0$	C	0.0	in/sec	$\dot{\gamma}$ at Time = 0
$\ddot{\gamma}$	V		in/sec <sup>2</sup>	Airplane C.G. acceleration in $\gamma$ Direction
$\gamma_{AXL}$	V(O)		in	{ M.G. Undelected Axle Location and Velocity in the $\gamma$ Direction
$\dot{\gamma}_{AXL}$	V(O)		in/sec	
$\gamma_{AXE}$	V(O)		in	
$\dot{\gamma}_{AXE}$	V(O)		in/sec	
$\gamma_{DLN}$	V		in	{ N.G. Lateral Deflection N.G. Lateral Delta Velocity M.G. Tire Footprint Location In the $\gamma$ Direction
$\dot{\gamma}_{DLN}$	V		in/sec	
$\gamma_{ML}$	V(I)		in	
$\dot{\gamma}_{MR}$	V(I)		in	

Table A8 Airplane System (6 Degree) Parameters (Sheet 8 of 9)

SYMBOL	TYPE	VALUE	UNITS	DESCRIPTION
$\dot{Y}_N$	V		in	N.G. Lateral Location ( $\gamma$ Direction)
$\dot{Y}_{NO}$	C	0.0	in	$\dot{Y}_N$ at Time = 0
$\ddot{Y}_N$	V		in/sec	N.G. Lateral Velocity
$\ddot{Y}_{NO}$	C	0.0	in/sec	$\ddot{Y}_N$ at Time = 0
$\ddot{Y}_N$	V		in/sec <sup>2</sup>	N.G. Lateral Acceleration
$\ddot{Z}$	V		in	Height of Apl C.G. above ground ref.
$\ddot{Z}_0$	C	02.36	in	$\ddot{Z}$ at Time = 0
$\dot{\ddot{Z}}$	V		in/sec	Apl vertical velocity
$\ddot{\ddot{Z}}$	C	0.0	in/sec	$\dot{\ddot{Z}}$ at Time = 0
$\ddot{\ddot{Z}}$	V		in/sec <sup>2</sup>	Apl Vertical acceleration
$\ddot{Z}_{GO}$	V(I)		in	Runway contour height
$\ddot{Z}_{GDP}$	V(I)		in/in	Runway contour slope ( $\alpha$ Direction)
$\ddot{Z}_{ELL}$	V		in	Distance from $W_u$ position to Axle
$\ddot{Z}_{GLR}$	V		in	M.G. Strut Velocity and Stroke
$\ddot{Z}_{SML}$	V		in	
$\ddot{Z}_{SML}$	V		in/sec	
$\ddot{Z}_{SMR}$	V		in	
$\ddot{Z}_{SMR}$	V		in/sec	
$\ddot{Z}_{SN}$	V		in	
$\ddot{Z}_{SN}$	V		in/sec	
$\ddot{Z}_{WML}$	V		in	N. G. Stroke
$\ddot{Z}_{WMR}$	V		in	N.G. Stroke Velocity
$\ddot{Z}_{WML0}$	C	20.91	in	M. G. Axle Height
$\ddot{Z}_{WMR0}$	C	20.91	in	M.G. Axle Height at Time = 0
$\ddot{Z}_{WML}$	V		in/sec	
$\ddot{Z}_{WMR}$	V		in/sec	M.G. Axle Velocity

Table A8 Airplane System (6 Degree) Parameters (Sheet 9 of 9)

SYMBOL	TYPE	VALUE	UNITS	DESCRIPTION
$\dot{Z}_{WMLO}$	C	0.0	in/sec	M.G. Axle Velocity at Time = 0
$\dot{Z}_{WMRO}$	C	0.0	in/sec	M.G. Axle Vertical Acceleration
$\dot{Z}_{WML}$	V		in/sec <sup>2</sup>	
$\dot{Z}_{WMR}$	V		in/sec <sup>2</sup>	
$\dot{Z}_{WLN}$	V		in	N. G. Axle Vertical Location
$\dot{Z}_{WNO}$	C	10.02	in	$\dot{Z}_{WN}$ at Time = 0
$\dot{Z}_{WLN}$	V		in/sec	N.G. Axle Vertical Velocity
$\dot{Z}_{WNO}$	C	0.0	in/sec	$\dot{Z}_{WN}$ at Time = 0
$\dot{Z}_{WLN}$	V		in/sec <sup>2</sup>	N. G. Axle Vertical Acceleration
$F_{OEV L}$	V(I)		lb	M. G. Tire Unbalance
$F_{OEV R}$	V(I)		lb	

#### 4a. WHEEL AND TIRE SYSTEM (FLYWHEEL)

Figure A33 shows the components of the wheel and tire system.

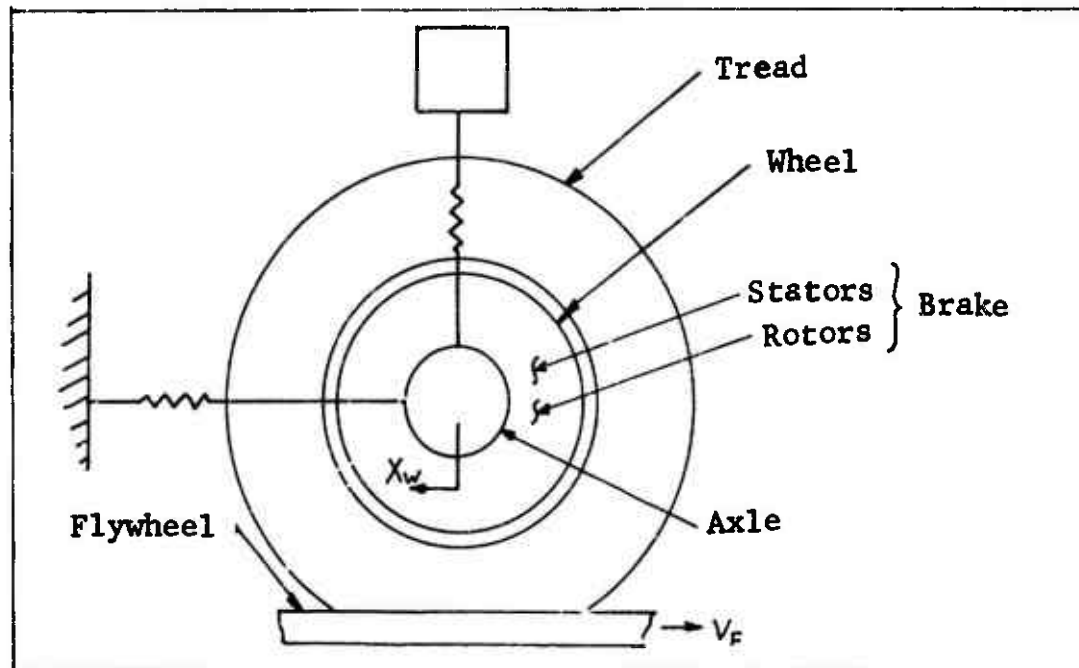


Figure A33 Components of the Wheel and Tire System

In the vertical, or Z direction, the axle, brake, wheel, tire, and lower shock strut are combined and operate as a single mass point. A description of this mode is found in the airplane system. The airplane system furnishes various inputs to the tire and wheel:  $V_F$  the airplane (flywheel surface) velocity;  $F_{NM}$ , the vertical load between the tire and pavement;  $S_M$ , the tire deflection. The brake torque  $T_{ST}$  is an input from the brake system.

The horizontal displacement of two mass points is considered. One mass point is made up of the axle, brake, wheel, and the inner part of the tire and its location is designated as  $X_w$ . The other mass point is the tire tread and its location is designated as  $X_{TT}$ .

In rotation, there are three mass points: the axle and stationary brake elements make up the first; the brake rotors, wheel, and inner tire make up the second; and the tire tread makes up the third. The angular positions of these three mass points are denoted respectively as  $\Theta_s$ ,  $\Theta_w$ , and  $\Theta_T$ . Let  $F_G$  be the horizontal force acting on the

axle and let  $F_{TT}$  be the net horizontal force between the wheel and tire tread. Figure A34 shows the location of these forces.  $F_{BT}$  is the horizontal force between the tire and the flywheel surface.

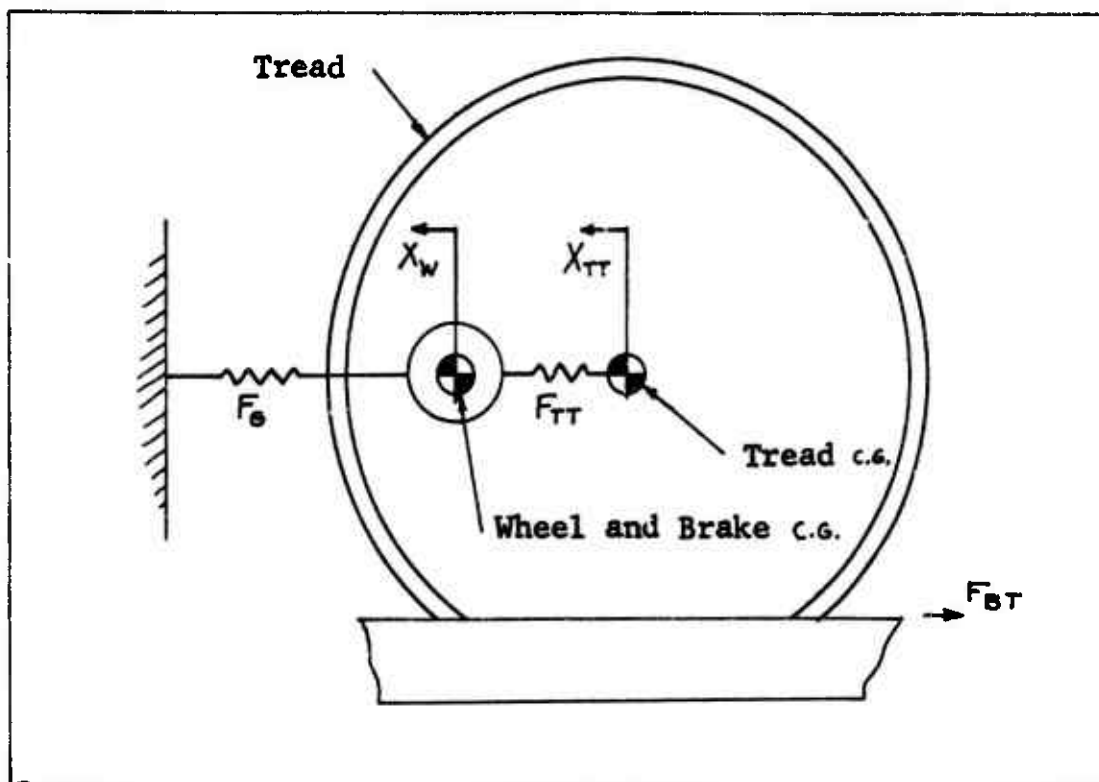


Figure A34 Tire Horizontal Model

#### A. Mathematical Description

Equations describing the tire and wheel behavior are developed by referring to Figure A34. Forces  $F_6$  and  $F_{TT}$  are defined by equations (4a.1), (4a.2), and (4a.3) as follows:

$$(4a.1) \quad F_6 = -C_{GN} X_W - D_{GN} \dot{X}_W$$

$$(4a.2) \quad F_{TT} = C_{TT} (X_{TT} - X_W) + E_{TT} (X_{TT} - X_V) + D_{TLV} (\dot{X}_{TT} - \dot{X}_W)$$

$$(4a.3) \quad D_{TT} (\dot{X}_V - \dot{X}_W) = E_{TT} (X_{TT} - X_V)$$

Equations (4a.2) and (4a.3) describe a type 2 spring-damper system as defined by Figure A38 and discussed in the parameter evaluation.

Let  $W_{GW}$  denote the mass of the axle, wheel, brake and inner part of the tire. Let  $W_{TE}$  denote the appropriate tire tread mass. Summing forces in the horizontal direction gives:

$$(4a.4) \quad W_{GW} \ddot{X}_W = F_G + F_{TT}$$

$$(4a.5) \quad W_{TE} \ddot{X}_{TT} = -F_{TT} - F_{BT} + F_{\Theta RH}$$

Where  $F_{\Theta RH}$  is a force produced by tire unbalance, the corresponding vertical part of this unbalance force is denoted by  $F_{\Theta RV}$ . These two forces are given in equations (4a.6) and (4a.7).

$$(4a.6) \quad F_{\Theta RH} = R_{\Theta} W_T^2 \sin\langle\Theta_T\rangle$$

$$(4a.7) \quad F_{\Theta RV} = R_{\Theta} W_T^2 \cos\langle\Theta_T\rangle$$

$W_T$  and  $\Theta_T$  are the rotational speed and position of the tire tread.

The rotational schematic of the wheel and tire system is shown in Figure A35 .

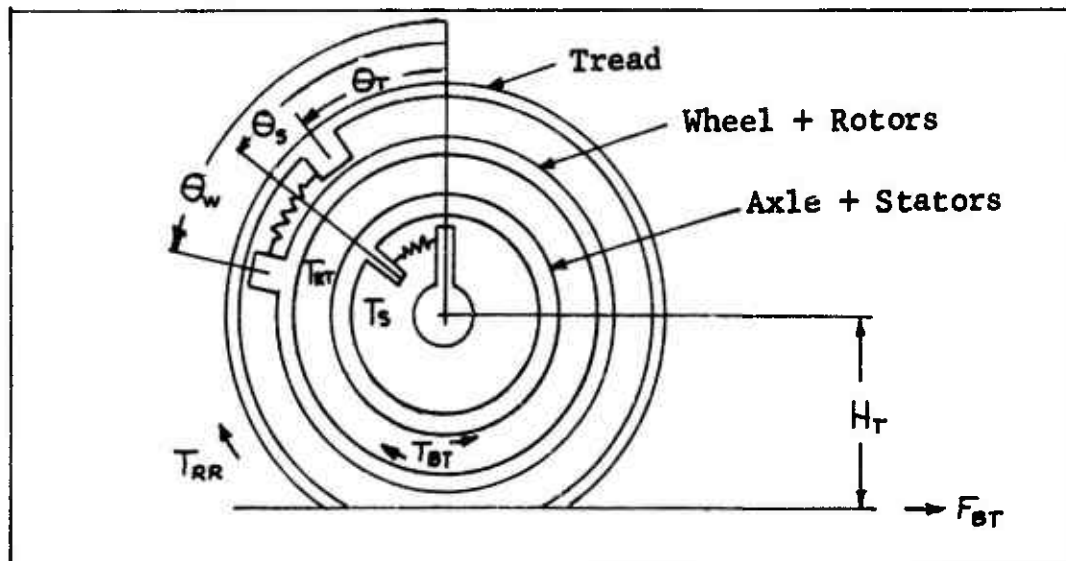


Figure A35 Tire Rotational Model

Let  $T_{RT}$  and  $T_s$  be defined by equations (4a.8), (4a.9), and (4a.10) as follows:

$$(4a.8) \quad T_{RT} = C_{RT}(\Theta_w - \Theta_T) + E_{RT}(\Theta_w - \Theta_Y) + D_{TRV}(\dot{\Theta}_w - \dot{\Theta}_T)$$

$$(4a.9) \quad D_{RT}(\dot{\Theta}_Y - \dot{\Theta}_T) = E_{RT}(\Theta_w - \Theta_Y)$$

$$(4a.10) \quad T_s = C_{RS} \theta_s + D_{RS} \dot{\theta}_s$$

Let  $H_T$  be the height of the axle above the ground. Let  $T_{RR}$  be the torque on the tire that produces rolling resistance. These two quantities are given by:

$$(4a.11) \quad H_T = R_{OT} - S_M$$

$$(4a.12) \quad T_{RR} = \begin{cases} S_M (D_{SR} + D_{VR} W_T) & \text{if } W_T > 0 \\ 0 & \text{if } W_T = 0 \\ S_M (-D_{SR} + D_{VR} W_T) & \text{if } W_T < 0 \end{cases}$$

If  $T_{BT}$  is the brake torque, then torques can be summed to obtain the following three equations:

$$(4a.13) \quad W_{IS} \ddot{\theta}_s = T_{BT} - T_s$$

$$(4a.14) \quad W_{IW} \ddot{\theta}_w = -T_{RT} - T_{BT}$$

$$(4a.15) \quad W_{IT} \ddot{\theta}_T = H_T F_{BT} + T_{RT} - T_{RR}$$

The rolling radius of the tire is obtained using the methods of Reference 1. Denoting the rolling radius as  $R_T$ , it is defined as:

$$(4a.16) \quad R_T = R_{OT} - \frac{1}{3} S_M - U_{RR} (X_{TT} - X_W)$$

Let  $V_{RS}$  denote the velocity of the tire footprint relative to the flywheel surface with  $W_T = 0$ , let  $V_R$  be the relative velocity including  $W_T$ .

$$(4a.17) \quad V_{RS} = V_F + \dot{X}_{TT}$$

$$(4a.18) \quad V_R = V_{RS} - R_T W_T$$

Here  $V_F$  is the velocity of the flywheel surface. Adopting the convention,  $W_T = \dot{\theta}_T$ ;  $W_s = \dot{\theta}_s$ ; and  $W_w = \dot{\theta}_w$ , the relative angular velocity between the stators and rotors is denoted by  $W_B$  and is established by:

$$(4a.19) \quad W_B = W_w - W_s$$

When a tire is moving over a runway with any appreciable amount of standing water or slush, a hydrodynamic "wedge"

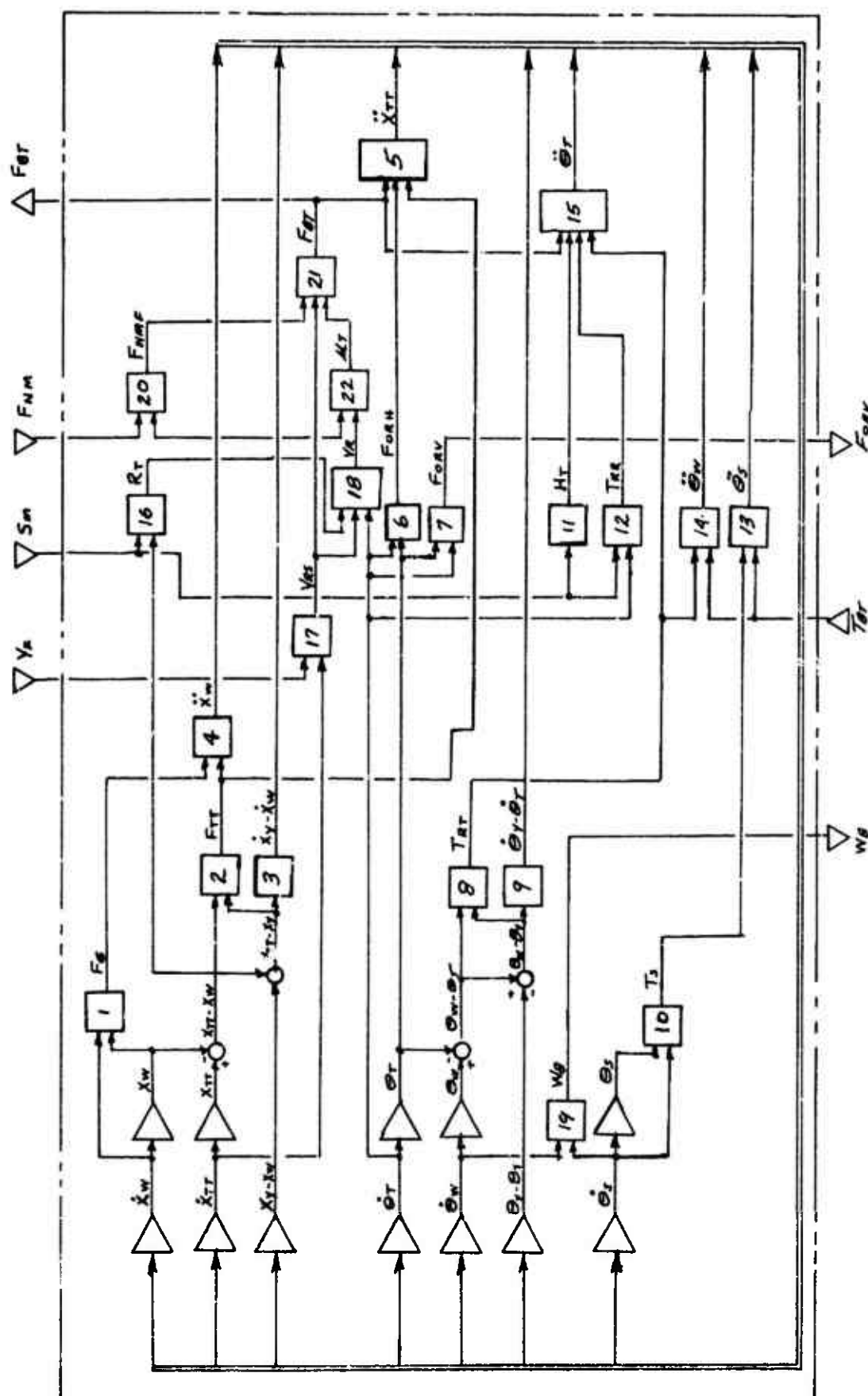


Figure A36 Wheel and Tire System (Flywheel) Equation Flow Diagram

of water starts separating the tread and runway surface. It is assumed that the length of this "wedge" is proportional to  $V_{RS}^2$  and at hydroplaning speed,  $V_{HY}$ , the tread is completely separated from the runway. In equations (4a.20) and (4a.21) the coefficients  $C_{HY}$  and  $D_{HY}$  are used to define hydroplaning effects and water drag on the wheel. For dry runway conditions,  $C_{HY}$  and  $D_{HY}$  are zero. The horizontal force between the tire tread footprint and the runway surface is established by equations (4a.20), (4a.21), and (4a.22) as follows:

$$(4a.20) F_{NMF} = F_{NM} (1 - C_{HY} (V_{RS}/V_{HY})^2)$$

$$(4a.21) F_{BT} = F_{NMF} U_T + D_H V_{RS}^2$$

$$(4a.22) U_T = \begin{cases} U_{T1} + (U_{T2} - E_T V_{RS}) e^{-\alpha V_R} & \text{if } V_R > V_{R0} \\ \left\{ [U_{T1} + (U_{T2} - E_T V_{RS}) e^{-\alpha V_{R0}}] \frac{V_R}{V_{R0}} \right\} & \text{if } V_{R0} < V_R < V_{R0} + V_{R0} \\ -U_{T1} (U_{T2} - E_T V_{RS}) e^{-\alpha V_R} & \text{if } V_R < V_{R0} \end{cases}$$

Figure A36 is an equation flow diagram showing the relation between equations (4a.1) through (4a.22).

## B. Parameter Evaluation

### Gear Characteristics

The mass  $W_{GW}$  is made up of the mass of half the shock strut, half the lateral beam, the axle, the wheel, the brakes, and all but one-third of the tire tread. The sum of the masses of these components totals 616 LBM. Thus,  $W_{GW} = 616/386 = 1.60 \text{ lb sec}^2/\text{in}$ . The fore and aft natural frequency of the gear (as calculated from deflection data) is  $21.84 \text{ cps} = 137.5 \text{ rad/sec}$ . Using the gear mass, with all of the tire included (644 LBM), the spring rate  $C_{GH}$  can be calculated as:

$$(4a.23) C_{GH} = m \omega_n^2 = \left( \frac{644}{386} \right) (137.5)^2 = 31,500 \text{ lb/in}$$

A typical approach to estimate the damping coefficient is to use 3% critical. Thus,

$$(4a.24) D_{GH} = (.03) 2 \sqrt{m C_G} = (.06) \sqrt{\left( \frac{644}{386} \right) 31500} = 13.8 \frac{\text{lb sec}}{\text{in}}$$

## Tire Tread Characteristics

The principle underlying the calculation of the tire friction coefficient is that compared to the rest of the tire, the tire "footprint" is totally inelastic. (The tire "footprint" is that portion of the tire tread which is in contact with the ground). Thus, if the velocity of the footprint and the friction vs. velocity curve for the rubber-surface interface are defined, the tire friction coefficient is established. In order to predict the motion of the footprint, the tire tread is assumed to behave like an inelastic ring which is supported on the wheel as shown in Figure A37.

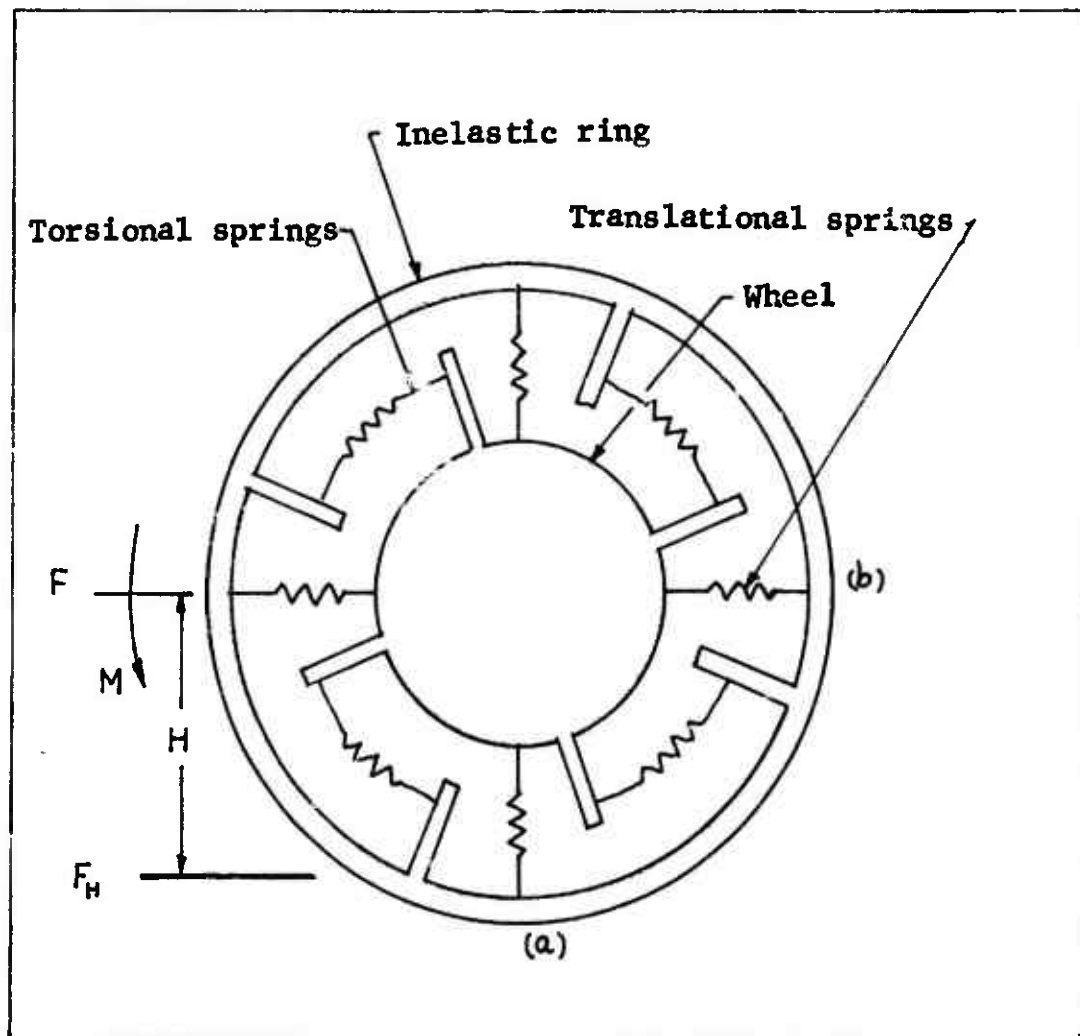


Figure A37 Tire Tread Model

The horizontal position of the footprint is assumed to be the same as the horizontal position of the ring center of gravity. A frictional force  $F_H$  applied at the ground can be resolved into a translational force  $F = F_H$  acting at the ring C.G., plus a moment  $M = F_H \cdot H$  acting about the ring C.G.

For an actual tire with distributed mass and elasticity approximately one-third of the tire would move with the footprint in response to force,  $F_H$ . Therefore, it is assumed for translation the mass of the ring,  $W_{TE}$ , is one-third of the tire tread mass, which is 84 LBM. Thus,  $W_{TE} = (84)/(3 \times 386) = 0.0725 \text{ LBF SEC}^2/\text{IN}$ .

For rotation the total tire tread mass is assumed to move in response to moment,  $M$ . Thus, the moment of inertia about its center of gravity is  $W_{IT} = MR^2 = (84/386) (23^2) = 115 \text{ LBF SEC}^2/\text{IN}$ .

References 1 (page 22) and 10 (Figure 8) are used to obtain values for the torsional and translational spring rates as shown in Figure A37. Under the application of the force  $F_H$ , the peripheral movement at point (b) is about 20% of the peripheral movement at point (a) in Figure A37. The expression for the footprint spring rate from Reference 1 is:

$$(4a.25) K_x = .6 d (P + 4 P_r) \sqrt[3]{S_o/d}$$

Where for the F-111 with a vertical tire load of 25,000 lb,

$d = 46.65 \text{ in.}$  = Tire diameter  
 $P = 150 \text{ psi}$  = Tire operating pressure  
 $P_r = 150 \text{ psi}$  = Tire rated pressure  
 $S_o = 2.75 \text{ in.}$  = Operating (static) deflection

Thus,

$$(4a.26) K_x = (.6)(46.65)(5)(150) \sqrt[3]{2.75/46.65} = 8150 \text{ lb/in}$$

The application of  $F_H = 8150 \text{ lb.}$  causes the footprint to move one inch. At point b, the movement is .2 inches. Assuming that the movement at point b is all due to rotation, the apparent torsional spring rate is:

$$(4a.27) C_{RT} = \left(\frac{d}{2}\right) \frac{H F_H}{(.2)} = \frac{(23.32)(20.57)(8150)}{(.2)} = 19.5 \times 10^6 \text{ IN LBF/RAD}$$

Since .8 inches of the 1.0 inch footprint motion is due to tread C.G. fore and aft translation, the apparent spring rate is:

$$(4a.28) C_{TT} = \frac{F_H}{.8} = \frac{8150}{.8} = 10,200 \text{ lb/in}$$

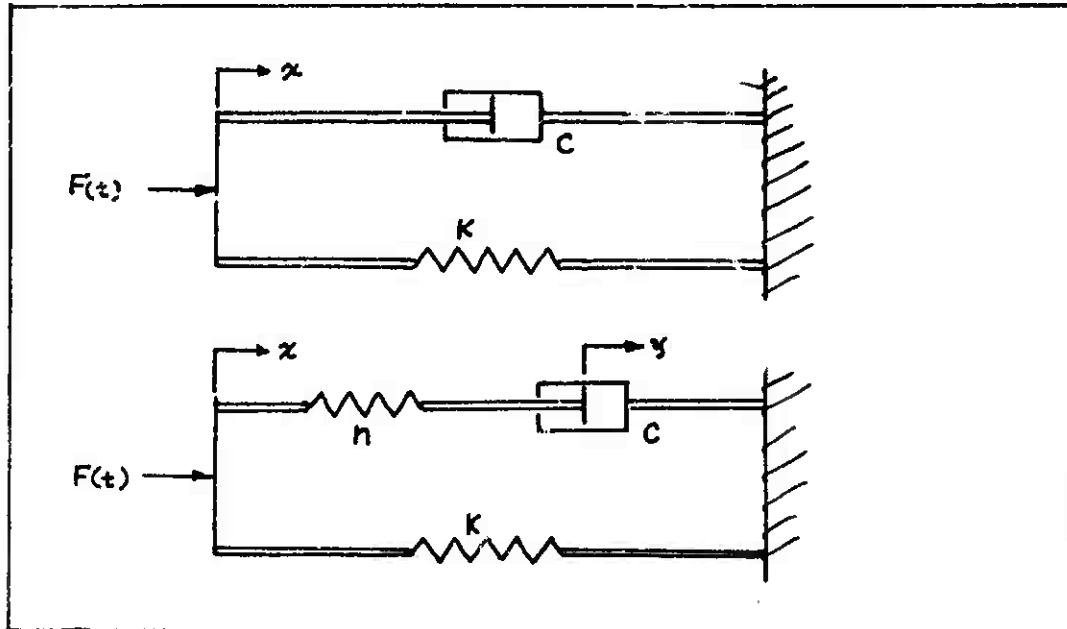


Figure A38 Tire Damping Models

It is well publicized and generally accepted that the elastic and damping characteristics of tires and other structural devices are not accurately described by the mathematically convenient linear spring-viscous damper representation over a wide frequency range. The behavior of rubber-like materials is particularly different than that described by the conventional model. To establish suitable mathematical descriptions of the various damping forces for tires and other elements of this study, several models were explored. Figure A38 depicts the two types of elastic systems which are used. The Type 1 model is a conventional system with viscous damping and Type 2 is a visco-elastic system, having elasticity and damping which varies with frequency. To compare the two, consider the effects of driving each with a variable force  $F(t) = F_0 \cos \omega t$ . In each case, the resultant deflection is  $x = x_0 \cos(\omega t - \phi)$

The loss coefficient,  $\beta$ , is defined by  $\beta = \tan \phi$ . For a conventional system (Type 1 with  $c$  and  $k$  constant), the loss coefficient which is a measure of the damping is

given by:

$$(4a.29) \beta = c\omega/k$$

Reference 1 assumes that  $c$  is of the form  $c = \eta k/\omega$  where  $\eta$  and  $k$  are constant. From this:

$$(4a.30) \beta = \eta$$

Reference 8 seems to indicate (p. 55) that the loss coefficient for tire tread rubber is somewhere between the above two values.

For the Type 2 system, shown in Figure constant, the loss coefficient is given by:

$$(4a.31) \beta = \left(\frac{c\omega}{k}\right) / \left(1 + \left(\frac{c\omega}{n}\right)^2 \left(1 + \frac{n}{k}\right)\right)$$

To represent a tire, the values  $(c/k) = 1.56 \times 10^{-3}$  sec. and  $(n/k) = 0.520$ , were used to compute values of  $\beta$  for a range of frequencies.  $\beta$  versus  $\omega$  is shown in Figure A39 for both Type 1 and Type 2 models, along with values of  $\beta$  taken from References 1 and 8. The value from Reference 1 is shown constant at all frequencies because the value is not identified with any frequency. The above values of  $(c/k)$  and  $(n/k)$  were chosen because they gave  $\beta$  values in best agreement with authoritative data.

Figure A39 shows both Type 1 and Type 2 models have relatively poor correlation with both data sources. Reference 8 indicates  $\beta$  is highly dependent upon temperature and tire rubber compound as might be expected. During damping model exploration, both Type 1 and Type 2 systems were examined dynamically on an analog computer. It was found that differences in their behavior were observable; however, since the damping forces are relatively small compared to the other forces, this difference was small. Either model is equally satisfactory for evaluating anti-skid operation. The Type 2 system is used for the tire because it is in closer agreement with recorded observations. The peak in the  $\beta$  versus frequency curve for the Type 2 system is in keeping with most of the contour plots for rubber-like materials as shown in Reference 7 and 8.

The tire elastic and damping coefficients are:

$$(4a.32) \quad \begin{cases} D_{TT} = (1.56 \times 10^3) C_{TT} = 15.9 \text{ lb sec/in} \\ E_{TT} = (.52) C_{TT} = 5300 \text{ lb/in} \\ D_{RT} = (1.56 \times 10^3) C_{RT} = 30,400 \text{ in lb sec/rad} \\ E_{RT} = (.52) C_{RT} = 10.15 \times 10^6 \text{ in lb/rad} \end{cases}$$

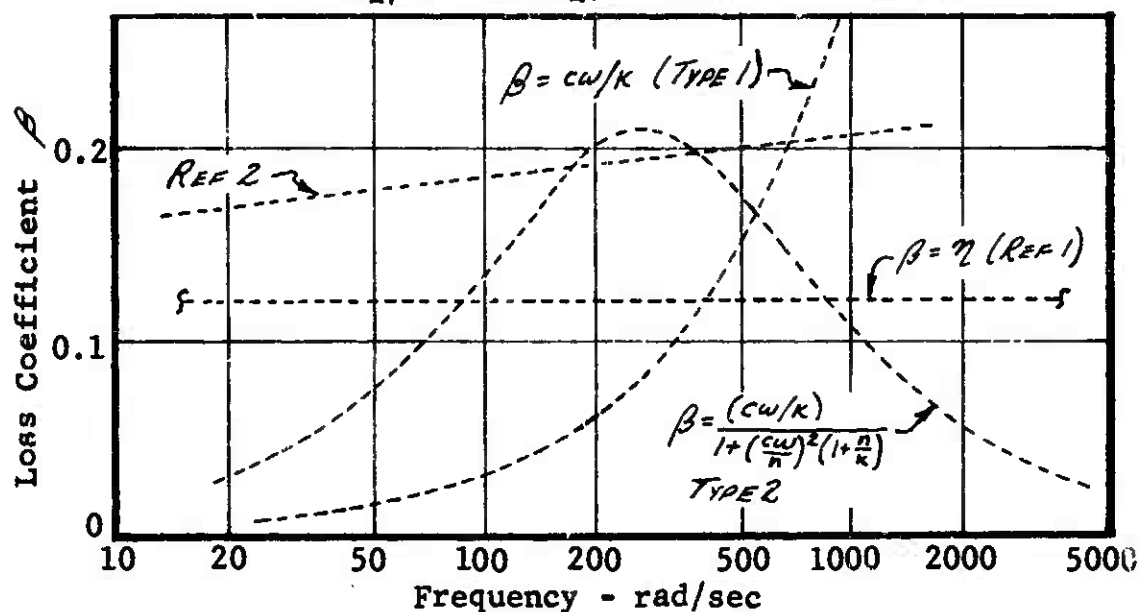


Figure A39 Model Loss Factors

The equation (4a.16) for the rolling radius  $R_T$  is a re-statement of equation (76 b) of Reference 1. To allow for circumferential decay length other than those equal to the outside free tire radius, a coefficient  $U_{RR}$  is provided. For this study  $U_{RR}$  is set equal to 1.0.

#### Axle Parameters

The observed torsional natural frequency of the axle (with brake stators) is 125 cps. The calculated value for its moment of inertia is 16.8 LBF SEC<sup>2</sup>/IN. Thus, the torsional spring rate,  $C_{RS}$ , is established as:

$$(4a.33) \quad C_{RS} = (2\pi 125)^2 (16.8) = 10.4 \times 10^6 \text{ in lb/rad}$$

For the steel axle, a value for  $\eta$  (in the type 1 system in Figure 38) is probably something less than .01 (Reference 7). Thus, at resonance, if  $c\omega/k = \eta$ , then the damping coefficient is established as:

$$(4a.34) \quad D_{RS} = k\eta/\omega = (10.4 \times 10^6)(.01)/(2\pi 125) = 132 \text{ in lb sec/rad}$$

## Tire Rolling Resistance

From Figure 17a of Reference 2, the rolling resistance coefficient,  $\mu_r$  is given by  $\mu_r = .012 + 1 \times 10^{-5}v$  where  $v$  is the axle speed in INCHES/SEC. Thus,

$$(4a.35) T_{RR} = \mu_r F_{RR} R_T = (.012 + 1 \times 10^{-5}V) F_{RR} R_T$$

$$\text{Or alternately, } = (.012 + 1 \times 10^{-5} \dot{\theta}_T R_T) (F_{RR}/\delta) (\delta) R_T$$

Since  $F_{RR}/\delta = C_{MT}$ , the rolling resistance coefficients are established as:

$$(4a.36) D_{SR} = .012 C_{MT} R_T = (.012)(9530)(20.57) = 2350 \text{ lb}$$

$$(4a.37) D_{VR} = 1 \times 10^{-5} C_{MT} R_T^2 = (9530 \times 10^{-5})(20.57)^2 = 40.3 \text{ lb sec}$$

Figure A40 shows the friction coefficient for a tire sliding (i.e. full skid) on a dry concrete runway as a function of velocity. This data is taken from Reference 3 and is applicable to a typical runway contaminated with rubber deposits from previous airplane operations. Table A9 below lists the appropriate coefficients for equation (4a.22) which apply for dry and wet runway surface conditions.

Table A9 Runway Friction Characteristics

SYMBOL	UNITS	WET CONCRETE	DRY CONCRETE
$U_{T1}$	-----	.050	.200
$U_{T2}$	-----	.180	.450
$E_T$	SEC/IN	$.065 \times 10^{-3}$	$.065 \times 10^{-3}$
$\alpha$	SEC/IN	$1.0 \times 10^{-3}$	$2.5 \times 10^{-3}$

## Initial Conditions

All initial conditions, except wheel and tire rotational speed, will be set to zero. From the airplane system at time = 0,  $V_F = 2400$  and  $S_M = 2.245$ . Using equation (4a.16) results in:

$$(4a.38) R_T = R_{\theta T} - \frac{1}{3} S_M = 23.32 - \frac{1}{3} (2.245) = 22.67 \text{ in}$$

In order that  $V_R$  be zero, equations (4a.18) and (4a.19) show that:

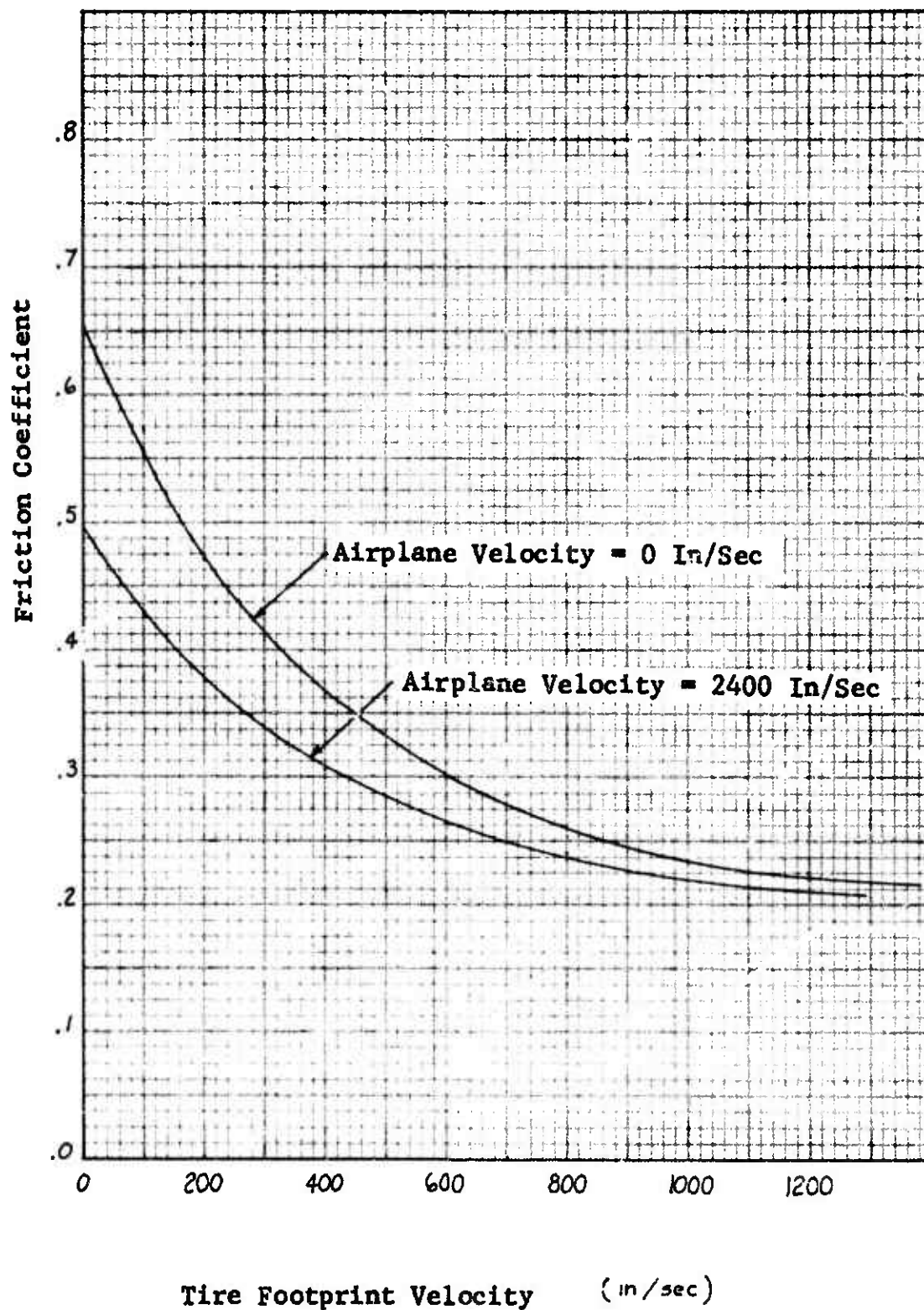


Figure A40 Tire Sliding Friction Coefficient

$$(4a.39) \quad \dot{\theta}_{T0} = \dot{\theta}_{W0} = V_F / R_T = 2400 / 22.67 = 105.9 \text{ rad/sec}$$

Table A10 Wheel and Tire System (Flywheel) Parameters (Sheet 1 of 4)

SYMBOL	TYPE	VALUE	UNITS	DESCRIPTION
$\alpha$	c	$2.5 \times 10^{-3}$	sec/in	Tire Friction Parameter
$C_{GH}$	c	3/500	lb/in	Fore and Aft Spring Rate at Axle
$C_{RS}$	c	$10.4 \times 10^6$	in lb/rad	Axle Rotational Spring Rate
$C_{RT}$	c	$19.5 \times 10^6$	in lb/rad	Tire to Wheel Rotational Spring Rate
$C_{HY}$	c	0.0	-	Controls Hydroplaning Influence
$C_{TT}$	c	10,200	lb/in	Tread to Wheel Spring Rate
$D_{GH}$	c	1/3.8	lb sec/in	Fore and Aft Damping Coefficient at Axle
$D_{HY}$	c	0.0	lb sec <sup>2</sup> /in <sup>2</sup>	Water Resistance Coefficient
$D_{RS}$	c	132.0	in lb sec/rad	Gear to Axle Rotational Damping Coefficient
$D_{RT}$	c	30,400	in lb sec/rad	Tire to Wheel Rotational Damping Coefficient
$D_{SR}$	c	2350	lb	Rolling Resistance Parameter
$D_{TT}$	c	15.9	lb sec/in	Tread to Wheel Damping Coefficient
$D_{VR}$	c	40.3	lb sec/rad	Rolling Resistance Parameter
$E_{RT}$	c	$10.15 \times 10^6$	in lb/rad	Tire to Wheel Coupling Spring Rate
$E_T$	c	$.65 \times 10^{-4}$	sec/in	Tire Friction Correction Coeff.
$E_{TT}$	c	5200	lb/in	Tread to Wheel Coupling Spring Rate
$F_{BT}$	v(o)		lb	Horizontal Force on Tire Footprint from Ground
$F_G$	v		lb	Horizontal Force at Axle
$F_{GEH}$	v		lb	Horizontal Wheel Unbalance Force
$F_{GEV}$	v(o)		lb	Vertical Wheel Unbalance Force
$F_{NM}$	v(I)		lb	Vertical Force between Tire and Ground
$F_{NMF}$	v		lb	Vertical Force not Supported by Water Film

Table A10 Wheel and Tire System (Flywheel) Parameters (Sheet 2 of 4)

SYMBOL	TYPE	VALUE	UNITS	DESCRIPTION
$F_{Tr}$	V		lb	Net Force Between Tread & Wheel
$H_T$	V		in	Axle Height Above Ground ( $H_T \leq R_{Gr}$ )
$\dot{\theta}_s$	V		rad	Axle Rotation
$\dot{\theta}_{s0}$	C	0.0	rad	Axle Rotation at Time = 0
$\ddot{\theta}_s$	V		rad/sec	Axle Rotational Speed
$\ddot{\theta}_{s0}$	C	0.0	rad/sec	Axle Rotational Speed at Time = 0
$\ddot{\theta}_s$	V		rad/sec <sup>2</sup>	Axle Rotational Acceleration
$\dot{\theta}_T$	V		rad	Tire Tread Rotation
$\dot{\theta}_{T0}$	C	0.0	rad	Tire Tread Rotation at Time = 0
$\ddot{\theta}_T$	V		rad/sec	Tire Tread Rotational Speed
$\ddot{\theta}_{T0}$	C	105.9	rad/sec	Tire Tread Rotational Speed at Time = 0
$\ddot{\theta}_T$	V		rad/sec <sup>2</sup>	Tire Tread Rotational Acceleration
$\dot{\theta}_w$	V		rad	Wheel Rotation
$\dot{\theta}_{w0}$	C	0.0	rad	Wheel Rotation at Time = 0
$\ddot{\theta}_w$	V		rad/sec	Wheel Rotational Speed
$\ddot{\theta}_{w0}$	C	105.9	rad/sec	Wheel Rotational Speed at Time = 0
$\ddot{\theta}_w$	V		rad/sec <sup>2</sup>	Wheel Rotational Acceleration
$\dot{\theta}_y$	V		rad	Dummy Variables used to
$\dot{\theta}_{y0}$	C		rad	Simulate Visco-elastic Tire
$\ddot{\theta}_y$	V		rad/sec	Characteristic
$R_{ko}$	C	0.0	rad/sec <sup>2</sup>	Unbalance Coefficient
$R_{Gr}$	C	0.0	lb sec <sup>2</sup> /rad <sup>2</sup>	Undelected Tire Radius
$R_T$	C	23.32	in	Tire Rolling Radius
$S_m$	V(I)		in	Tire Deflection
$T_{Br}$	V(I)		in lb	Brake Torque

Table A10 Wheel and Tire System (Flywheel) Parameters (Sheet 3 of 4)

SYMBOL	TYPE	VALUE	UNITS	DESCRIPTION
$T_{RZ}$	V		in lb	Torque Producing Rolling Resistance
$T_{RT}$	V		in lb	Torque between Tire (Tread) and Wheel
$T_s$	V		in lb	Axle Torque
$U_{RE}$	C	1.0	-	Rolling Radius Parameter
$U_T$	V		-	Tire Friction Coefficient
$U_{T1}$	C	.20	-	Tire Friction Parameters
$U_{T2}$	C	.45	-	
$V_F$	V(I)		in/sec	Flywheel Surface Velocity
$V_{HY}$	C		in/sec	Tire Hydroplaning Speed
$V_R$	V	2400	in/sec	Velocity of Tire Footprint Relative to Flywheel
$V_{ES}$	V		in/sec	Same as $V_R$ except Rotational Effects Ignored
$W_0$	V(O)		rad/sec	Relative Rotational Speed Between Stators and Rotors
$W_{GW}$	C	1.60	lb sec <sup>2</sup> /in	Effective Tire, Wheel, and Brake Mass
$W_{IS}$	C	16.8	in lb sec <sup>2</sup> /rad	Axle Moment of Inertia (+ Stators)
$W_{IT}$	C	115.0	in lb sec <sup>2</sup> /rad	Tread Moment of Inertia
$W_{IW}$	C	66.0	in lb sec <sup>2</sup> /rad	Wheel & Rotors Moment of Inertia
$W_s$	V		rad/sec	$W_s = \dot{\theta}_s$
$W_T$	V		rad/sec	$W_T = \dot{\theta}_T$
$W_{TE}$	C	.0725	lb sec <sup>2</sup> /in	Equivalent Tire Tread Mass
$W_W$	V		rad/sec	$W_W = \dot{\theta}_W$
$X_{TT}$	V		in	Location of Tire Tread C.G.
$X_{TTO}$	C	0.0	in	Location of Tire Tread C.G. at Time = 0

Table A10 Wheel and Tire System (Flywheel) Parameters (Sheet 4 of 4)

SYMBOL	TYPE	VALUE	UNITS	DESCRIPTION
$\dot{X}_{TT}$	V		IN/SEC	Tread CG Velocity
$\dot{X}_{TTO}$	C	0.0	IN/SEC	Tread CG Velocity at Time = 0
$\ddot{X}_{TT}$	V		IN/SEC <sup>2</sup>	Tread CG Acceleration
$X_W$	V		IN	Horizontal Axle Location
$X_{WO}$	C	0.0	IN	Horizontal Axle Location at Time = 0
$\dot{X}_W$	V		IN/SEC	Horizontal Axle Velocity
$\dot{X}_{WO}$	C	0.0	IN/SEC	Horizontal Axle Velocity at Time = 0
$\ddot{X}_W$	V		IN/SEC <sup>2</sup>	Horizontal Axle Acceleration
$X_Y$	V		IN	Dummy Variables Used to Simulate Visco-elastic Tire Characteristic
$X_{YO}$	C	0.0	IN	
$\dot{X}_Y$	V		IN/SEC	
$\dot{D}_{TRV}$	C	9500	IN LBF SEC/RAD	Tire Tread Radial Damping Coeff
$\dot{D}_{TRL}$	C	5.45	LBF SEC/IN	Tire Tread Longitudinal Damping Coeff
$V_{RO}$	C	25.0	IN/SEC	Tire Friction Threshold Velocity

#### 4b. WHEEL AND TIRE SYSTEM (3 DEGREE)

Figure A41 shows the components of the wheel and tire system. The wheel and tire system

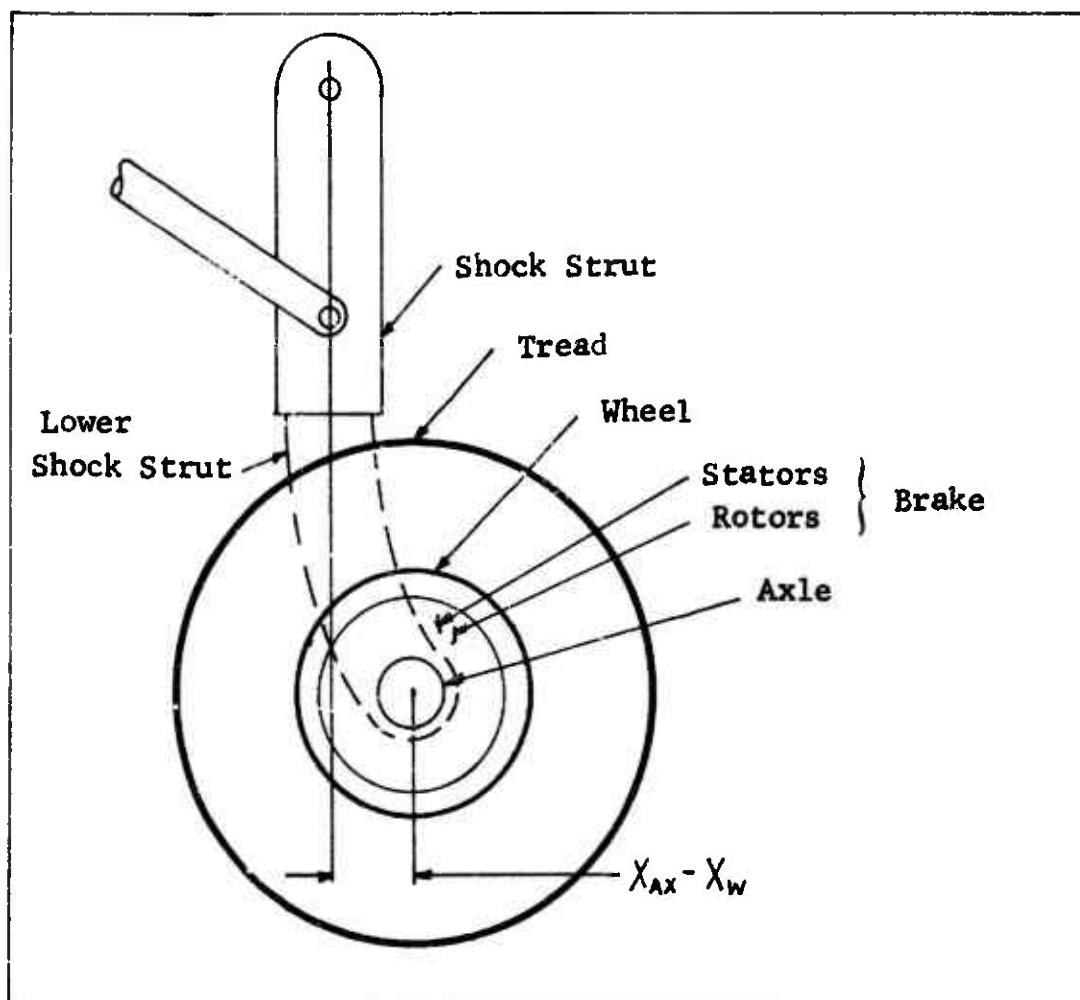


Figure A41 Components of the Wheel and Tire System

for the 3 degree airplane system is essentially the same as for the flywheel model. The Airplane System still furnishes the tire deflection  $S_M$  and the tire vertical load  $F_{NM}$ . The ground speed, however, is no longer furnished by the Airplane System, but is found by summing forces on the tire, wheel, brake, and axle mass. The horizontal force exerted on the axle by the airplane is calculated by obtaining the translational ( $X_{Ax}$ ) and rotational ( $\theta_g$ ) gear positions from the Airplane System.

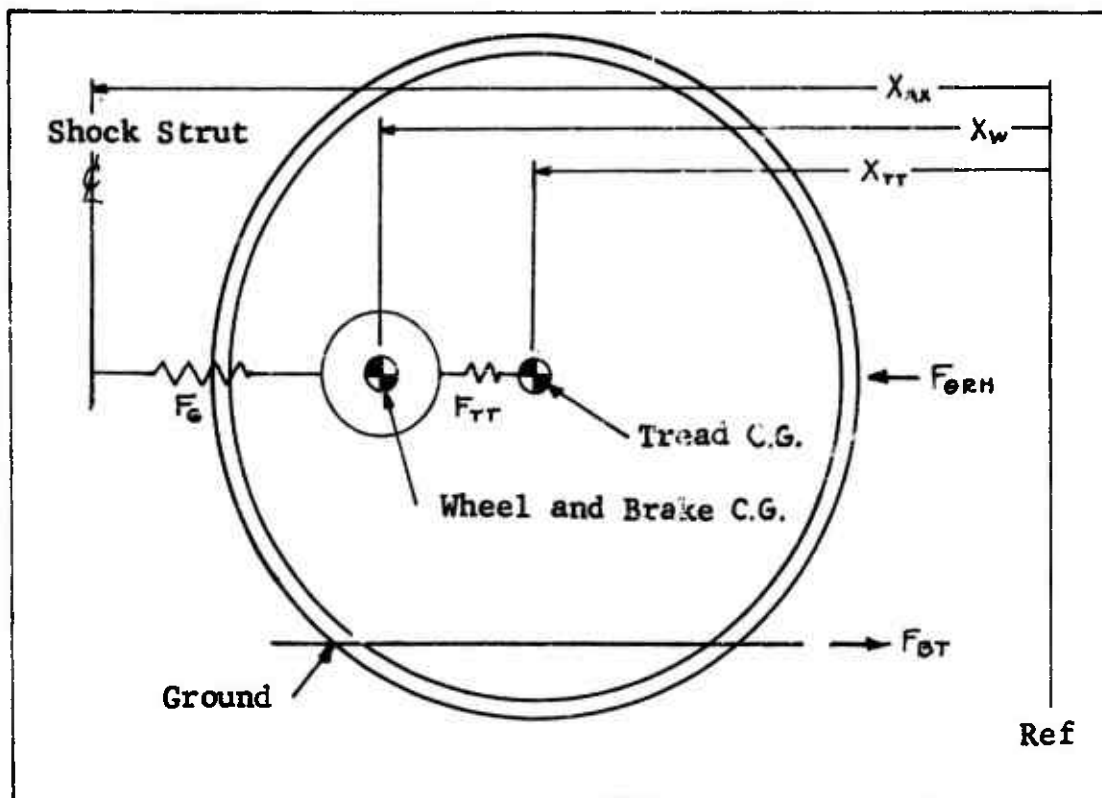


Figure A42 Tire Horizontal Model

Referring to Figure A42 equation (4a.1) in the flywheel system changes to

$$(4b.1) F_G = C_G (X_{AX} - X_W) + D_G (\dot{X}_{AX} - \dot{X}_W)$$

Equations (4b.2) through (4b.9) are listed for completeness, although they are the same as (4a.2) through (4a.9).

$$(4b.2) F_{TT} = C_{TT} (X_{TT} - X_W) + E_{TT} (X_{TT} - X_Y) + D_{TLV} (\dot{X}_{TT} - \dot{X}_W)$$

$$(4b.3) D_{TT} (\dot{X}_Y - \dot{X}_W) = E_{TT} (X_{TT} - X_Y)$$

$$(4b.4) W_{GW} \ddot{X}_W = F_G + F_{TT}$$

$$(4b.5) W_{TE} \ddot{X}_{TT} = -F_{TT} - F_{BT} + F_{\Theta RH}$$

$$(4b.6) F_{\Theta RH} = R_{K\Theta} W_T^2 \sin \langle \Theta_T \rangle$$

$$(4b.7) F_{\Theta RV} = R_{K\Theta} W_T^2 \cos \langle \Theta_T \rangle$$

Figure A43 shows the rotational model of the wheel, tire, axle, and lower strut with the gear rotation  $\theta_G$  added. Including the effect of  $\theta_G$  there follows:

$$(4b.8) T_{RT} = C_{RT}(\theta_w - \theta_T) + E_{RT}(\theta_w - \theta_Y) + D_{TRV}(\dot{\theta}_w - \dot{\theta}_T)$$

$$(4b.9) D_{RT}(\dot{\theta}_Y - \dot{\theta}_T) = E_{RT}(\theta_w - \theta_Y)$$

$$(4b.10) T_S = C_{RS}(\theta_S + \theta_G) + D_{RS}(\dot{\theta}_S + \dot{\theta}_G)$$

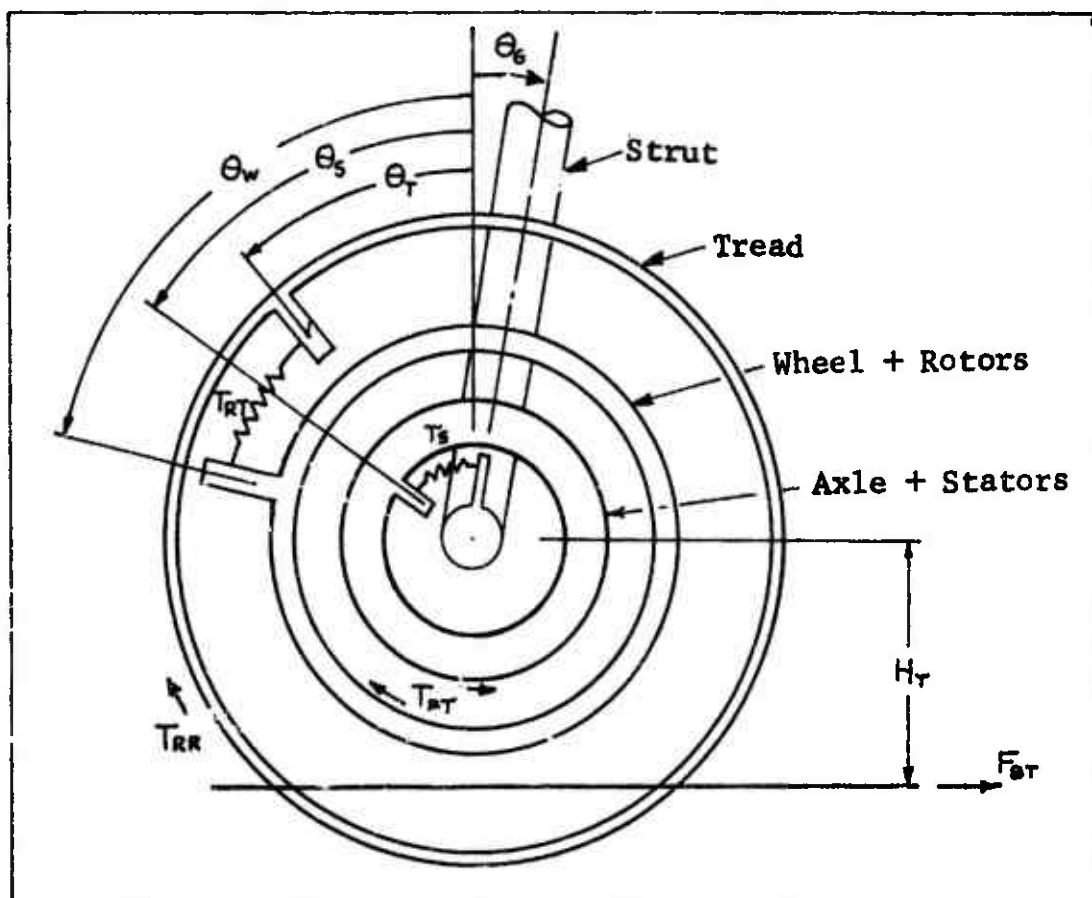


Figure A43 Tire Rotational Model

Equations (4b.11) through (4b.16) are the same as (4a.11) through (4a.16).

$$(4b.11) H_T = R_{OT} - S_M$$

$$(4b.12) T_{RR} = \begin{cases} S_M (D_{SR} + D_{VR} W_T) & \text{if } W_T > 0 \\ C & \text{if } W_T = 0 \\ S_M (-D_{SR} + D_{VR} W_T) & \text{if } W_T < 0 \end{cases}$$

$$(4b.13) W_{IS} \ddot{\Theta}_S = T_{BT} - T_S$$

$$(4b.14) W_{IW} \ddot{\Theta}_W = -T_{RT} - T_{BT}$$

$$(4b.15) W_{IT} \ddot{\Theta}_T = H_T F_{BT} + T_{RT} - T_{RR}$$

$$(4b.16) R_T = R_{BT} - \frac{1}{3} S_M - U_{RR} (X_{TT} - X_W)$$

Because the ground is now stationary equation (4a.17) becomes

$$(4b.17) V_{RS} = \dot{X}_{TT}$$

The remaining equations are unchanged except for noting that the outputs  $X_{WM}$  and  $\dot{X}_{WM}$  required for the Airplane System are obtained by renaming  $X_{TT}$ . Thus  $X_{WM} = X_{TT}$  and  $\dot{X}_{WM} = \dot{X}_{TT}$ . Continuing,

$$(4b.18) V_R = V_{RS} - R_T W_T \quad (\text{WHERE } W_T = \dot{\Theta}_T)$$

$$(4b.19) W_B = W_W - W_S$$

$$(4b.20) F_{NMF} = F_{NM} (1 - C_{HY} (V_{RS} / V_{HY})^2)$$

$$(4b.21) F_{BT} = F_{NMF} U_T + D_{HY} V_{RS}^2$$

$$(4b.22) U_T = \begin{cases} U_{T1} + (U_{T2} - E_T V_{RS}) e^{-\alpha V_R} & \text{if } V_R > V_{R0} \\ \left\{ [U_{T1} + (U_{T2} - E_T V_{RS}) e^{-\alpha V_{R0}}]^{1/V_{R0}} \right\} V_R & \text{if } V_{R0} > V_R > -V_{R0} \\ -U_{T1} - (U_{T2} - E_T V_{RS}) e^{\alpha V_R} & \text{if } V_R < -V_{R0} \end{cases}$$



## B. Parameter Evaluation

The parameter values for this system are essentially the same as for the wheel and tire system that corresponds to the flywheel system. One difference is the values for  $C_G$  and  $D_G$  which are derived in the Airplane System (3 degree). These values are

$$(4b.23) \quad \begin{cases} C_G = 200,000 \text{ lb/in} \\ D_G = 78.6 \text{ lb sec/in} \end{cases}$$

Since this system moves with the airplane the initial conditions should match the Airplane model. Thus

$$(4b.24) \quad \begin{cases} X_{TTO} = 0.774 \text{ in} \\ \dot{X}_{TTO} = 2400 \text{ in/sec} \end{cases}$$

$$(4b.25) \quad \begin{cases} X_{WO} = 0.774 \text{ in} \\ \dot{X}_{WO} = 2400 \text{ in/sec} \end{cases}$$

From equation (4b.16)

$$(4b.26) \quad R_T = R_{ET} - \frac{1}{3} S_M = 23.32 - .80 = 22.52 \text{ IN}$$

Thus for a "spun up" tire, we have from equation (18)

$$(4b.27) \quad W_T = V_{RS} / R_T = 2400 / 22.52 = 106.7 \text{ rad/sec}$$

Then

$$(4b.28) \quad \dot{\Theta}_{TO} = \dot{\Theta}_{WO} = 106.7 \text{ rad/sec}$$

Also from equation (10), choose  $\Theta_{SO}$  so that zero torque is produced.

$$(4b.29) \quad \Theta_{SO} = \Theta_{GO} = .0329 \text{ rad/sec}$$

Table A11 Wheel and Tire System (3 Degree) Parameters (Sheet 1 of 4)

SYMBOL	TYPE	VALUE	UNITS	DESCRIPTION
$\alpha$	c	$2.5 \times 10^{-3}$	sec/in	Tire Friction Parameter
$C_g$	c	$2.0 \times 10^5$	lb/in	Fore and Aft Spring Rate at Axle
$C_{RS}$	c	$10.4 \times 10^6$	in lb/rad	Axle Rotational Spring Rate
$C_{RT}$	c	$19.5 \times 10^4$	in lb/rad	Tire to Wheel Rotational Spring Rate
$C_{HY}$	c	0.0	-	Controls Hydroplaning Influence
$C_{TT}$	c	10,200	lb/in	Tread to Wheel Spring Rate
$D_g$	c	78.6	lb sec/in	Fore and Aft Damping Coeff. at Axle
$D_{HY}$	c	0.0	lb sec <sup>2</sup> /in <sup>2</sup>	Water Resistance Coeff.
$D_{RS}$	c	132	in lb sec/rad	Gear To Axle Rotational Damping Coeff.
$D_{RT}$	c	30,400	in lb sec/rad	Tire to Wheel Rotational Damping Coeff.
$D_{SL}$	c	2350	lb	Rolling Resistance Parameter
$D_{TT}$	c	15.9	lb sec/in	Tread to Wheel Damping Coeff.
$D_{VR}$	c	40.3	lb sec/rad	Rolling Resistance Parameter
$E_{RT}$	c	$10.15 \times 10^6$	in lb/rad	Tire to Wheel Coupling Spring Rate
$E_T$	c	$.65 \times 10^{-4}$	sec/in	Tire Friction Correction Coeff.
$E_{TT}$	c	5300	lb/in	Tread to Wheel Coupling Spring Rate
$F_{BT}$	v		lb	Horizontal Force on Tire Footprint from Ground
$F_g$	v(0)		lb	Horizontal Force at Axle
$F_{GRH}$	v		lb	Horizontal Wheel Unbalance Force
$F_{GRV}$	v(0)		lb	Vertical Wheel Unbalance Force
$F_{GM}$	v(1)		lb	Vertical Force Between Tire and Ground
$F_{GMF}$	v		lb	Vertical Force Not Supported by Water Film
$F_{TR}$	v		lb	Net Force Between Tread and Wheel

Table All Wheel and Tire System (3 Degree) Parameters (Sheet 2 of 4)

SYMBOL	TYPE	VALUE	UNITS	DESCRIPTION
$H_T$	v		in	Axle Height Above Ground ( $H_T \leq R_{OT}$ )
$\Theta_s$	v	.0329	rad	Axle Rotation
$\dot{\Theta}_{s0}$	c		rad	Axle Rotation at Time = 0
$\dot{\Theta}_s$	v		rad/sec	Axle Rotational Speed
$\dot{\Theta}_{s0}$	c	0.0	rad/sec	Axle Rotational Speed at Time = 0
$\ddot{\Theta}_s$	v		rad/sec <sup>2</sup>	Axle Rotational Acceleration
$\Theta_T$	v		rad	Tire Tread Rotation
$\Theta_{T0}$	c	0.0	rad	Tire Tread Rotation at Time = 0
$\dot{\Theta}_T$	v		rad/sec	Tire Tread Rotational Speed
$\dot{\Theta}_{T0}$	c	106.7	rad/sec	Tire Tread Rotational Speed at Time = 0
$\ddot{\Theta}_T$	v		rad/sec <sup>2</sup>	Tire Tread Rotational Acceleration
$\Theta_W$	v		rad	Wheel Rotation
$\Theta_{W0}$	c	0.0	rad	Wheel Rotation at Time = 0
$\dot{\Theta}_W$	v		rad/sec	Wheel Rotational Speed
$\dot{\Theta}_{W0}$	c	106.7	rad/sec	Wheel Rotational Speed at Time = 0
$\ddot{\Theta}_W$	v		rad/sec <sup>2</sup>	Wheel Rotational Acceleration
$\Theta_Y$	v		rad	Dummy Variables Used to
$\Theta_{Y0}$	c	0.0	rad	Simulate Visco-Elastic Tire
$\dot{\Theta}_Y$	v		rad/sec	Characteristic.
$R_{k\theta}$	c	0.0	lb sec <sup>2</sup> /rad <sup>2</sup>	Unbalance Coeff.
$R_{OT}$	c	23.32	in	Undelected Tire Radius
$R_T$	v		in	Tire Rolling Radius
$S_n$	v(i)		in	Tire Deflection

Table All Wheel and Tire System (3 Degree) Parameters (Sheet 3 of 4)

SYMBOL	TYPE	VALUE	UNITS	DESCRIPTION
$T_{BT}$	v(i)		in lb	Brake Torque
$T_{RE}$	v		in lb	Torque Producing Rolling Resistance
$T_{RT}$	v		in lb	Torque Between Tire (Tread) and Wheel
$T_s$	v(o)		in lb	Axle Torque
$U_{BR}$	c	1.0	-	Rolling Radius Parameter
$U_T$	v		-	Tire Friction Coefficient
$U_{T1}$	c	.20	-	} Tire Friction Parameters
$U_{T2}$	c	.45	-	
$V_{HY}$	c	2400	in/sec	
$V_R$	v		in/sec	
$V_{ES}$	v		in/sec	Tire Hydroplaning Speed
$W_B$	v(o)		rad/sec	Velocity of Tire Footprint Relative to Flywheel
$W_{EW}$	c	1.6	lb sec <sup>2</sup> /in	Same as $V_R$ except Rotational Effects Ignored
$W_{TS}$	c	16.8	in lb sec <sup>2</sup> /rad	Relating Rotational Speed Between Stators & Rotors
$W_{IT}$	c	115.0	in lb sec <sup>2</sup> /rad	Effective Tire, Wheel, & Brake Mass
$W_{IW}$	c	66.0	in lb sec <sup>2</sup> /rad	Axle Moment of Inertia (+ Stators)
$W_s$	v		rad/sec	Tread Moment of Inertia
$W_T$	v		rad/sec	Wheel and Rotors Moment of Inertia
$W_{TE}$	c	.0725	lb sec <sup>2</sup> /in	$W_s = \dot{\Theta}_s$ $W_T = \dot{\Theta}_T$
$W_w$	v		rad/sec	Equivalent Tire Tread Mass
$X_{TT}$	v		in	$W_w = \dot{\Theta}_w$
$X_{TTO}$	c	0.774	in	Location of Tire Tread C.G. Location of Tire Tread C.G. at Time = 0

Table All Wheel and Tire System (3 Degree) Parameters (Sheet 4 of 4)

SYMBOL	TYPE	VALUE	UNITS	DESCRIPTION
$\dot{X}_{TT}$	v		in/sec	Tread C.G. Velocity
$\dot{X}_{TTO}$	c	2400	in/sec	Tread C.G. Velocity at Time = 0
$\ddot{X}_{TT}$	v		in/sec <sup>2</sup>	Tread C.G. Acceleration
$X_W$	v	0.774	in	Horizontal Axle Location
$X_{WO}$	c		in	Horizontal Axle Location at Time = 0
$\dot{X}_W$	v		in/sec	Horizontal Axle Velocity
$\dot{X}_{WO}$	c	2400	in/sec	Horizontal Axle Velocity at Time = 0
$\ddot{X}_W$	v		in/sec <sup>2</sup>	Horizontal Axle Acceleration
$X_Y$	v		in	Dummy Variables Used to
$X_{YO}$	c	0.0	in	Simulate Visco-Elastic Tire
$\dot{X}_Y$	v		in/sec	Characteristic.
$\dot{\Theta}_G$	v(i)		rad/sec	Gear Rotation
$\dot{\Theta}_G$	v(i)		rad/sec	Gear Rotational Velocity
$X_{AX}$	v(i)		in	Undelected Axle Position
$\dot{X}_{AX}$	v(i)		in/sec	Undelected Axle Velocity
$X_{WM}$	v(o)		in	Footprint Location (x Direction)
$\dot{X}_{WM}$	v(o)		in/sec	Footprint Velocity (x Direction)
$DTRV$	c	9500	in LBF SEC/RAD	Tire Tread Radial Damping Coeff.
$DTLV$	c	5.45	LBF SEC/IN	Tire Tread Longitudinal Damping Coeff.
$VR0$	c	25.0	in/sec	Tire Friction Threshold Velocity

#### 4c. TIRE AND WHEEL SYSTEM (6 DEGREE)

The wheel and tire system for the six degree problem is the same as that described in the three degree system except for inclusion of the lateral mode. Equations (4c.1) through (4c.17) are the same as (4b.1) through (4b.17) in the three degree system.

##### A. Mathematical Description

$$(4c.1) \quad F_G = C_G (X_{AX} - X_W) + D_G (\dot{X}_{AX} - \dot{X}_W)$$

$$(4c.2) \quad F_{TT} = C_{TT}(X_{TT} - X_W) + E_{TT}(X_{TT} - X_Y) + D_{TLV}(\dot{X}_{TT} - \dot{X}_W)$$

$$(4c.3) \quad D_{TT}(\dot{X}_Y - \dot{X}_W) = E_{TT}(X_{TT} - X_Y)$$

$$(4c.4) \quad W_{GW} \ddot{X}_W = F_G + F_{TT}$$

$$(4c.5) \quad W_{TE} \ddot{X}_{TT} = -F_{TT} - F_{BT} + F_{ORH}$$

$$(4c.6) \quad F_{ORH} = R_{KH} W_T^2 \sin(\theta_T)$$

$$(4c.7) \quad F_{ORV} = R_{KV} W_T^2 \cos(\theta_T)$$

$$(4c.8) \quad T_{RT} = C_{RT}(\theta_W - \theta_T) + E_{RT}(\theta_W - \theta_Y) + D_{TRV}(\dot{\theta}_W - \dot{\theta}_T)$$

$$(4c.9) \quad D_{RT}(\dot{\theta}_Y - \dot{\theta}_T) = E_{RT}(\theta_W - \theta_Y)$$

$$(4c.10) \quad T_S = C_{RS}(\theta_S - \theta_G) + D_{RS}(\dot{\theta}_S - \dot{\theta}_G)$$

$$(4c.11) \quad H_T = R_{\theta T} - S_M$$

$$(4c.12) \quad T_{RR} = \begin{cases} S_M (D_{SR} + D_{VR} W_T) & \text{if } W_T > 0 \\ 0 & \text{if } W_T = 0 \\ S_M (-D_{SR} + D_{VR} W_T) & \text{if } W_T < 0 \end{cases}$$

$$(4c.13) \quad W_{IS} \ddot{\theta}_S = T_{BT} - T_S$$

$$(4c.14) \quad W_{IW} \ddot{\theta}_W = -T_{RT} - T_{BT}$$

$$(4c.15) \quad W_{IT} \ddot{\theta}_T = H_T F_{BT} + T_{RT} - T_{RR}$$

$$(4c.16) \quad R_T = R_{\theta T} - \frac{1}{3} S_M - U_{RR}(X_{TT} - X_W)$$

$$(4c.17) \quad V_{RS} = \dot{X}_{TT} = \dot{X}_{WM} \quad \text{also } X_{WM} = X_{TT}$$

Equation (4b.18) which gives the relative velocity between the footprint and the ground is changed to account for the lateral footprint velocity  $\dot{Y}_M$ .

$$(4c.18) \quad V_R = \sqrt{V_{Rx}^2 + \dot{Y}_M^2}$$

Equations (4b.19) and (4b.20) are unchanged.

$$(4c.19) \quad W_B = W_W - W_S$$

$$(4c.20) \quad F_{NMF} = F_{NM} (1 - C_{HY} (V_{RS} / V_{HY})^2)$$

Now  $V_{Rx}$  is the relative velocity in the x direction so

$$(4c.21) \quad V_{Rx} = V_{RS} - R_T W_T$$

Thus, the angle  $\beta_T$  which defines the friction force direction as shown in Figure A45 is given by

$$(4c.22) \quad \beta_T = \tan^{-1} \langle \dot{Y}_M / V_{Rx} \rangle$$

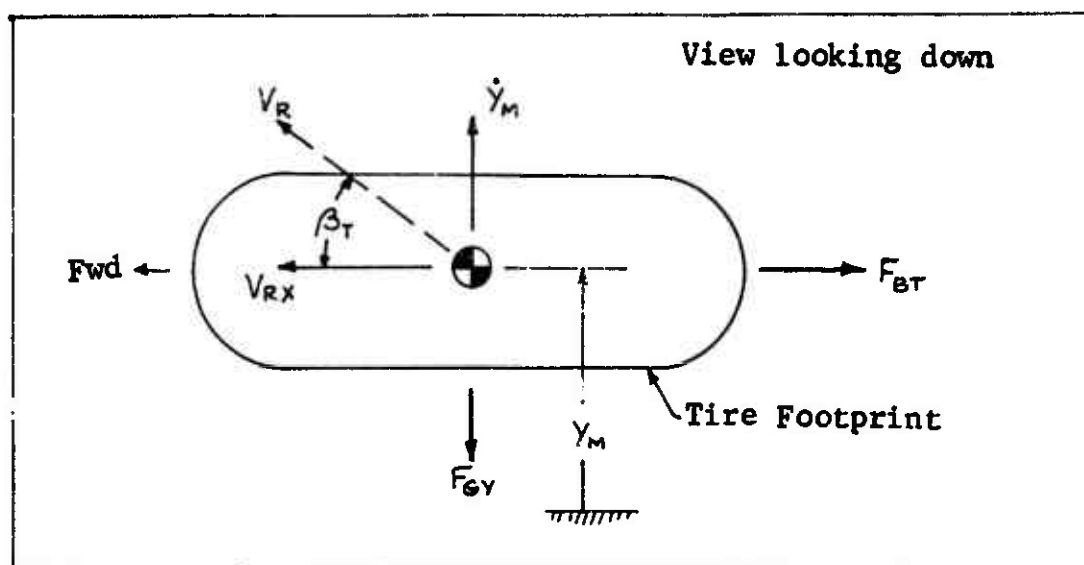


Figure A45 Footprint Friction Components

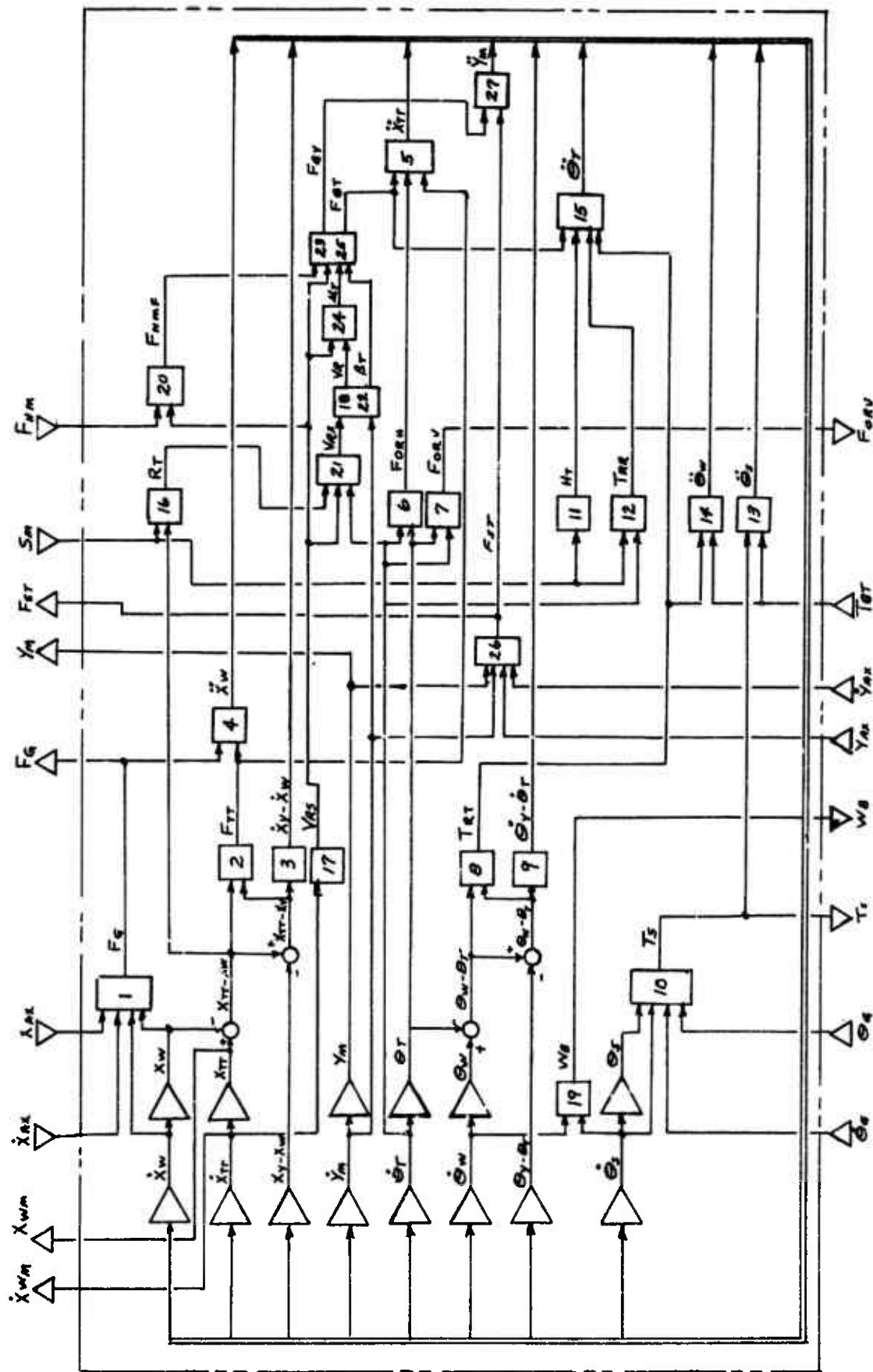


Figure A46 Wheel and Fire System (6 Degree) Equation Flow Diagram

Thus,  $F_{BT}$  is now given by

$$(4c.23) F_{BT} = F_{NMF} U_T \cos \langle \beta_T \rangle + D_{HY} V_{RS}^2$$

and

$$(4c.24) U_T = \begin{cases} U_{T1} + (U_{T2} - E_T V_{RS}) e^{-\alpha V_R} & \text{if } V_R > V_{R0} \\ \{ [U_{T1} + (U_{T2} - E_T V_{RS}) e^{-\alpha V_{R0}}]^{1/V_{R0}} \} V_R & \text{if } V_{R0} > V_R \geq 0 \end{cases}$$

The lateral friction force  $F_{\epsilon Y}$  is given by

$$(4c.25) F_{\epsilon Y} = F_{NMF} U_T \sin \langle \beta_T \rangle$$

The airplane produces a lateral position  $Y_{AX}$  of the axle. If  $Y_M$  is the lateral location of the footprint, then a lateral force  $F_{ST}$  is produced and

$$(4c.26) F_{ST} = C_{ST} (Y_{AX} - Y_M) + D_{ST} (\dot{Y}_{AX} - \dot{Y}_M)$$

Finally, forces can be summed laterally on the footprint to obtain

$$(4c.27) W_{TE} \ddot{Y}_M = F_{ST} - F_{\epsilon Y}$$

## B. Parameter Evaluation

### Wheel and Tire System Parameters

Most of the parameter values were derived in the wheel and tire system that was used with the flywheel. The only addition is the evaluation of  $C_{ST}$  and  $D_{ST}$ .

From reference 1 (p.15)

$$(4c.28) K_\lambda = \tau_\lambda \omega (P + .24 P_R) (1 - .7(s_0/\omega))$$

Assuming that  $s_0 = 2.245$  in., then

$$(4c.29) C_{ST} = (2)(18)(1.24)(150)(1 - .7(2.245/18))$$

$$(4c.30) C_{ST} = 6460 \text{ lb/in}$$

$$\text{Using } \omega_n = \sqrt{K/m} = \sqrt{6460/.0725} = 298.4$$

Using  $\eta = .1$  (from page 50 of Ref. 1) results in

$$(4c.31) D_{ST} = \eta C_{ST} / \omega_n = (.1)(6460)/298.4 = 2.165$$

### Initial Conditions

The only difference between this and the three degree system is evaluating  $y_{M0}$  and  $\dot{y}_{M0}$ . It should be that  $y_{M0} = y_{Ax}(0)$ . Since this system is used for both right and left sides, then  $y_{M0}$  will differ. Assume that this system is used as the right wheel and tire. Then,  $y_{M0} = y_{AxR}$  as in equation (4c.56). From this equation at Time = 0, (since  $R = P = 0$ ), then

$$(4c.32) \quad y_{M0} = y_{AxR} = y_0 + S_{6W} = 0 + 60 = 60 \text{ in}$$

Similarly

$$(4c.33) \quad \dot{y}_{M0} = \dot{y}_{AxR} = \dot{y}_0 = 0.0 \text{ in/sec}$$

Table A12 Wheel and Tire System (6 Degree) Parameters

(Sheet 1 of 5)

SYMBOL	TYPE	VALUE	UNITS	DESCRIPTION
$\mu$	C	$2.5 \times 10^{-3}$	sec/in	Tire Friction Parameter
$\beta_T$	V		rad	Tire Footprint Friction Angle
$C_e$	C	$2.0 \times 10^5$	lb/in	Fore and Aft Spring Rate at Axle
$C_{RS}$	C	$10.4 \times 10^6$	in lb/rad	Axle Rotational Spring Rate
$C_{RT}$	C	$19.5 \times 10^6$	in lb/rad	Tire to Wheel Rotational Spring Rate
$C_{HY}$	C	0.0	-	Controls Hydroplaning Influence
$C_{ST}$	C	6460	lb/in	Tire Lateral Spring Rate
$C_{TT}$	C	10,200	lb/in	Tread to Wheel Spring Rate
$D_e$	C	78.6	lb sec/in	Fore and Aft Damping Coefficient at Axle
$D_{HY}$	C	0.0	lb sec <sup>2</sup> /in <sup>2</sup>	Water Resistance Coefficient
$D_{RS}$	C	132	in lb sec/rad	Gear to Axle Rotational Damping Coeff.
$D_{RT}$	C	30,400	in lb sec/rad	Tire to Wheel Rotational Damping Coeff.
$D_{SR}$	C	2350	lb	Rolling Resistance Parameter
$D_{ST}$	C	2.165	lb sec/in	Tire Lateral Damping Coefficient
$D_{TT}$	C	15.9	lb sec/in	Tread to Wheel Damping Coefficient
$D_{VZ}$	C	40.3	lb sec/rad	Rolling Resistance Parameter
$E_{RT}$	C	$10.15 \times 10^6$	in lb/rad	Tire to Wheel Coupling Spring Rate
$E_T$	C	$.65 \times 10^4$	sec/in	Tire Friction Correction Coefficient
$E_{TT}$	C	5300	lb/in	Tread to Wheel Coupling Spring Rate
$F_{BT}$	V		lb	Horizontal Force on Tire Footprint from Ground
$F_G$	V(o)		lb	Horizontal Force at Axle
$F_{GY}$	V		lb	Lateral Tire Load (On Ground)
$F_{GRH}$	V		lb	Horizontal Wheel Imbalance Force
$F_{GRV}$	V(o)		lb	Vertical Wheel Imbalance Force

Table A12 Wheel and Tire System (6 Degree) Parameters (Sheet 2 of 5)

SYMBOL	TYPE	VALUE	UNITS	DESCRIPTION
$F_{NM}$	$v(I)$		lb	Vertical Force between Tire and Ground
$F_{NMF}$	$v$		lb	Vertical Force not supported by Water Film
$F_{ST}$	$v(O)$		lb	Lateral Tire Load (On Apl)
$F_{TT}$	$v$		lb	Net Force between Tread and Wheel
$H_T$	$v$		in	Axle Height Above Ground
$\theta_G$	$v(I)$		rad	Gear Rotation
$\dot{\theta}_G$	$v(I)$		rad/sec	Gear Rotational Velocity
$\theta_S$	$v$		rad	Axle Rotation
$\dot{\theta}_{SO}$	$c$	- .0329	rad	Axle Rotation at Time = 0
$\dot{\theta}_S$	$v$		rad/sec	Axle Rotational Speed
$\dot{\theta}_{SO}$	$c$	0.0	rad/sec	Axle Rotational Speed at Time = 0
$\ddot{\theta}_S$	$v$		rad/sec <sup>2</sup>	Axle Rotational Acceleration
$\dot{\theta}_T$	$v$		rad	Tire Tread Rotation
$\dot{\theta}_{TD}$	$c$	0.0	rad	Tire Tread Rotation at Time = 0
$\ddot{\theta}_T$	$v$		rad/sec	Tire Tread Rotational Speed
$\dot{\theta}_{TD}$	$c$	106.7	rad/sec	Tire Tread Rotational Speed at Time = 0
$\ddot{\theta}_T$	$v$		rad/sec <sup>2</sup>	Tire Tread Rotational Acceleration
$\dot{\theta}_W$	$v$		rad	Wheel Rotation
$\dot{\theta}_{WD}$	$c$	0.0		Wheel Rotation at Time = 0
$\ddot{\theta}_W$	$v$		rad/sec	Wheel Rotational Speed
$\dot{\theta}_{WD}$	$c$	106.7	rad/sec	Wheel Rotational Speed at Time = 0
$\ddot{\theta}_W$	$v$		rad/sec <sup>2</sup>	Wheel Rotational Acceleration
$\theta_Y$	$v$		rad	} Dummy Variables used to } Simulate Visco-Elastic Tire } Characteristic
$\dot{\theta}_{YO}$	$c$	0.0	rad	
$\ddot{\theta}_Y$	$v$		rad/sec	

Table A12 Wheel and Tire System (6 Degree) Parameters (Sheet 3 of 5)

SYMBOL	TYPE	VALUE	UNITS	DESCRIPTION
$R_{k\theta}$	c	0.0	lb sec <sup>2</sup> /rad <sup>2</sup>	Unbalance Coefficient
$R_{\theta T}$	c	23.32	in	Undelected Tire Radius
$R_T$	v		in	Tire Rolling Radius
$S_M$	v(I)		in	Tire Deflection
$T_{\theta T}$	v(I)		in lb	Brake Torque
$T_{RR}$	v		in lb	Torque Producing Rolling Resistance
$T_{RT}$	v		in lb	Torque Between Tire (Tread) and Wheel
$T_s$	v(o)		in lb	Axle Torque
$U_{RR}$	c	1.0	—	Rolling Radius Parameter
$U_T$	v		—	Tire Friction Coefficient
$U_{T1}$	c	.20	—	} Tire Friction Parameters
$U_{T2}$	c	.45	—	
$V_{HY}$	c	2400	in/sec	Tire Hydroplaning Speed
$V_R$	v		in/sec	Velocity of Tire Footprint Relative to Flywheel
$V_{RS}$	v		in/sec	Same as $V_{RX}$ except rotational effects ignored
$V_{RX}$	v		in/sec	Tire Footprint Relative Velocity in X Direction
$W_B$	v(o)		rad/sec	Relative Rotational Speed between Slaters and Rotors
$W_{\theta W}$	c	1.6	lb sec <sup>2</sup> /in	Effective Tire, Wheel, and Brake Mass
$W_{IS}$	c	12.8	in lb sec <sup>2</sup> /rad	Axle Moment of Inertia (+ Stators)
$W_{IT}$	c	115	in lb sec <sup>2</sup> /rad	Tread Moment of Inertia
$W_{IW}$	c	66.0	in lb sec <sup>2</sup> /rad	Wheel and Rotors Moment of Inertia

Table A12 Wheel and Tire System (6 Degree) Parameters (Sheet 4 of 5)

SYMBOL	TYPE	VALUE	UNITS	DESCRIPTION
$W_s$	V		rad/sec	$W_s = \dot{\theta}_s$
$W_T$	V		rad/sec	$W_T = \dot{\theta}_T$
$W_{TE}$	C	0.0725	lb sec <sup>2</sup> /in	Equivalent Tire Tread Mass
$W_w$	V		rad/sec	$W_w = \dot{\theta}_w$
$X_{TT0}$	V		in	Location of Tire Tread C. G.
$\dot{X}_{TT}$	V	0.0	in/sec	Location of Tire Tread C. G. at Time = 0
$\ddot{X}_{TT0}$	C		in/sec	Tread C. G. Velocity
$\ddot{X}_{TT}$	C	2400	in/sec <sup>2</sup>	Tread C. G. Velocity at Time = 0
$\ddot{X}_{TT}$	V		in/sec <sup>2</sup>	Tread C. G. Acceleration
$X_W$	V		in	Horizontal Axle Location
$\dot{X}_{W0}$	C	0.0	in/sec	Horizontal Axle Location at Time = 0
$\dot{X}_W$	V		in/sec	Horizontal Axle Velocity
$\ddot{X}_{W0}$	C	2400	in/sec <sup>2</sup>	Horizontal Axle Velocity at Time = 0
$\ddot{X}_W$	V		in/sec <sup>2</sup>	Horizontal Axle Acceleration
$X_Y$	V		in	Dummy Variables used to
$X_{Y0}$	C	0.0	in	Simulate Visco-Elastic Tire
$\dot{X}_Y$	V		in/sec	Characteristic
$Y_{AX}$	V(I)		in	Undelected Axle Location (y Direction)
$\dot{Y}_{AX}$	V(I)		in/sec	Undelected Axle Velocity (y Direction)
$X_{AX}$	V(I)		in	Undelected Axle Location (x Direction)
$\dot{X}_{AX}$	V(I)		in/sec	Undelected Axle Velocity (x Direction)
$Y_M$	V(O)		in	Footprint Location (y Direction)
$Y_{M0}$	C	±60.0	in	Ym at Time = 0 ( $Y_{M20} = +60$ , $Y_{M10} = -60$ )
$\dot{Y}_M$	V		in/sec	Footprint Velocity
$\dot{Y}_{M0}$	C	0.0	in/sec	Ym at Time = 0

Table A12 Wheel and Tire System (6 Degree) Parameters (Sheet 5 of 5)

SYMBOL	TYPE	VALUE	UNITS	DESCRIPTION
$\ddot{y}_M$	v		in/sec <sup>2</sup>	Footprint Acceleration
$x_{wm}$	v(o)		in	Footprint Position (x Direction)
$\dot{x}_{wm}$	v(o)		in/sec	Footprint Velocity
DTRV	c	9500	in Lbf Sec/RAD	Tire Tread Radial Damping Coeff.
DTLV	c	5.45	Lbf Sec/in	Tire Tread Longitudinal Damping Coeff.
VR0	c	25.0	in/sec	Tire Friction Threshold Velocity

## 5. WHEEL SPEED SENSOR

The primary input parameter to an electronic antiskid control circuit is an airplane wheel speed signal. For conventional control circuitry the input must be a direct current voltage. The wheel speed sensor may have any of several forms such as a D.C. tachometer or an A.C. tachometer with variable voltage or frequency converted to a direct current voltage by suitable electronic circuitry. The control circuit input signal,  $E_G$ , is a function of the wheel's angular velocity relative to the axle (tachometer mount) and the characteristics of any associated electronic circuitry used for radio interference suppression and/or for conversion of A.C. frequency or voltage signals to D.C. voltage. To provide the means for mathematically describing the control circuit input signal for a variety of wheel speed sensors, two approaches are taken. The first, identified as Option 1, is applicable whenever there is a perceptible phase lag between actual wheel speed and the antiskid circuit input as is generally the case where A.C. voltage signals are converted to D.C. or where a D.C. tachometer is driven through an elastic coupling. A second simpler mathematical description, called Option 2, is provided to minimize computation difficulty and expense where no significant phase lag exists.

### A. Mathematical Description

#### Option 1

Assume that a D.C. tachometer generator is mounted on the axle and is driven by the wheel. The output of the hypothetical generator is assumed to be applied to a linear force motor which acts upon a single degree of freedom damped spring mass system as shown on Figure A47. The control circuit input signal,  $E_G$ , is proportional to the mass displacement. By adjusting the relative characteristics of the linear force motor, hypothetical generator, spring, mass and damper a mathematical description of a wide variety of wheel speed sensors can be accommodated.

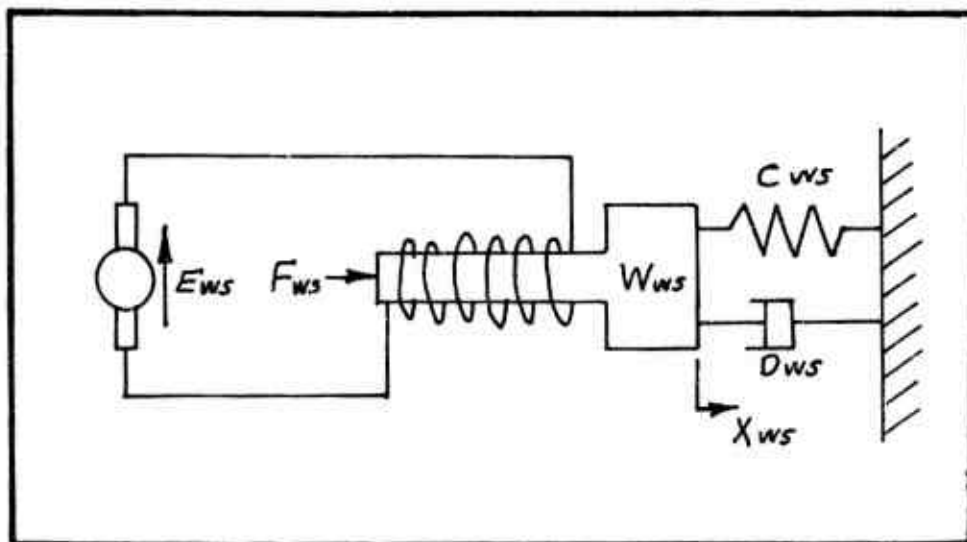


Figure A47 Wheel Speed Signal System

The output of the hypothetical generator,  $E_{ws}$ , is proportional to the wheel's angular velocity relative to the axle,  $W_B$ , as defined by equation (5.1). Angular velocity,  $W_B$ , is obtained as an output of the tire and wheel system.

$$(5.1) \quad E_{ws} = G_{ws} W_B$$

The force produced by the linear force motor,  $F_{ws}$ , is proportional to the generator output,  $E_{ws}$ , as defined by equation (5.2).

$$(5.2) \quad F_{ws} = C_{wg} E_{ws}$$

The hypothetical mass displacement,  $X_{ws}$ , is obtained from equation (5.3) which results from summing forces on the hypothetical mass,  $W_{ws}$ .

$$(5.3) \quad \ddot{X}_{ws} = \frac{F_{ws}}{W_{ws}} - \frac{C_{ws}}{W_{ws}} (X_{ws}) - \frac{D_{ws}}{W_{ws}} (\dot{X}_{ws})$$

The antiskid circuit wheel speed input voltage signal,  $E_G$ , is proportional to the hypothetical mass displacement,  $X_{ws}$ , as defined by equation (5.4).

$$(5.4) \quad E_G = C_{gv} X_{ws} + E_{sn}$$

In equation (5.4),  $E_{sn}$  is any extraneous "noise" which might be present due to the operation of other aircraft systems, etc.

The equation flow diagram is shown on Figure A48.

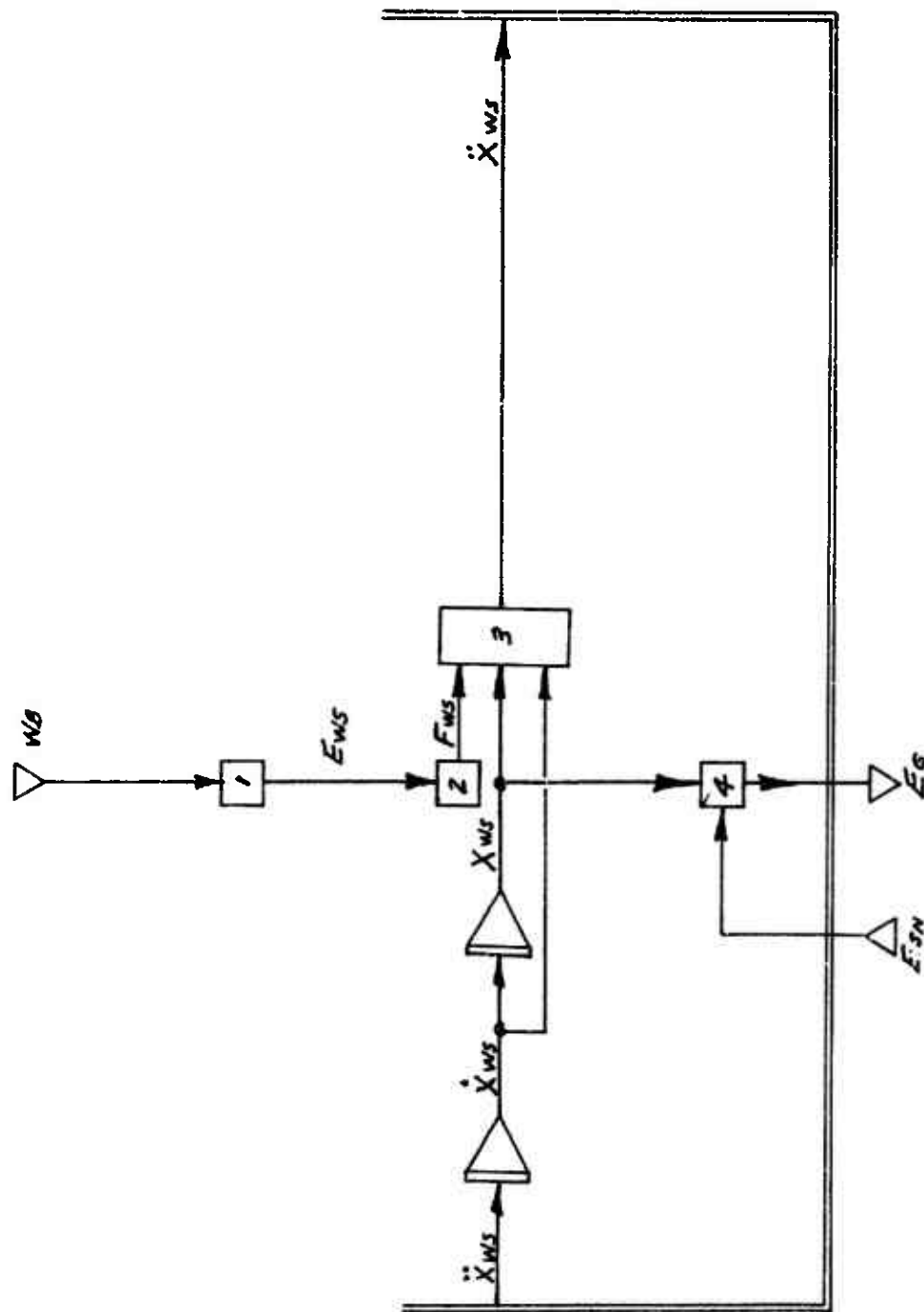


Figure A48 Wheel Speed Sensor Equation Flow Diagram (Option 1)

## Option 2

For cases where the wheel speed transducer is a D.C. tachometer, or equivalent, driven through a rigid coupling (such as the F-104 and F-111) there is usually very small difference between the actual wheel speed and antiskid control circuit input (i.e., very low phase lag or attenuation) and the extra mathematical complication incurred by using a very high gain second order equation is not justified. For these cases the antiskid control circuit input voltage may be considered proportional to the wheel's angular velocity as defined by equation (5.5).

$$(5.5) \quad E_G = G_{WDC} W_B + E_{SN}$$

No equation flow diagram is shown for Option 2.

### B. Parameter Evaluation

#### Option 1

The objective of using a single degree of freedom damped spring mass system to describe the antiskid control circuit input is to provide a mathematical "tool" whereby phase lag within the wheel speed sensor device can be accounted for. Consequently, the values for mass, spring rate and damping coefficient are chosen to produce the desired effect rather than to describe physical devices. The other coefficients are chosen to achieve compatibility with the control circuit. For the F-111 modulated antiskid circuit let the hypothetical tachometer coefficient be the same as for the actual F-111 tachometer, 12 volts per thousand RPM. Therefore:

$$(5.6) \quad G_{WS} = \frac{12 \times 60}{1000 \times 2\pi} = 0.1147 \text{ VOLT SEC/RAD}$$

Let the force motor coefficient, the elastic system spring rate and output voltage coefficient all be equal to unity so that for steady state conditions the control circuit input,  $E_G$ , is the tachometer output. Therefore:

$$(5.7) \quad \begin{aligned} C_{WG} &= 1.0 \text{ lbf/VOLT} \\ C_{WS} &= 1.0 \text{ lbf/INCH} \\ C_{GV} &= 1.0 \text{ VOLT/INCH} \end{aligned}$$

Based on information furnished by the Goodyear Aerospace Corp. the component characteristics and arrangement which is usually utilized for converting A.C. frequency to D.C. voltage produces about 30 degrees (or greater) phase lag at 5 cps. The following equations from reference 12 describe the single degree of freedom system's behavior when an oscillatory force  $X_0 K \sin \omega t$  is applied.

$$(5.8) \quad \frac{X}{X_0} = \frac{1}{\sqrt{[1 - (\omega/\omega_n)^2]^2 + (2\zeta\omega/\omega_n)^2}}$$

$$\tan \phi = \frac{2(\omega/\omega_n)\zeta}{1 - (\omega/\omega_n)^2}$$

In these equations  $\phi$  is the phase angle,  $\zeta = D_{ws}/2W_{ws}\omega_n$  is the damping factor,  $\omega_n = \sqrt{C_{ws}/W_{ws}}$  is the undamped natural frequency,  $\omega$  is the frequency of applied oscillatory loading, and  $X/X_0$  is the magnification factor. If the degree of attenuation and phase angle are known at a particular frequency, the undamped natural frequency and damping factor are established. Assuming two percent attenuation and 30 degree phase lag at 5 cps, the equations above give an undamped natural frequency of 14.6 cps (91.8 RAD/SEC) and a damping factor of 0.746.

For an undamped natural frequency of 91.8 RAD/SEC and a spring rate,  $C_{ws}$ , of 1.0 lbf/in the mass,  $W_{ws}$ , is established as  $0.1185 \times 10^{-3}$  lbf sec<sup>2</sup>/in. The damping coefficient,  $D_{ws}$ , is established from the mass and damping factor as

$$(5.9) \quad D_{ws} = 0.1623 \times 10^{-2} \text{ lbf sec/in}$$

#### Option 2

For use with the F-111 modulated antiskid control circuit, use the actual F-111 tachometer output of 12 volts D.C. per 1000 RPM. Therefore:

$$(5.10) \quad G_{WDC} = \frac{12 \times 60}{1000 \times 2\pi} = 0.1147 \text{ VOLT SEC/RAD}$$

For use with the on-off antiskid circuit as installed on the F-104 (and B-58) the tachometer output is 20 volts per 1000 RPM. To make the on-off circuit compatible with the F-111 requires that the difference in tire size (46.5 inch dia. for F-111 versus 22 inch dia. for B-58) also be accounted for. Therefore, for the on-off antiskid circuit use:

$$(5.11) \quad G_{WOC} = (0.1147) \left( \frac{46.5}{22} \right) \left( \frac{20}{12} \right) = 0.4 \text{ VOLT SEC/RAD}$$

Table A13 Wheel Speed Sensor Parameters

(Sheet 1 of 2)

SYMBOL	TYPE	VALUE	UNITS	DESCRIPTION
<u>OPTION 1 FOR USE WITH F-111 MODULATED CIRCUIT</u>				
C <sub>CGV</sub>	C	1.0	VOLT/IN	Output Voltage Coefficient
C <sub>WG</sub>	C	1.0	lbf/VOLT	Hypothetical Linear Force Motor Coefficient
C <sub>WS</sub>	C	1.0	lbf/IN	Spring Rate (Hypothetical Spring)
D <sub>WS</sub>	C	$0.1623 \times 10^{-2}$	lbf sec/IN	Damping Coefficient (Hypothetical Damper)
E <sub>G</sub>	V(O)		VOLTS	Antiskid Control Circuit Input Signal
E <sub>WS</sub>	V		VOLTS	Hypothetical Tachometer Voltage
F <sub>WS</sub>	V		lbf	Hypothetical Linear Force Motor Output Force
G <sub>WS</sub>	C	0.1147	VOLT sec/RAO	Hypothetical Tachometer Voltage-Speed Coefficient
E <sub>SN</sub>	V(I)	0.0	VOLTS	Input Signal "Noise"
W <sub>WS</sub>	C	$0.1185 \times 10^{-3}$	lbf sec <sup>3</sup> /IN	Mass (Hypothetical Mass)
W <sub>B</sub>	V(I)		RAO/sec	Wheel Angular Velocity Relative to Angle
X <sub>WS</sub>	V		INCH	Hypothetical Mass Displacement
X <sub>WSO</sub>	C	0.0	INCH	Hypothetical Mass Displacement at Time Zero
X <sub>WS</sub>	V		IN/sec	Hypothetical Mass Velocity
X <sub>WSO</sub>	C	0.0	IN/sec	Hypothetical Mass Velocity at Time Zero
X <sub>WS</sub>	V		IN/sec <sup>2</sup>	Hypothetical Mass Acceleration
<u>OPTION 2 FOR USE WITH F-111 MODULATED CIRCUIT</u>				
G <sub>WOC</sub>	C	0.1147	VOLT sec/RAO	
E <sub>SN</sub>	V(I)	0.0	VOLTS	

Table A13 Wheel Speed Sensor Parameters (Sheet 2 of 2)

SYMBOL	TYPE	VALUE	UNITS	DESCRIPTION
<u>OPTION 2 FOR USE WITH F104 ON-OFF CIRCUIT</u>				
$G_{WOC}$ $E_{SN}$	$C$ $V(I)$	0.4 0.0	VOLT SEC / RAD VOLTS	

## 6a. MODULATED ANTISKID CONTROL CIRCUIT

After introduction of on-off type antiskid systems, it became apparent from various analyses and studies of test results and operational performance that braking effectiveness could be increased if the number of antiskid cycles and their intensity could be minimized. To minimize antiskid cycling occurrences and intensity, it is necessary to control the amount of brake torque being applied such that the available friction torque is not exceeded for as much of the time as is possible. A number of devices utilizing various principles of operation have been used for this purpose. These devices predominately utilize the principle of regulating or "modulating" brake pressure to keep its value as near as possible to that which will produce a skid. One of the first of these type devices is a hydraulic pressure modulator comprised of an orifice and accumulator installed upstream from the pilot's metering valve and configured such that repetitive antiskid cycling causes a temporary reduction in pilot's metered pressure. The Convair Model 880 airplane's Hytrol MKI antiskid system with hydraulic modulation is a typical example of this type installation.

A subsequent development was the Bendix system which is used on Grumman A6A and Lockheed C141 aircraft. This system combines hydraulic modulation accomplished within the off-on type control valve with two levels of skid detection, (i.e., brake pressure reduction in two steps controlled by skid intensity). Further improvements have been achieved by utilizing a servo type pressure regulating valve with electronic control to achieve a wide range of control characteristics and better accommodate widely varying runway friction conditions encountered during aircraft operation. The Goodyear Adaptive system used on General Dynamics F-111 aircraft and the Hytrol MK II system used on McDonnell-Douglas F4C and LTV A7A aircraft are examples of the servo valve type systems. Within each of the types or classes of systems there are a number of variations in circuitry and component arrangement depending upon the aircraft type, landing gear arrangement and configuration, and the airplane's mission requirements. For this program a mathematical model of the F-111 airplane's Goodyear Adaptive Antiskid Control Circuit is developed. Models for other type circuits can be developed using similar procedures.

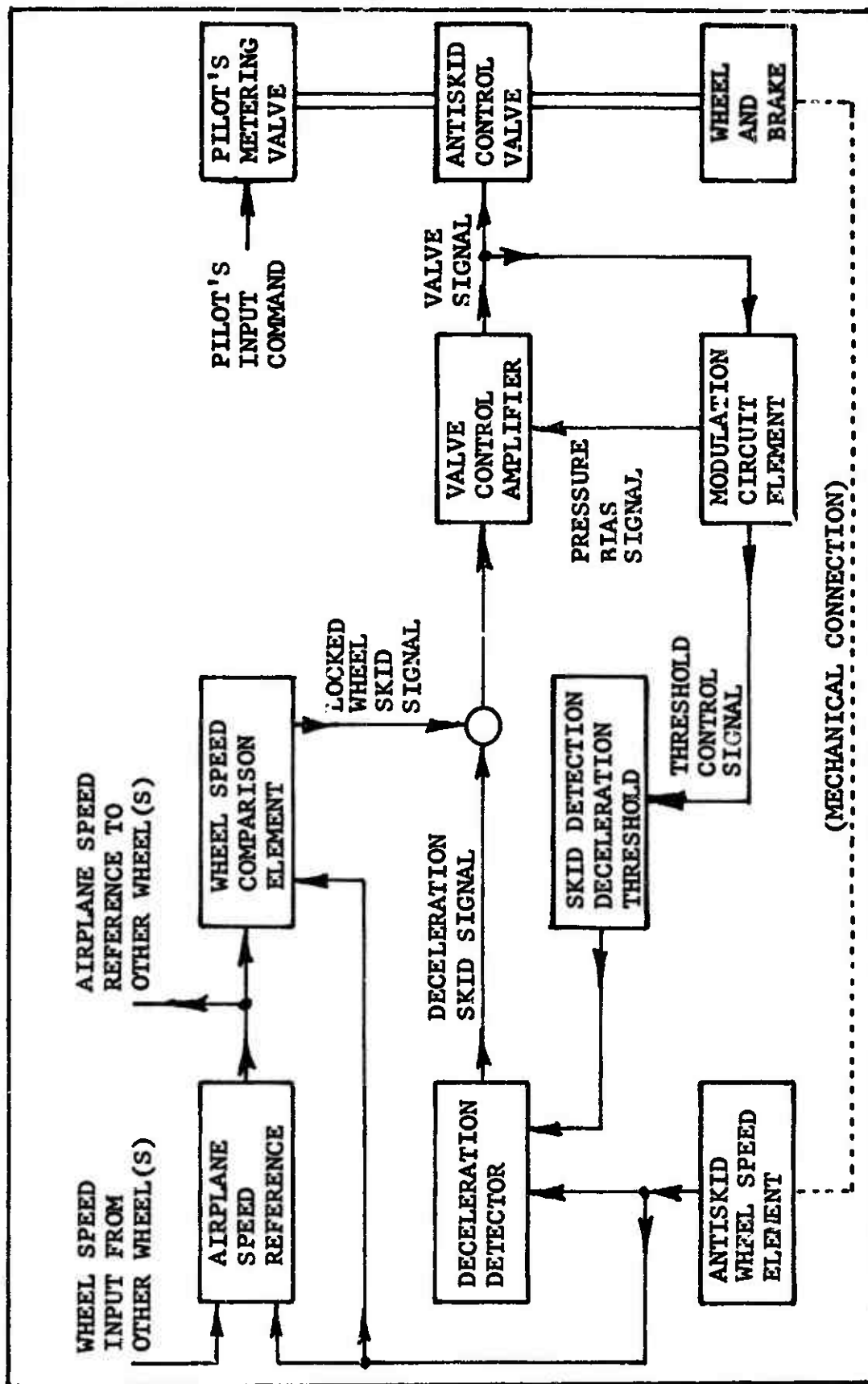


Figure A49 Modulated Antiskid Control Functional Block Diagram

Figure A49 is a block diagram showing the basic functional elements of the Goodyear adaptive antiskid control circuit as used on the F-111 airplane and showing the relationship of the control circuit to the other brake system components. During antiskid circuit operation, a wheel speed signal is provided as an input to a deceleration detector. Within the deceleration detector the wheel's deceleration rate is computed and compared to a threshold value provided by a skid detection threshold circuit element. The deceleration detector produces a skid signal proportional to the amount by which the wheel's deceleration rate exceeds the threshold value. The skid signal is applied to a valve control amplifier which in turn produces a valve control signal proportional to the input skid signal plus any pressure bias signal which might exist. The valve control signal is supplied to the antiskid control valve (a servo type pressure regulator) for brake pressure control and to a modulation circuit element. The modulation circuit element interprets the valve control signal and provides a pressure bias signal to the valve control amplifier and a threshold control signal to the skid detection threshold circuit element. The wheel speed signal is also supplied to the locked wheel prevention circuit elements consisting of an airplane speed reference and a wheel speed comparison element. When the airplane speed reference indicates that the airplane's speed exceeds "locked wheel arming speed" (usually 20 mph) and simultaneously the wheel speed is less than that which should exist for a slightly lower airplane speed (usually 10 mph), the wheel speed comparison circuit element produces a skid signal sufficient to fully release the brake. Locked wheel arming speed is chosen as some reasonably low speed below which a locked wheel is not particularly detrimental. The locked wheel feature is deactivated below locked wheel arming speed so that the airplane can be brought to a complete stop. The aircraft circuit also incorporates circuit elements for failure detection, automatic cutoff and prevention of brake application prior to touchdown. These logic type functions do not affect aircraft stopping performance and are not included in this analysis.

#### A. Modulated Antiskid Circuit Mathematical Description

A simplified schematic diagram of the Goodyear adaptive antiskid circuit for one wheel as used on F-111 type aircraft is shown on Figure A50. This circuit accom-

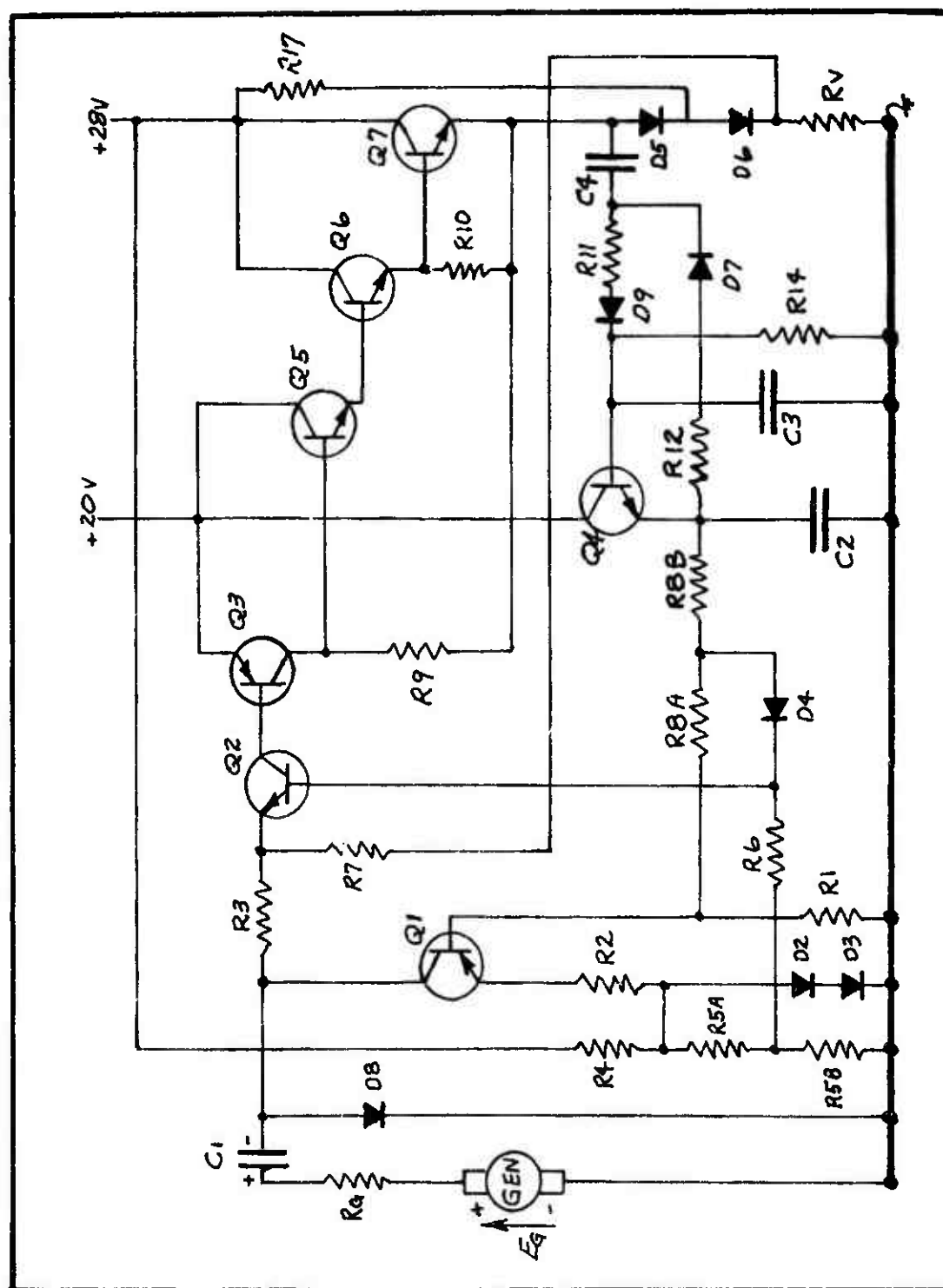


Figure A 50 Modulated Antiskid Control Circuit Schematic

plishes deceleration skid control as previously described in the control circuit functional description as follows. An input voltage,  $E_g$ , is provided by a wheel driven D. C. tachometer generator (GEN).  $E_g$  charges the deceleration detector, capacitor,  $C_1$ , through resistance  $R_4$  and diode  $D_8$  during wheel spin-up. For normal wheel deceleration rates, with no incipient skidding, the generator voltage will decrease relatively slowly and a small current will flow from the positive side of  $C_1$  through  $R_4$ , the generator,  $R_4$ ,  $R_2$ , and transistor  $Q_1$  to the negative side of  $C_1$ . This current discharges capacitor  $C_1$  and causes its voltage to closely follow  $E_g$ . Transistor  $Q_1$  is the skid detection threshold circuit element.  $Q_1$  is a current-limiting device that offers very low impedance to current below its threshold value and extremely high impedance to any current above that threshold. The threshold is controlled by  $R_2$ . Diodes  $D_2$  and  $D_3$  provided bias voltage for the operation of  $Q_1$ . When an incipient skid occurs, the generator voltage decreases rapidly and since  $Q_1$  limits the discharge current into  $C_1$ , the voltage at the negative side of  $C_1$  decreases and causes current to flow through  $R_{5A}$ ,  $R_6$ ,  $Q_2$ , and  $R_3$ . The current into the base of  $Q_2$  is amplified by  $Q_2$ ,  $Q_3$ ,  $Q_5$ ,  $Q_6$  and  $Q_7$ , (the valve control amplifier) to produce a voltage across  $R_v$ , the antiskid valve coil. Voltage applied to the antiskid valve causes brake pressure to be reduced proportionally and thereby alleviate the incipient skid. Antiskid valve voltage is feedback to the amplifier input through  $R_7$  to stabilize amplifier gain against changes due to temperature and component characteristic variations.

Antiskid valve voltage pulses are transmitted to the modulation circuit elements through capacitor  $C_4$ . Within the modulation circuit element, consisting of  $C_4$ ,  $R_{11}$ ,  $R_{14}$ ,  $R_{12}$ ,  $D_7$ ,  $C_3$ ,  $C_2$ ,  $D_9$  and  $Q_4$ , each increase in voltage to the valve produces an increase in the charge on  $C_3$ . Voltage on  $C_3$  causes  $Q_4$  to charge  $C_2$ . Since  $C_2$  discharges through  $R_{8B}$ ,  $R_{8A}$ , and  $R_1$ , the voltage on  $C_2$  provides a threshold control signal to  $Q_1$ . The charge on  $C_3$ , and in turn on  $C_2$ , is a function of the amplitude and frequency of valve voltage pulses. Voltage on  $C_2$  is also applied to  $Q_2$  through  $R_{8B}$  and  $D_4$  to provide a pressure bias signal to the valve control amplifier. The operation of the modulation circuit element results in an automatic threshold change to the skid sensing circuit and a bias to the valve control amplifier to match the braking conditions being encountered.

The mathematical description of the operation of the Goodyear adaptive electronic antiskid control circuit as shown on Figure A50 is developed with conventional circuit analysis techniques using Kirchhoff's Laws. Figure A51 is the schematic diagram from Figure A50 with the transistors and diodes shown in terms of their equivalent circuits and the various currents and voltages identified. The transistor and diode equivalent circuits are adaptations of equivalent circuits developed and described in references 13, 14 and 15. Some of the diode forward resistances are combined with other resistance in series with the diodes and are not shown separately. Also, since the current through  $R_6$  (the output resistance of the wheel speed signal source) has three non-mutually influencing components,  $R_6$  is included in  $R_3$ ,  $R_{08}$  and  $R_{15}$  to simplify equations. Other simplifications will be described and discussed during the development of equations.

Referring to Figure A51, the circuit equations are developed as follows:

The voltage across capacitor  $C_1$  is defined as:

$$(1) \quad V_{C_1} = \int \dot{V}_{C_1} dt$$

$$(A1) \quad \dot{V}_{C_1} = A_{C_1}/C_1 \quad \text{OR} \quad \dot{V}_{C_1} = A_{C_1} C_{608}$$

$A_{C_1}$  is the current through  $C_1$  and  $C_1$  is the capacitance.  $A_{C_1}$  is established by summing currents at node (N11) as:

$$(N11) \quad A_{C_1} = A_{08} - A_{12}$$

Using Ohm's law and summing voltages around the loop of which  $R_{08}$  is a part,  $A_{08}$  is established as:

$$(R10) \quad A_{08} = (E_G - V_{C_1} - E_{08})/R_{08} \quad \text{FOR } (E_G - V_{C_1} - E_{08}) > 0$$

$$= 0 \quad \text{FOR } (E_G - V_{C_1} - E_{08}) \leq 0$$

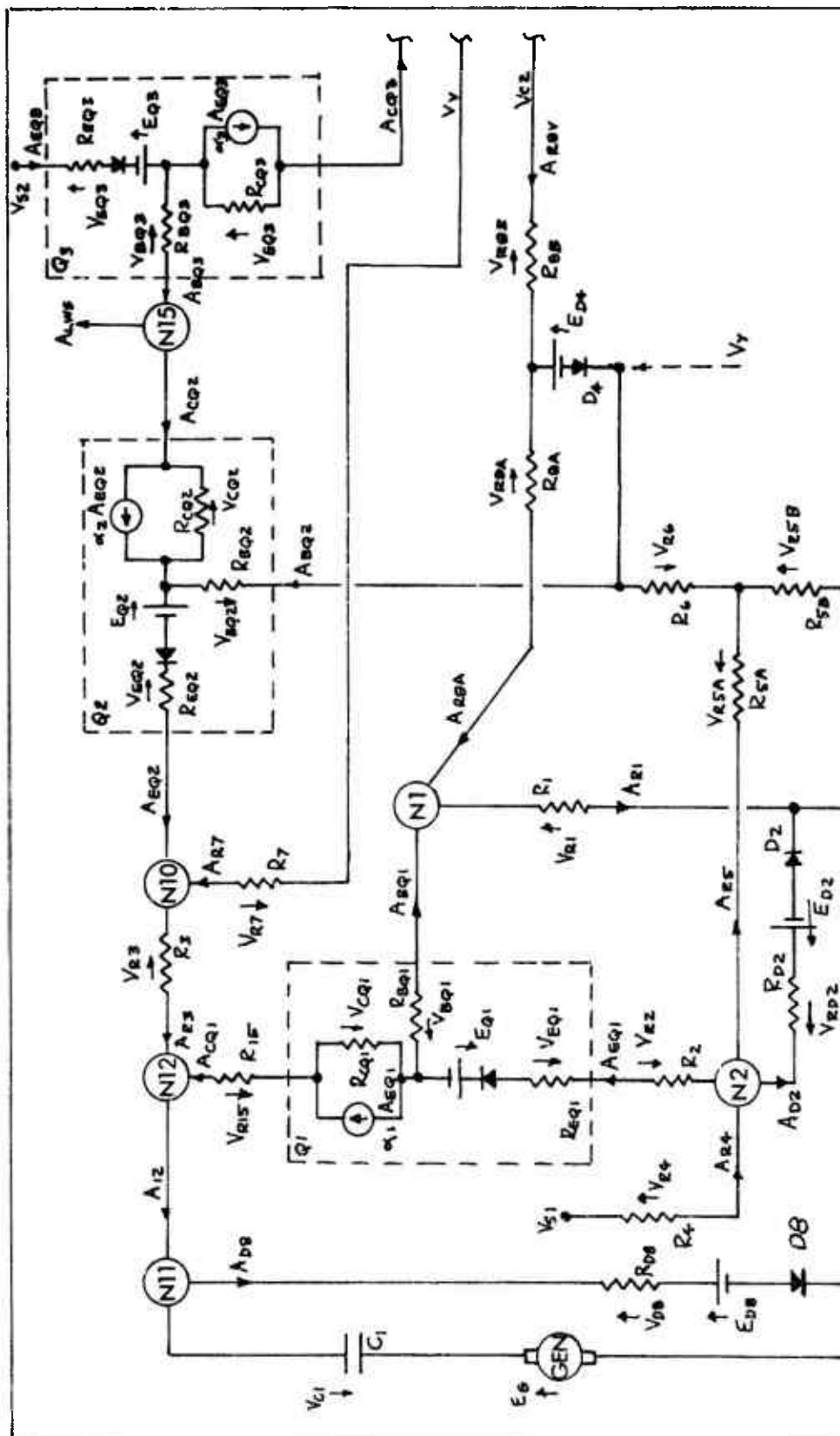
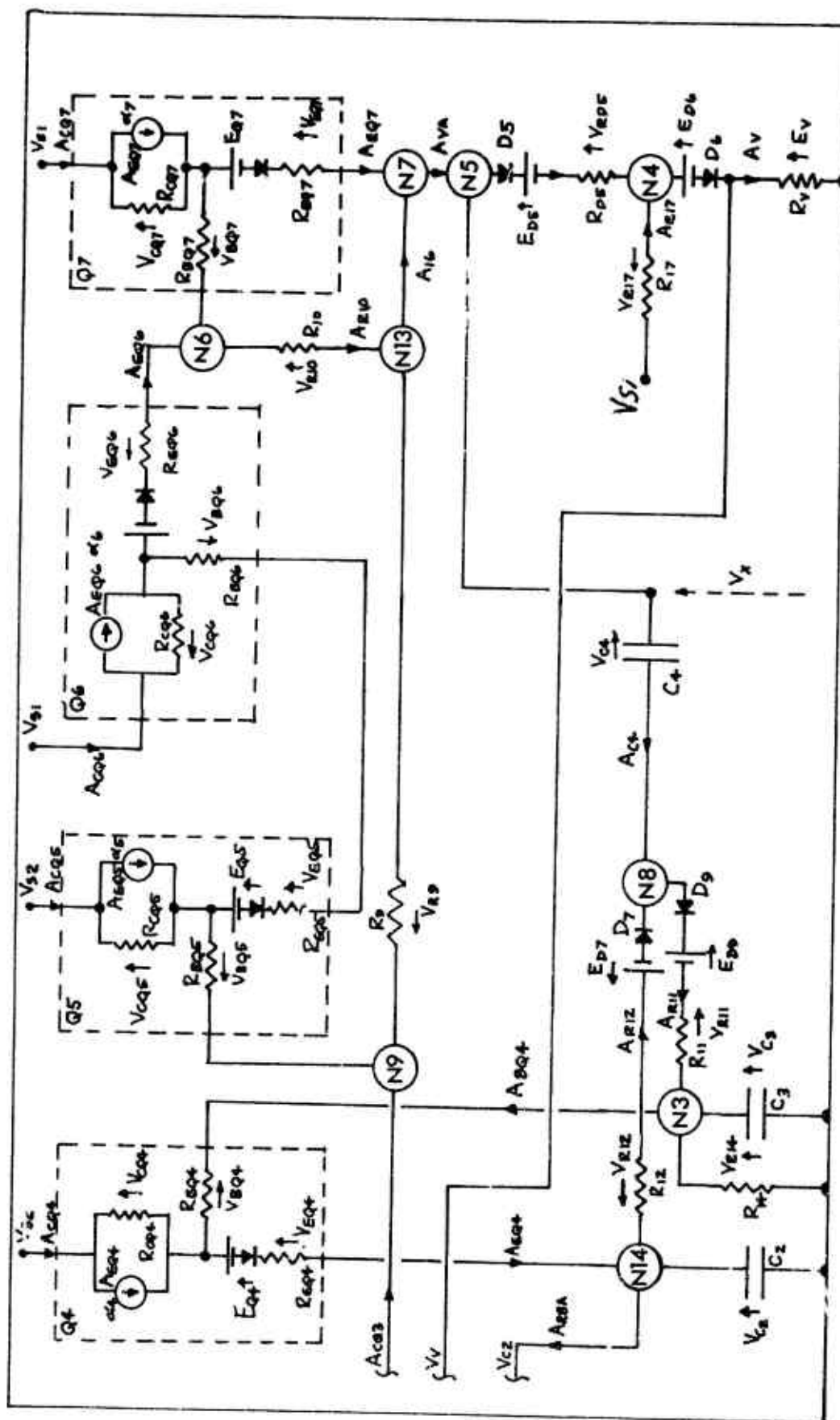


Figure A51 Modulated Antiskid Schematic with Mathematical Identification and Incorporating Equivalent Circuits for Transistors and Diodes (Sheet 1 of 2)



**Figure A51**    **Modulated Antiskid Schematic with Mathematical Identification and Incorporating Equivalent Circuits for Transistors and Diodes (Sheet 2 of 2)**

Noting that because of diode  $D_3$ ,  $A_{D3}$  is restricted to positive values only.

To combine constants, write equation (R10) as:

$$(R10) \quad A_{D3} = (E_G - V_{C1}) C_{620} - C_{621} \quad \text{FOR } (E_G - V_{C1}) > C_{620}/C_{621} \\ = 0 \quad \text{FOR } (E_G - V_{C1}) \leq C_{620}/C_{621}$$

By summing currents at Node (N12), current  $A_{I2}$  is established as:

$$(N12) \quad A_{I2} = A_{R3} + A_{CQ1}$$

Substituting equation (N12) into equation (N11) gives:

$$(N11)' \quad A_{C1} = A_{D3} - A_{R3} - A_{CQ1}$$

To compute  $A_{CQ1}$  it is desirable to first obtain equations for the voltages at the base and emitter of  $Q_1$  in terms of the base and emitter currents and the appropriate voltage sources. The voltage at the base of  $Q_1$  is  $V_{R1}$ . Summing currents at Node (N1) establishes current  $A_{R1}$  as:

$$(N1) \quad A_{R1} = A_{BQ1} + A_{RBA}$$

Summing voltages around the loop  $R_1, R_{BA}, R_{BB}$  to  $V_{C2}$  gives:  $V_{RBA} + V_{RBB} = V_{C2} - V_{R1}$ . If the current through diode  $D_4$  is assumed negligible, then  $A_{RBA} = A_{RBB}$ . (Because of the relative resistances, the current through  $D_4$  is a very small fraction of the current through  $R_{BB}$ ). By Ohm's law,  $V_{RBA} + V_{RBB} = A_{RBA} (R_{BA} + R_{BB})$  and  $V_{R1} = A_{R1} R_1$ . Substitution into equation (N1) and solving for  $V_{R1}$  gives:

$$(N1)' \quad V_{R1} = R_1 \left( A_{BQ1} + \frac{V_{C2}}{R_{BA} + R_{BB}} \right) / \left( 1 + \frac{R_1}{R_{BA} + R_{BB}} \right)$$

The voltage at Node (N2) is  $E_{D2} + V_{R_{D2}}$ . (Here two diodes  $D_2$  and  $D_3$  as shown on Figure 50 are combined in an equivalent single diode). Summing currents at Node (N2) establishes current  $A_{D2}$  as:

$$(N2): \quad A_{D2} = A_{R4} - A_{R5} - A_{EQ1}$$

By Ohm's law,  $V_{R_{D2}} = A_{D2} R_{D2}$ ,  $V_{R4} = A_{R4} R_4$ , and  $(V_{R5A} + V_{R5B}) = A_{R5} (R_{5A} + R_{5B})$  (Note: Because of the relative resistances,  $A_{R6}$  is a very small component of the current in  $R_{5A}$  and is assumed to be zero when computing  $V_{R_{D2}}$ .) Summing voltages around the appropriate loops establishes that  $V_{R4} = V_{S1} - V_{R_{D2}} - E_{D2}$  and  $V_{R5A} + V_{R5B} = V_{R_{D2}} + E_{D2}$ . By substitution into equation (N2) and solving for  $V_{R_{D2}}$  gives:

$$(N2)' \quad V_{R_{D2}} = \frac{\left[ \frac{V_{S1}}{R_4} - E_{D2} \left( \frac{1}{R_4} + \frac{1}{R_{5A} + R_{5B}} \right) - A_{EQ1} \right]}{\left( \frac{1}{R_{D2}} + \frac{1}{R_4} + \frac{1}{R_{5A} + R_{5B}} \right)}$$

Summing voltages around the loop through which  $A_{BQ1}$  (the base of current  $Q_1$ ) flows results in:

$$(Q-1) \quad E_{D2} + V_{R_{D2}} - V_{R2} - V_{EQ1} - E_{Q1} - V_{BQ1} - V_{R1} = 0$$

By substituting  $V_{R2} = A_{EQ1} R_2$ ,  $V_{EQ1} = A_{EQ1} R_{EQ1}$  and  $V_{BQ1} = A_{BQ1} R_{BQ1}$  (From Ohm's Law) along with equations (N1)', (N2)', and the basic transistor relationship  $A_{EQ1} = (h_{FE1} + 1) A_{BQ1}$  into equation (Q-1) and solving for  $A_{EQ1}$

$$(Q-1)' \quad A_{EQ1} = C_{602} - C_{603} V_{C2} \quad , \quad \text{WHERE}$$

$$C_{602} = \frac{\left\{ E_{D2} \left[ 1 - \left( \frac{1}{R_4} + \frac{1}{R_5} \right) / \left( \frac{1}{R_{D2}} + \frac{1}{R_4} + \frac{1}{R_5} \right) \right] + V_{S1} \left( \frac{1}{R_4} \right) / \left( \frac{1}{R_{D2}} + \frac{1}{R_4} + \frac{1}{R_5} \right) - E_{Q1} \right\}}{\left\{ R_2 + R_{EQ1} + \frac{R_{BQ1}}{(h_{FE1} + 1)} + \frac{R_1}{(h_{FE1} + 1)} / \left( 1 + \frac{R_1}{R_B} \right) + 1 / \left( \frac{1}{R_{D2}} + \frac{1}{R_4} + \frac{1}{R_5} \right) \right\}}$$

$$C_{603} = \frac{\frac{R_1}{R_1 + R_B}}{\left\{ R_2 + R_{EQ1} + \frac{R_{BQ1}}{(h_{FE1} + 1)} + \frac{R}{(h_{FE1} + 1)} / \left( 1 + \frac{R_1}{R_B} \right) + 1 / \left( \frac{1}{R_{D2}} + \frac{1}{R_4} + \frac{1}{R_5} \right) \right\}}$$

And where in the above  $R_5 = R_{5A} + R_{5B}$  and  $R_6 = R_{6A} + R_{6B}$ .

For  $Q_1$  to operate as a transistor,  $V_{CQ1}$  must be positive. Using equation (Q-1)', the basic transistor characteristic (Q2)  $A_{CQ1} = h_{FE1} A_{EQ1} / (h_{FE1} + 1)$  and by writing the voltage loop equation through  $D_2, Q_1, R_{15}, C_1$  and  $(GEN)$  it can be shown that  $V_{CQ1}$  is positive for  $(E_G - V_{C1})$  negative; therefore, equation (Q-1)' is applicable only for  $(E_G - V_{C1}) < 0$ . Substituting (Q-1) into (Q-2) gives the following equation:

$$\begin{aligned} (Q-1C) \quad A_{CQ1} &= C_{604} - C_{605} V_{C2} \quad \text{FOR } (E_G - V_{C1}) < 0 \\ &= 0 \quad \text{FOR } (E_G - V_{C1}) \geq 0 \\ &= 0 \quad \text{FOR } V_{C2} \geq C_{604} / C_{605} \end{aligned}$$

$$C_{604} = C_{602} \left( \frac{h_{FE1}}{h_{FE1} + 1} \right)$$

$$C_{605} = C_{603} \left( \frac{h_{FE1}}{h_{FE1} + 1} \right)$$

By summing currents at node  $(N10)$ , current  $AR_3$  is established as:

$$(N10) \quad AR_3 = A_{EQ2} + AR_7$$

To compute the components of  $AR_3$  (i.e.,  $A_{EQ2}$  and  $AR_7$ ) it is desirable to have equation (N10) in a form where  $AR_7$  is expressed in terms of the appropriate voltages and resistances. By summing voltages around the loop  $R_V, R_7, R_3, C_1$  and  $GEN$ ,  $V_{R7}$  is established as:

$$(V7) \quad V_{R7} = E_V - V_{R3} - (E_G - V_{C1})$$

Substituting equation (V7) along with  $V_{R3} = AR_3 R_3$  and  $V_{R7} = AR_7 R_7$  into (N10) gives:

$$(N10)' \quad AR_3 = \frac{A_{EQ2}}{1 + R_3/R_7} + \frac{E_V}{(R_7 + R_3)} - \frac{(E_G - V_{C1})}{(R_7 + R_3)}$$

To combine constants write as:

$$(N10)' \quad AR_3 = A_{EQ2} C_{612} + [E_V - (E_G - V_{C1})] C_{613}$$

To compute current  $A_{EQ2}$ , sum voltages around the loop through which  $A_{BQ2}$  flows:

$$(Q-2) \quad V_Y - V_{BQ2} - E_{Q2} - V_{EQ2} - V_{R3} - (E_6 - V_{C1}) = 0$$

Here voltage  $V_Y$  is the base voltage on Q2 and is either  $(V_{R5B} - V_{R6})$  or  $(V_{C2} - V_{RBB} - E_{D4})$  whichever is the largest; therefore, there will be a version of equation (Q-2) for each of these conditions. To establish which condition exists, it is necessary to compute  $(V_{R5B} - V_{R6})$  and  $(V_{C2} - V_{RBB} - E_{D4})$

During derivation of Equation (N2)' it was observed that  $V_{R5A} + V_{R5B} = V_{RD2} + E_{D2}$  and it was assumed that  $A_{R6}$  was small when compared to  $A_{R5}$ . Using the same assumption  $V_{R5B}$  is established as follows by Ohm's Law:

$$(R-5) \quad V_{R5B} = A_{R5} R_{5B}$$

By substituting  $A_{R5} (R_{5A} + R_{5B}) = V_{R5A} + V_{R5B}$  into equation (R-5) above gives:

$$(R-5)' \quad V_{R5B} = R_{5B} (V_{RD2} + E_{D2}) / (R_{5A} + R_{5B})$$

By substituting equation (N2)' for  $V_{RD2}$  and investigating the influence of  $A_{EQ1}$  within its allowable range, it can be seen that for practical purposes  $V_{R5B}$  is a constant.

To compute  $V_{R6}$ , it can be seen that  $A_{R6}$  equals  $A_{BQ2}$  when  $V_Y$  is  $V_{R5B} - V_{R6}$ ; therefore,  $V_{R6} = A_{BQ2} R_6$  by Ohm's law.

By Ohm's Law  $V_{RBB} = A_{RBB} R_{BB}$ . Since the current through D4 is very small and may be assumed zero, and since  $A_{BQ1}$  is such a small component of the current through R1 that it can be assumed zero, by Ohm's Law:

$$(V8) \quad A_{RBB} = A_{RBA} = V_{C2} / (R_1 + R_{BA} + R_{BE})$$

Therefore:

$$(V_{C2} - V_{RBB} - E_{D4}) = \left[ V_{C2} \left( \frac{R_1 + R_{BA}}{R_1 + R_{BA} + R_{BB}} \right) - E_{D4} \right]$$

To establish whether  $V_Y = (V_{R5B} - V_{R6})$  or

$$V_Y = \left[ V_{C2} \left( \frac{R_1 + R_{BA}}{R_1 + R_{BA} + R_{BB}} \right) - E_{D4} \right]$$

A voltage  $V_B$  will be defined as follows:

$$(VB) \quad V_B = \left[ V_{C2} \left( \frac{R_1 + R_{BA}}{R_1 + R_{BA} + R_{BB}} \right) - E_{D4} \right] - (V_{R5B} - R_6 A_{BQ2})$$

$$\text{if } V_B > 0, (VY-1) \quad V_Y = [V_{C2} C_m - E_{D4}]$$

$$\text{if } V_B \leq 0, (VY-2) \quad V_Y = [V_{R5B} - R_6 A_{BQ2}]$$

where  $C_m$  above is defined as:

$$C_m = \left( \frac{R_1 + R_{BA}}{R_1 + R_{BA} + R_{BB}} \right)$$

To combine constants and expressing  $A_{BQ2}$  as  $A_{EQ2}/h_{FE2} + 1$  equation (VB) may be written in the following form:

$$(VB) \quad V_B = V_{C2} C_m + A_{EQ2} C_{B01} - C_{B00}$$

Before proceeding with the computation of  $A_{R3}$ , the valve control amplifier and modulation circuit elements will be examined to develop equations for  $E_V$  and  $V_{C2}$ .

By summing currents at Node (N5) current  $A_{D5}$  is established as:

$$(N5) \quad A_{D5} = A_{VA} - A_{C4}$$

The voltage at Node (N5) is defined as  $V_X$ . Summing voltages around the loop  $R_V$ ,  $D_6$ ,  $D_5$  and  $V_X$  gives:

$$(VX) \quad V_X = E_V + E_{D6} + V_{R05} + E_{D5}$$

By summing currents at Node (N4), current  $A_{R17}$  is established as:

$$(N4) \quad A_{R17} = A_V - A_{D5}$$

By substituting equations (N4), (N5), and (EV) into equation (VX) and by using Ohm's Law to establish that  $E_V = A_V R_V$ ,  $V_{R17} = A_{R17} R_{17}$  and  $V_{D5} = A_{D5} R_{D5}$ , VX is established as:

$$(VX)' \quad V_X = A_{D5} C_{400} + C_{401}$$

By substituting equation (EV) into (N4) and using the relationships  $E_V = A_V R_V$  and  $V_{R17} = A_{R17} R_{17}$  EV is established as:

$$(N4)' \quad E_V = A_{D5} C_{406} + C_{407}$$

The operation of transistors Q2, Q3, Q5, Q6, and Q7 will now be considered to develop an equation for current  $A_{VA}$  (Valve Control Amplifier Output Current).

By summing currents at Node (N7), current  $A_{VA}$  is established as:

$$(N7) \quad A_{VA} = A_{EQ7} + A_{16}$$

By summing currents at Node (N13), current  $A_{16}$  is established as:

$$(N13) \quad A_{16} = A_{R10} + A_{R9}$$

By summing currents at Node (N6), current  $A_{R10}$  is established as:

$$(N6) \quad A_{R10} = A_{EQ6} - A_{BQ7}$$

By summing currents at Node (N9), current  $A_{R9}$  is established as:

$$(N9) \quad A_{R9} = A_{CQ3} - A_{BQ5}$$

Summing voltages around the loop,  $R_{EQ7}$ ,  $R_{BQ7}$  and  $R_{10}$  gives:

$$(V10) \quad V_{R10} = V_{EQ7} + E_{Q7} + V_{BQ7}$$

By using the relationships  $V_{R10} = A_{R10} R_{10}$ ,  $V_{EQ7} = A_{EQ7} R_{EQ7}$  and  $V_{BQ7} = A_{BQ7} R_{BQ7}$  as established by Ohm's law along with the transistor characteristic  $A_{EQ7} = (h_{FE7} + 1) A_{BQ7}$  and substitution equation (N6) into (V10) and solving for  $A_{BQ7}$ :

$$(V10)' \quad A_{BQ7} = \frac{A_{EQ6} R_{10} - E_{Q7}}{[(h_{FE7} + 1) R_{EQ7} + R_{BQ7} + R_{10}]}$$

By substituting (V10)' and (N6) into the relationship  $V_{R10} = A_{R10} R_{10}$

$$(A10) \quad V_{R10} = A_{EQ6} C_{402} + C_{403} E_{Q7}$$

Summing voltages around the loop  $R_{10}$ ,  $R_{EQ6}$ ,  $R_{BQ6}$ ,  $R_{EQ5}$ ,  $R_{BQ5}$  and  $R_9$  gives:

$$(V9) \quad 0 = V_{R10} + V_{EQ6} + E_{Q6} + V_{BQ6} + V_{EQ5} + E_{Q5} + V_{BQ5} - V_{R9}$$

By substituting equations (A10) and (N9) into (V9) along with transistor characteristics  $A_{EQ6} = (h_{FE6} + 1) A_{BQ6}$  and  $A_{EQ5} = (h_{FE5} + 1) A_{BQ5}$  and the Ohm's Law relationships  $V_{R9} = A_{R9} R_9$ ,  $V_{EQ6} = A_{EQ6} R_{EQ6}$ ,  $V_{BQ6} = A_{BQ6} R_{BQ6}$ ,  $V_{EQ5} = A_{EQ5} R_{EQ5}$  and  $V_{BQ5} = A_{BQ5} R_{BQ5}$  and solving for  $A_{EQ6}$ :

(V9)'

$$A_{EQ6} = \frac{A_{R9} R_9 - (E_{Q6} + E_{Q5} + C_{403} E_{Q7})}{\left[ C_{402} + R_{EQ6} + \frac{R_{BQ6} + R_{EQ5}}{(h_{FE6} + 1)} + \frac{R_{BQ5} + R_9}{(h_{FE5} + 1)(h_{FE6} + 1)} \right]}$$

Substituting equations (N13), (N6), (N9), and (V9)' into equation (N7) along with transistor characteristics  $A_{EQ5} = (h_{FE5} + 1) A_{BQ5}$  and  $A_{EQ6} = (h_{FE6} + 1) A_{BQ6}$  and solving for  $A_{VA}$  gives:

$$(N7)' \quad A_{VA} = A_{CQ3} C_{404} - C_{405}$$

It should be noted that these operations involving Q5, Q6, and Q7 assume that  $A_{CQ3}$  is large enough such that  $A_{VA}$  is not negative and that the applicable supply voltages,  $V_{S1}$  and  $V_{S2}$ , are large enough to keep  $V_{CQ1}$ ,  $V_{CQ6}$  and  $V_{CQ5}$  positive at all times. The latter assumption can be proven to be true for the range of currents experienced during circuit operation. If  $A_{CQ3}$  is not greater than  $C_{405}/C_{404}$ , insufficient voltage is developed across  $R_9$  to cause Q5, Q6 and Q7 to operate. For  $A_{CQ3}$  less than  $C_{405}/C_{404}$  all of  $A_{CQ3}$  goes through  $R_9$  and  $A_{VA} = A_{CQ3}$ ; therefore, equation (N7)' has two forms depending on the value of  $A_{CQ3}$ . Write these two forms as follows:

$$(N7)'' \quad A_{VA} = A_{CQ3} C_{404} - C_{405} \quad \text{FOR } A_{CQ3} > C_{405}/C_{404}$$

$$= A_{CQ3} \quad \text{FOR } A_{CQ3} \leq C_{405}/C_{404}$$

Supply voltage  $V_{S2}$  is large enough so that voltages  $V_{CQ3}$  and  $V_{EQ3}$  are always positive and a small leakage current  $A_{CQ30}$  flows. All the equations developed here are for the increment of  $A_{CQ3}$  above the leakage value.

By using the transistor characteristics  $A_{CQ3} = h_{FE3} A_{BQ3}$   
 $A_{CQ2} = A_{EQ2} h_{FE2} / (h_{FE2} + 1)$

And if at Node N15  $A_{LWS} = 0$ ,  $A_{BQ3} = A_{CQ2}$  then:

$$(Q3) \quad A_{CQ3} = A_{EQ2} C_{606}$$

$$\text{WHERE} \quad C_{606} = \frac{(h_{FE2})(h_{FE2})}{(h_{FE2} + 1)}$$

The operation of the modulating circuit element will now be examined. To compute valve voltage  $E_V$  from equation (N4)' the value of current  $A_{D5}$  which is established by Equation (N5) is required. Equation (N5) shows that a

component of  $A_{D5}$  is  $A_{C4}$ . Before developing equations for computing  $A_{C4}$  some observations relative to the operation of C4 and Q4 are helpful.

By summing currents at Node (N8) current  $A_{C4}$  is established as:

$$(N8) \quad A_{C4} = A_{R11} - A_{R12}$$

However, because of diodes D7 and D9 currents  $A_{R11}$  and  $A_{R12}$  have limitations depending upon the direction of voltage across the diodes. Summing voltages around the loop C3, R11, D9, C4 to VX gives:

$$(V11) \quad V_{C3} + V_{R11} + E_{D9} + V_{C4} - V_X = 0$$

Substituting equation (V11) into the expression  $V_{R11} = A_{R11} R_{11}$  as established by Ohm's law gives:

$$(V11)' \quad A_{R11} = \frac{V_X - V_{C4} - E_{D9} - V_{C3}}{R_{11}} \quad \text{FOR } (V_X - V_{C4} - E_{D9} - V_{C3}) > 0$$

Because of D9,  $A_{R11} = 0$  FOR  $(V_X - V_{C4} - E_{D9} - V_{C3}) \leq 0$

Summing voltages around the loop C3, R12, D7, C4, to VX gives:

$$(V12) \quad V_{C2} - V_{R12} - E_{D7} + V_{C4} - V_X = 0$$

Substituting equation (V12) into the expression  $V_{R12} = A_{R12} R_{12}$  as established by Ohm's law gives:

$$(V12)' \quad A_{R12} = \frac{V_{C2} - E_{D7} + V_{C4} - V_X}{R_{12}} \quad \text{FOR } (V_{C2} - E_{D7} + V_{C4} - V_X) > 0$$

Because of D7  $A_{R12} = 0$  FOR  $(V_{C2} - E_{D7} + V_{C4} - V_X) \leq 0$

Summing voltages around the loop C3 through Q4 to C2 gives:

$$(V-Q4) \quad V_{C3} - V_{BQ4} - E_{Q4} - V_{EQ4} - V_{C2} = 0$$

Since the currents  $A_{BQ4}$  and  $A_{EQ4}$  in transistor Q4 are restricted to positive values only, voltages  $V_{BQ4}$  and  $V_{EQ4}$  are always positive; therefore, equation (V-Q4) shows that  $V_{C2}$  is always less than  $V_{C3}$  by an amount at least equal to  $E_{Q4}$ . Also, because of diodes D7 and D9, no current can flow from C3 through R11, D9, D7 and R12 to C2. For these circumstances, it is observed (1) that for  $A_{C4}$  positive, all of  $A_{C4}$  passes through R11 and all of  $A_{R11}$  is  $A_{C4}$  and (2) that for  $A_{C4}$  negative, all of  $A_{C4}$  passes through R12 and all of  $A_{R12}$  is  $-A_{C4}$ .

Since there cannot be positive  $A_{R11}$  and positive  $A_{R12}$  simultaneously, equation (N8) evolves to:

$$\begin{aligned} (N8)' \quad A_{C4} &= A_{R11} && \text{FOR } A_{R11} > 0 \\ A_{C4} &= 0 && \text{FOR } A_{R11} = 0 \text{ AND } A_{R12} = 0 \\ A_{C4} &= -A_{R12} && \text{FOR } A_{R12} > 0 \end{aligned}$$

By substituting equations (N5), (VX)' and (N7)" into equations (V11)' and (V12)', equations for  $A_{C4}$  are developed for each case.

The remaining equations for the modulation circuit element will now be developed. Substituting the expressions  $V_{BQ4} = A_{BQ4} R_{BQ4}$  and  $V_{EQ4} = A_{EQ4} R_{EQ4}$  as established by Ohm's law along with the transistor characteristic  $A_{EQ4} = (h_{FE4} + 1) A_{BQ4}$  into equation (V-Q4) and solving for  $A_{BQ4}$  gives:

$$\begin{aligned} (V-Q4)' \quad A_{BQ4} &= \frac{V_{C3} - E_{Q4} - V_{C2}}{[R_{BQ4} + (h_{FE4} + 1) R_{EQ4}]} \\ &\quad \text{FOR } (V_{C3} - E_{Q4} - V_{C2}) > 0 \\ &= 0 && \text{FOR } (V_{C3} - E_{Q4} - V_{C2}) \leq 0 \end{aligned}$$

To combine constants, write equation (V-Q4) as:

$$\begin{aligned}
 \text{(V-Q4)} \quad ABQ4 &= (V_{C3} - V_{C2}) C_{622} - C_{623} \\
 &\quad \text{FOR } (V_{C3} - V_{C2}) > C_{623}/C_{622} \\
 &= 0 \quad \text{FOR } (V_{C3} - V_{C2}) \leq C_{623}/C_{622}
 \end{aligned}$$

Also, since current AEQ4 is needed, define the transistor characteristic as equation Q4:

$$\begin{aligned}
 \text{(Q-4)} \quad AEQ4 &= ABQ4 C_{614} \\
 \text{where } C_{614} &= (\beta_{FE4} + 1)
 \end{aligned}$$

By summing currents at Node (N14) current AC2 is established as:

$$\text{(N14)} \quad AC2 = AEQ4 - AR12 - AR8A$$

Using the same assumption relative to AR8A as was made for equations (N1)' and (V8) and by Ohm's Law AR8A is established by equation (V8) as:

$$\text{(V8)} \quad AR8A = \frac{V_{C2}}{R_1 + R_{8A} + R_{8B}} \quad \text{(Repeated)}$$

By summing currents at Node (N3) current AC3 is established as:

$$\text{(N3)} \quad AC3 = AR11 - AR14 - ABQ4$$

Current AR14 is computed from  $V_{C3} = AR14 R_{14}$  established by Ohm's law and ABQ4 is computed from equation (V-Q4)' and Equation (Q-4).

Equation (N8)' establishes that:

$$\begin{aligned} AR_{12} &= -Ac_4 & \text{FOR } Ac_4 < 0 \\ &= 0 & \text{FOR } Ac_4 \geq 0 \end{aligned}$$

$$\begin{aligned} AR_{11} &= Ac_4 & \text{FOR } Ac_4 > 0 \\ &= 0 & \text{FOR } Ac_4 \leq 0 \end{aligned}$$

Substituting the above and equations (V8) and (Q-4) into equation (N14) gives:

$$\begin{aligned} (N14)' \quad Ac_2 &= ABQ_4 C_{614} + Ac_4 - Vc_2 C_{618} & \text{FOR } Ac_4 < 0 \\ &= ABQ_4 C_{614} - Vc_2 C_{618} & \text{FOR } Ac_4 \geq 0 \end{aligned}$$

Similarly, by substituting the above  $AR_{11}$  to  $Ac_4$  relationship and  $Vc_3 = AR_{14} R_{14}$  into equation (N3)  $Ac_3$  is established as:

$$\begin{aligned} (N3)' \quad Ac_3 &= Ac_4 - Vc_3 C_{619} - ABQ_4 & \text{FOR } Ac_4 > 0 \\ &= -Vc_3 C_{619} - ABQ_4 & \text{FOR } Ac_4 \leq 0 \end{aligned}$$

The voltages across capacitors C2, C3 and C4 are established by:

$$(2) \quad Vc_2 = \int Vc_2' dt$$

$$(A2) \quad Vc_2' = C_{609} Ac_2$$

$$(3) \quad Vc_3 = \int Vc_3' dt$$

$$(A3) \quad Vc_3' = C_{610} Ac_3$$

$$(4) \quad Vc_4 = \int Vc_4' dt$$

$$(A4) \quad \dot{V}_{c4} = C_{611} A_{c4}$$

All of the equations describing the antiskid circuit's operation have now been developed; however, to obtain a computer solution of these equations, they have to be converted to a suitable form so that there are no "closed loops." Also, since the equations for  $A_{EQ2}$ ,  $A_{VA}$  and  $A_{c4}$  have different forms depending upon which circumstances exist, a procedure must be established to define which form of equations (Q2), (N7)" and (N8)" applies for each instance. There are twelve (12) possible combinations of circumstances as shown on Table A14. The procedure for defining which condition exists will be to assume a condition and develop a set of equations based on the assumption. Using these equations, the assumption will be tested. If the test is affirmative, the assumed condition exists. If the test is negative, the assumption is incorrect and other assumed conditions are tested until an affirmative test result is obtained. To illustrate this procedure, the equations for circuit condition 4 will be developed:

For circuit condition 4  $A_{c4}$  is positive,  $A_{cQ3}$  greater than  $C_{405}/C_{404}$  and  $V_B$  greater than zero. Substitute equation (N5) and the applicable version of equation (N7)" into equation (VX)".

$$(VX)''-4 \quad V_X = (A_{cQ3} C_{404} - C_{405} - A_{c4}) C_{400} + C_{401}$$

From equations (N8)" and (V11)"  $A_{c4}$  is established as:

$$(N8)'' - P \quad A_{c4} = \frac{V_X - V_{c4} - E_{09} - V_{c3}}{R_{11}}$$

Substitute (VX)''-4 into (N8)''-P and solve for  $A_{c4}$

$$(N8)''-P4$$

$$A_{c4} = \frac{A_{cQ3} C_{404} C_{400}}{R_{11} + C_{400}} - \frac{(V_{c4} + V_{c3})}{R_{11} + C_{400}} - \frac{(E_{09} + C_{405} C_{400} - C_{401})}{R_{11} + C_{400}}$$

Table A14 Modulated Antiskid Circuit Conditions

Circuit Condition	Capacitor C4 Current Mode (See Note 1)	Valve Amplifier Operating Mode (See Note 2)	Pressure Bias Signal Condition (See Note 3)
1	$A_{C4} > 0$	$A_{EQ2} \leq C_{607}$	$V_B \leq 0$
2	$A_{C4} > 0$	$A_{EQ2} \leq C_{607}$	$V_B > 0$
3	$A_{C4} > 0$	$A_{EQ2} > C_{607}$	$V_B \leq 0$
4	$A_{C4} > 0$	$A_{EQ2} > C_{607}$	$V_B > 0$
5	$A_{C4} = 0$	$A_{EQ2} \leq C_{607}$	$V_B \leq 0$
6	$A_{C4} = 0$	$A_{EQ2} \leq C_{607}$	$V_B > 0$
7	$A_{C4} = 0$	$A_{EQ2} > C_{607}$	$V_B \leq 0$
8	$A_{C4} = 0$	$A_{EQ2} > C_{607}$	$V_B > 0$
9	$A_{C4} < 0$	$A_{EQ2} \leq C_{607}$	$V_B \leq 0$
10	$A_{C4} < 0$	$A_{EQ2} \leq C_{607}$	$V_B > 0$
11	$A_{C4} < 0$	$A_{EQ2} > C_{607}$	$V_B \leq 0$
12	$A_{C4} < 0$	$A_{EQ2} > C_{607}$	$V_B > 0$

## Notes:

1. Capacitor C4 is charging for  $A_{C4} > 0$ , static for  $A_{C4} = 0$  and discharging for  $A_{C4} < 0$ .
2. The valve amplifier is amplifying for  $A_{EQ2} > C_{607}$  and is cutoff for  $A_{EQ2} \leq C_{607}$ .
3. A pressure bias signal exists for  $V_B > 0$  and does not exist for  $V_B \leq 0$ .

Now substitute equations (N5), (N7)" and (N8)'-P4 into equation (N4)' and solve for EV

$$(N4)'-4 \quad EV = \frac{R_V}{R_{11} + C_{400}} \left[ A_{EQ3} C_{404} R_{11} C_{406} + (V_{C4} + V_{C2}) C_{406} - (C_{405} R_{11} - E_{04} + C_{401}) C_{406} + C_{407} (R_{11} + C_{400}) \right]$$

Substituting equations (N4)'-4, (N10)', (Vy-1), and (Q3) into equation (Q-2) and solving for  $A_{EQ2}$  gives:

$$(Q-2)-4 \quad A_{EQ2} = -(E_6 - V_{C4}) C_{449} + V_{C2} C_{450} - (V_{C3} + V_{C4}) C_{451} + C_{452}$$

By substituting equation (Q3) into equation (N8)'-P4 an equation is obtained for computing  $AC4$  using the value of  $A_{EQ2}$  obtained from equation (Q-2)-4 above and making this substitution and combining constants, equation (N8)'-P4 can be written as:

$$(N8)-4 \quad AC4 = (A_{EQ2}) C_{806} - (V_{C3} + V_{C4}) C_{804} - C_{807}$$

if  $[(A_{EQ2}) C_{806} - (V_{C3} + V_{C4}) C_{804} - C_{807}] > 0$

The value of  $A_{EQ2}$  from equation (Q-2)-4 may also be used for computing VB.

Using equations (Q-2)-3, (VB) and (N8)-4 the assumption that  $AC4 > 0$ ,  $ACQ3 > C_{405}/C_{404}$  and  $VB > 0$  can be tested. If the test is affirmative, then values for  $AC4$ ,  $AR3$  and EV can be computed. If the test is negative another conditions must be tested for.

Tables A15 and A16 are a summary of test equations developed in the same manner as above. Since equation (Q3) establishes a linear relationship between  $A_{EQ2}$  and  $ACQ3$  and since  $A_{EQ2}$  needs to be computed as a step in the computation of  $AR3$ , the test equations for  $ACQ3$  will be performed implicitly by computing  $A_{EQ2}$  and comparing its computed value to C607 where C607 is defined as:

$$C607 = \frac{C_{405}}{(C_{404})(C_{606})}$$

Currents  $AC4$  and  $A_{EQ2}$  are computed using the applicable test condition equations.

Table A15 Valve Amplifier Operating Mode Test Equations

Circuit Condition, n	Applicable Equation (6a-Q2-n) (See Note)
1	$AEQ2 = -(EG - VC1) C456 - (VC3 + VC4) C457 + C458$
2	$AEQ2 = VC2 C461 - (EG - VC1) C459 - (VC3 + VC4) C460 + C462$
3	$AEQ2 = -(EG - VC1) C446 - (VC3 + VC4) C447 + C448$
4	$AEQ2 = VC2 C450 - (EG - VC1) C449 - (VC3 + VC4) C451 + C452$
5	$AEQ2 = -(EG - VC1) C531 + C532$
6	$AEQ2 = VC2 C533 - (EG - VC1) C534 - C535$
7	$AEQ2 = -(EG - VC1) C526 + C527$
8	$AEQ2 = VC2 C528 - (EG - VC1) C529 - C530$
9	$AEQ2 = -(EG - VC1) C565 - (VC2 + VC4) C566 + C567$
10	$AEQ2 = VC2 C568 - (EG - VC1) C569 - (VC2 + VC4) C570 - C571$
11	$AEQ2 = -(EG - VC1) C575 - (VC2 + VC4) C576 + C577$
12	$AEQ2 = VC2 C578 - (EG - VC1) C579 - (VC2 + VC4) C580 - C581$
<p>Notes:</p> <ol style="list-style-type: none"> <li>1. For circuit conditions 1, 2, 5, 6, 9 and 10 - if <math>AEQ2 &lt; 0</math>, set <math>AEQ2 = 0</math></li> <li>2. For circuit conditions 3, 4, 7, 8, 11 and 12 - if <math>AEQ2 &gt; C802</math>, set <math>AEQ2 = C802</math></li> </ol>	

Table A16 Capacitor C4 Current Mode Test Equations

Circuit Condition, n	Applicable Equation (6a-N8-n)
1 & 2	$AC4 = (AEQ2) C806 - (VC3 + VC4) C804 - C807$ $\text{IF } [(AEQ2) C806 - (VC3 + VC4) C804 - C807] > 0$
3 & 4	$AC4 = (AEQ2) C803 - (VC3 + VC4) C804 - C805$ $\text{IF } [(AEQ2) C803 - (VC3 + VC4) C804 - C805] > 0$
5 & 6	$AC4 = 0 \text{ IF } [(AEQ2) C806 - (VC3 + VC4) C804 - C807] \leq 0$ <p style="text-align: center;">AND</p> $[(AEQ2) C811 - (VC2 + VC4) C809 - C812] \geq 0$
7 & 8	$AC4 = 0 \text{ IF } [(AEQ2) C803 - (VC3 + VC4) C804 - C805] \leq 0$ <p style="text-align: center;">AND</p> $[(AEQ2) C808 - (VC2 + VC4) C809 - C810] \geq 0$
9 & 10	$AC4 = (AEQ2) C811 - (VC2 + VC4) C809 - C812$ $\text{IF } [(AEQ2) C811 - (VC2 + VC4) C809 - C812] < 0$
11 & 12	$AC4 = (AEQ2) C808 - (VC2 + VC4) C809 - C810$ $\text{IF } [(AEQ2) C808 - (VC2 + VC4) C809 - C810] < 0$

For the cases where  $AEQ2 > C607$  an upper limit must be established to represent saturation of the valve drive amplifier. This upper limit is called C802 and applies to the applicable circuit conditions noted on Table A15.

Table A17      Summary of Equations for Computing  
Current  $A_{05}$

Circuit Condition, n	Applicable Equation 6a-N5-n (See Note)
1 & 2	$A_{05} = A_{VAI} C_{606} - A_{C4}$
3 & 4	$A_{05} = A_{VAI} C_{606} C_{404} - C_{405} - A_{C4}$
5 & 6	$A_{05} = A_{VAI} C_{606}$
7 & 8	$A_{05} = A_{VAI} C_{606} C_{404} - C_{405}$
9 & 10	$A_{05} = A_{VAI} C_{606} - A_{C4}$
11 & 12	$A_{05} = A_{VAI} C_{606} C_{404} - C_{405} - A_{C4}$
Note: For all circuit conditions if $A_{05} < 0$ , set $A_{05} = 0$	

As shown on Figure A49 the locked wheel prevention circuit elements also have an input to the valve control amplifier. In the equations thus far it has been assumed that the locked wheel skid signal,  $ALWS$  at node (N15), is zero. When computing the valve voltage, it is necessary that the non-zero value of  $ALWS$  be accounted for. If  $ALWS$  is not zero then equation (Q3) is:

$$(Q3-1) \quad ACQ3 = C606 A_{EQ2} + hFE3 ALWS$$

Since  $ALWS$  is a two valued variable (i.e. either zero or the value required to drive the amplifier as necessary to achieve full brake release) insofar as valve voltage computation is concerned, it can be considered as a current which can be added to  $A_{EQ2}$  in Equation (Q3). If we define a current  $A_{VAI}$ , valve amplifier input current, as:

$$(LW-1) \quad A_{VAI} = A_{EQ2} + ALWS$$

and treat this current like  $A_{EQ2}$  in equation (Q3) and if we substitute equations (Q3) and (N7)" into equation (N5) an equation for computing  $A_{DS}$  is formulated for each circuit condition. Current  $A_{DS}$  is then used in equation (N4) to compute EV. Table A17 lists the version of equation (N5) which is to be used for computing current  $A_{DS}$  for each circuit condition.

Since the variables EG and VC1 are always used in the form of their difference, we will define the difference as equation (5)

$$(5) \quad EG - VC_1 = (E_G - V_{C_1})$$

For the cases where the antiskid control circuit mathematical model is used with the flywheel system or three dimensional airplane system, the flywheel velocity,  $V_F$ , or the airplane velocity,  $X$ , as applicable, will be used as the airplane speed reference circuit element. The wheel speed comparison element will be described as follows:

$$(6) \quad \begin{aligned} ALWS &= C617 \quad \text{FOR } V_F > C615 \text{ AND } E_G < C616 \\ &= 0 \quad \text{FOR } V_F \leq C615 \text{ OR } E_G \geq C616 \end{aligned}$$

Table A18      Modulated Antiskid Circuit Equation Summary  
(Sheet 1 of 2)

Equation No.	Equation
(6a-1)	$V_{C1} = \int \dot{V}_{C1} dt$
(6a-A1)	$\dot{V}_{C1} = A_{C1} C_{608}$
(6a-2)	$V_{C2} = \int \dot{V}_{C2} dt$
(6a-A2)	$\dot{V}_{C2} = A_{C2} C_{609}$
(6a-3)	$V_{C3} = \int \dot{V}_{C3} dt$
(6a-A3)	$\dot{V}_{C3} = A_{C3} C_{610}$
(6a-4)	$V_{C4} = \int \dot{V}_{C4} dt$
(6a-4A)	$\dot{V}_{C4} = A_{C4} C_{611}$
(6a-5)	$(E_G - V_{C1}) = E_G - V_{C1}$
(6a-6)	$A_{LWS} = \begin{cases} C_{617} & \text{FOR } V_F > C_{615} \text{ AND } E_G < C_{616} \\ 0 & \text{FOR } V_F \leq C_{615} \text{ OR } E_G \geq C_{616} \end{cases}$
(6a-LW-1)	$A_{VAI} = A_{EQ2} + A_{LWS}$
(6a-N3)	$A_{C3} = \begin{cases} A_{C4} - V_{C3} C_{619} - A_{BQ4} & \text{FOR } A_{C4} > 0 \\ -V_{C3} C_{619} - A_{BQ4} & \text{FOR } A_{C4} \leq 0 \end{cases}$
(6a-N4)	$E_V = A_{D5} C_{406} + C_{407}$
(6a-N5-n)	See Table A17
(6a-N8-n)	See Table A16

Table A18      Modulated Antiskid Circuit Equation Summary  
(Sheet 2 of 2)

Equation No.	Equation
(6a-N10)	$AR3 = AEQ2 C612 + [EV - (E6 - V61)] C613$
(6a-N11)	$AC1 = AD8 - AR3 - ACQ1$
(6a-N14)	$AC2 = \begin{cases} ABQ4 C614 + AC4 - VC2 C618 & \text{FOR } AC4 < 0 \\ ABQ4 C614 - VC2 C613 & \text{FOR } AC4 \geq 0 \end{cases}$
(6a-Q2-n)	See Table A15
(6a-Q-1C)	$ACQ1 = \begin{cases} C604 - C605 VC2 & \text{FOR } (E6 - V61) < 0 \\ 0 & \text{FOR } (E6 - V61) \geq 0 \\ 0 & \text{FOR } VC2 \geq C604 / C605 \end{cases}$
(6a-R10)	$AD8 = \begin{cases} (E6 - V61) C620 - C621 & \text{FOR } (E6 - V61) > C621 / C620 \\ 0 & \text{FOR } (E6 - V61) \leq C621 / C620 \end{cases}$
(6a-VB)	$VB = VC2 C_m + AEQ2 C801 - C800$
(6a-VQ4)	$ABQ4 = \begin{cases} (VC3 - VC2) C622 - C623 & \text{FOR } (VC3 - VC2) > C623 / C622 \\ 0 & \text{FOR } (VC3 - VC2) \leq C623 / C622 \end{cases}$

The conditions which define the circuit's mode of operation at a particular instant are: (1) the current,  $Ac_4$ , into capacitor  $C_4$  is either positive, negative or zero, (2) the valve control amplifier is operating either in the cutoff mode or in the amplification mode, and (3) the modulating circuit element is either providing a pressure bias signal or it is not. The valve amplifier condition is indicated by current  $Aeq_2$  being equal to or less than C607 in the cutoff mode and being greater than C607 in the amplification mode. The pressure bias signal is indicated as existing when voltage  $V\theta$  is greater than zero and as not existing when  $V\theta$  is equal to or less than zero.

Table A18 summarizes the modulated antiskid circuit equations and the equation flow diagram is shown on Figure A52.

#### B. Parameter Evaluation

Table A19 lists the parameters defining the modulated circuit's operation. The values for the constants are computed from various circuit element characteristics (resistance, capacitance, etc.) as described in reference 13 and in the semiconductor component manufacturers catalogs.

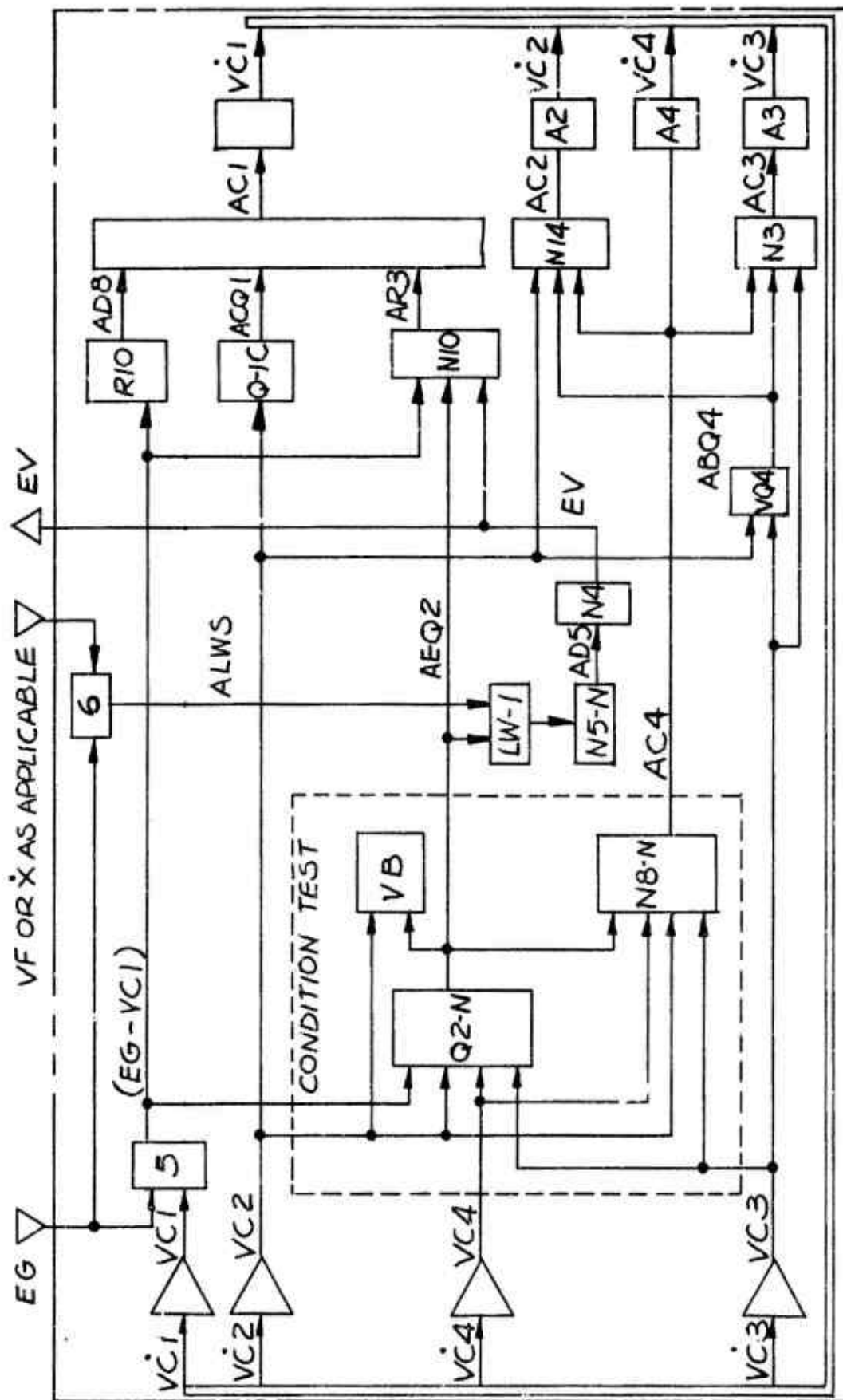


Figure A52 Modulated Antiskid Circuit Equation Flow Diagram

Table A19 Modulated Control System Parameters

(Sheet 1 of 4)

Symbol	Type	Value	Units	Description (See Note)
ABQ4	V		Amps	Transistor Q4 Base Current
Ac1	V		Amps	Current thru Capacitor C1
Ac2	V		Amps	Current thru Capacitor C2
Ac3	V		Amps	Current thru Capacitor C3
Ac4	V		Amps	Current thru Capacitor C4
Acq1	V		Amps	Transistor Q1 Collector Current
Ad5	V		Amps	Current thru Diode D5
Ad8	V		Amps	Current thru Diode D8
Aeq2	V		Amps	Transistor Q2 Emitter Current
Aeq4	V		Amps	Transistor Q4 Emitter Current
AR3	V		Amps	Current thru Resistor R3
EG	V(I)		Volts	Input Signal from Wheel Speed Sensor
V8	V		Volts	Circuit Condition Determination Voltage
Vc1	V		Volts	Voltage Across Capacitor C1
Vc10	C	12.08	Volts	Voltage across Capacitor C1 at Time Zero
Vc2	V		Volts	Voltage across Capacitor C2
Vc20	C	0.0	Volts	Voltage across Capacitor C2 at Time Zero
Vc3	V		Volts	Voltage across Capacitor C3
Vc30	C	0.0	Volts	Voltage across Capacitor C3 at Time Zero
Vc4	V		Volts	Voltage across Capacitor C4
Vc40	C	0.0	Volts	Voltage across Capacitor C4 at Time Zero
Ev	V(O)		Volts	Antiskid Valve Voltage
ALws	V		Amps	Locked Wheel Skid Signal
Vf	V(I)		In/Sec	Flywheel Velocity
Cm	C	0.23	Dimls	VG2 Voltage Coefficient EQU VB-n
N	V		Dimls	Circuit Condition Number, Integer 1-12

Note: All equation numbers in Description are preceded by 6a. For example, EQU VB-n means equations number 6a-VB-n.

Table A19 Modulated Control System Parameters

(Sheet 2 of 4)

Symbol	Type	Value	Units	Description (See Note page )
C404	c	2476.0	Dimls	ACQ3 Coeff. EQU N7, N5-3-4, N5-7-8, N5-11-12
C405	c	0.106	Amps	Const EQU N7, N5-3-4, N5-78, N5-11-12
C406	c	66.0	Ohms	AD5 Coefficient EQU N4
C407	c	1.51	Volts	Const. EQU N4
C446	c	$1.825 \times 10^{-6}$	Mhos	(EG-VCL) Coefficient EQU Q2-3
C447	c	$0.144 \times 10^{-8}$	Mhos	(VC3 + VC4) Coefficient EQU Q2-3
C448	c	$0.465 \times 10^{-6}$	Amps	Const EQU Q2-3
C449	c	$1.86 \times 10^{-6}$	Mhos	(EG-VCL) Coefficient EQU Q2-4
C450	c	$0.474 \times 10^{-6}$	Mhos	VC2 Coefficient EQU Q2-4
C451	c	$0.144 \times 10^{-8}$	Mhos	(VC3 + VC4) Coefficient EQU Q2-4
C452	c	$-1.567 \times 10^{-6}$	Amps	Const EQU Q2-4
C456	c	$34.0 \times 10^{-6}$	Mhos	(EG-VCL) Coefficient EQU Q2-1
C457	c	$0.027 \times 10^{-6}$	Mhos	(VC3 + VC4) Coefficient EQU Q2-1
C458	c	$-17.1 \times 10^{-6}$	Amps	Const EQU QL-1
C459	c	$52.0 \times 10^{-6}$	Mhos	(EG-VCL) Coefficient EQU Q2-2
C460	c	$0.027 \times 10^{-6}$	Mhos	(VC3 + VC4) Coefficient EQU Q2-2
C461	c	$13.25 \times 10^{-6}$	Mhos	VC2 Coefficient EQU Q2-2
C462	c	$-83.4 \times 10^{-6}$	Amps	Const EQU Q2-2
C526	c	$1.825 \times 10^{-6}$	Mhos	(EG-VCL) Coefficient EQU Q2-7
C527	c	$0.465 \times 10^{-6}$	Amps	Const EQU Q2-7
C528	c	$0.474 \times 10^{-6}$	Mhos	VC2 Coefficient EQU Q2-8
C529	c	$1.86 \times 10^{-6}$	Mhos	(EG-VCL) Coefficient EQU Q2-8
C530	c	$1.567 \times 10^{-6}$	Amps	Const. EQU Q2-8
C531	c	$34.0 \times 10^{-6}$	Mhos	(EG-VCL) Coefficient EQU Q2-5
C532	c	$-17.1 \times 10^{-6}$	Amps	Const. EQU Q2-5
C533	c	$13.25 \times 10^{-6}$	Mhos	VC2 Coefficient EQU Q2-6
C534	c	$52.0 \times 10^{-6}$	Mhos	(EG-VCL) Coefficient EQU Q2-6
C535	c	$83.4 \times 10^{-6}$	Amps	Const. EQU Q2-6
C56	c	$34.0 \times 10^{-6}$	Mhos	(EG-VCL) Coefficient EQU Q2-9

Table A19 Modulated Control System Parameters

(Sheet 3 of 4)

Symbol	Type	Value	Units	Description (See Note page )
C566	c	$0.014 \times 10^{-6}$	Mhos	(VC2 + VC4) Coefficient EQU Q2-9
C567	c	$-17.1 \times 10^{-6}$	Amps	Const. EQU Q2-9
C568	c	$13.25 \times 10^{-6}$	Mhos	VC2 Coefficient EQU Q2-10
C569	c	$52.0 \times 10^{-6}$	Mhos	(EG-VC1) Coefficient EQU Q2-10
C570	c	$0.014 \times 10^{-6}$	Mhos	(VC2 + VC4) Coefficient EQU Q2-10
C571	c	$66.5 \times 10^{-6}$	Amps	Const. EQU Q2-10
C575	c	$1.825 \times 10^{-6}$	Mhos	(EG-VC1) Coefficient EQU Q2-11
C576	c	$0.001 \times 10^{-6}$	Mhos	(VC2 + VC4) Coefficient EQU Q2-11
C577	c	$0.465 \times 10^{-6}$	Amps	Const. EQU Q2-11
C578	c	$0.474 \times 10^{-6}$	Mhos	VC2 Coefficient EQU Q2-12
C579	c	$1.86 \times 10^{-6}$	Mhos	(EG-VC1) Coefficient EQU Q2-12
C580	c	$0.001 \times 10^{-6}$	Mhos	(VC2 + VC4) Coefficient EQU Q2-12
C581	c	$-1.567 \times 10^{-6}$	Amps	Const. EQU Q2-12
C604	c	$16.1 \times 10^{-6}$	Amps	Const. EQU Q-1C
C605	c	$7.25 \times 10^{-6}$	Mhos	VC2 Coefficient EQU Q-1C
C606	c	29.2	Dimensionless	Q3 Collector - Q2 Emitter Current Ratio
C607	c	$1.46 \times 10^{-6}$	Amps	AEQ2 Comparison Constant
C608	c	$0.037 \times 10^{-6}$	Volts/Amp Sec	Reciprocal of Capacitance C1
C609	c	$3.03 \times 10^{-6}$	Volts/Amp Sec	Reciprocal of Capacitance C2
C610	c	$0.833 \times 10^{-5}$	Volts/Amp Sec	Reciprocal of Capacitance C3
C611	c	$0.222 \times 10^{-6}$	Volts/Amp Sec	Reciprocal of Capacitance C4
C612	c	0.901	Dimensionless	AEQ2 Coefficient EQU N10
C613	c	$5.19 \times 10^{-6}$	Mhos	EV-(EG-VC1) Coefficient EQU N10
C614	c	36.0	Dimensionless	ABQ4 Coefficient EQU N14 - Q4
C615	c	352.0	In/Sec	Locked Wheel Arming Speed
C616	c	0.92	Volts	Locked Wheel Signal Detection Speed
C617	c	$3.76 \times 10^{-6}$	Amps	Locked Wheel Signal Current
C618	c	$7.7 \times 10^{-6}$	Mhos	VC2 Coefficient EQU N14
C619	c	$7.7 \times 10^{-6}$	Mhos	VC3 Coefficient EQU N3

Table A19 Modulated Control System Parameters (Sheet 4 of 4)

Symbol	Type	Value	Units	Description (See Note page )
C620	c	0.001	Mhos	(EG-VC1) Coefficient EQU R10
C621	c	$600.0 \times 10^{-6}$	Amps	Const. EQU R10
C622	c	$846.0 \times 10^{-6}$	Mhos	(VC3-VC2) Coefficient EQU VQ4
C623	c	$593.0 \times 10^{-6}$	Amps	Const. EQU VQ4
C800	c	0.994	Volts	Constant EQU VB
C801	c	9167	Ohms	AEQ2 Coefficient EQU VB
C802	c	$4.29 \times 10^{-6}$	Amps	Maximum Value for AEQ2 in EQU-Q2-N
C803	c	536.2	Dimls	AEQ2 Coefficient EQU N8-3, 4, 7 & 8
C804	c	$109.1 \times 10^{-6}$	Mhos	(VC3 + VC4) Coefficient EQU N8-1,2,3,4,5,6,7,8
C805	c	$552.0 \times 10^{-6}$	Amps	Constant EQU N8-3, 4, 7 & 8
C806	c	0.2166	Dimls	AEQ2 Coefficient EQU N8-1, 2, 5 & 6
C807	c	$-230.4 \times 10^{-6}$	Amps	Constant EQU N8-1, 2, 5 & 6
C808	c	222.8	Dimls	AEQ2 Coefficient EQU N8-7, 8, 11 & 12
C809	c	$4.53 \times 10^{-6}$	Mhos	(VC2 + VC4) Coefficient EQU N8-5, 6, 7, 8, 9, 10, 11 & 12
C810	c	$175.8 \times 10^{-6}$	Amps	Constant EQU N8-7, 8, 11 & 12
C811	c	0.090	Dimls	AEQ2 Coefficient EQU N8-5, 6, 9 & 10
C812	c	$-150.1 \times 10^{-6}$	Amps	Constant EQU N8-5, 6, 9 & 10
N0	c	1	Dimls	Circuit Condition at Time Zero
VC1	v		Volts/Sec	Capacitor C1 Voltage Change Rate
VC10	c	0.0	Volts/Sec	Capacitor C1 Voltage Change Rate at Time Zero
VC2	v		Volts/Sec	Capacitor C2 Voltage Change Rate
VC20	c	0.0	Volts/Sec	Capacitor C2 Voltage Change Rate at Time Zero
VC3	v		Volts/Sec	Capacitor C3 Voltage Change Rate
VC30	c	0.0	Volts/Sec	Capacitor C3 Voltage Change Rate at Time Zero
VC4	v		Volts/Sec	Capacitor C4 Voltage Change Rate
VC40	c	0.0	Volts/Sec	Capacitor C4 Voltage Change Rate at Time Zero

## 6b. ON-OFF ANTISKID CONTROL CIRCUIT

Most aircraft on-off type antiskid systems operate according to the functional block diagram shown on Figure A53. The various functional elements may be electrical, mechanical or a combination of electrical and mechanical devices. If during braking the brake torque applied to the wheel exceeds the amount which can be reacted by friction at the tire-ground interface, the antiskid system operates to prevent tire skids as follows. A wheel speed signal is provided to a deceleration detection element where the wheel's deceleration rate is computed and compared to a threshold value which is provided by a skid detection threshold element. The deceleration detector produces a skid signal whenever the wheel's deceleration rate exceeds the threshold value. The wheel speed signal is also supplied to a wheel speed reference element and a wheel speed comparison element. The wheel speed reference element is a "memory" device which produces a "comparison index." The "comparison index" is the wheel's initial unbraked speed minus an adjustment to account for the aircraft's deceleration. The wheel speed comparison element compares wheel speed to the "comparison index" and produces a skid signal whenever the wheel speed is less than the "comparison index." The deceleration detection element initiates a skid signal and the wheel speed comparison element maintains the skid signal until the wheel has regained most of its initial speed. The skid signals from both the deceleration detection element and the wheel speed comparison element are transmitted to a valve control element which acts to control the antiskid valve such that the brake is released when a skid signal exists and the brake is applied when a skid signal does not exist.

An electrical system of the form shown on Figure A54 or a mechanical device as shown on Figure A56 are the most common means used for implementing the on-off antiskid system function.

### Electrical On-Off Antiskid System

Figure A54 is a schematic diagram of the Goodyear electrical on-off antiskid control circuit as used on the Lockheed F104 and General Dynamics B-58 aircraft. This circuit accomplishes on-off antiskid control according to the preceding functional description as follows: The wheel speed

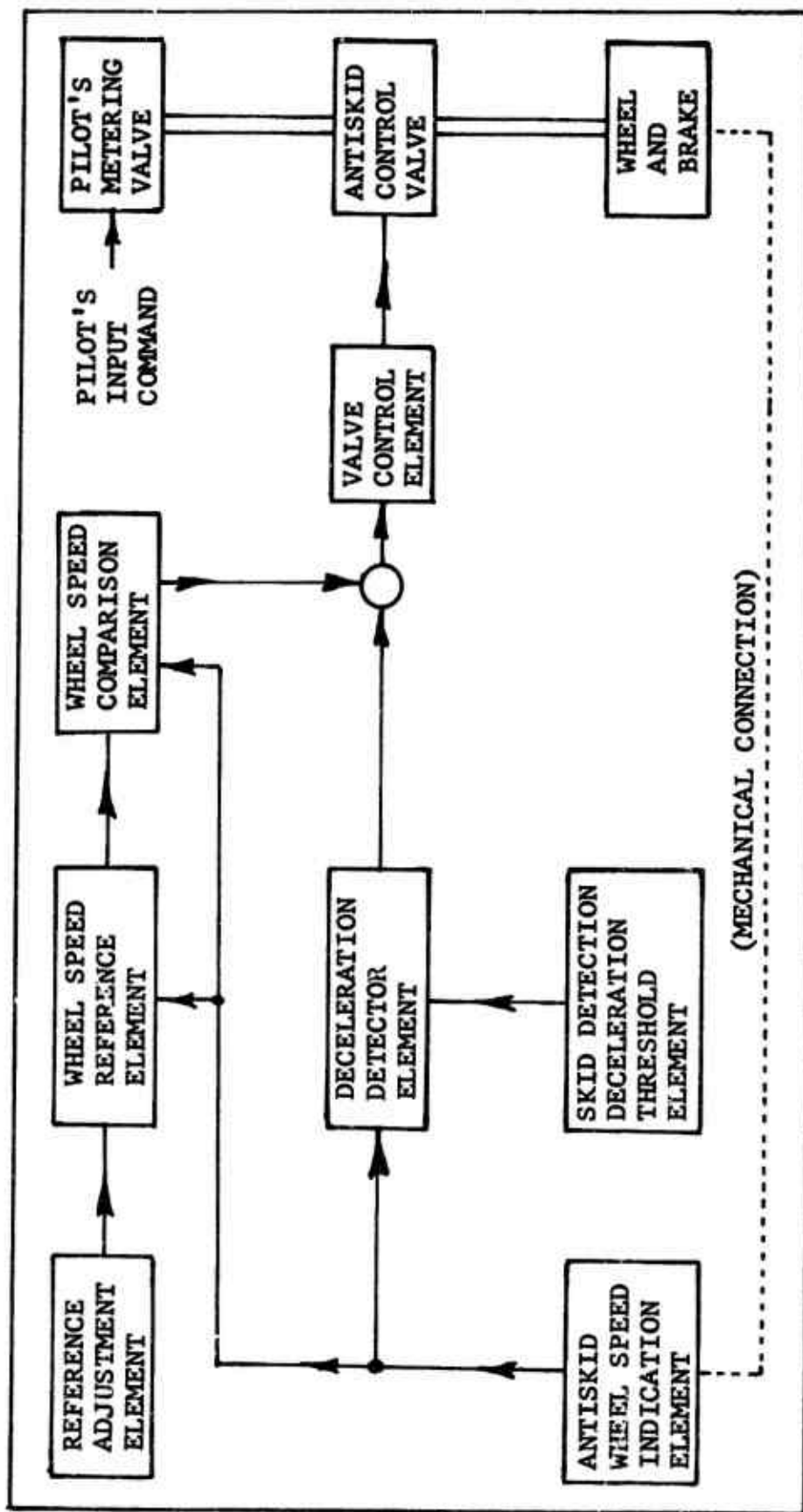
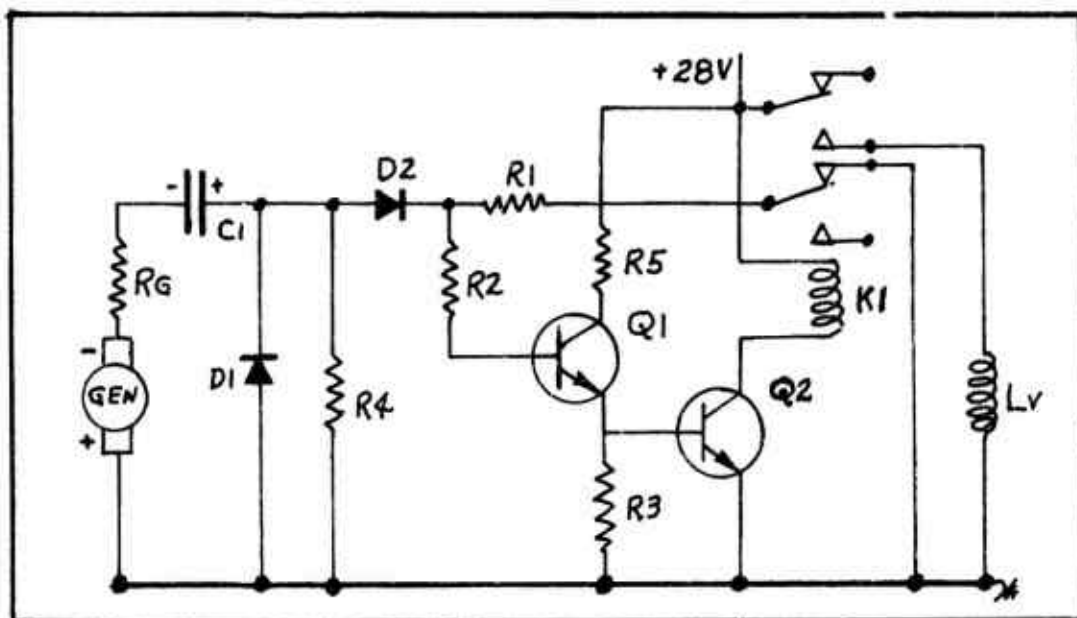
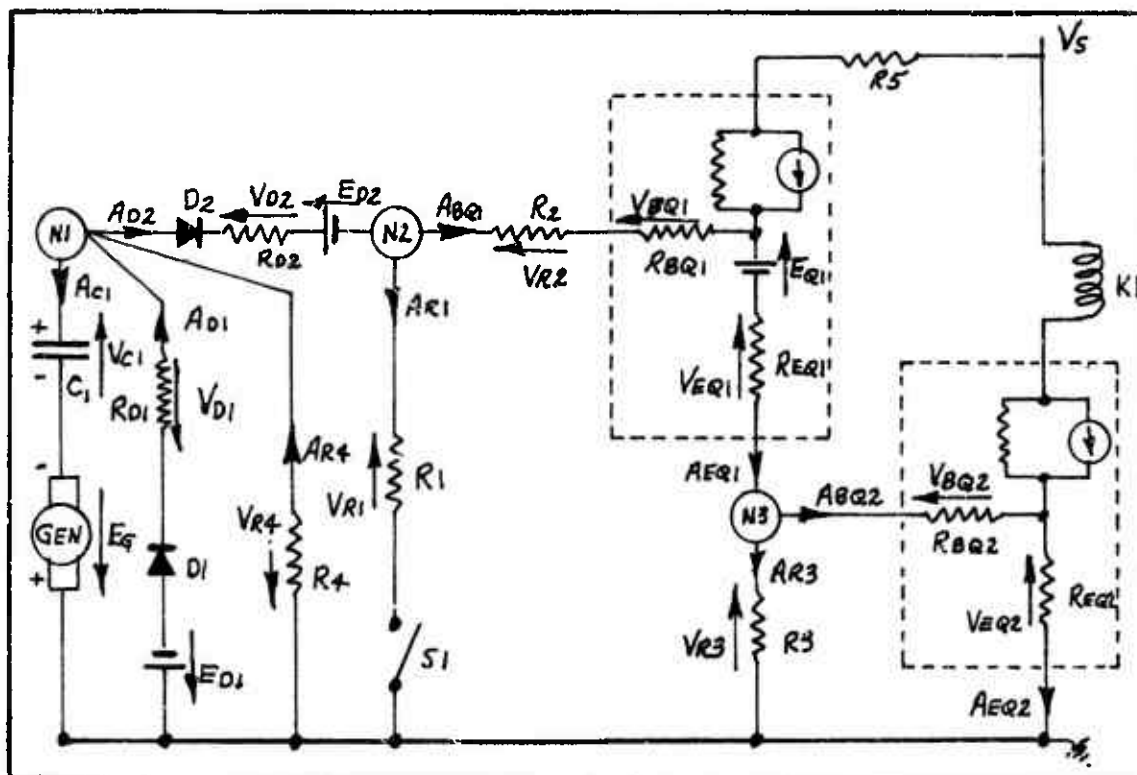


Figure A53 On-Off Antiskid Control Functional Block Diagram



(A) Schematic Diagram



(B) Mathematical Identification Showing Transistors and Diodes in Terms of their Equivalent Circuits

Figure A54 Electrical On-Off Antiskid Control Circuit

indication element, a wheel driven D. C. tachometer generator (GEN), supplies an input voltage EG which is proportional to wheel speed. EG charges capacitor C1 through R5, Diode D1 and Resistance RG during wheel spin-up. Capacitor C1 is both the deceleration detector and the wheel speed reference element. For normal wheel deceleration rates, with no incipient skidding, the generator voltage decreases relatively slowly and a small current will flow from the positive side of C1 through R5 and through D2 and R1, (GEN) and RG to the negative side of C1. This current discharges C1 and causes its voltage to closely follow EG. The amplifier comprised of R2, Q1, R3, R4 and Q2 acts as the skid detection deceleration threshold element, the wheel speed comparison element, and, in conjunction with relay K1, the valve control element. When an incipient skid occurs, the generator voltage decreases rapidly. R5 and R1 limit the discharge current flow into C1 so that the voltage at the positive side of C1 increases. The value of the voltage at the positive side of C1 is proportional to wheel deceleration rate. The amplifier characteristics are set so that when the voltage at the positive side of C1 is a value  $V_{SDT}$  or greater, enough current flows into the base of Q1 to cause Q2 to conduct sufficiently for relay K1 to actuate. When relay K1 actuates the supply voltage is applied to the antiskid valve coil LV. The voltage across the antiskid valve coil, EV, is equal to the supply voltage. Actuation of relay K1 also causes R1 to be disconnected from ground so that the resistance in the discharge path of C1 is increased to aid its action as a wheel speed reference. Voltage  $V_{SDT}$  is the skid detection threshold. More modern versions of this circuit utilize transistors to perform the function of relay K1; however, their operation is the same. Resistor R5 is the speed reference adjustment element.

## A-1 Electrical On-Off Mathematical Description

The mathematical description of the electrical circuit's operation is developed from Figure A54(b) which is the schematic from Figure A54(a) with the transistors and diodes shown in terms of their equivalent circuits and the appropriate currents and voltages identified.

The voltage across capacitor C1 is defined by:

$$(6b-1-1) \quad V_{C1} = \int V_{C1} dt$$

$$\text{where (6b-1-A1)} \quad \dot{V}_{C1} = A_{C1} C_{705} \quad (C_{705} = 1/C_1)$$

Current AC1 is established by summing currents at node (N1) as:

$$(6b-1-N1) \quad A_{C1} = A_{D1} + A_{R4} - A_{D2}$$

Using Ohm's law and summing voltages around the loop of which RD1 is a part, current AD1 is established as:

$$(6b-1-R1) \quad A_{D1} = \frac{E_G - V_{C1} - E_{D1}}{R_{D1}} \quad \text{FOR } (E_G - V_{C1} - E_{D1}) > 0$$

$$= 0 \quad \text{FOR } (E_G - V_{C1} - E_{D1}) \leq 0$$

To combine constants, write equation (6b-1-R1) as:

$$A_{D1} = (E_G - V_{C1}) C_{706} - C_{707} \quad \text{FOR } (E_G - V_{C1}) > \frac{C_{707}}{C_{706}}$$

$$= 0 \quad \text{FOR } (E_G - V_{C1}) \leq \frac{C_{707}}{C_{706}}$$

Noting that because of diode D1,  $A_{D1}$  is restricted to positive values only.

In a similar manner, using Ohm's law and summing voltages around the loop containing R4, current AR4 is established as:

$$(6b-1-V2) \quad A_{R4} = (E_G - V_{C1}) / R_4 \quad \text{OR} \quad A_{R4} = (E_G - V_{C1}) C_{708}$$

Summing currents at node N2 and noting that because of diode D2, current AD2 cannot be negative gives:

$$\begin{aligned} (6b-1-N2) \quad A_{D2} &= A_{BQ1} + A_{R1} && \text{FOR } (A_{BQ1} + A_{R1}) \geq 0 \\ &= 0 && \text{FOR } (A_{BQ1} + A_{R1}) < 0 \end{aligned}$$

By Ohm's law the voltage across RD2 is

$$(6b-1-V3) \quad V_{D2} = A_{D2} R_{D2}$$

For the case where no skid signal exists and relay K1 is not actuated, R1 is connected to ground and a current AR1 may flow. Using Ohm's law and by summing voltages around the loop R1, D2, C1 and (GEN), AR1 is established as:

$$(6b-1-V4) \quad A_{R1} = (V_{C1} - E_G - E_{D2} - V_{D2}) / R_1$$

Since the variables EG and VC1 are always used in the form of their difference, define the difference as:

$$(6b-1-3) \quad (E_G - V_{C1}) = E_G - V_{C1}$$

By substituting (6b-1-V3) and (6b-1-N2) into (6b-1-V4),

$$(6b-1-V4)' \quad A_{R1} = \frac{(V_{C1} - E_G - E_{D2})}{R_{D2} + R_1} - \frac{A_{BQ1} R_{D2}}{R_{D2} - R_1}$$

By summing currents at node (N3), current AEQ1 is

$$(6b-1-N3) \quad A_{EQ1} = A_{BQ2} + A_{R3}$$

By summing voltages around the loop containing R3 and the base and emitter of Q2,

$$(6b-1-V5) \quad 0 = V_{R3} - V_{BQ2} - V_{EQ2}$$

Note: For Q2 the base-emitted junction potential has been omitted to reduce mathematical complexity. This is justified because whether or not Q2 is conducting has negligible effect on current  $A_{C1}$ .

By substituting (6b-1-N3) along with the Ohm's law expressions  $A_{BQ2} = V_{BQ2}/R_{BQ2}$  AND  $A_{EQ2} = V_{EQ2}/R_{EQ2}$  and the transistor characteristic  $A_{EQ2} = (h_{FE2} + 1) A_{BQ2}$  into (6b-1-V5) and solving for  $A_{BQ2}$ ,

$$(6b-1-V5)' \quad A_{BQ2} = \frac{A_{EQ1} R_3}{R_{BQ2} + R_3 + R_{EQ2} (h_{FE2} + 1)}$$

By substituting (6b-1-V5)' and (6b-1-N3) into the Ohm's law expression  $V_{R3} = A_{R3} R_3$

$$(6b-1-2) \quad V_{R3} = R_3 A_{EQ1} \left[ 1 - \frac{R_3}{R_{BQ2} + R_3 + R_{EQ2} (h_{FE2} + 1)} \right]$$

By summing voltages around the loop R3, REQ1, EQ1, RBQ1, R2, RD2, C1 and (GEN)

$$(6b-1-V6) \quad 0 = V_{R3} + V_{EQ1} + E_{Q1} + V_{BQ1} + V_{R2} + E_{D2} + V_{D2} - V_{C1} + E_G$$

By substituting (6b-1-2) and (6b-1-V4) along with the Ohm's law expressions  $V_{EQ1} = A_{EQ1} R_{EQ1}$ ,  $V_{BQ1} = A_{BQ1} R_{BQ1}$  and  $V_{R2} = A_{BQ1} R_2$  and the transistor characteristic  $A_{EQ1} = (h_{FE1} + 1) A_{BQ1}$  into (6b-1-V6) and solving for  $A_{BQ1}$ :

$$(6b-1-V6)' \quad A_{BQ1} = (V_{C1} - E_G) \frac{C_{701} - C_{702}}{C_{701}} \quad \text{FOR } (V_{C1} - E_G) > \frac{C_{702}}{C_{701}}$$

$$= 0 \quad \text{FOR } (V_{C1} - E_G) \leq \frac{C_{702}}{C_{701}}$$

For the case where relay K1 is actuated and R1 is disconnected from ground the same substitution is made except that  $V_{D2} = A_{BQ1} R_{D2}$  is used in place of equation (6b-1-V4). For the actual circuit components used on the aircraft, the resulting equation has coefficients that are negligibly different from (6b-1-V6)'; therefore, equation

(6b-1-V6)' will be used for both cases.

The value of  $ABQ_1$  which causes relay K1 to be actuated is defined as, C700, the skid detection threshold current. From this definition and equation (6b-1-V4)'

$$\begin{aligned} (6b-1-V4-1) \quad AR_1 &= (V_C - E_S) C_{709} - C_{710} - ABQ_1 C_{711} \\ &\quad \text{FOR } ABQ_1 < C_{700} \\ &= 0 \quad \text{FOR } ABQ_1 \geq C_{700} \end{aligned}$$

When relay K1 is not actuated  $EV = 0$ , when relay K1 is actuated  $EV = VS$ ; therefore,

$$\begin{aligned} (6b-1-EV) \quad EV &= 0 \quad \text{FOR } ABQ_1 < C_{700} \\ &= VS \quad \text{FOR } ABQ_1 \geq C_{700} \end{aligned}$$

The equation flow diagram for the electrical on-off control circuit is shown on Figure A55.

#### B-1 Electrical On-Off Parameter Evaluation

Table A20 lists the parameters and their values as applicable for the General Dynamics B-58 control circuit. (The same circuit is used on the Lockheed F-104.)

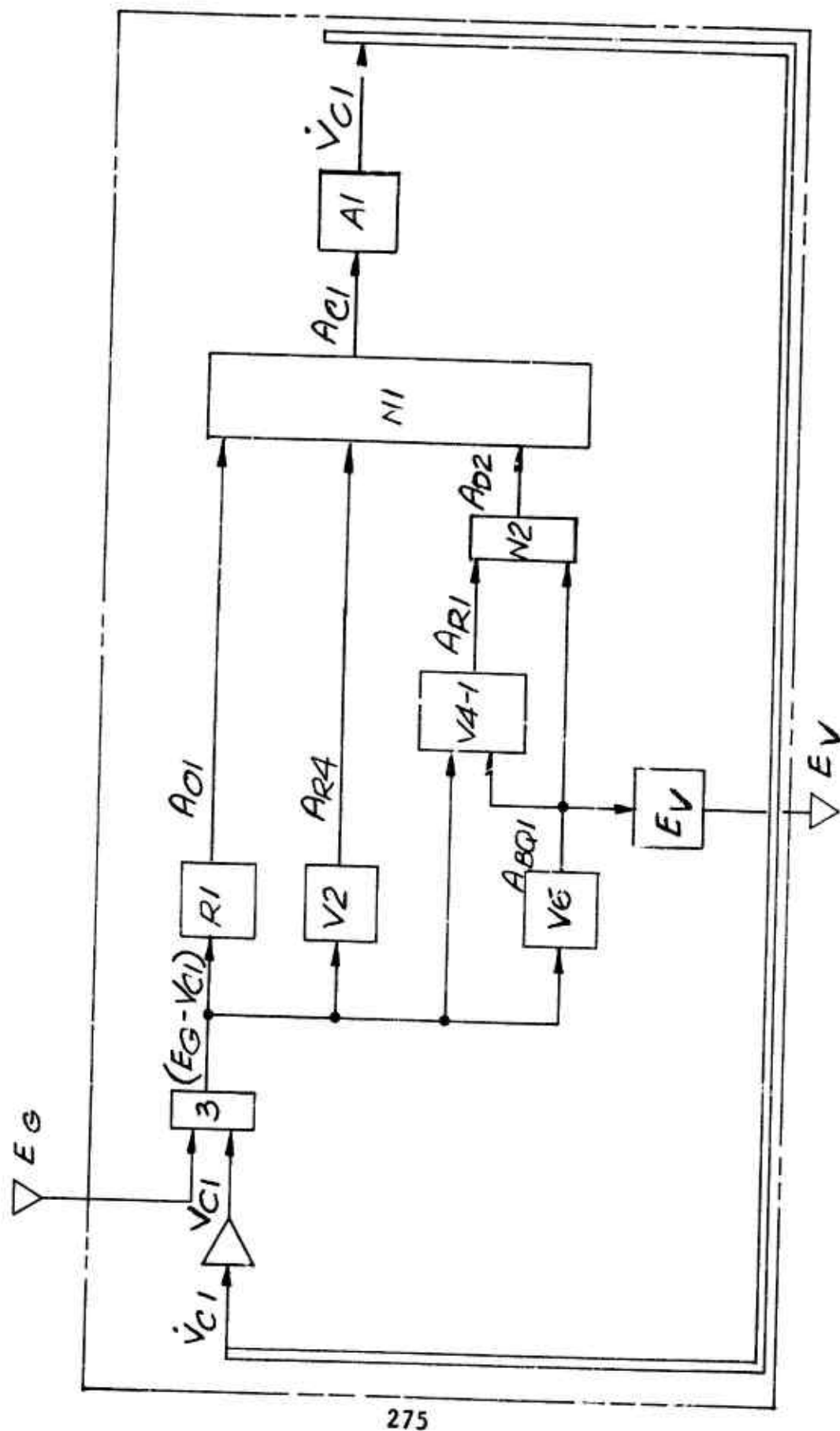


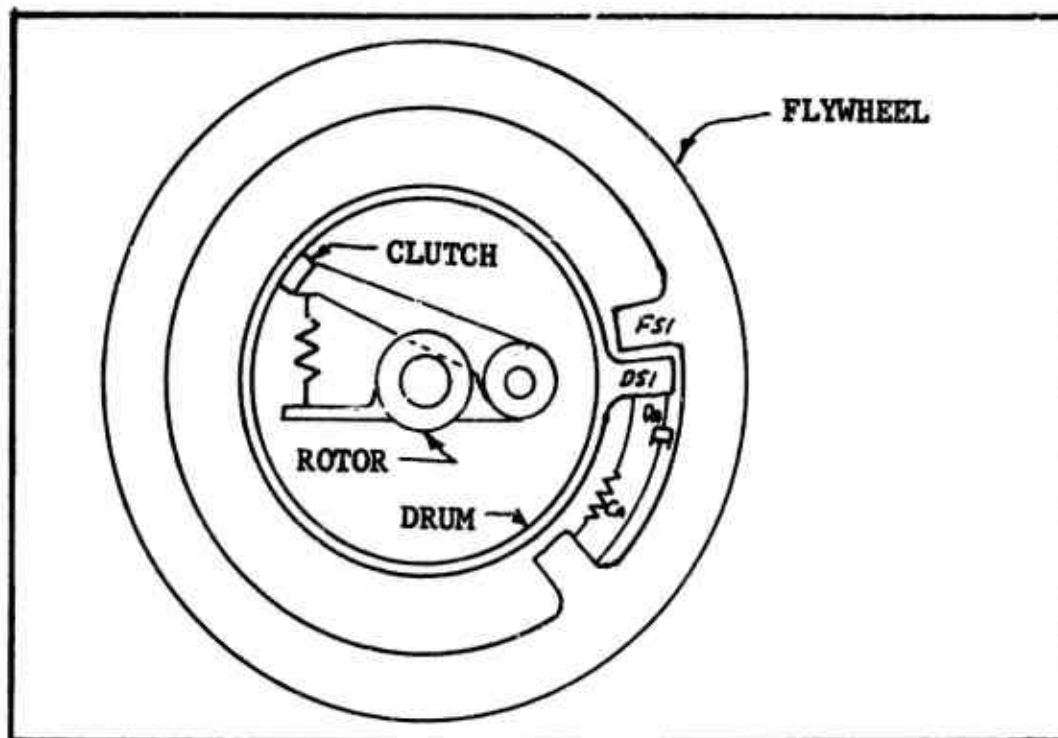
Figure A55 Electrical On-Off Circuit Equation Flow Diagram

Table A20 On-Off Control System Parameters

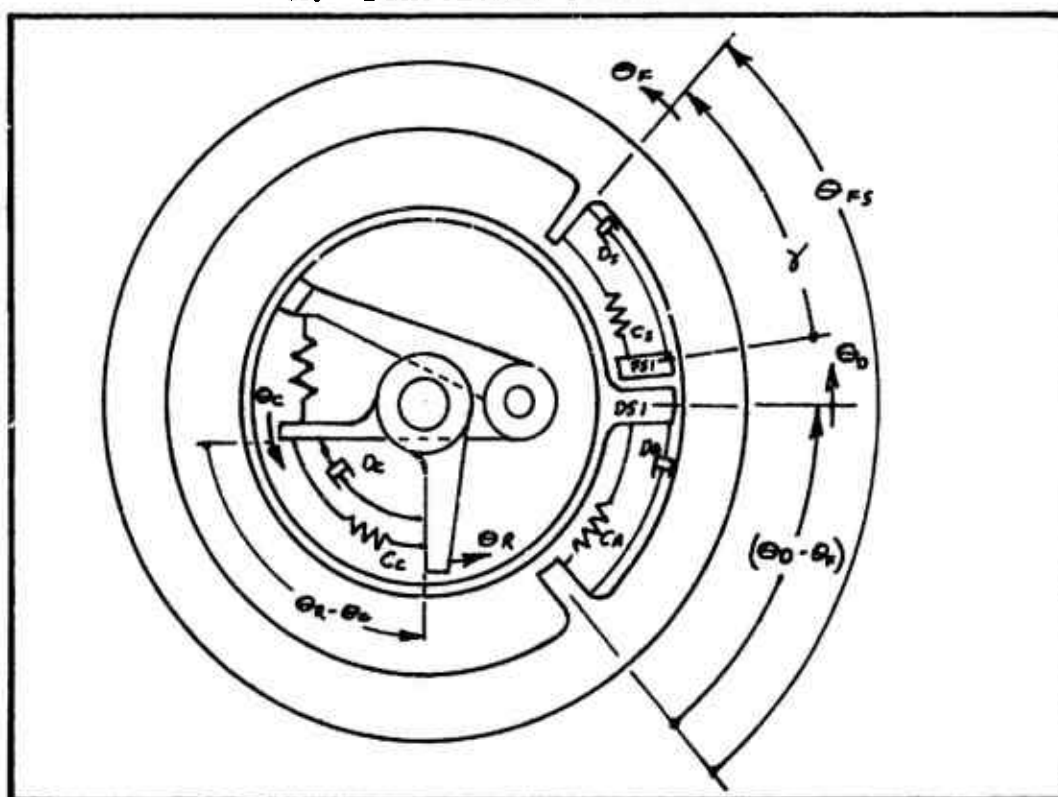
Symbol	Type	Value	Units	Description
ABQ1	V		Amps	Transistor Q1 Base Current
AC1	V		Amps	Current thru Capacitor C1
AD1	V		Amps	Current thru Diode D1
AR1	V		Amps	Current thru Resistor R1
AR4	V		Amps	Current thru Resistor R4
EG	V(I)		Volts	Input Signal from Wheel Speed Sensor
EV	V(C)		Volts	Antiskid Valve Voltage
VC1	V		Volts	Voltage across Capacitor C1
VC10	C	0.0	Volts	Voltage across Capacitor C1 at Time Zero
VC1	V		Volts/Sec	Capacitor C1 Voltage Change Rate
V5	C	28.0	Volts	Supply Voltage
C700	C	$17.5 \times 10^{-6}$	Amps	Skid Detection Threshold Current
C701	C	$6.6 \times 10^{-6}$	Mhos	(EG - VC1) Coefficient EQU V6
C702	C	$0.86 \times 10^{-6}$	Amps	Constant EQU V6
C705	C	$0.04 \times 10^{-6}$	Volt/Amp Sec	Reciprocal of Capacitance C1
C706	C	$1667.0 \times 10^{-6}$	Mhos	(EG - VC1) Coefficient EQU R1
C707	C	$1000.0 \times 10^{-6}$	Amps	Constant EQU R1
C708	C	$19.35 \times 10^{-6}$	Mhos	(EG-VC1) Coefficient EQU V2
C709	C	$161 \times 10^{-6}$	Mhos	(EG-VC1) Coefficient EQU V4-1
C710	C	$96.8 \times 10^{-6}$	Amps	Constant EQU V4-1
C711	C	0.0968	Dimls	ABQ1 Coefficient EQU V4-1

## Mechanical On-Off Antiskid Device

Figure A56 is a schematic drawing showing the operating principles of a commonly used mechanical on-off antiskid device of which the Hydroaire Hytrol Mk I and Dunlop Maxaret units are typical examples. The device operates as follows. The rotor (the wheel speed indication element) is connected to the aircraft wheel by some positive means such as a direct connection or gear train, etc., so that the rotor's angular velocity is a constant ratio of aircraft wheel speed. During spinup the motion of the rotor is transmitted through the clutch to the drum. The clutch is configured such that it is self-energizing for rotation in the direction of wheel rotation associated with forward airplane motion, shown here as counterclockwise. Stop (DS1) on the drum engages stop (FS1) on the flywheel, thereby transmitting torque to cause the velocity of the flywheel to be the same as the drum. The flywheel and the drum are connected by spring (CA) and damper (DA). As the aircraft wheel and rotor decelerate, a clockwise torque is transmitted through the clutch to the drum and from the drum through spring (CA) and damper (DA) to the flywheel. The amount of this torque is proportional to the product of the rotor's deceleration rate and the flywheel's inertia. The torque compresses spring (CA) so that the flywheel moves counterclockwise with respect to the drum. For steady airplane wheel deceleration the amount of relative motion between the flywheel and drum is proportional to the deceleration rate. A suitable mechanism (usually a set of electrical contact points or a cam device) connected between the flywheel and drum causes a valve to be actuated so that brake pressure is relieved whenever a pre-established amount of relative motion occurs. The clutch is also configured so that when the torque from the rotor to the drum is clockwise, the torque capacity is limited to some slightly greater amount than that required to initiate brake release. If the rotor experiences greater deceleration than that required to initiate brake release, the clutch slips and allows the drum and flywheel to overrun the rotor. The flywheel's inertia reacted by the drag of the clutch maintains a torque on spring (CA) so that the relative motion between the drum and flywheel (skid signal) is sustained until the flywheel's kinetic energy is dissipated or until the rotor has regained sufficient speed to eliminate clutch slippage. For this device the flywheel's inertia causing displacement of spring (CA) and damper (DA) is the



A. Functional Schematic



B. Mathematical Representation

Figure A56 Mechanical On-Off Antiskid Device

deceleration detector element, the clutch's overrunning drag torque on the drum is the reference adjustment element, the clutch is the wheel speed comparison element and the rotational kinetic energy of the flywheel is the wheel speed reference element.

## A-2 Mechanical On-Off Mathematical Description

The mathematical description of the mechanical on-off anti-skid device is developed by referring to figure A56(B) which defines the applicable parameters and shows flywheel stop (FS1) represented by a spring-damper system. Also, a spring-damper system is added between the rotor and clutch carrier to represent the small motion which actually occurs during clutch operation.

At flywheel stop (FS1) there is a torque,  $T_S$ , which is exerted on the flywheel by the drum, if drum stop (DS1) is in contact with FS1. If the mass of FS1 is considered small in comparison to the stop spring (CS) and stop damper (DS) then, setting the sum of torques on FS1 at zero:

$$(6b-2-1) \quad T_S = C_S (\gamma_0 - \gamma) - D_S \dot{\gamma}$$

Where  $C_S(\gamma_0 - \gamma)$  is the stop spring torque,  $(-D_S \dot{\gamma})$  is the stop damper torque and  $\gamma_0$  is the free length of spring CS.

Since  $T_S$  results from a contact force, it cannot be less than zero; therefore, if  $\gamma + (\theta_0 - \theta_F)$  is less than  $\theta_{FS}$  then  $T_S = 0$ . Rewriting equation (1) solving for  $\dot{\gamma}$  gives:

$$(6b-2-2) \quad \dot{\gamma} = (C_S (\gamma_0 - \gamma) - T_S) / D_S$$

$\gamma$  is then established by:

$$(6b-2-3) \quad \gamma = \int \dot{\gamma} dt$$

$\gamma$  as computed from (6b-2-2) and (6b-2-3) is compared to  $\theta_{FS} - (\theta_0 - \theta_F)$  to establish TS. If TS is other than zero, it is computed from (6b-2-1) using  $\gamma = \theta_{FS} - (\theta_0 - \theta_F)$  AND  $\dot{\gamma} = -(\dot{\theta}_0 - \dot{\theta}_F)$ .

Substituting the above expressions for  $\gamma$  and  $\dot{\gamma}$  into (6b-2-1) gives:

$$(6b-2-1-1) \quad TS = CS \left[ \gamma_0 - \theta_{FS} + (\theta_D - \theta_F) \right] + DS (\dot{\theta}_D - \dot{\theta}_F) \\ \text{FOR } [\gamma + (\theta_D - \theta_F) - \theta_{FS}] \geq 0 \\ = 0 \quad \text{FOR } [\gamma + (\theta_D - \theta_F) - \theta_{FS}] < 0$$

Summing torques on the flywheel gives:

$$(6b-2-4) \quad \ddot{\theta}_F = [T_S + C_A(\theta_D - \theta_F) + D_A(\dot{\theta}_D - \dot{\theta}_F)] / W_{FW}$$

Summing torques on the drum gives:

$$(6b-2-5) \quad \ddot{\theta}_D = [-T_S - C_A(\theta_D - \theta_F) - D_A(\dot{\theta}_D - \dot{\theta}_F) + T_C] / W_D$$

Where  $T_C$  is the clutch torque.

Subtracting (6b-2-4) from (6b-2-5) results in:

$$(6b-2-6) \quad (\ddot{\theta}_D - \ddot{\theta}_F) = \left( \frac{1}{W_D} + \frac{1}{W_{FW}} \right) [-T_S - C_A(\theta_D - \theta_F) - D_A(\dot{\theta}_D - \dot{\theta}_F)] \\ + T_C / W_D$$

By integrating (6b-2-6) twice,  $(\dot{\theta}_D - \dot{\theta}_F)$  and  $(\theta_D - \theta_F)$  are established as

$$(6b-2-7) \quad (\dot{\theta}_D - \dot{\theta}_F) = \int (\ddot{\theta}_D - \ddot{\theta}_F) dt$$

$$(6b-2-8) \quad (\theta_D - \theta_F) = \int (\dot{\theta}_D - \dot{\theta}_F) dt$$

Substituting values for  $(\theta_D - \theta_F)$  and  $(\dot{\theta}_D - \dot{\theta}_F)$  computed from (6b-2-7) and (6b-2-8) into equation (6b-2-4) and integrating once establishes  $\dot{\theta}_F$  as follows:

$$(6b-2-9) \quad \dot{\theta}_F = \int \ddot{\theta}_F dt$$

Combining the results from (6b-2-7) and (6b-2-9) establishes  $\dot{\theta}_D$  as:

$$(6b-2-10) \quad \dot{\theta}_D = (\dot{\theta}_D - \dot{\theta}_F) + \dot{\theta}_F$$

The clutch will now be examined.

The torque exerted on the clutch carrier by the rotor,  $T_c$ , is defined by:

$$(6b-2-11) \quad T_c = C_c (\theta_R - \theta_c) + D_c (\dot{\theta}_R - \dot{\theta}_c)$$

If, as for the flywheel stop, it is assumed that the clutch carrier inertia is negligibly small, the torque between the clutch and the drum equals the torque between the rotor and the clutch carrier. In this case equation (6b-2-11) may be solved for  $(\dot{\theta}_R - \dot{\theta}_c)$  and by integrating once  $(\theta_R - \theta_c)$  is obtained:

$$(6b-2-12) \quad (\theta_R - \theta_c) = \int (\dot{\theta}_R - \dot{\theta}_c) dt$$

Where  $(\dot{\theta}_R - \dot{\theta}_c)$  is obtained from the following version of (6b-2-11)

$$(6b-2-11-1) \quad (\dot{\theta}_R - \dot{\theta}_c) = [T_c - C_c (\theta_R - \theta_c)] / D_c$$

It follows that:

$$(6b-2-13) \quad \dot{\theta}_c = \dot{\theta}_R - (\dot{\theta}_R - \dot{\theta}_c)$$

If the clutch is configured so that there is no slipping for counterclockwise torque on the drum,  $\dot{\theta}_c$  must equal  $\dot{\theta}_d$  and any difference between  $\dot{\theta}_R$  and  $\dot{\theta}_d$  must be relative velocity between the clutch carrier and the rotor (i.e.  $\dot{\theta}_R - \dot{\theta}_c$ ). If  $\dot{\theta}_d$  is substituted for  $\dot{\theta}_c$  in equation (6b-2-11) then the resulting equation can be used to compute the torque required to force  $\dot{\theta}_c$  to be equal to  $\dot{\theta}_d$ . Therefore, making this substitution,

$$(6b-2-11-2) \quad T_c = C_c (\theta_R - \theta_c) + D_c (\dot{\theta}_R - \dot{\theta}_d)$$

Equation (6b-2-11-2) adequately describes the component of clutch torque due to relative velocity; however, the component due to relative displacement is not satisfactorily described because the torque direction is independent of relative position. To compute the clutch torque for all conditions, equation (6b-2-11-2) will be modified and

a procedure for establishing the clutch condition will be defined. The clutch condition is established by the torque direction. The torque direction is determined by examining the direction the drum is attempting to move relative to the clutch. The direction of the drum's attempted movement relative to the clutch is established by comparing the drum velocity,  $\dot{\Theta}_D$ , to the velocity,  $\dot{\Theta}_{CH}$ , of a hypothetical or "index" clutch. The "index" clutch will be permitted to have slight slippage on the drum for counterclockwise torque so that there is a preceivable circumstance to indicate torque direction. To describe the "index" clutch motion relative to the rotor, equation (6b-2-11-1) is modified by substituting  $\Theta_{CH}$  and  $\dot{\Theta}_{CH}$  for  $\Theta_C$  and  $\dot{\Theta}_C$  as follows:

$$(6b-2-11-1M) \quad (\dot{\Theta}_R - \dot{\Theta}_{CH}) = [\tau_C - C_C(\Theta_R - \Theta_{CH})] / D_C$$

The clutch torque,  $\tau_C$ , is defined by equation (6b-2-11-3).

$(\Theta_R - \Theta_{CH})$  is obtained from equation (6b-2-12) and  $\dot{\Theta}_{CH}$  is then established from equation (6b-2-13), noting that in each case  $\Theta_{CH}$  and  $\dot{\Theta}_{CH}$  are used in place of  $\Theta_C$  and  $\dot{\Theta}_C$ . The clutch condition is established by the difference between  $\dot{\Theta}_{CH}$  and  $\dot{\Theta}_D$  as follows:

For  $(\dot{\Theta}_{CH} - \dot{\Theta}_D) > 0$  Clutch torque is positive on the drum (clutch attempting to have positive velocity with respect to drum)

For  $(\dot{\Theta}_{CH} - \dot{\Theta}_D) = 0$  Clutch is not attempting to move relative to drum

For  $(\dot{\Theta}_{CH} - \dot{\Theta}_D) < 0$  Clutch torque is negative on the drum. (Drum is attempting to have positive velocity with respect to clutch).

Now that the clutch condition is defined, equation (6b-2-11-2) is modified so that the torque direction is established by the direction of relative velocity between the drum and the clutch as follows:

$$\begin{aligned}
 (6b-2-11-3) \quad T_C &= G_C \langle \dot{\theta}_{CH} - \dot{\theta}_0 \rangle \left| C_C (\theta_R - \theta_{CH}) \right| + D_C (\dot{\theta}_R - \dot{\theta}_0) \\
 &\quad \text{FOR } \left\{ G_C \langle \dot{\theta}_{CH} - \dot{\theta}_0 \rangle \left| C_C (\theta_R - \theta_{CH}) \right| + D_C (\dot{\theta}_R - \dot{\theta}_0) \right\} > C750 \\
 &= C750 \\
 &\quad \text{FOR } \left\{ G_C \langle \dot{\theta}_{CH} - \dot{\theta}_0 \rangle \left| C_C (\theta_R - \theta_{CH}) \right| + D_C (\dot{\theta}_R - \dot{\theta}_0) \right\} \leq C750
 \end{aligned}$$

The function  $G_C \langle \dot{\theta}_{CH} - \dot{\theta}_0 \rangle$  is defined as follows:

$$\begin{aligned}
 (6b-2-14) \quad G_C \langle \dot{\theta}_{CH} - \dot{\theta}_0 \rangle &= +1.0 \quad \text{FOR } (\dot{\theta}_{CH} - \dot{\theta}_0) > 0 \\
 &= 0 \quad \text{FOR } (\dot{\theta}_{CH} - \dot{\theta}_0) = 0 \\
 &= -1.0 \quad \text{FOR } (\dot{\theta}_{CH} - \dot{\theta}_0) < 0
 \end{aligned}$$

The constant C750 is the value of clutch drag torque when the drum is overrunning the clutch.

The amount of relative motion between the flywheel and drum  $(\theta_0 - \theta_F)$  is the skid signal. To be compatible with the electrical antiskid control circuits, assume the skid signal is produced by a set of electrical contact points; therefore,

$$\begin{aligned}
 (6b-2-15) \quad E_V &= V_S \quad \text{FOR } (\theta_0 - \theta_F) \geq C751 \\
 &= 0 \quad \text{FOR } (\theta_0 - \theta_F) < C751
 \end{aligned}$$

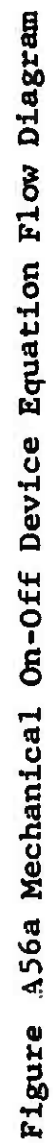
C751 is the skid detection threshold value of  $(\theta_0 - \theta_F)$ . Also, for compatibility with the other parts of the analysis, let the input be derived from the wheel speed sensor output, EG, as follows:

$$(6b-2-16) \quad \dot{\theta}_R = C752 E_G$$

C752 is the conversion coefficient. The equation flow diagram for the mechanical on-off antiskid device is shown on Figure A56a.

## B-2 Mechanical On-Off Parameter Evaluation

No parameter evaluation has been accomplished for the mechanical on-off device because it is not applicable to the aircraft being considered.



## 7. ANTISKID CONTROL VALVE

Aircraft antiskid control systems typically utilize a two-stage electrically operated pressure control valve. The first stage contains an electro-mechanical device such as a torque motor, solenoid or linear force motor which positions a hydraulic flow regulating element (flapper, nozzle or spool) such that a control pressure is produced. The control pressure is a function of the valve input pressure and the electrical input signal. The first stage control pressure is applied to the second stage hydraulic flow controlling power spool. The second stage spool is positioned by forces produced by the control pressure and valve output pressure in a manner such that output pressure is controlled in proportion to the first stage control pressure.

### A. Mathematical Description

#### First Stage

The function of the first stage can be described mathematically by considering the control pressure producing element to be a single degree of freedom damped spring mass system as shown in Figure A57 acted upon by a force,  $F_{cv}$ , proportional to the electrical input signal.

$$(7.1) \quad F_{cv} = C_{scv} E_v$$

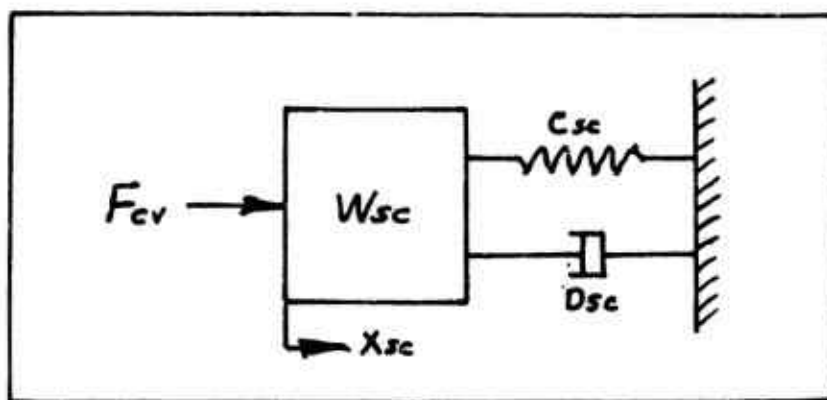


Figure A57 First Stage Spring Mass System

The first stage control pressure,  $P_{sc}$ , is defined as a function of the mass position,  $X_{sc}$ , according to Figure A58.  $X_{sc}$  is established by equation (7.2) which results from summing forces on the first stage mass,  $W_{sc}$ .

$$(7.2) \quad \ddot{X}_{sc} = \frac{F_{cv}}{W_{sc}} - \frac{C_{sc}}{W_{sc}} \dot{X}_{sc} - \frac{D_{sc}}{W_{sc}} X_{sc}$$

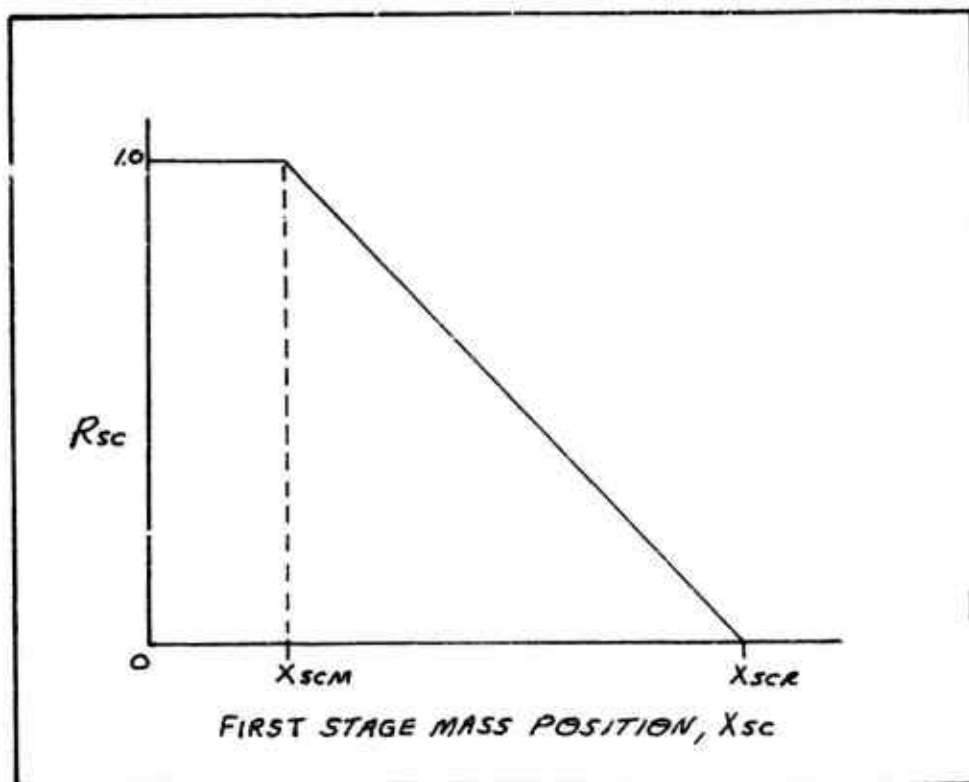


Figure A58 First Stage Control Pressure - Mass Position Relationship

$$(7.3) \quad P_{sc} = R_{sc} (P_{mv} - P_{cvr}) + P_{cvr}$$

$$(7.4) \quad R_{sc} = \begin{cases} 1.0 & \text{IF } X_{sc} \leq X_{scm} \\ \frac{X_{scr} - X_{sc}}{X_{scr} - X_{scm}} & \text{IF } X_{scm} < X_{sc} < X_{scr} \\ 0 & \text{IF } X_{sc} \geq X_{scr} \end{cases}$$

## Second Stage

The physical arrangement of the F-111 antiskid valve second stage is shown schematically in Figure A59. Most other antiskid valves have the same operating principles.

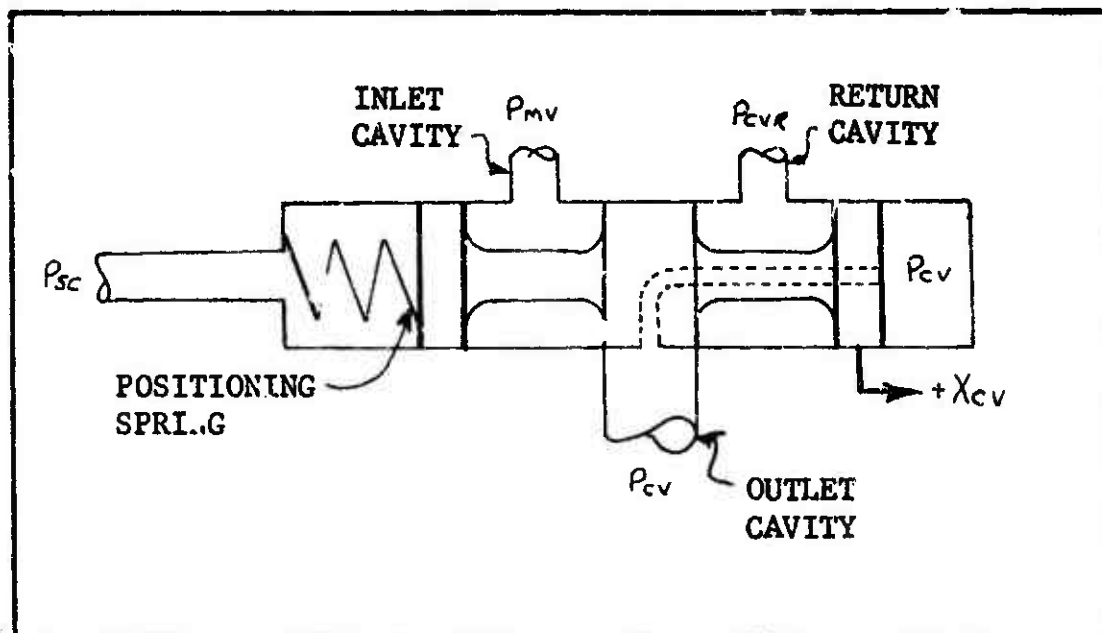


Figure A 59 Antiskid Valve Second Stage

As described in the hydraulic system, the metering valve output pressure,  $P_{mv}$ , is supplied to the antiskid control valve second stage inlet. When the second stage spool is displaced in a positive direction a fluid passage opens permitting hydraulic flow from the metering valve to the antiskid valve outlet cavity. When the second stage spool is displaced in a negative direction a fluid passage opens permitting hydraulic flow from the outlet cavity to return. Therefore, the second stage spool position defines the hydraulic flow areas. To permit computation flexibility and economy, two options for establishing the second stage spool position are provided.

### Option No. 1

For Option No. 1 the second stage spool position,  $X_{CV}$ , is established by equation (7.5) which results from summing forces on the spool mass,  $W_{CV}$ . Figure A60 shows a schematic of a single degree of freedom damped spring mass system representing the antiskid valve second stage spool. Springs,  $C_{CVS}$ , and dampers,  $D_{CVS}$ , are stops representing the spool's longitudinal restraining caused by its contact with the valve body. The forces acting on the second stage spool are the positioning spring force, damping force, stop forces and forces due to outlet cavity pressure,  $P_{CV}$ , and first stage control pressure,  $P_{SC}$ .

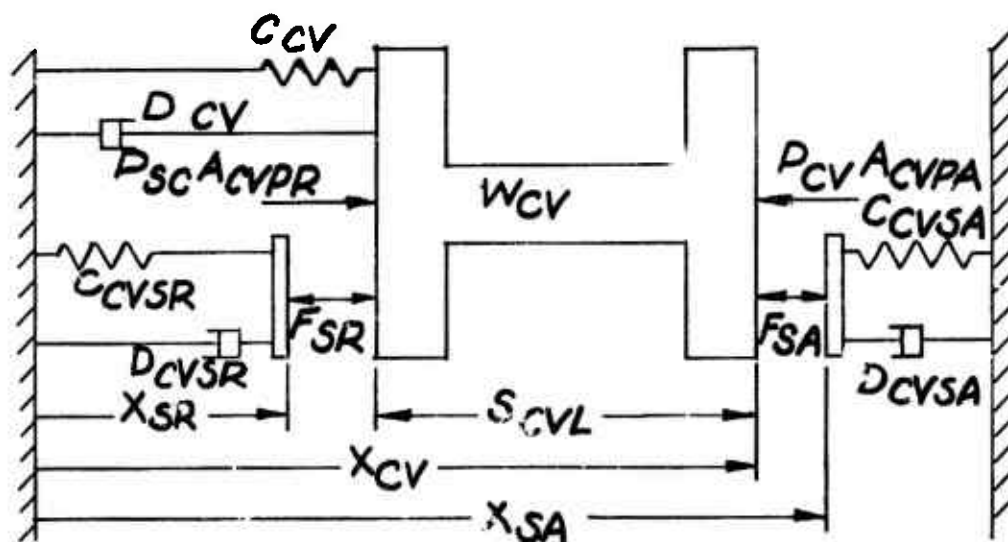


Figure A60 Second Stage Spool Forces

Summing forces on the second stage spool gives:

$$(7.5) \quad \ddot{X}_{CV} = \frac{[(P_{SC})(A_{CVPR}) - (P_{CV})(A_{CVPA})]}{W_{CV}} + \frac{(X_{CVP} - X_{CV})C_{CV}}{W_{CV}} - \frac{\dot{X}_{CV}(D_{CV})}{W_{CV}} + \frac{F_{SR}}{W_{CV}} - \frac{F_{SA}}{W_{CV}}$$

Integrating twice gives:

$$(7.6) \quad \dot{X}_{CV} = \int \ddot{X}_{CV} dt$$

$$(7.7) \quad \dot{X}_{CV} = \int \ddot{X}_{CV} dt$$

In equation (7.5) the forces  $F_{SA}$  and  $F_{SR}$  are the forces between the spool and the stops. Since the stop forces are contact forces, they cannot be less than zero. Forces  $F_{SA}$  and  $F_{SR}$  are defined as follows:

$$(7.8) \quad F_{SA} = 0, \text{ FOR } \dot{X}_{CV} \leq \dot{X}_{SA}$$

$$F_{SA} = C_{CVS}(\dot{X}_{SA} - \dot{S}_{SA}) + \ddot{X}_{CV} D_{CVS}, \text{ FOR } \dot{X}_{CV} > \dot{X}_{SA}$$

$$(7.9) \quad F_{SR} = 0, \text{ FOR } (\dot{X}_{CV} - \dot{S}_{CVL}) \geq \dot{X}_{SR}$$

$$F_{SR} = C_{CVS}(\dot{S}_{SR} - \dot{X}_{SR}) - \ddot{X}_{CV} D_{CVS}, \text{ FOR } (\dot{X}_{CV} - \dot{S}_{CVL}) < \dot{X}_{SR}$$

In equation (7.9),  $\dot{S}_{CVL}$ , is the spool length and  $\dot{S}_{SR}$  is the undeflected position of stop,  $S_R$ . The positions of the spool stops,  $\dot{X}_{SA}$  and  $\dot{X}_{SR}$ , are established as follows: Let the mass of the stop in the brake application direction of spool movement,  $S_A$ , be zero. Therefore, summing forces on  $S_A$  and solving for  $\dot{X}_{SA}$  gives:

$$(7.10) \quad \dot{X}_{SA} = [F_{SA} - (\dot{X}_{SA} - \dot{S}_{SA}) C_{CVS}] / D_{CVS}$$

In equations (7.8) and (7.10),  $\dot{S}_{SA}$  is the undeflected position of stop,  $S_A$ . It follows that:

$$(7.11) \quad \dot{X}_{SA} = \int \ddot{X}_{SA} dt$$

Using the same procedure as above for the stop in the brake release direction of spool movement,  $S_R$ ;

$$(7.12) \quad \dot{X}_{SR} = [C_{CVS}(\dot{S}_{SR} - \dot{X}_{SR}) - F_{SR}] / D_{CVS}$$

And it follows that:

$$(7.13) \quad \dot{X}_{SR} = \int \ddot{X}_{SR} dt$$

The hydraulic system contains provision for leakage flow associated with first stage pressure regulation and spool fit. Since these small flows have no effect on the valve's performance in the case under consideration, they have not been computed. Therefore, the following equations apply:

$$(7.14) \quad Q_{CV1} = 0$$

$$(7.15) \quad Q_{CV2} = 0$$

$$(7.16) \quad Q_{CV3} = 0$$

Figure A61 shows the Option No. 1 Control Valve Equation Flow Diagram.

#### Option No. 2

Since the time interval which elapses during second stage spool movement from one extreme position to the other is very short in comparison with overall control valve response time and since all of the control valve lag can be accounted for in the first stage, the second stage spool position,  $X_{CV}$ , can be established as a function of the direction of pressure differential thusly:

$$\begin{aligned} (7.17) \quad X_{CV} &= 0 && \text{FOR } (P_{CV} - P_{CVB}) = P_{SC} \\ X_{CV} &= +S_{CV0} && \text{FOR } (P_{CV} - P_{CVB}) < P_{SC} \\ X_{CV} &= -S_{CV0} && \text{FOR } (P_{CV} - P_{CVB}) > P_{SC} \end{aligned}$$

In equation (7.17)  $S_{CV0}$  is the second stage spool position for full flow area as described in the hydraulic system and  $P_{CVB}$  is the second stage apparent bias pressure equivalent to the positioning spring force.

Figure A62 is the Equation Flow Diagram for Option No. 2.

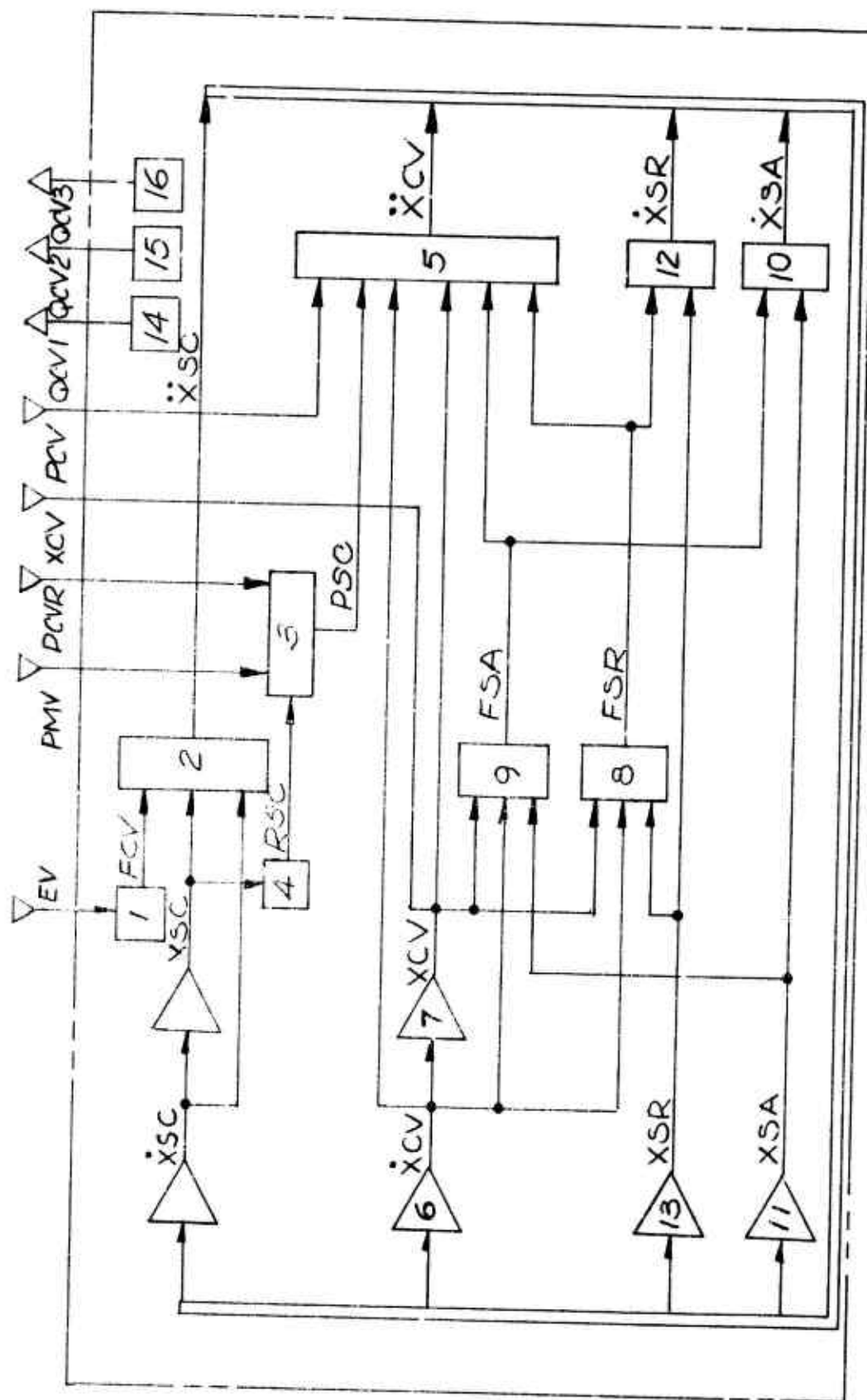


Figure A61 Antiskid Control Valve Equation Flow Diagram (Option No. 1)



## B. Parameter Evaluation

The parameters used for describing the antiskid valve's first stage behavior are established from measured frequency response performance characteristics along with some features of its physical construction. Frequency response test results from the F-111 antiskid valve show 25 degrees phase lag at 5 cps. From various experiments it is known that the first stage accounts for most of the phase lag. The F-111 valve's approximate 700 cps undamped natural frequency is quite high compared to a more usual 100 cps value. Since antiskid operation is generally 10 cps or less and since the low frequency phase lag can be accurately described with a lower natural frequency system, an undamped natural frequency of 100 cps will be used to minimize computation difficulty.

Coefficients  $C_{scv}$  and  $C_{sc}$  are set arbitrarily so that static values of  $X_{sc}$  will be compatible with values of  $X_{scm}$  and  $X_{scr}$  (which are also arbitrarily chosen) and the proper valve voltage - output pressure relationship is achieved. In this example the following values are assigned:

$$\begin{aligned} C_{scv} &= 1.2 \text{ lbf/volt} \\ C_{sc} &= 1.0 \text{ lbf/inch} \\ (7.14) \quad X_{scm} &= 3.6 \text{ inches} \\ X_{scr} &= 14.4 \text{ inches} \end{aligned}$$

For 100 cps (628 RAD/SEC) undamped natural frequency and  $C_{sc} = 1.0 \text{ lbf/in}$ , the mass  $W_{sc}$  is computed from  $(\omega_n)^2 = C_{sc}/W_{sc}$

$$(7.15) \quad W_{sc} = 2.54 \times 10^{-6} \text{ lbf sec}^2/\text{in}$$

Using the equations relating natural frequency and phase angle listed in the wheel speed sensor parameter evaluation and assuming the first stage has 20 degrees phase lag at 5 cps, the damping factor is established as 3.63. For the values of  $W_{sc}$  and  $C_{sc}$  above this damping factor results in:

$$(7.16) \quad D_{sc} = 11.6 \times 10^{-3} \text{ lbf sec/inch}$$

The area,  $A_{cVP}$ , the stop clearances,  $S_{cVA}$  and  $S_{cVR}$ , and the mass of the second stage spool,  $W_{cV}$ , are computed from the spool's physical dimensions as shown on the valve drawing.

$$\begin{aligned} A_{cVP} &= 0.05 \text{ IN}^2 \\ W_{cV} &= 41.5 \times 10^{-6} \text{ lbf sec}^2/\text{IN} \\ (7.17) \quad S_{cVA} &= 0.03 \text{ INCH} \\ S_{cVR} &= 0.03 \text{ INCH} \end{aligned}$$

The positioning spring rate,  $C_{cV}$ , and spool damping coefficient were established based on the valve's transient response characteristic where it was observed that a 50 cps about .5 critically damped transient pressure oscillation appeared. From this observation

$$\begin{aligned} C_{cV} &= 4.0 \text{ lbf/IN} \\ (7.18) \quad D_{cV} &= 13.0 \times 10^{-3} \text{ lbf sec/IN} \end{aligned}$$

The stop spring,  $C_{cVS}$ , and damper,  $D_{cVS}$ , characteristics are arbitrarily chosen to be as high as possible within computation capability.

$$\begin{aligned} C_{cVS} &= 5000 \text{ lbf/IN} \\ (7.19) \quad D_{cVS} &= 50 \text{ lbf sec/IN} \end{aligned}$$

The undeflected positioning spring length was computed assuming it produced approximately the same force on the valve spool as 25 PSI pressure differential.

$$(7.20) \quad X_{cVP} = 0.2 \text{ INCH}$$

Table A21 lists the parameters and their values which are applicable to the F-111 antiskid control valve. For Option 1 mathematical description and Table A22 lists the parameters which are applicable to Option 2.

Table A21 Antiskid Control Valve Parameters (Option No. 1) (Sheet 1 of 2)

SYMBOL	TYPE	VALUE	UNITS	DESCRIPTION
ACVPA	c	0.05	IN <sup>2</sup>	Second Stage Spool Area, Output Pressure End
ACVPR	c	0.05	IN <sup>2</sup>	Second Stage Spool Area, Control Pressure End
CSCV	c	1.2	LBF/VOLT	First Stage Volts - Force Coefficient
CSC	c	1.0	LBF/IN	First Stage Spring Rate
CCV	c	4.0	LBF/IN	Second Stage Positioning Spring Rate
CCVS	c	5000	LBF/IN	Second Stage Stop Spring Rate
DSC	c	$11.6 \times 10^{-3}$	LBF/SEC/IN	First Stage Damping Coefficient
DCV	c	$13.0 \times 10^{-3}$	LBF/SEC/IN	Second Stage Damping Coefficient
DCVS	c	50	LBF/SEC/IN	Second Stage Stop Damping Coefficient
EV	v(I)		VOLTS	Antiskid Valve Volts
FCV	v		LBF	First Stage Driving Force
FSA	v		LBF	Second Stage Stop Force - Positive Spool Displacement
FSR	v		LBF	Second Stage Stop Force - Negative Spool Displacement
PCV	v(I)		LBF/IN <sup>2</sup>	Antiskid Valve Outlet Cavity Pressure
PMV	v(I)		LBF/IN <sup>2</sup>	Metering Valve Output Pressure
PSC	v		LBF/IN <sup>2</sup>	First Stage Output Control Pressure
PCVR	v(I)		LBF/IN <sup>2</sup>	Antiskid Valve Return Cavity Pressure
QCV1	v(O)		IN <sup>3</sup> /SEC	Leakage Flow into Control Valve Inlet Cavity
QCV2	v(O)		IN <sup>3</sup> /SEC	Leakage Flow into Control Valve Outlet Cavity
QCV3	v(O)		IN <sup>3</sup> /SEC	Leakage Flow into Control Valve Return Cavity
RSC	v		DIMENSIONLESS	First Stage Pressure Regulation Coefficient
SSA	c	0.03	IN	Undelected Stop Position - Second Stage Spool Positive Displacement
SSR	c	-0.03	IN	Undelected Stop Position - Second Stage Spool Negative Displacement
SCVL	c	1.0	IN	Second Stage Spool Length

Table A21 Antiskid Control Valve Parameters (Option No. 1) (Sheet 2 of 2)

SYMBOL	TYPE	VALUE	UNITS	DESCRIPTION
$W_{SC}$	C	$2.54 \times 10^{-6}$	$LBF \cdot SEC^2 / IN$	First Stage Mass
$W_{CV}$	C	$41.5 \times 10^{-6}$	$LBF \cdot SEC^2 / IN$	Second Stage Spool Mass
$X_{SC}$	V	0.0	IN	First Stage Mass Displacement
$X_{SCO}$	C	0.0	IN	First Stage Mass Displacement at Time Zero
$\dot{X}_{SC}$	V	0.0	IN/SEC	First Stage Mass Velocity
$\dot{X}_{SCO}$	C	0.0	IN/SEC	First Stage Mass Velocity at Time Zero
$\ddot{X}_{SC}$	V	3.6	IN/SEC <sup>2</sup>	First Stage Mass Acceleration
$X_{SCM}$	C	3.6	IN	First Stage Mass Position for Zero Regulation
$X_{SCR}$	C	14.4	IN	First Stage Mass Position for Max Regulation
$X_{CV}$	V	0.03	IN	Second Stage Spool Displacement
$\dot{X}_{CV}$	C	0.03	IN	Second Stage Spool Displacement at Time Zero
$\dot{X}_{CVO}$	V	0.0	IN/SEC	Second Stage Spool Velocity
$\ddot{X}_{CV}$	C	0.0	IN/SEC <sup>2</sup>	Second Stage Spool Velocity at Time Zero
$\ddot{X}_{CVO}$	V	0.0	IN/SEC <sup>2</sup>	Second Stage Spool Acceleration
$X_{SA}$	V	0.03	IN	Positive Motion Stop Displacement
$X_{SAO}$	C	0.03	IN	Positive Motion Stop Displacement at Time Zero
$\dot{X}_{SA}$	V	-1.03	IN/SEC	Positive Motion Stop Velocity
$X_{SR}$	V	-1.03	IN	Negative Motion Stop Displacement
$X_{SRO}$	C	-1.03	IN	Negative Motion Stop Displacement at Time Zero
$\dot{X}_{SR}$	V	0.2	IN/SEC	Negative Motion Stop Velocity
$X_{CVP}$	C	0.2	IN	Second Stage Positioning Spring Undeflected Spool Position

Table A22 Antiskid Control Valve Parameters (Option No. 2)

SYMBOL	TYPE	VALUE	UNITS	DESCRIPTION
CSCV	c	1.2	LB/IN <sup>2</sup> /VOLT	First Stage Volts - Force Coefficient
CSC	c	1.0	LB/IN	First Stage Spring Rate
DSC	c	11.6 x 10 <sup>-3</sup>	LB/SEC/IN	First Stage Damping Coefficient
EV	v(I)		VOLTS	Antiskid Valve Volts
FCV	v		LB/IN	First Stage Driving Force
PCV	v(I)		LB/IN <sup>2</sup>	Antiskid Valve Outlet Cavity Pressure
PCV0	c	15	LB/IN <sup>2</sup>	Second Stage Bias Pressure
PCVR	v(I)		LB/IN <sup>2</sup>	Antiskid Valve Return Cavity Pressure
PMV	v(I)		LB/IN <sup>2</sup>	Metering Valve Output Pressure
PSC	v		LB/IN <sup>2</sup>	First Stage Output Control Pressure
RSC	v		DIMENSIONLESS	First Stage Regulation Coefficient
*SCV0	c	0.03	IN	Second Stage Spool Displacement for Max Flow Area
WSC	c	2.54 x 10 <sup>-6</sup>	LB/SEC <sup>2</sup> /IN	First Stage Mass
XCV	v(o)		IN	Second Stage Spool Displacement
XSC	v		IN	First Stage Mass Displacement
XSC0	c	0.0	IN	First Stage Mass Displacement at Time Zero
XSC	v		IN/SEC	First Stage Mass Velocity
XSC0	c	0.0	IN/SEC	First Stage Mass Velocity at Time Zero
XSC	v		IN/SEC <sup>2</sup>	First Stage Mass Acceleration
XSCM	c	3.6	IN	First Stage Position for Zero Regulation
XSCR	c	14.4	IN	First Stage Position for Maximum Regulation
QCV1	v(o)	0.0	IN <sup>3</sup> /SEC	Leakage Flow into Control Valve Inlet Cavity
QCV2	v(o)	0.0	IN <sup>3</sup> /SEC	Leakage Flow into Control Valve Outlet Cavity
QCV3	v(o)	0.0	IN <sup>3</sup> /SEC	Leakage Flow into Control Valve Return Cavity

\*See Hydraulic System

## 8. HORIZONTAL TAIL CONTROL

In the 3 degree and 6 degree airplane models, the tail position can be controlled by two different means. The first is simply to require that the horizontal tail rotation be fixed at some value  $S_{HT}$ . The second is to fix the input commands  $S_{EST}$  and  $F_{PX}$  and then let the stability augmentation system adjust the tail setting  $S_{HT}$ .

### A. Mathematical Description

Figure A63 shows a control system representation of the stability augmentation system.

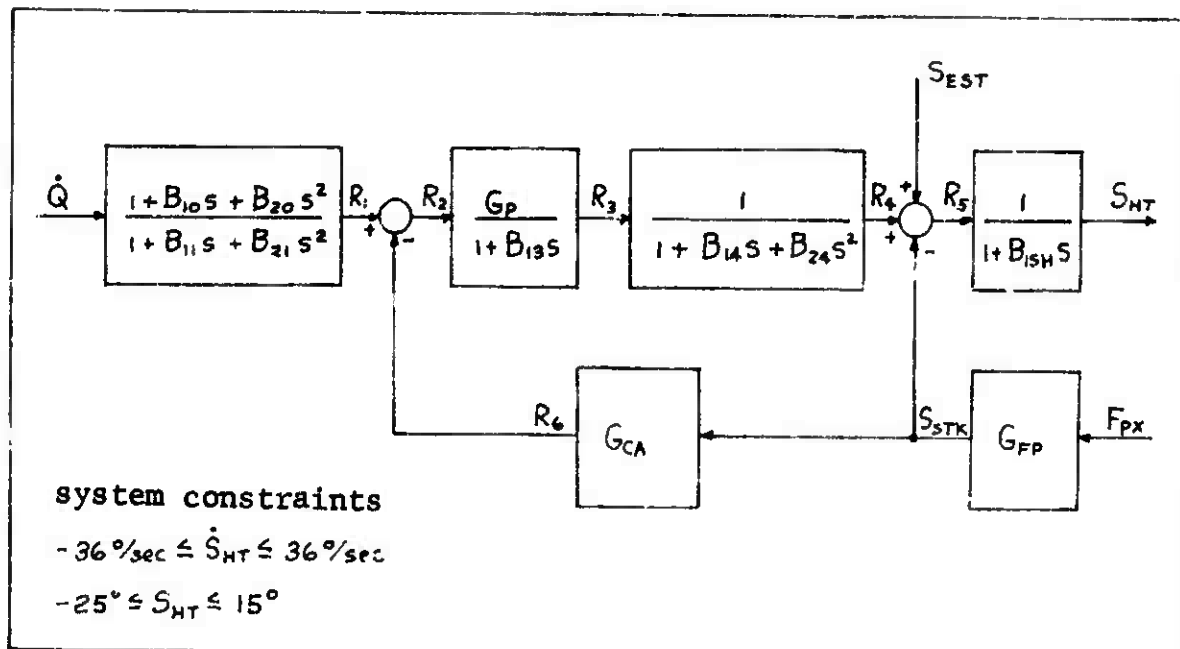


Figure A63 Stability Augmentation System

Using figure A63 as a guide, the following equations describe the stability augmentation system.

$$(8.1) S_{STK} = G_{FP} F_{PX}$$

Where  $F_{PX}$  is the force exerted by the pilot on the stick.

$$(8.2) R_6 = G_{CA} S_{STK}$$

Let  $U_Q$  and  $U_{QQ}$  be defined by

$$(8.3) \quad U_Q = \left(\frac{180}{\pi}\right) \int \dot{Q} dt$$

$$(8.4) \quad U_{QQ} = \int U_Q dt$$

Also, let  $U_{R1}$  and  $U_{RR1}$  be defined by

$$(8.5) \quad U_{R1} = \int R_1 dt$$

$$(8.6) \quad U_{RR1} = \int U_{R1} dt$$

Then

$$(8.7) \quad R_1 = (U_{QQ} + B_{10} U_Q + B_{20} \dot{Q} - U_{RR1} - B_{11} U_{R1}) / B_{21}$$

$$(8.8) \quad R_2 = R_1 - R_6$$

Let  $U_{R2}$ ,  $U_{R3}$ ,  $U_{RR3}$ ,  $U_{R4}$ , and  $U_{RR4}$  be defined by

$$(8.9) \quad U_{R2} = \int R_2 dt$$

$$(8.10) \quad U_{R3} = \int R_3 dt$$

$$(8.11) \quad U_{RR3} = \int U_{R3} dt$$

$$(8.12) \quad U_{R4} = \int R_4 dt$$

$$(8.13) \quad U_{RR4} = \int U_{R4} dt$$

Then

$$(8.14) \quad R_3 = (G_P U_{R2} - U_{R3}) / B_{13}$$

$$(8.15) \quad R_4 = (U_{RR3} - U_{RR4} - B_{14} U_{R4}) / B_{24}$$

$$(8.16) \quad R_5 = R_4 + S_{EST} - S_{STR}$$

Because of rate and position limits, the equations that describe  $S_{HT}$  in terms of  $R_5$  must be modified to reflect these limits. Let  $S_{HTP}$  be defined by

$$(8.17) \quad S_{HTP} = (R_5 - S_{HT}) / B_{15H}$$

Then

$$(8.18) \ S_{HT1} = \begin{cases} S_{HTDMX} & \text{if } S_{HTP} > S_{HTDMX} \\ S_{HTP} & \text{if } -S_{HTDMX} \leq S_{HTP} \leq S_{HTDMX} \\ -S_{HTDMX} & \text{if } S_{HTP} < -S_{HTDMX} \end{cases}$$

$$(8.19) \ \dot{S}_{HT} = \begin{cases} \min\{0.0, S_{HT1}\} & \text{if } S_{HT} \geq S_{HTMAX} \\ S_{HT1} & \text{if } S_{HTMIN} < S_{HT} < S_{HTMAX} \\ \max\{0.0, S_{HT1}\} & \text{if } S_{HT} \leq S_{HTMIN} \end{cases}$$

Finally the stick position  $F_{PX}$  may be positioned as a function of time by specifying two times and two loads.

$$(8.20) \ F_{PX} = \begin{cases} 0 & \text{if } T_{PX2} \leq T_{PX1} \\ F_{PX1} & \text{if } T \leq T_{PX1} < T_{PX2} \\ F_{PX2} & \text{if } T_{PX1} < T_{PX2} \leq T \\ F_{PX1} + (F_{PX2} - F_{PX1})(T - T_{PX1}) / (T_{PX2} - T_{PX1}) & \text{if } T_{PX1} < T < T_{PX2} \end{cases}$$

#### B. Parameter Evaluation

The values for the F-111A system parameters are listed in Table A23. In using this system for a braking problem the usual procedure is to first choose a steadystate value for  $S_{HT}(S_{HTSS})$ . Set  $S_{HT0} = S_{HTSS} = S_{GST}$  and set  $F_{PX} = 0$  ( $T_{PX1} = T_{PX2} = 0$ ). Set all other initial conditions to zero.



Table A23 Horizontal Tail Control Parameters

SYMBOL	TYPE	VALUE	UNITS	DESCRIPTION
B <sub>10</sub>	C	0.4	sec	SAS Constants
B <sub>11</sub>	C	0.05	sec	
B <sub>13</sub>	C	0.50	sec	
B <sub>14</sub>	C	0.00269	sec	
B <sub>15H</sub>	C	0.05	sec	
B <sub>20</sub>	C	3.58	sec <sup>2</sup> deg/ rad	Stick Force
B <sub>21</sub>	C	0.000555	sec <sup>2</sup>	
B <sub>24</sub>	C	0.00037	sec <sup>2</sup>	
F <sub>FX</sub>	V	0.0	lb	Determine Stick Force
F <sub>PX1</sub>	C	0.0	lb	
F <sub>PX2</sub>	C	0.0	lb	
G <sub>CA</sub>	C	3.6	sec <sup>-1</sup>	Command Augmentation Gain
G <sub>FP</sub>	C	0.51	deg/lb	Stick Force Gain
G <sub>P</sub>	C	0.375	sec <sup>-1</sup>	Augmentation Gain
Q	V(i)		rad/sec	Airplane Pitch Rate
R <sub>1</sub>	V		deg/sec	
R <sub>2</sub>	V		deg/sec	
R <sub>3</sub>	V		deg/sec	Intermediate SAS Variables
R <sub>4</sub>	V		deg/sec	
R <sub>5</sub>	V		deg/sec	
R <sub>6</sub>	V		deg/sec	Series Trim Input
S <sub>EST</sub>	C	-5.0	deg/sec	

Table A23 Horizontal Tail Control Parameters (Sheet 2 of 3)

SYMBOL	TYPE	VALUE	UNITS	DESCRIPTION
$S_{HT}$	V(o)		deg	Horizontal Tail Deflection
$S_{HTO}$	C	-5.0	deg	when Time = 0
$\dot{S}_{HT}$	V		deg/sec	Horizontal Tail Deflection Rate
$S_{HT1}$	V		deg/sec	Used to Calculate $\dot{S}_{HT}$
$S_{HTP}$	V		deg/sec	
$S_{HTDMX}$	C	36.0	deg/sec	Maximum Tail Deflection Rate
$S_{HTMAX}$	C	15.0	deg	Maximum Tail Deflection
$S_{HTMIN}$	C	-25.0	deg	Minimum Tail Deflection
$S_{STK}$	V		deg	Stick Position
$T$	V(i)		sec	Time
$T_{PX1}$	C	0.0	sec	Used to Determine $\bar{r}_{px}$
$T_{PX2}$	C	0.0	sec	
$U_Q$	V		deg	
$U_{Q0}$	C	0.0	deg	
$U_{QQ}$	V		deg/sec	
$U_{QQC}$	C	0.0	deg/sec	
$U_{R1}$	V		deg	
$U_{R10}$	C	0.0	deg	
$U_{RR1}$	V		deg/sec	
$U_{RR10}$	C	0.0	deg/sec	
$U_{R2}$	V		deg	
$U_{R20}$	C	0.0	deg	
				SAS Variables and Initial Conditions

Table A23 Horizontal Tail Control Parameters (Sheet 3 of 3)

SYMBOL	TYPE	VALUE	UNITS	DESCRIPTION
U <sub>R3</sub>	V		deg	} SAS Variables and Initial Conditions
U <sub>R30</sub>	C	0.0	deg	
U <sub>RR3</sub>	V		deg sec	
U <sub>RR30</sub>	C	0.0	deg sec	
U <sub>R4</sub>	V		deg sec	
U <sub>R40</sub>	C	0.0	deg sec <sup>2</sup>	
U <sub>RR4</sub>	V		deg sec <sup>2</sup>	
U <sub>RR40</sub>	C	0.0	deg sec <sup>2</sup>	

## 9a. RUNWAY SYSTEM (FLYWHEEL AND 3 DEGREE)

This runway system is essentially the same as the runway system for the 6 degree. In fact, the relation between the two is given by  $Z_{6D}\langle x \rangle = Z_{6D}\langle x, 0 \rangle$  and  $Z_{6DP}\langle x \rangle = Z_{6PP}\langle x, 0 \rangle$ . Even though this system is like the 6 degree system, the equations are listed below which take advantage of the fact that it takes less computer time to calculate  $Z_{6D}\langle x \rangle$  than  $Z_{6D}\langle x, 0 \rangle$ . The data describing the runway is in tabular form and consists of runway elevation values as shown in table A25 as described in discussion of the 6 degree runway system. The data is from the center strip from station 4574 to station 6574.

### A. Mathematical Description

Let  $H_{RC}(i)$ ,  $i = 1, 2, \dots, 1001$  denote the elevations at two foot intervals. As an example,  $H_{RC}(5) = 9.686$ . If  $x$  is a distance measured down the runway where  $x$  is in inches, then  $z = Z_{6D}\langle x \rangle$  and  $w = Z_{6DP}\langle x \rangle$  correspond to the elevation in inches and the slope in inches per inch. The values for  $z$  and  $w$  are determined as outlined below. The function  $Z_{6D}$  will have the property that  $Z_{6D}\langle 0 \rangle = 0$ .

Let  $X_{LRO}$  be a constant such that  $0 \leq X_{LRO} < 2000$ . The input  $X_{LRF}$  in feet is derived from  $x$  such that  $0 \leq X_{LRF} < 2000$  and for some integer  $k$

$$(9a.1) \quad X_{LRF} = X_{LRO} + x/12 - 2000k$$

Let  $n$  be an integer such that  $2(n-1) \leq X_{LRO} < 2n$  and define  $Z_{6CO}$  by

$$(9a.2) \quad Z_{6CO} = H_{RC}(n) + (H_{RC}(n+1) - H_{RC}(n))(X_{LRO} - 2n + 2)/2$$

If  $m$  is an integer such that  $2(m-1) \leq X_{LRF} < 2m$  then  $z$  and  $w$  are given by

$$(9a.3) \quad z = 12(H_{RC}(m) + (H_{RC}(m+1) - H_{RC}(m))(X_{LRF} - 2m + 2)/2 - Z_{6CO})$$

$$(9a.4) \quad w = (H_{RC}(m+1) - H_{RC}(m))/2$$

Table A24 Runway System Parameters (Flywheel and 3 Degree)

SYMBOL	TYPE	VALUE	UNITS	DESCRIPTION
$H_{RC}(i)$	C	*	Ft.	Center Runway Elevation Profile
$\omega$	$v(o)$		In/In	Runway Slope at $\alpha$ ( $\omega = Z_{GDP} < \alpha >$ )
$\alpha$	$v(L)$		In.	Distance Down Runway
$X_{LRO}$	C	0.0	Ft.	Determines starting point (at time = 0) on Runway Profile
$X_{L2F}$	V		Ft.	Determines position on runway profile
$z$	$v(o)$		In.	Runway elevation at $\alpha$
$Z_{GCO}$	$\#$ C		Ft.	Correction height

# Determined from the constant  $X_{LRO}$

\* See Table A24 of the 6 degree runway system (use center, sta. 4574 to 6574)

## 9b. RUNWAY SYSTEM (6 DEGREE)

The runway system is not actually a "system" in the same sense as the brake system, for example. The runway system is simply a function called by the airplane system to supply values for ground slope and elevation. The data describing the runway is in tabular form and consists of runway elevation values as shown in Table A25. Except for a slight modification, the data in Table A25 is taken from station 4574 to station 6574 of runway 25 from reference 11. The left elevations and right elevations are 10 ft. to the left and 10 ft. to the right of center respectively. The elevations have been modified slightly so that the elevations at station 4574 match those at station 6574. This is done to provide an essentially "endless" runway by repeated use of a basic 2000 ft. strip.

### A. Mathematical Description

Let  $H_L(i)$ ,  $H_{RC}(i)$ ,  $H_{RL}(i)$ ,  $i = 1, 2, \dots, 1001$  denote the elevations at two foot increments of the right, center, and left runway strips respectively. As an example,  $H_{RL}(11) = 9.550$  and  $H_{RC}(5) = 9.686$ . If  $x$  is a distance measured down the runway, and  $y$  is a distance measured out from the center of the runway where  $x$  and  $y$  are in inches, then  $z = Z_{GD}(x, y)$  and  $\omega = Z_{SD}(x, y)$  correspond to the elevation in inches and the slope in inches per inch. The values for  $z$  and  $\omega$  are determined as outlined below. The function  $Z_{GD}$  will be chosen in such a way that  $Z_{GD}(0, y) = 0.0$  inches.

Let  $X_{LRF}$  and  $Y_{LRF}$  be the inputs in feet. Thus,

$$(9c.1) \quad Y_{LRF} = y/12$$

Let  $X_{LRO}$  be a constant such that  $0 \leq X_{LRO} < 2000$ .  $X_{LRF}$  is a number such that  $0 \leq X_{LRF} < 2000$  and which also satisfies the following equation for some integer  $K$ .

$$(9c.2) \quad X_{LRF} = X_{LRO} + x/12 - 2000K$$

Now let  $n$  be an integer such that  $2(n-1) \leq X_{LRO} < 2n$ .  
 Define  $Z_{GRO}$ ,  $Z_{GCO}$ ,  $Z_{GLO}$  as follows:

$$(9c.3) \quad Z_{GRO} = H_{RR}(n) + \frac{1}{2}(H_{RR}(n+1) - H_{RR}(n))(X_{LRO} - 2n + 2)$$

$$(9c.4) \quad Z_{GCO} = H_{RC}(n) + \frac{1}{2}(H_{RC}(n+1) - H_{RC}(n))(X_{LRO} - 2n + 2)$$

$$(9c.5) \quad Z_{GLO} = H_{RL}(n) + \frac{1}{2}(H_{RL}(n+1) - H_{RL}(n))(X_{LRO} - 2n + 2)$$

Now let  $m$  be an integer such that  $2(m-1) \leq X_{LRF} < 2m$ .  
 Define  $Z_{GRX}$ ,  $Z_{GCX}$ , and  $Z_{GLX}$  as follows:

$$(9c.6) \quad Z_{GRX} = H_{RR}(m) + \frac{1}{2}(H_{RR}(m+1) - H_{RR}(m))(X_{LRF} - 2m + 2) - Z_{GRO}$$

$$(9c.7) \quad Z_{GCX} = H_{RC}(m) + \frac{1}{2}(H_{RC}(m+1) - H_{RC}(m))(X_{LRF} - 2m + 2) - Z_{GCO}$$

$$(9c.8) \quad Z_{GLX} = H_{RL}(m) + \frac{1}{2}(H_{RL}(m+1) - H_{RL}(m))(X_{LRF} - 2m + 2) - Z_{GLO}$$

If  $Y_{LRF} \geq 0$ , then

$$(9c.10) \quad z = 12 (Z_{GCX} + (Z_{GRX} - Z_{GCX})(Y_{LRF}/10))$$

$$(9c.11) \quad w = (Y_{LRF}/20)(H_{RR}(m+1) - H_{RR}(m) - H_{RC}(m+1) + H_{RC}(m)) \\ + \frac{1}{2}(H_{RC}(m+1) - H_{RC}(m))$$

If  $Y_{LRF} < 0$ , then

$$(9c.12) \quad z = 12 (Z_{GCX} + (Z_{GCX} - Z_{GLX})(Y_{LRF}/10))$$

$$(9c.13) \quad w = (Y_{LRF}/20)(H_{RC}(m+1) - H_{RC}(m) - H_{RL}(m+1) + H_{RL}(m)) \\ + \frac{1}{2}(H_{RC}(m+1) - H_{RC}(m))$$

**Table A.25 Three Track Elevation Profiles**

(Stations and elevations are in feet)

(Sheet 1 of 6)

STATION	ELEVATION		
	LEFT	CENTER	RIGHT
4574	9.597	9.703	9.593
4576	9.596	9.699	9.586
4578	9.593	9.696	9.581
4580	9.590	9.696	9.580
4582	9.590	9.686	9.580
4584	9.589	9.696	9.622
4586	9.580	9.688	9.629
4588	9.574	9.685	9.625
4590	9.570	9.686	9.616
4592	9.563	9.693	9.622
4594	9.564	9.704	9.634
4596	9.563	9.692	9.616
4598	9.556	9.676	9.611
4600	9.558	9.676	9.613
4602	9.592	9.694	9.612
4604	9.594	9.699	9.627
4606	9.595	9.711	9.641
4608	9.600	9.704	9.601
4610	9.604	9.703	9.605
4612	9.594	9.696	9.602
4614	9.585	9.697	9.606
4616	9.572	9.699	9.608
4618	9.569	9.702	9.607

Table A25 Three Track Elevation Profiles

(Stations and elevations are in feet)  
(Sheet 2 of 6)

Station	Elevation			Station	Elevation			Station	Elevation		
	Left	Center	Right		Left	Center	Right		Left	Center	Right
4620	9.565	9.697	9.531	4763	9.557	9.667	9.567	4900	9.590	9.716	9.603
4622	9.572	9.698	9.631	4762	9.560	9.668	9.564	4901	9.593	9.714	9.582
4624	9.578	9.677	9.536	4764	9.560	9.668	9.561	4904	9.593	9.717	9.585
4626	9.583	9.687	9.589	4766	9.565	9.676	9.568	4906	9.598	9.714	9.589
4628	9.583	9.690	9.593	4768	9.567	9.676	9.567	4908	9.591	9.711	9.584
4630	9.583	9.681	9.593	4770	9.563	9.666	9.564	4910	9.589	9.716	9.578
4632	9.584	9.694	9.537	4772	9.561	9.660	9.557	4912	9.589	9.713	9.585
4634	9.591	9.699	9.634	4774	9.563	9.670	9.561	4914	9.592	9.712	9.581
4636	9.593	9.658	9.601	4776	9.565	9.676	9.561	4916	9.588	9.711	9.585
4638	9.594	9.693	9.537	4778	9.564	9.677	9.567	4918	9.587	9.710	9.592
4640	9.597	9.691	9.570	4780	9.560	9.678	9.574	4920	9.589	9.705	9.585
4642	9.588	9.691	9.538	4782	9.557	9.678	9.575	4922	9.586	9.696	9.578
4644	9.586	9.687	9.559	4784	9.552	9.683	9.574	4924	9.588	9.685	9.576
4646	9.594	9.667	9.531	4786	9.554	9.686	9.580	4926	9.589	9.695	9.572
4648	9.583	9.668	9.569	4788	9.571	9.682	9.586	4928	9.585	9.701	9.571
4650	9.568	9.673	9.557	4790	9.572	9.703	9.587	4930	9.586	9.702	9.577
4652	9.573	9.669	9.569	4792	9.573	9.702	9.591	4932	9.590	9.711	9.571
4654	9.574	9.674	9.559	4794	9.580	9.704	9.594	4934	9.594	9.707	9.568
4656	9.572	9.681	9.556	4796	9.582	9.703	9.597	4936	9.590	9.699	9.569
4658	9.565	9.665	9.567	4798	9.576	9.702	9.588	4938	9.590	9.692	9.567
4660	9.570	9.654	9.564	4800	9.567	9.697	9.590	4940	9.588	9.684	9.566
4662	9.573	9.659	9.561	4802	9.580	9.696	9.586	4942	9.583	9.687	9.573
4664	9.575	9.674	9.554	4804	9.553	9.699	9.593	4944	9.581	9.688	9.566
4666	9.574	9.669	9.569	4806	9.590	9.700	9.588	4946	9.582	9.682	9.562
4668	9.572	9.677	9.555	4808	9.590	9.698	9.585	4948	9.580	9.692	9.567
4670	9.577	9.677	9.554	4810	9.588	9.694	9.579	4950	9.576	9.679	9.569
4672	9.573	9.694	9.674	4812	9.555	9.697	9.581	4952	9.576	9.678	9.578
4674	9.568	9.691	9.551	4814	9.581	9.698	9.583	4954	9.571	9.687	9.578
4676	9.571	9.685	9.587	4816	9.578	9.700	9.583	4956	9.575	9.682	9.579
4678	9.577	9.690	9.591	4818	9.579	9.693	9.579	4958	9.581	9.689	9.585
4680	9.576	9.687	9.595	4820	9.572	9.686	9.578	4960	9.581	9.686	9.581
4682	9.554	9.631	9.599	4822	9.534	9.679	9.574	4962	9.582	9.678	9.585
4684	9.564	9.630	9.587	4824	9.589	9.676	9.574	4964	9.583	9.695	9.589
4686	9.535	9.632	9.536	4826	9.589	9.680	9.568	4966	9.580	9.699	9.588
4688	9.569	9.627	9.590	4828	9.590	9.686	9.571	4968	9.576	9.709	9.587
4690	9.571	9.656	9.594	4830	9.593	9.689	9.574	4970	9.574	9.696	9.585
4692	9.578	9.685	9.597	4832	9.595	9.684	9.581	4972	9.576	9.685	9.585
4694	9.578	9.632	9.597	4834	9.596	9.693	9.585	4974	9.571	9.682	9.584
4696	9.577	9.693	9.632	4836	9.595	9.695	9.594	4976	9.576	9.690	9.579
4698	9.555	9.733	9.676	4838	9.590	9.698	9.599	4978	9.576	9.685	9.580
4700	9.573	9.694	9.631	4840	9.590	9.701	9.603	4980	9.573	9.679	9.583
4702	9.567	9.696	9.630	4842	9.588	9.710	9.598	4982	9.580	9.678	9.588
4704	9.557	9.735	9.539	4844	9.586	9.704	9.596	4984	9.579	9.691	9.592
4706	9.571	9.702	9.996	4846	9.590	9.691	9.597	4986	9.585	9.688	9.591
4708	9.573	9.734	9.630	4848	9.591	9.689	9.596	4988	9.593	9.695	9.595
4710	9.568	9.696	9.598	4850	9.586	9.695	9.595	4990	9.590	9.699	9.589
4712	9.556	9.694	9.595	4852	9.579	9.694	9.598	4992	9.589	9.689	9.591
4714	9.562	9.695	9.593	4854	9.577	9.693	9.595	4994	9.593	9.695	9.592
4716	9.558	9.691	9.596	4856	9.580	9.693	9.595	4996	9.597	9.704	9.597
4718	9.563	9.698	9.591	4858	9.586	9.696	9.593	4998	9.598	9.709	9.590
4720	9.562	9.691	9.593	4860	9.588	9.694	9.587	5000	9.603	9.702	9.594
4722	9.554	9.689	9.593	4862	9.591	9.690	9.585	5002	9.602	9.715	9.602
4724	9.565	9.658	9.592	4864	9.595	9.686	9.595	5004	9.608	9.703	9.610
4726	9.555	9.687	9.592	4866	9.595	9.683	9.602	5006	9.607	9.724	9.609
4728	9.576	9.690	9.596	4868	9.594	9.680	9.601	5008	9.605	9.728	9.610
4730	9.590	9.693	9.632	4870	9.589	9.692	9.603	5010	9.608	9.730	9.613
4732	9.582	9.690	9.604	4872	9.590	9.685	9.600	5012	9.609	9.721	9.614
4734	9.579	9.699	9.533	4874	9.587	9.685	9.598	5014	9.607	9.710	9.611
4736	9.579	9.693	9.539	4876	9.591	9.678	9.596	5016	9.597	9.703	9.604
4738	9.578	9.691	9.594	4878	9.584	9.677	9.595	5018	9.587	9.711	9.599
4740	9.578	9.696	9.587	4880	9.593	9.673	9.594	5020	9.586	9.701	9.592
4742	9.575	9.674	9.587	4882	9.595	9.685	9.594	5022	9.587	9.691	9.583
4744	9.573	9.676	9.575	4884	9.599	9.688	9.595	5024	9.588	9.682	9.580
4746	9.577	9.695	9.572	4886	9.610	9.693	9.594	5026	9.581	9.666	9.577
4748	9.583	9.685	9.573	4888	9.632	9.699	9.596	5028	9.582	9.671	9.575
4750	9.587	9.670	9.571	4890	9.632	9.704	9.599	5030	9.581	9.672	9.574
4752	9.582	9.664	9.573	4892	9.596	9.703	9.598	5032	9.582	9.679	9.578
4754	9.581	9.680	9.572	4894	9.590	9.713	9.597	5034	9.590	9.684	9.583
4756	9.583	9.675	9.574	4896	9.595	9.715	9.596	5036	9.589	9.692	9.585
4758	9.572	9.674	9.571	4898	9.596	9.715	9.593	5038	9.588	9.691	9.587

Table A25 Three Track Elevation Profiles

(Stations and elevations are in feet)  
(Sheet 3 of 6)

Station	Elevation			Station	Elevation			Station	Elevation		
	Left	Center	Right		Left	Center	Right		Left	Center	Right
5043	9.581	9.689	9.587	5180	9.586	9.735	9.630	5320	9.657	9.805	9.695
5042	9.580	9.686	9.582	5182	9.577	9.745	9.633	5322	9.658	9.810	9.692
5044	9.577	9.682	9.578	5184	9.597	9.745	9.638	5324	9.667	9.803	9.693
5046	9.585	9.683	9.573	5186	9.612	9.755	9.643	5326	9.668	9.799	9.692
5048	9.572	9.680	9.570	5188	9.599	9.756	9.640	5328	9.576	9.797	9.689
5050	9.571	9.683	9.563	5190	9.591	9.750	9.637	5330	9.675	9.803	9.690
5052	9.575	9.684	9.568	5192	9.595	9.757	9.641	5332	9.677	9.806	9.695
5054	9.579	9.686	9.575	5194	9.621	9.756	9.650	5334	9.680	9.812	9.697
5056	9.580	9.655	9.588	5196	9.597	9.752	9.652	5336	9.686	9.811	9.702
5058	9.589	9.699	9.531	5198	9.535	9.745	9.639	5338	9.689	9.823	9.702
5060	9.588	9.702	9.593	5200	9.595	9.741	9.633	5340	9.683	9.812	9.704
5062	9.582	9.696	9.591	5202	9.591	9.747	9.635	5342	9.680	9.811	9.703
5064	9.577	9.686	9.593	5204	9.622	9.758	9.648	5344	9.675	9.807	9.705
5066	9.558	9.679	9.579	5206	9.610	9.752	9.655	5346	9.572	9.813	9.699
5068	9.569	9.663	9.555	5208	9.623	9.767	9.659	5348	9.680	9.816	9.701
5070	9.575	9.662	9.557	5210	9.630	9.779	9.662	5350	9.694	9.818	9.704
5072	9.574	9.665	9.551	5212	9.623	9.772	9.661	5352	9.699	9.810	9.704
5074	9.568	9.666	9.562	5214	9.624	9.755	9.659	5354	9.705	9.813	9.706
5076	9.571	9.670	9.557	5216	9.623	9.768	9.660	5356	9.710	9.811	9.708
5078	9.569	9.675	9.555	5218	9.619	9.773	9.657	5358	9.714	9.817	9.707
5080	9.558	9.679	9.566	5220	9.620	9.772	9.650	5360	9.707	9.809	9.699
5082	9.565	9.690	9.553	5222	9.622	9.765	9.659	5362	9.699	9.813	9.700
5084	9.559	9.697	9.570	5224	9.627	9.761	9.648	5364	9.697	9.804	9.703
5086	9.566	9.695	9.555	5226	9.628	9.766	9.652	5366	9.697	9.808	9.701
5088	9.555	9.664	9.557	5228	9.624	9.757	9.658	5368	9.702	9.802	9.708
5090	9.553	9.664	9.556	5230	9.633	9.756	9.657	5370	9.708	9.797	9.706
5092	9.565	9.663	9.557	5232	9.634	9.772	9.661	5372	9.713	9.799	9.706
5094	9.565	9.674	9.553	5234	9.643	9.777	9.661	5374	9.719	9.811	9.705
5096	9.564	9.672	9.566	5236	9.637	9.765	9.662	5376	9.731	9.822	9.711
5098	9.552	9.675	9.559	5238	9.625	9.777	9.659	5378	9.737	9.835	9.715
5100	9.565	9.694	9.574	5240	9.627	9.778	9.650	5380	9.744	9.832	9.721
5102	9.555	9.702	9.576	5242	9.622	9.775	9.668	5382	9.746	9.833	9.722
5104	9.565	9.706	9.577	5244	9.638	9.779	9.675	5384	9.751	9.835	9.732
5106	9.573	9.704	9.581	5246	9.643	9.780	9.684	5386	9.760	9.837	9.733
5108	9.569	9.712	9.575	5248	9.641	9.779	9.689	5388	9.764	9.852	9.729
5110	9.564	9.699	9.582	5250	9.645	9.780	9.695	5390	9.768	9.850	9.733
5112	9.571	9.697	9.577	5252	9.653	9.771	9.697	5392	9.769	9.854	9.735
5114	9.568	9.694	9.583	5254	9.655	9.783	9.702	5394	9.773	9.865	9.736
5116	9.554	9.698	9.577	5256	9.654	9.783	9.703	5396	9.780	9.862	9.731
5118	9.561	9.659	9.575	5258	9.657	9.792	9.725	5398	9.781	9.865	9.735
5120	9.552	9.676	9.553	5260	9.652	9.793	9.714	5400	9.777	9.871	9.737
5122	9.542	9.675	9.555	5262	9.653	9.787	9.739	5402	9.777	9.860	9.737
5124	9.544	9.676	9.570	5264	9.663	9.782	9.708	5404	9.777	9.870	9.743
5126	9.539	9.677	9.571	5266	9.664	9.784	9.705	5406	9.783	9.862	9.742
5128	9.537	9.672	9.567	5268	9.664	9.786	9.592	5408	9.781	9.858	9.745
5130	9.536	9.657	9.555	5270	9.650	9.787	9.675	5410	9.782	9.868	9.757
5132	9.547	9.667	9.567	5272	9.657	9.785	9.683	5412	9.785	9.865	9.760
5134	9.549	9.657	9.555	5274	9.655	9.782	9.681	5414	9.786	9.864	9.763
5136	9.539	9.661	9.561	5276	9.650	9.789	9.575	5416	9.783	9.871	9.763
5138	9.535	9.652	9.553	5278	9.641	9.780	9.667	5418	9.777	9.873	9.762
5140	9.542	9.653	9.549	5280	9.633	9.774	9.562	5420	9.775	9.877	9.760
5142	9.545	9.651	9.557	5282	9.629	9.766	9.662	5422	9.780	9.883	9.766
5144	9.548	9.664	9.555	5284	9.624	9.757	9.557	5424	9.787	9.880	9.770
5146	9.552	9.678	9.573	5286	9.621	9.775	9.645	5426	9.783	9.872	9.775
5148	9.555	9.672	9.574	5288	9.635	9.775	9.557	5428	9.785	9.869	9.777
5150	9.552	9.675	9.573	5290	9.639	9.773	9.667	5430	9.787	9.862	9.784
5152	9.565	9.664	9.570	5292	9.643	9.775	9.666	5432	9.790	9.857	9.786
5154	9.565	9.674	9.573	5294	9.655	9.780	9.666	5434	9.797	9.875	9.793
5156	9.578	9.698	9.535	5296	9.664	9.793	9.650	5436	9.796	9.887	9.793
5158	9.590	9.705	9.590	5298	9.652	9.801	9.567	5438	9.795	9.883	9.792
5160	9.599	9.715	9.611	5300	9.657	9.801	9.674	5440	9.787	9.882	9.787
5162	9.589	9.718	9.604	5302	9.653	9.805	9.557	5442	9.786	9.887	9.785
5164	9.599	9.723	9.607	5304	9.661	9.808	9.689	5444	9.781	9.877	9.783
5166	9.598	9.719	9.613	5306	9.657	9.804	9.685	5446	9.777	9.870	9.774
5168	9.632	9.723	9.617	5308	9.657	9.802	9.691	5448	9.785	9.866	9.773
5170	9.631	9.735	9.615	5310	9.659	9.801	9.644	5450	9.791	9.865	9.767
5172	9.599	9.730	9.623	5312	9.652	9.809	9.699	5452	9.754	9.857	9.764
5174	9.592	9.738	9.627	5314	9.652	9.808	9.701	5454	9.770	9.855	9.763
5176	9.592	9.732	9.633	5316	9.655	9.807	9.730	5456	9.771	9.866	9.767
5178	9.597	9.734	9.634	5318	9.660	9.805	9.702	5458	9.772	9.850	9.767

Table A25 Three Track Elevation Profiles

(Stations and elevations are in feet)  
(Sheet 4 of 6)

Station	Elevation			Station	Elevation			Station	Elevation		
	Left	Center	Right		Left	Center	Right		Left	Center	Right
5463	9.777	9.869	9.753	5631	9.838	9.917	9.862	5740	9.964	13.058	9.944
5462	9.769	9.861	9.789	5632	9.837	9.926	9.851	5742	9.967	13.052	9.943
5464	9.769	9.859	9.787	5604	9.831	9.921	9.862	5744	9.964	13.056	9.945
5466	9.767	9.868	9.791	5506	9.831	9.931	9.866	5746	9.962	13.049	9.946
5468	9.769	9.852	9.788	5608	9.836	9.937	9.876	5748	9.970	13.056	9.959
5470	9.785	9.886	9.792	5513	9.828	9.936	9.875	5750	9.972	13.064	9.966
5472	9.797	9.893	9.795	5612	9.827	9.926	9.874	5752	9.972	13.089	9.974
5474	9.801	9.897	9.803	5514	9.824	9.932	9.876	5754	9.967	13.088	9.977
5476	9.803	9.900	9.797	5616	9.818	9.946	9.879	5756	9.966	13.092	9.981
5478	9.804	9.896	9.795	5618	9.829	9.953	9.876	5758	9.974	13.091	9.983
5480	9.810	9.915	9.799	5620	9.837	9.952	9.887	5760	9.982	13.098	9.985
5482	9.811	9.929	9.803	5622	9.841	9.956	9.884	5762	9.980	13.101	9.982
5484	9.812	9.927	9.806	5624	9.846	9.953	9.881	5764	9.976	13.097	9.985
5486	9.819	9.929	9.813	5626	9.846	9.961	9.879	5766	9.975	13.098	9.983
5488	9.818	9.922	9.807	5628	9.846	9.973	9.885	5768	9.979	13.100	9.976
5490	9.815	9.927	9.807	5630	9.843	9.972	9.887	5770	9.978	13.087	9.975
5492	9.807	9.931	9.801	5532	9.849	9.978	9.893	5772	9.967	13.094	9.976
5494	9.807	9.920	9.793	5634	9.850	9.977	9.896	5774	9.973	13.087	9.975
5496	9.793	9.919	9.783	5535	9.859	9.979	9.906	5776	9.970	13.092	9.974
5498	9.792	9.918	9.776	5638	9.860	9.986	9.909	5778	9.967	13.097	9.975
5500	9.795	9.905	9.774	5640	9.864	9.993	9.916	5780	9.963	13.095	9.976
5502	9.797	9.903	9.771	5642	9.867	9.999	9.925	5782	9.963	13.089	9.979
5504	9.800	9.905	9.775	5644	9.862	10.006	9.927	5784	9.957	13.084	9.976
5506	9.797	9.904	9.779	5646	9.857	10.008	9.929	5786	9.943	13.077	9.977
5508	9.799	9.905	9.754	5548	9.862	10.011	9.936	5788	9.934	13.067	9.979
5510	9.799	9.906	9.788	5650	9.873	10.017	9.945	5790	9.930	13.067	9.983
5512	9.802	9.902	9.735	5652	9.880	10.021	9.951	5792	9.927	13.064	9.982
5514	9.801	9.904	9.784	5654	9.887	10.023	9.952	5794	9.914	13.062	9.980
5516	9.801	9.903	9.795	5656	9.897	10.041	9.955	5796	9.915	13.066	9.978
5518	9.803	9.902	9.790	5558	9.903	10.043	9.956	5798	9.912	13.074	9.975
5520	9.803	9.904	9.795	5660	9.907	10.039	9.956	5800	9.910	13.071	9.975
5522	9.802	9.892	9.800	5562	9.910	12.039	9.954	5802	9.923	13.073	9.984
5524	9.801	9.900	9.800	5664	9.910	12.046	9.949	5804	9.925	13.091	9.987
5526	9.806	9.904	9.804	5566	9.914	12.039	9.945	5806	9.927	13.088	9.994
5528	9.809	9.899	9.807	5668	9.911	12.033	9.942	5808	9.933	13.105	10.001
5530	9.797	9.887	9.815	5570	9.913	12.033	9.939	5810	9.942	13.131	10.002
5532	9.797	9.904	9.824	5672	9.916	12.028	9.932	5812	9.947	13.125	9.994
5534	9.799	9.913	9.827	5574	9.914	12.028	9.926	5814	9.963	13.123	9.991
5536	9.814	9.909	9.826	5676	9.926	12.037	9.929	5816	9.965	13.108	9.984
5538	9.818	9.929	9.827	5578	9.929	12.044	9.937	5818	9.973	13.113	9.987
5540	9.817	9.933	9.827	5680	9.926	12.049	9.944	5820	9.970	13.134	9.985
5542	9.825	9.937	9.825	5582	9.925	12.057	9.950	5822	9.975	13.101	9.985
5544	9.823	9.933	9.835	5684	9.934	12.062	9.949	5824	9.973	13.095	9.986
5546	9.823	9.927	9.835	5586	9.933	12.052	9.949	5826	9.967	13.091	9.987
5548	9.828	9.938	9.839	5688	9.930	12.052	9.951	5828	9.963	13.095	9.998
5550	9.826	9.927	9.843	5590	9.923	12.054	9.954	5830	9.961	13.105	10.004
5552	9.820	9.930	9.843	5692	9.936	12.055	9.952	5832	9.963	13.137	10.011
5554	9.822	9.933	9.847	5594	9.947	12.053	9.949	5834	9.960	13.118	10.015
5556	9.821	9.922	9.850	5696	9.944	12.045	9.942	5836	9.959	13.121	10.014
5558	9.822	9.930	9.854	5598	9.939	12.028	9.937	5838	9.963	13.115	10.013
5560	9.829	9.937	9.863	5700	9.939	12.032	9.929	5840	9.960	13.111	10.017
5562	9.833	9.947	9.855	5702	9.914	12.029	9.929	5842	9.967	13.105	10.015
5564	9.847	9.956	9.858	5704	9.917	12.024	9.925	5844	9.963	13.108	10.009
5566	9.893	9.947	9.862	5706	9.913	12.030	9.932	5846	9.957	13.115	10.004
5568	9.849	9.947	9.861	5708	9.921	12.036	9.936	5848	9.964	13.112	10.003
5570	9.849	9.961	9.863	5710	9.929	12.040	9.943	5850	9.977	13.103	9.996
5572	9.856	9.948	9.854	5712	9.931	12.044	9.947	5852	9.985	13.115	9.995
5574	9.841	9.963	9.871	5714	9.929	12.044	9.942	5854	9.990	13.111	9.993
5576	9.841	9.962	9.878	5716	9.934	12.052	9.952	5856	9.991	13.105	9.993
5578	9.843	9.963	9.877	5718	9.933	12.055	9.954	5858	9.988	13.105	9.994
5580	9.845	9.963	9.875	5720	9.934	12.056	9.953	5860	9.987	13.100	10.003
5582	9.840	9.970	9.875	5722	9.938	12.068	9.962	5862	9.988	13.095	10.003
5584	9.839	9.953	9.874	5724	9.938	12.050	9.949	5864	9.983	13.091	9.999
5586	9.861	9.954	9.862	5726	9.940	12.054	9.957	5866	9.971	13.088	9.992
5588	9.843	9.954	9.861	5728	9.943	12.049	9.956	5868	9.962	13.082	9.988
5590	9.845	9.943	9.861	5730	9.943	12.054	9.955	5870	9.957	13.081	9.985
5592	9.836	9.934	9.862	5732	9.950	12.053	9.956	5872	9.952	13.088	9.979
5594	9.834	9.935	9.862	5734	9.953	12.043	9.949	5874	9.950	13.073	9.976
5596	9.833	9.911	9.865	5736	9.958	12.041	9.949	5876	9.943	13.064	9.973
5598	9.833	9.916	9.853	5738	9.958	12.049	9.939	5878	9.947	13.061	9.965

Table A25 Three Track Elevation Profiles

(Stations and elevations are in feet)  
(Sheet 5 of 6)

Station	Elevation		
	Left	Center	Right
5880	9.945	13.055	9.957
5882	9.943	13.041	9.954
5884	9.947	13.025	9.947
5886	9.943	13.026	9.946
5888	9.945	13.028	9.952
5890	9.952	13.021	9.957
5892	9.957	13.038	9.967
5894	9.961	13.053	9.968
5896	9.953	13.065	9.994
5898	9.971	13.071	10.005
5900	9.973	13.075	10.036
5902	9.989	13.072	10.038
5904	10.002	10.081	10.009
5906	13.008	13.089	13.037
5908	10.017	13.102	10.003
5910	13.032	13.112	9.997
5912	10.027	13.114	10.002
5914	13.039	10.117	10.034
5916	10.038	13.116	13.038
5918	10.040	13.115	10.010
5920	13.041	13.115	13.035
5922	10.038	13.109	10.001
5924	10.050	13.123	13.072
5926	10.013	13.113	9.998
5928	9.994	13.105	10.000
5930	9.983	10.111	13.074
5932	9.970	13.110	10.074
5934	9.957	10.098	10.070
5936	9.987	10.134	9.997
5938	9.953	13.098	9.993
5940	9.982	13.093	9.991
5942	9.983	13.091	9.956
5944	9.980	10.099	9.980
5946	9.976	13.098	9.975
5948	9.982	13.092	9.980
5950	9.993	13.091	9.984
5952	10.003	13.095	9.987
5954	13.078	13.101	9.992
5956	10.079	13.125	9.997
5958	13.110	13.123	13.010
5960	10.033	10.135	13.037
5962	13.070	13.138	10.002
5964	9.995	13.128	9.997
5966	9.994	13.115	9.988
5968	9.958	13.103	9.954
5970	9.987	10.100	9.977
5972	9.957	13.094	9.974
5974	9.984	13.097	9.955
5976	9.957	13.099	9.959
5978	9.991	13.095	9.954
5980	9.993	10.098	9.955
5982	9.992	13.095	9.951
5984	9.997	10.090	9.947
5986	9.975	13.092	9.955
5988	9.987	10.094	9.957
5990	9.954	13.093	9.963
5992	9.983	13.083	9.957
5994	9.975	13.038	9.966
5996	9.976	13.038	9.954
5998	9.975	10.086	9.965
6000	9.977	13.075	9.954
6002	9.960	13.071	9.959
6004	9.953	13.070	9.955
6006	9.945	13.073	9.965
6008	9.953	13.071	9.968
6010	9.956	13.068	9.977
6012	9.957	13.077	9.981
6014	9.953	13.079	9.934
6016	9.967	13.083	9.987
6018	9.955	13.079	9.955

Station	Elevation		
	Left	Center	Right
6020	9.962	10.082	9.979
6022	9.954	10.083	9.975
6024	9.955	10.086	9.972
6026	9.953	10.080	9.975
6028	9.957	10.076	9.971
6030	9.960	10.085	9.975
6032	9.963	10.096	9.972
6034	9.969	10.092	9.959
6036	9.973	10.096	9.964
6038	9.973	10.093	9.960
6040	9.973	10.089	9.959
6042	9.978	10.089	9.958
6044	9.976	10.087	9.955
6046	9.975	10.088	9.955
6048	9.973	10.054	9.951
6050	9.972	10.084	9.946
6052	9.950	10.073	9.946
6054	9.931	10.082	9.946
6056	9.952	10.089	9.951
6058	9.958	10.093	9.945
6060	9.933	10.092	9.954
6062	9.950	10.093	9.952
6064	9.979	10.091	9.942
6066	9.970	10.093	9.943
6068	9.970	10.082	9.942
6070	9.975	10.076	9.955
6072	9.976	10.085	9.963
6074	9.977	10.086	9.968
6076	9.953	10.085	9.973
6078	9.955	10.088	9.981
6080	9.980	10.103	9.980
6082	9.933	10.108	9.986
6084	9.937	10.105	9.985
6086	9.930	10.089	9.996
6088	9.930	10.092	9.998
6090	9.933	10.085	9.996
6092	9.977	10.096	9.996
6094	9.976	10.089	9.991
6096	9.964	10.092	9.982
6098	9.965	10.083	9.983
6100	9.953	10.085	9.986
6102	9.956	10.076	9.988
6104	9.941	10.081	9.988
6106	9.957	10.079	9.986
6108	9.955	10.076	9.987
6110	9.952	10.074	9.958
6112	9.946	10.072	9.985
6114	9.944	10.077	9.952
6116	9.943	10.075	9.975
6118	9.941	10.071	9.977
6120	9.941	10.079	9.975
6122	9.938	10.063	9.960
6124	9.938	10.070	9.969
6126	9.935	10.074	9.968
6128	9.940	10.073	9.972
6130	9.934	10.077	9.977
6132	9.935	10.076	9.974
6134	9.937	10.059	9.970
6136	9.943	10.077	9.969
6138	9.940	10.070	9.967
6140	9.934	10.061	9.970
6142	9.935	10.073	9.971
6144	9.937	10.066	9.972
6146	9.933	10.067	9.977
6148	9.936	10.066	9.981
6150	9.932	10.074	9.987
6152	9.930	10.069	9.996
6154	9.933	10.066	10.004
6156	9.932	10.082	10.005
6158	9.936	10.071	10.006

Station	Elevation		
	Left	Center	Right
6160	9.937	10.079	10.011
6162	9.957	10.086	10.012
6164	9.938	10.078	10.013
6166	9.940	10.096	10.016
6168	9.940	10.095	10.014
6170	9.958	10.096	10.009
6172	9.940	10.076	9.999
6174	9.945	10.085	10.006
6176	9.942	10.080	10.005
6178	9.939	10.079	10.002
6180	9.942	10.070	10.002
6182	9.938	10.062	9.999
6184	9.942	10.059	9.995
6186	9.955	10.063	9.995
6188	9.946	10.057	9.986
6190	9.943	10.065	9.985
6192	9.934	10.062	9.973
6194	9.936	10.049	9.962
6196	9.930	10.048	9.955
6198	9.929	10.059	9.954
6200	9.927	10.049	9.954
6202	9.929	10.081	9.955
6204	9.922	10.075	9.949
6206	9.914	10.071	9.940
6208	9.912	10.061	9.945
6210	9.900	10.071	9.949
6212	9.897	10.060	9.953
6214	9.894	10.058	9.949
6216	9.887	10.062	9.949
6218	9.889	10.061	9.944
6220	9.887	10.063	9.941
6222	9.886	10.068	9.935
6224	9.880	10.061	9.929
6226	9.877	10.055	9.925
6228	9.873	10.065	9.916
6230	9.867	10.061	9.914
6232	9.860	10.055	9.912
6234	9.853	10.043	9.915
6236	9.850	10.044	9.922
6238	9.846	10.041	9.921
6240	9.841	10.031	9.919
6242	9.844	10.021	9.918
6244	9.854	10.015	9.909
6246	9.848	10.018	9.903
6248	9.840	9.997	9.899
6250	9.844	10.009	9.898
6252	9.840	10.018	9.896
6254	9.836	10.015	9.899
6256	9.853	10.022	9.903
6258	9.827	10.013	9.899
6260	9.827	10.001	9.891
6262	9.821	10.004	9.886
6264	9.821	9.987	9.883
6266	9.826	9.956	9.879
6268	9.828	9.958	9.881
6270	9.830	9.963	9.882
6272	9.830	9.964	9.881
6274	9.831	9.972	9.879
6276	9.832	9.978	9.884
6278	9.830	9.984	9.886
6280	9.827	9.984	9.885
6282	9.823	9.974	9.890
6284	9.824	9.973	9.891
6286	9.824	9.967	9.890
6288	9.823	9.958	9.882
6290	9.820	9.949	9.879
6292	9.815	9.957	9.870
6294	9.806	9.952	9.863
6296	9.807	9.948	9.855
6298	9.819	9.941	9.853

Table A25 Three Track Elevation Profiles

(Stations and elevations are in feet)

(Sheet 6 of 6)

Station	Elevation			Station	Elevation			Station	Elevation		
	Left	Center	Right		Left	Center	Right		Left	Center	Right
6330	9.818	9.937	9.852	6392	9.754	9.864	9.779	6484	9.691	9.752	9.657
6302	9.817	9.935	9.853	6394	9.743	9.856	9.775	6486	9.691	9.755	9.657
6374	9.822	9.937	9.849	6396	9.727	9.853	9.772	6488	9.648	9.731	9.648
6306	9.815	9.934	9.855	6398	9.723	9.846	9.765	6490	9.643	9.737	9.645
6308	9.811	9.928	9.852	6400	9.719	9.854	9.781	6492	9.641	9.734	9.639
6310	9.809	9.931	9.851	6432	9.716	9.849	9.780	6494	9.636	9.730	9.637
6312	9.807	9.936	9.847	6404	9.721	9.855	9.779	6496	9.636	9.732	9.640
6314	9.806	9.937	9.855	6406	9.727	9.854	9.780	6498	9.635	9.730	9.643
6316	9.803	9.939	9.843	6408	9.734	9.846	9.784	6500	9.637	9.734	9.637
6318	9.796	9.943	9.841	6410	9.744	9.849	9.787	6502	9.641	9.736	9.635
6320	9.794	9.944	9.835	6412	9.750	9.850	9.786	6504	9.642	9.738	9.641
6322	9.799	9.949	9.822	6414	9.753	9.855	9.776	6506	9.640	9.736	9.642
6324	9.784	9.947	9.829	6416	9.757	9.856	9.774	6508	9.641	9.739	9.641
6326	9.781	9.948	9.830	6418	9.759	9.858	9.773	6510	9.640	9.737	9.639
6328	9.783	9.949	9.832	6420	9.758	9.862	9.771	6512	9.638	9.739	9.637
6330	9.782	9.941	9.833	6422	9.755	9.859	9.775	6514	9.639	9.735	9.639
6332	9.783	9.944	9.832	6424	9.752	9.861	9.765	6516	9.637	9.735	9.637
6334	9.786	9.938	9.835	6426	9.754	9.862	9.753	6518	9.635	9.733	9.635
6336	9.787	9.956	9.842	6428	9.751	9.856	9.760	6520	9.633	9.736	9.638
6338	9.794	9.956	9.841	6430	9.749	9.859	9.755	6522	9.627	9.742	9.637
6340	9.796	9.950	9.839	6432	9.739	9.852	9.791	6524	9.626	9.733	9.634
6342	9.793	9.954	9.835	6434	9.712	9.847	9.743	6526	9.623	9.731	9.630
6344	9.792	9.934	9.834	6436	9.729	9.834	9.733	6528	9.620	9.727	9.625
6346	9.794	9.938	9.823	6438	9.724	9.830	9.724	6530	9.612	9.721	9.620
6348	9.793	9.923	9.826	6440	9.721	9.831	9.720	6532	9.608	9.713	9.616
6350	9.784	9.931	9.823	6442	9.717	9.827	9.720	6534	9.610	9.704	9.609
6352	9.783	9.921	9.825	6444	9.716	9.826	9.714	6536	9.607	9.702	9.604
6354	9.783	9.929	9.820	6446	9.716	9.822	9.713	6538	9.602	9.713	9.597
6356	9.779	9.924	9.812	6448	9.717	9.822	9.707	6540	9.597	9.694	9.594
6358	9.782	9.914	9.814	6450	9.720	9.821	9.711	6542	9.599	9.701	9.595
6360	9.786	9.927	9.804	6452	9.721	9.827	9.713	6544	9.597	9.698	9.592
6362	9.790	9.910	9.798	6454	9.718	9.830	9.714	6546	9.674	9.696	9.591
6364	9.794	9.909	9.793	6456	9.721	9.831	9.719	6548	9.677	9.699	9.593
6366	9.797	9.914	9.786	6458	9.721	9.830	9.720	6550	9.593	9.702	9.600
6368	9.795	9.912	9.786	6460	9.720	9.824	9.720	6552	9.588	9.706	9.604
6370	9.794	9.914	9.785	6462	9.724	9.829	9.711	6554	9.588	9.692	9.625
6372	9.794	9.906	9.794	6464	9.718	9.827	9.711	6556	9.590	9.704	9.603
6374	9.793	9.905	9.786	6466	9.727	9.817	9.710	6558	9.591	9.707	9.603
6376	9.787	9.904	9.783	6468	9.698	9.812	9.704	6560	9.588	9.708	9.601
6378	9.782	9.898	9.791	6470	9.693	9.809	9.696	6562	9.589	9.704	9.594
6380	9.793	9.908	9.788	6472	9.693	9.811	9.683	6564	9.591	9.692	9.587
6382	9.778	9.903	9.784	6474	9.682	9.799	9.682	6566	9.590	9.695	9.585
6384	9.776	9.901	9.783	6476	9.680	9.786	9.681	6568	9.590	9.696	9.589
6386	9.774	9.888	9.784	6478	9.677	9.777	9.680	6570	9.591	9.702	9.594
6388	9.773	9.884	9.779	6480	9.660	9.766	9.673	6572	9.597	9.701	9.593
6390	9.762	9.879	9.776	6482	9.653	9.758	9.663	6574	9.587	9.703	9.583

Table A26 Runway System Parameters (6 Degree)

SYMBOL	TYPE	VALUE	UNITS	DESCRIPTION
$H_{RC}(i)$	C	*	Ft	Center runway elevation profile
$H_{RL}(i)$	C	*	Ft	Left runway elevation profile
$H_{RR}(i)$	C	*	Ft	Right runway elevation profile
$\omega$	V (O)		In/In	Runway slope at coordinate (X,Y)
$\alpha$	V (I)		In	Distance down the runway
$X_{LRO}$ ★	C	0.0	Ft	Determines starting point (at time = 0) on runway profile
$X_{LRF}$	V		Ft	Determines position on runway profile
$\eta$	V (I)		In	Distance from runway C., Inches
$Y_{LRF}$	V		Ft	Distance from runway C., Feet
$Z$	V (O)		In	Runway elevation at coordinate (X,Y)
$Z_{GCO}$	C	#	Ft	Center profile height at time = 0
$Z_{GCX}$	V		Ft	Center profile height
$Z_{GLO}$	C	#	Ft	Left profile height at time = 0
$Z_{GLX}$	V		Ft	Left profile height
$Z_{GRO}$	C	#	Ft	Right profile height at time = 0
$Z_{GRX}$	V		Ft	Right profile height

\* See Table A25 for values of  $H_{RC}$ ,  $H_{RL}$  and  $H_{RR}$ . Use station 4574 to 6574.

# Determined from the constant  $X_{LRO}$

★ This input allows starting the airplane on a different part of the runway profile even though its distance down the runway is the same.

## APPENDIX B

### DIGITAL COMPUTER PROGRAM FOR SIMPLIFIED ANTISKID ANALYSIS PROCEDURE

The user's instructions for CDC 6600 procedure A6A which is a program for solving the equations for the simplified antiskid analysis procedure as described in Section III are as follows:

#### INPUT DATA

Input card data shall be tabulated on Data Sheets according to the following format for all cards:

1-66	67-72	73	74-75	76-79
Problem Data	Job	"P"	PN	CS

PN-- problem number, CS--card sequence number (numbered sequentially from 0001).

The problem data is defined by the following formats. Unless otherwise indicated, data should be entered as floating point.

#### Card 1

Card Columns

1-30		37-45		47
ID		JOB		M

#### Columns

1-30

37-45

47

#### Variable Description

ID -- Alphanumeric Identification

JOB -- Problem Name (alphanumeric)

M = 1 printed output only

= 2 microfilm output only

= 3 printed and microfilm output

Card 2

Card Columns

1-10	11-20	21-30	31-40
TSTEP	TINTP	TEND	TRITE

Variable

Description

TSTEP	Time between steps
TINTP	Internal print interval
TEND	System run time
TRITE	System print interval

Card 3

Card Columns

1-10	11-20	21-30	31-40	41-45
ACVRO	ACVSO	PCVB	VMIN	NR

Variable

Description

ACVRO	Control valve return full flow coefficient
ACVSO	Control valve supply full flow coefficient
PCVB	Control valve bias pressure
VMIN	Flywheel velocity for terminating problem
NR	Number of Brake rotors

# Simplified Brake Control System (Cards 4-11)

1-10	11-20	21-30	31-40	41-50	51-60	Cards.
ALPHA	ALPHB	ABP	ABPS	XGDD	VFD	4
ACVL	CBPL	CBPU	CG	CSCVR	DG	5
ET	FNM	GCV	PBO	PCP	PFB	6
PR	RBT	RR	RTD	SCL	SCVO	7
SCVA	SCVR	TCP	UB1	UB2	UT1	8
UT2	VF	VRO	WG	WTO	WIT	9
XCVO	XSCM	XSCR	XBO	XGO	XDGO	10
XFO	XFDO					11

Variable	Description
ALPHA	Tire Friction Parameter ( $\alpha$ )
ALPHB	Brake Lining Friction Parameter ( $\alpha_B$ )
ABP	Piston area/brake
ABPS	Piston area/control valve
XGDD	Axle horizontal acceleration ( $\ddot{x}_g$ )
VFD	Flywheel peripheral acceleration ( $\ddot{v}_f$ )
ACVL	Control valve leakage flow coefficient
CBPL	Brake P-V slope (disk not in contact)
CBPU	Brake P-V slope (disc in contact)
CG	Fore and aft spring rate at axle
CSCVR	Control valve input coefficient
DG	Fore and aft damping coefficient at axle.
ET	Tire friction velocity correction coefficient
FNM	Vertical force on tire from ground
GCV	Control valve gain
PBO	Brake pressure (at time zero)
PCP	Pilots command brake pressure
PFB	Brake piston friction hysteresis pressure
PR	Hydraulic system reservoir pressure
RBT	Brake piston torque producing radius
RR	Tire effective rolling radius
RTD	Axle height (above ground)
SCL	Control valve overlap

<u>Variable</u>	<u>Description</u>
SCVO	Control valve full open spool travel
SCVA	Control valve maximum application travel
SCVR	Control valve maximum release travel
TCP	Time to reach maximum command pressure
UB1	Brake lining friction parameter
UB2	Brake lining friction parameter
UT1	Tire friction parameter
UT2	Tire friction parameter
VF	Flywheel peripheral velocity
VRO	Tire - friction vs. velocity - parameter
WG	Mass of: Wheel, Tire, Brake, & supporting structure
WTO	Angular velocity of Tire & Wheel (at time zero)
WIT	Moment of Inertia: Tire, Wheel, & Brake rotor
XCVO	Control valve spool position (at time zero)
XSCM	Value of $X_{SC}$ for maximum regulation '
XSCR	Value of $X_{SC}$ for zero regulation'
XBO	Brake piston position (at time zero)
XGO	Axle horizontal position (at time zero) ( $X_{GO}$ )
XDGO	Axle horizontal velocity (at time zero) ( $X_{GO}$ )
XFO	Flywheel peripheral distance (at time zero) ( $X_{FO}$ )
XFDO	Flywheel peripheral velocity (at time zero) ( $X_{FO}$ )

1)  $X_{SC}$  is the control valve pressure regulation parameter.

## Wheel Speed Sensor System

Card 12 (follows the Simplified Brake Control Systems cards)

2	Card
IOPT	12

<u>Variable</u>	<u>Description</u>
IOPT=1	the control circuit input signal is proportional to the mass displacement
IOPT=2	the control circuit input voltage is considered proportional to the wheel's angular velocity.

The wheel speed sensor system has two approaches as mentioned above. The problem data varies for each approach taken.

IOPT=1

Card Columns

1-10	11-20	21-30	31-40	41-50	51-60	Card
CCGV	CWG	CWS	DWS	GWS	WWS	13
ESN	XWS	XWS	EG			14

<u>Variable</u>	<u>Description</u>
CCGV	Output voltage coefficient (volt/in)
CWG	Hypothetical linear force motor coefficient (lbf/volt)
CWS	Spring rate (hypothetical spring) (lbf/in)
DWS	Damping coefficient (hypothetical damper) (lbf/in)
GWS	Hypothetical tachometer voltage-speed coefficient (volt sec/rad)
WWS	Mass (hypothetical mass) (lbf sec <sup>2</sup> /in)
ESN	Input signal "noise" (volts)
XWS	Hypothetical mass displacement at time=0 (in)
XWS	Hypothetical mass velocity at time=0 (in/sec)
EG	Anti-skid control circuit input signal (volts)

IOPT=2

Card Columns

1-10	11-20	21-30	Card
GWOC	ESN	EG	13

<u>Variable</u>	<u>Description</u>
GWOC	D.C. tachometer voltage-speed coefficient (volt sec/rad)
ESN	Input signal "noise" (volts)
EG	Anti-skid control circuit input signal (volts)

Card Group A (follows wheel)

2	Card
I	A1

<u>Variable</u>	<u>Description</u>
I=1	a modulated (brake pressure) circuit will be used to simulate the control system.
I=2	an electrical on-off circuit will be used to simulate the control system.

# Modulated Circuit

## Card Columns

1-10	11-20	21-30	31-40	41-50	51-60	Card
CM	C404	C405	C406	C407	C446	A2
C447	C448	C449	C450	C451	C452	A3
C456	C457	C458	C459	C460	C461	A4
C462	C526	C527	C528	C529	C530	A5
C531	C532	C533	C534	C535	C565	A6
C566	C567	C568	C569	C570	C571	A7
C575	C576	C577	C578	C579	C580	A8
C581	C604	C605	C606	C607	C608	A9
C609	C610	C611	C612	C613	C614	A10
C615	C616	C617	C618	C619	C620	A11
C621	C622	C623	C800	C801	C802	A12
C803	C804	C805	C806	C807	C808	A13
C809	C810	C811	C812	VC1	VC2	A14
VC3	VC4	VC1	VC2	VC3	VC4	A15
EV						A16

## Variable

## Description

CM	VC2 voltage coefficient equ VB
C404	ACQ3 coeff equ N7, N5-3-4, N5-7-8, N5-11-12 (DIMLS)
C405	Const equ N7, N5-3-4, N5-78, N5-11-12 (AMPS)
C406	AD5 coeff equ N4 (OHMS)
C407	Const equ N4 (VOLTS)
C446	(EG-VC1) coeff equ Q2-3 (MHOS)
C447	(VC3+VC4) coeff equ Q2-3 (MHOS)
C448	Const equ Q2-3 (AMPS)
C449	(EG-VC1) coeff equ Q2-4 (MHOS)
C450	VC2 coeff equ Q2-4 (MHOS)
C451	(VC3+VC4) coeff equ Q2-4 (MHOS)
C452	Const equ Q2-4 (AMPS)
C456	(EG-VC1) coeff equ Q2-1 (MHOS)
C457	(VC3+VC4) coeff equ Q2-1 (MHOS)
C458	Const equ Q2-1 (AMPS)
C459	(EG-VC1) coeff equ Q2-2 (MHOS)
C460	(VC3+VC4) coeff equ Q2-2 (MHOS)
C461	VC2 coeff equ Q2-2 (MHOS)
C462	Const equ Q202 (AMPS)

<u>Variable</u>	<u>Description</u>
C526	(EG-VC1) coeff equ Q2-7 (MHOS)
C527	Const equ Q2-7 (AMPS)
C528	VC2 coeff equ Q2-8 (MHOS)
C529	(EG-VC1) coeff equ Q2-8 (MHOS)
C530	Const equ Q2-8 (AMPS)
C531	(EG-VC1) Coeff equ Q2-5 (MHOS)
C532	Const Equ Q2-5 (AMPS)
C533	VC2 coeff equ Q2-6 (MHOS)
C534	(EG-VC1) coeff equ Q2-6 (MHOS)
C535	Const equ Q2-6 (AMPS)
C565	(EG-VC1) coeff equ Q2-9 (MHOS)
C566	(VC2+VC4) coeff equ Q2-9 (MHOS)
C567	Const equ Q2-9 (AMPS)
C568	VC2 coeff equ Q2-10 (MHOS)
C569	(EG-VC1) coeff equ Q2-10 (MHOS)
C570	(VC2+VC4) coeff equ Q2-10 (MHOS)
C571	Const equ Q2-10 (AMPS)
C575	(EG-VC1) coeff equ Q2-11 (MHOS)
C576	(VC2+VC4) coeff equ Q2-11 (MHOS)
C577	Const equ Q2-11 (AMPS)
C578	VC2 coeff equ Q2-12 (MHOS)
C579	(EG-VC1) coeff equ Q2-12 (MHOS)
C580	(VC2+VC4) coeff equ Q2-12 (MHOS)
C581	Const equ Q2-12 (AMPS)
C604	Const equ Q1C (AMPS)
C605	VC2 coeff equ Q-1C (MHOS)
C606	Q3 collector - Q2 emitter current ratio
C607	AEQ2 comparison constant (AMPS)
C608	Reciprocal of capacitance C1 (VOLT/AMP SEC)
C609	Reciprocal of capacitance C2 (VOLT/AMP SEC)
C610	Reciprocal of capacitance C3 (VOLT/AMP SEC)
C611	Reciprocal of capacitance C4 (VOLT/AMP SEC)
C612	AEQ2 coeff equ N10
C613	VV-EG+VC1 coeff equ N10 (MHOS)
C614	Emitter-base current ratio - Q4
C615	Locked wheel arming speed (IN/SEC)
C616	Locked wheel signal detection speed (VOLTS)
C617	Locked wheel signal current (AMPS)
C618	VC2 coeff equ 14 (MHOS)
C619	VC3 coeff equ N3 (MHOS)
C620	(EG-VC1) coeff equ R10 (MHOS)
C621	Const equ R10 (AMPS)
C622	(VC3-VC2) coeff equ VC4 (MHOS)
C623	Const equ VQ4 (AMPS)
C800	Constant equ VB (VOLTS)

Variable      Description

C801      AEQ2 coeff equ VB (OHMS)  
C802      Max. valve for AEQ2 equ Q2-N (AMPS)  
C803      AEQ2 coeff equ N8-3, 4, 7 & 8 (DIMLS)  
C804      (VC3+VC4) coeff equ N8-1 to N8-8 (MHOS)  
C805      Constant equ N8-3, 4, 7 & 8 (AMPS)  
C806      AEQ2 coeff equ N8-1, 2, 5 & 6 (DIMLS)  
C807      Constant equ N8-1, 2, 5 & 6 (AMPS)  
C808      AEQ2 coeff equ N8-7, 8, 11 & 12 (DIMLS)  
C809      (VC2+VC4) coeff equ N8-5 to N8-12 (MHOS)  
C810      Constant equ N8-7, 8, 11 & 12 (AMPS)  
C811      AEQ2 coeff equ N8-5, 6, 9 & 10 (DIMLS)  
C812      Constant equ N8-5, 6, 9 & 10 (AMPS)  
VC1      Voltage across capacitor C1 at time=0 (VOLTS)  
VC2      Voltage across capacitor C2 at time=0 (VOLTS)  
VC3      Voltage across capacitor C3 at time=0 (VOLTS)  
VC4      Voltage across capacitor C4 at time=0 (VOLTS)  
VC1      Capacitor C1 voltage change rate (volts/sec)  
VC2      Capacitor C2 voltage change rate (volts/sec)  
VC3      Capacitor C3 voltage change rate (volts/sec)  
VC4      Capacitor C4 voltage change rate (volts/sec)  
EV      Anti-skid valve voltage (VOLTS)

Electrical On-Off Circuit

Card Columns

1-10	11-20	21-30	31-40	41-50	51-60	Card
VS	C700	C701	C702	C705	C706	A2
C707	C708	C709	C710	C711	VC1	A3
VC1	EV					A4

Variable      Description

VS      Supply voltage (volts)  
C700      Skid detection threshold current (amps)  
C701      (EG-VC1) coeff equ V6 (MHOS)  
C702      Const equ V6 (AMPS)  
C705      Reciprocal of capacitance C1 (volt/  
amp sec)  
C706      (EG-VC1) coeff equ R1 (MHOS)  
C707      Const equ R1 (AMPS)

<u>Variable</u>	<u>Description</u>
C708	(EG-VC1) coeff equ V2 (MHOS)
C709	(EG-VC1) coeff equ V4-1 (MHOS)
C710	Const equ V4-1 (AMPS)
C711	ABQ1 coeff equ V4-1 (DIMLS)
VC1	Voltage across capacitor C1 at time=0 (VOLTS)
VC1	Capacitor C1 voltage change rate (volts/sec)
EV	Anti-skid valve voltage (VOLTS)

## OUTPUT DATA

If microfilm output data is expected, indicate "16mm print" on job sheet and write "33-4020 PR" under Setups. Only the data outputted from the modules will be microfilmed. This data is printed every "P" seconds (see Card 1) of the total run "R" (see Card 1). The internal data print is an optional print, after the outputted data print, which consists of data inside a particular module, not outputted to other modules.

## RESTRICTIONS AND ERRORS

### A. Restrictions

No single time step should be greater than the run time of the problem. Each time step should be greater than zero. The internal print frequencies may be zero, but the print frequency for external data should never be zero.

### B. Errors

If any of the following errors occur, a message giving the error number will be printed out.

<u>Error</u>	<u>Explanation</u>
100	Microfilm option not 1, 2, or 3
101	Run time is zero
102	External print frequency is zero
103 or 120	Brake time step is zero
104 or 131	Hydraulic time step is zero
105 or 125	Airplane time step is zero
106 or 130	Wheel and tire time step is zero
107 or 127	Wheel speed sensor time step is zero

<u>Error</u>	<u>Explanation</u>
108, 133 or 126	Control system time step is zero
109 or 128	Control valve time step is zero
110 or 160	Pitch control time step is zero
111	Airplane runway option no. 1 or 2
112	Wheel speed sensor option not 1 or 2
113	Number of points for nose gear airload curve less than one or greater than 20
114	Number of points for nose gear damping curve less than one or greater than 20
115	Number of points for main gear airload curve is less than 1 or greater than 20
116	Number of points for main gear damping curve (ZSM 0) less than 1 or greater than 20
117	Hydraulic option is not 1, 2, or 3

The Simplified Antiskid Analysis Procedure Digital Computer Program Listing, CDC 6600 Procedure A6A, follows.

PROGRAM A6A (INPUT,OUTPUT,TAPE5=INPUT,TAPE6=OUTPUT,TAPE22<

C  
C  
C  
C  
C

# ANTISKID BRAKE SYSTEM — SIMPLIFIED MODEL

```
COMMON /KEY/ TSTEP, TEND, TRITE, MICRC, IDPT(2), T, TINTP
1 /SIMS/ ALPHA, ALPHB, ABP, ABPS, XGDD, VFD, ACVL,
2 CBPL, CBPU, CG, CSCVR, DG, ET, FNM, GCV, PBO, PCP, PFB,
3 PR, RBT, RR, RTD, SCL, SCVD, SCVA, SCVR, TCP, UBI, UB2,
4 UT1, UT2, VF, VRO, WG, WT, WIT, XCV, XSCN, XSCR, XB, XG, XGD,
5 XF, XFE /AFTI/ XCVD, WTD, XBC
5 /ICHECK/ IT
6 /HSD/EG
7 /CSO/ EV
```

```
8 /A6AC1/ VMIN, ACVRD, ACVSD, NR, PCVB /FRST/ FLG1, FLG3
9 /CSI/ VC1, VC2, VC3, VC4, VC1D, VC2D, VC3D, VC4D
A /CSU/ VC1D1, VC2D1, VC3D1, VC4D1
DATA WF /26.29/
```

```
FL(XD,XD1,X1,H) = (H/2.) * (XD+XD1) + X1
FN(XD,XD1,XD2,X1,H) = (H/12.) * (5.*XD + 8.*XD1 - XD2) + X1
```

C  
C

## SIMPLIFIED BRAKE CONTROL

```
5 CALL INPUT
KNT = D
FLG1 = 0.
TOUT = TINTP
T = 0.
```

```
TOUT = TRITE
VC1D1 = VC1D
VC2D1 = VC2D
VC3D1 = VC3D
VC4D1 = VC4D
```

```
10 FLG3 = 0.
FLG2 = 1.0
```

```
20 XGDD1 = XGDD
XGD2 = XGD1
XGD1 = XGD
XG1 = AG
```

A6AAD01  
A6AAD02  
A6AAD03  
A6AAD04  
A6AAD05  
A6AAD06  
A6AAD07  
A6AAD08  
A6AAD09  
A6AAD10  
A6AAD11  
A6AAD12  
A6AAD13  
A6AAD14  
A6AAD15  
A6AAD16  
A6AAD17  
A6AAD18  
A6AAD19  
A6AAD20  
A6AAD21  
A6AAD22  
A6AAD23  
A6AAD24  
A6AAD25  
A6AAD26  
A6AAD27  
A6AAD28  
A6AAD29  
A6AAD30  
A6AAD31  
A6AAD32  
A6AAD33  
A6AAD34  
A6AAD35  
A6AAD36  
A6AAD37  
A6AAD38  
A6AAD39

A6AA040  
 A6AA041  
 A6AA042  
 A6AA043  
 A6AA044  
 A6AA045  
 A6AA046  
 A6AA047  
 A6AA048  
 A6AA049  
 A6AA050  
 A6AA051  
 A6AA052  
 A6AA053  
 A6AA054  
 A6AA055  
 A6AA056  
 A6AA057  
 A6AA058  
 A6AA059  
 A6AA060  
 A6AA061  
 A6AA062  
 A6AA063  
 A6AA064  
 A6AA065  
 A6AA066  
 A6AA067  
 A6AA068  
 A6AA069  
 A6AA070  
 A6AA071  
 A6AA072  
 A6AA073  
 A6AA074  
 A6AA075  
 A6AA076  
 A6AA077  
 A6AA078

```

X802 = XBD1
X801 = X8D
X81 = X8
XCVD2 = XCVD1
XCVD1 = XCV
XCV1 = XCV
WTD2 = WTD1
WTD1 = WTD
WT1 = WT
VFD2 = VFD1
VFD1 = VFD
VF1 = VF
XFD2 = XFD1
XFD1 = XFD
XF1 = XF

C
C
EQUATION 3
IF (T - TCP) 30,30,40
30 PMV = T * (PCP - PR)/TCP + PR
GO TO 50
40 PMV = PCP

C
C
EQUATION 4
50 IF (XCV - SCL - SCVD) 60, 70, 70
60 ACVS = AMAX1 (ACVL, (XCV - SCL)*ACVSD/SCVD)
GO TO 80
70 ACVS = ACVSD

C
C
EQUATION 5
80 IF (-XCV - SCL - SCVD) 90, 100, 100
90 ACVR = AMAX1 (ACVL, (-SCL - XCV)*ACVRG/SCVD)
GO TO 110
100 ACVR = ACVRO
110 CONTINUE

C
C
C
EQUATION 10
IF (XB) 150, 150, 160
150 PB # CBPL * XB & PB0
  
```

```

GO TO 170
160 PB = CBPU * X8 & P80
    EQUATION 6 AND 7
170 QCVS = ACVS * SIGN(1.,PMV-P8) * Sqrt (ABS(PMV - P8))
    QCVR = ACVR * SIGN(1.,P8-PR) * Sqrt (ABS(P8-PR))
C
C
    EQUATION 8
    QB = QCVS - QCVR
C
C
    EQUATION 9
    XBD = QB/ABPS
C
C
    EQUATION 11
    XSC = C SCVR * EV
C
C
    EQUATION 12
    IF (XSC.LE.XSCM) GO TO 200
    IF (XSC.LT.XSCR) GO TO 210
    RSC = 0.
    GO TO 220
200 RSC = 1.
    GO TO 220
210 RSC = (XSCR - XSC)/(XSCR - XSCM)
C
C
    EQUATION 13
    PSC = RSC * (PMV - PR) + PR + PCVE
C
C
    EQUATION 14
    VCV = GCV * (PSC - P8)
C
C
    EQUATION 15
    IF (XCV.GE.SCVA) GO TO 240
    IF (XCV.GT.SCVR) GO TO 230
    XCVD = AMAX1 (0,VCV)
    GO TO 250
230 XCVD = VCV
    GO TO 250
240 XCVD = AMIN1 (0,VCV)
C

```

A6AA079  
A6AA080  
A6AA081  
A6AA082  
A6AA083  
A6AA084  
A6AA085  
A6AA086  
A6AA087  
A6AA088  
A6AA089  
A6AA090  
A6AA091  
A6AA092  
A6AA093  
A6AA094  
A6AA095  
A6AA096  
A6AA097  
A6AA098  
A6AA099  
A6AA100  
A6AA101  
A6AA102  
A6AA103  
A6AA104  
A6AA105  
A6AA106  
A6AA107  
A6AA108  
A6AA109  
A6AA110  
A6AA111  
A6AA112  
A6AA113  
A6AA114  
A6AA115  
A6AA116  
A6AA117

```

C      EQUATION 16
250  TEMP = PF8 * SIGN(1.,XBD)
    PE = AMAX1 (0,PB-PBO-TEMP)
C
C      EQUATION 17
    VB = RBT * WT
C
C      EQUATION 18
    IF (VB) 300, 310, 320
300  UB = -UB1 - UB2 * EXP(ALPHA * VB)
    GO TO 330
310  UB = 0.
    GO TO 330
320  UB = UB1 + UB2 * EXP (-ALPHA * VB)
C
C      EQUATION 19
330  TBT = ABP * RBT * 2.0 * NR * PE * UB
C
C      EQUATION 20
    FG = -CG*XG - DG*XGD
C
C      EQUATION 23
    VR = VF + XGD - RR*WT
C
C      EQUATION 25
    IF (VR-ET*VRO) GO TO 400
    IF (VR-GT--VRO) GO TO 410
    UT = -UT1 -(UT2 - ET * VF) * EXP (ALPHA*(VR+VRO))
    GO TO 420
400  UT = UT1 + (UT2 - ET *VF) * EXP(-ALPHA*(VR-VRO))
    GO TO 420
410  UT = (VR/VRO) * (UT1+UT2-ET*VF)
C
C      EQUATION 24
420  FBT = FNM * UT
C
C      EQUATION 26
    VFD = -FBT / MF
C

```

A6AA118  
A6AA119  
A6AA120  
A6AA121  
A6AA122  
A6AA123  
A6AA124  
A6AA125  
A6AA126  
A6AA127  
A6AA128  
A6AA129  
A6AA130  
A6AA131  
A6AA132  
A6AA133  
A6AA134  
A6AA135  
A6AA136  
A6AA137  
A6AA138  
A6AA139  
A6AA140  
A6AA141  
A6AA142  
A6AA143  
A6AA144  
A6AA145  
A6AA146  
A6AA147  
A6AA148  
A6AA149  
A6AA  
A6AA151  
A6AA152  
A6AA153  
A6AA154  
A6AA155  
A6AA156

```

C      EQUATION 27
XFO = VF / 12.0

C      EQUATION 21
XGDO = (FG - FBT)/WG

C      EQUATION 22
WTD = (FBT * RTO - TBT)/WIT
IF3FLG1.NE.0.< GOTO 433
IF3FLG2.NE.0.< GOTO 434
XGDO1 = XGDO
433 IF (FLG2.EQ.0.) GO TO 500
434 IF (TINTP.EQ.0.) GO TO 500
IF (T - TIOUT) 500, 450, 450
450 TIOUT = TIOUT + TINTP
FLG3 = 1.
WRITE (22,2000) T, ACVR, ACVS, EV, FG, FBT, PB, PE, PMV,
IPSC, QB, QCVR, QCVS, RSC, TBT, U8, UT, V8, VCV, WT, WTD,
2XCV, XCV0, XSC, X8, XBC, XG, XGC, XCC, VR
2000 FORMAT (* *,*SIMPLIFIED BRAKE CCNTRCL INTERNAL DATA*/
1 *      T=*,F15.8,* ACVR=*,E11.4,* ACVS=*,E11.4,
2 *      EV=*,E11.4,* FG=*,E11.4,* FBT=*,E11.4/
3 *      P9=*,E11.4,* PE=*,E11.4,* PMV=*,E11.4,
4 *      PSC=*,E11.4,* QB=*,E11.4,* QCVR=*,E11.4/
5 *      QCVS=*,E11.4,* RSC=*,E11.4,* TBT=*,E11.4,
6 *      U8=*,E11.4,* UT=*,E11.4,* VB=*,E11.4/
7 *      VCV=*,E11.4,* WT=*,E11.4,* WTD=*,E11.4,
8 *      XCV=*,E11.4,* XCV0=*,E11.4,* XSC=*,E11.4/
9 *      X8=*,E11.4,* XBD=*,E11.4,* XG=*,E11.4,
A *      XGO=*,E11.4,* XGDO=*,E11.4,* VR=*,E11.4/)
500 XGD = F1(XGCD,XGOD1,XGD1,TSTEP)
IF (FLG1.NE.0.) GO TO 510
XG = F1(XGD,XGD1,XG1,TSTEP)
XB = F1(XBC,XBD1,XB1,TSTEP)
XCV = F1(XCV0,XCVD1,XCV1,TSTEP)
WT = F1(WTC,MTD1,WT1,TSTEP)
VF = F1(VFD,VFD1,VF1,TSTEP)
XF = F1(XFO,XFD1,XF1,TSTEP)
GO TO 520

```

A6AA157  
A6AA158  
A6AA159  
A6AA160  
A6AA161  
A6AA162  
A6AA163  
A6AA164  
A6AA165  
A6AA166  
A6AA167  
A6AA168  
A6AA169  
A6AA170  
A6AA171  
A6AA172  
A6AA173  
A6AA174  
A6AA175  
A6AA176  
A6AA177  
A6AA178  
A6AA179  
A6AA180  
A6AA181  
A6AA182  
A6AA183  
A6AA184  
A6AA185  
A6AA186  
A6AA187  
A6AA188  
A6AA189  
A6AA190  
A6AA191  
A6AA192  
A6AA193  
A6AA194  
A6AA195

```

510 XG = FN(XGD,XG01,XG02,XG1,TSTEP)
XB = FN(XBD,XB01,XB02,XB1,TSTEP)
XCV = FN(XCVD,XCVD1,XCVD2,XCV1,TSTEP)
WT = FN(WTO,MTD1,MT02,WT1,TSTEP)
VF = FN(VFD,VFD1,VFD2,VF1,TSTEP)
XF = FN(XFO,XF01,XF02,XF1,TSTEP)
520 IF (FLG2.NE.0.) GO TO 530
    FLG2 = 1.
    GO TO 20
530 CALL WHSPSN
    IF(10*PI*2<.EQ.2< GO TO 540
    CALL CONSYS
    GO TO 545
540 CALL CONCI
545 FLG1 = 1.
    T = T + TSTEP
    IF (VF .LE. VMIN) GO TO 600
    IF (T - TEND) 550, 605, 605
550 IF (T - TOUT) 10, 600, 600
600 TOUT = TOUT + TRITE
605 WRITE (6,6010) T, TBT, XB, PB, PMV, XCV, EG, EV, WT, XF, XG, VF
6010 FORMAT (*0*,T50,*TIME =*,F16.8/* *,T14,*SIMPLIFIED BRAKE*/ * *,
    1T14,*CONTROL SYSTEM*,T30,* TBT=*,E11.4,* XE=*,E11.4,* PB=*,
    2E11.4/* *,T30,* PMV=*,E11.4,* XCV=*,E11.4,* EG=*,E11.4/
    3 * *,T30,* EV=*,E11.4,* WT=*,E11.4,* XF=*,E11.4/
    4 * *,T30,* XG=*,E11.4,* VF=*,E11.4/)
    IF (VF .LE. VMIN) GO TO 5
    IF (T - TEND) 610, 5, 5
610 KNT = KNT + 1
    IF (MOD(KNT,8)) 10, 620, 10
620 CALL EJECT
    GO TO 10
END

```

A6AA196  
A6AA197  
A6AA198  
A6AA199  
A6AA200  
A6AA201  
A6AA202  
A6AA203  
A6AA204  
A6AA205  
A6AA206  
A6AA207  
A6AA208  
A6AA209  
A6AA210  
A6AA211  
A6AA212  
A6AA213  
A6AA214  
A6AA215  
A6AA216  
A6AA217  
A6AA218  
A6AA219  
A6AA220  
A6AA221  
A6AA222  
A6AA223  
A6AA224  
A6AA225  
A6AA226  
A6AA227  
A6AA228

```

C
C
C
      SUBROUTINE      W H S P S N
      THE WHEEL SPEED SENSOR SYSTEM

      COMMON /KEY/ TSTEP,TEND,TRITE,MICRO,IOP1(2),T,TINTP
1     /FRST/ FLG1,FLG3 /CSO/ EV
2     /WSC/ CCGV, CWG, CWS, DWS, GWS, GWCC, WWS, ESN
3     /WSI/ XWS, XWSD
4     /WSO/ EG
5     /SIMS/ SIMP(44)
      EQUIVALENCE (WT,SIMP(35))
C
      IF(IOP1(1).EQ.2) GO TO 60
      FLG4 = 0.
C
10    XWSD01 = XWSD0
      XWSD2 = XWSD1
      XWSD1 = XWSD
      XWS1 = XWS
C
      EQUATION (1)
      EWS = GWS * WT
C
      EQUATION (2)
      FWS = CWG * EWS
C
      EQUATION (3)
      XWSD0 = FWS/WWS - (CWS/WWS) * XWS - (CWS/WWS) * XWSD
C
      EQUATION (4)
      EG = CCGV * XWS + ESN
C
      CHECK FOR INTERNAL PRINT
      IF (FLG4.EQ.0.) GO TO 30
      IF (FLG3.EQ.0.) GO TO 30
20    WRITE(22,6000) T, ESN, EG, EWS, FWS, XWS, XWSD, XWSD0
6000  FORMAT(1X,WHEEL SPEED SENSOR OPT=1,
1      * T=*,E15.8,* ESN=*,E11.4,* EG=*,E11.4,
2      * EWS=*,E11.4,* FWS=*,E11.4,* XWS=*,E11.4/

```

```

3* XWSD=*,E11.4,* XWSD0=*,E11.4)
C
C   PERFORM INTEGRATION
30 XSWD = (TSTEP/2.) * (XWSD0 + XWSD1) + XWSD1
  IF (FLG1.NE.0.) GO TO 40
  XWS = (TSTEP/2.) * (XWSD + XWSD1) + XWS1
  GO TO 50
40 XWS = (TSTEP/12.) * (5.*XWSD + 8.*XWSD1 - XWSD2) + XWS1
50 IF (FLG4.NE.0.) GO TO 55
  FLG4 = 1.
  GO TO 10
55 RETURN
C
C   EQUATION (5)   OPTION 2
60 EG = GWOC * WT + ESN
  IF ( TINTP.EQ.0.) GO TO 80
  IF ( FLG3.EQ.0.) GC TO 80
  WRITE (22,6010) T, EG, WT, ESN
6010 FORMAT(10 WHEEL SPEED SENSOR*/% T=*,F15.8,
1* EG=*,E11.4,* WT=*,E11.4,* ESN=*,E11.4)
80 RETURN
C
C   END
C
C

```

A6AI040  
A6AI041  
A6AI042  
A6AI043  
A6AI044  
A6AI045  
A6AI046  
A6AI047  
A6AI048  
A6AI049  
A6AI050  
A6AI051  
A6AI052  
A6AI053  
A6AI054  
A6AI055  
A6AI056  
A6AI057  
A6AI058  
A6AI059  
A6AI060  
A6AI061  
A6AI062  
A6AL001  
A6AL002

A6AL003  
A6AL004  
A6AL005  
A6AL006  
A6AL007  
A6AL008  
A6AL009  
A6AL010  
A6AL011  
A6AL012  
A6AL013  
A6AL014  
A6AL015  
A6AL016  
A6AL017  
A6AL018  
A6AL019  
A6AL020  
A6AL021  
A6AL022  
A6AL023  
A6AL024  
A6AL025  
A6AL026  
A6AL027  
A6AL028  
A6AL029  
A6AL030  
A6AL031  
A6AL032  
A6AL033  
A6AL034  
A6AL035  
A6AL036  
A6AL037  
A6AL038  
A6AL039  
A6AL040  
A6AL041

# S U B R O U T I N E C O N S Y S

## THE MODULATED ANTISKIO CCNTRCL CIRCUIT

COMMON /KEY/ TSTEP, TENO, TRITE, MICRG, IQPT(2), T, TINTP

1 /SIMS/ SIMP(44)

2 /FRST/ FLG1, FLG3

3 /CSI/ VC1, VC2, VC3, VC4, VC10, VC20, VC30, VC40

4 /CSO/ EV

5 /WSO/ EG

COMMON /CSC/ CM, C404, C405, C406, C407, C446, C447, C448,  
C449, C450, C451, C452, C456, C457, C458, C459,  
C460, C461, C462, C526, C527, C528, C529, C530,  
C531, C532, C533, C534, C535, C565, C566, C567,  
C568, C569, C570, C571, C575, C576, C577, C578,  
C579, C580, C581, C604, C605, C606, C607, C608,  
C609, C610, C611, C612, C613, C614, C615, C616,  
C617, C618, C619, C620, C621, C622, C623, C624,  
C801, C802, C803, C804, C805, C806, C807, C808,  
C809, C810, C811, C812, N

A /CSU/ VC101, VC201, VC301, VC401

EQUIVALENCE (VF, SIMP(32))

F1(X0, X01, X1, H) = H\*.5\*(X0 + XD1) + X1

FN(X0, X01, X02, X1, H) = (H/12.)\*(5.\*XD + 8.\*X01 - XD2) + X1

T0 = TSTEP

FLG5 = 1.0

10 VC102 = VC101

VC101 = VC10

VC11 = VC1

VC202 = VC201

VC201 = VC20

VC21 = VC2

VC302 = VC301

VC301 = VC30

VC31 = VC3

VC402 = VC401

VC401 = VC40

```

C          VC41 = VC4
C          EQUATION (5)
C          EGMVC1 = EG - VC1
C
C          EQUATION (R10)
C          VALUE = C621 / C620
C          AD8 = 0.
C          IF (EGMVC1 .GT. VALUE) AD8 = EGMVC1 * C620 - C621
C
C          EQUATION (Q-1C)
C          IF (EGMVC1) 20, 25, 25
C          20 ACQ1 = C604 - C605 * VC2
C          IF (VC2 - C604/C605) 30, 25, 25
C          25 ACQ1 = 0.
C
C          EQUATION (6)
C          30 ALWS = 0.
C          IF (VF .GT. C615 .AND. EG .LT. C616) GC TC 600
C
C          EQUATION (VQ4)
C          VALU = VC3 - VC2
C          ABQ4 = 0.
C          IF (VALU .GT. C623/C622) ABQ4 = VALU * C622 - C623
C
C          CIRCUIT CONDITION TEST EQUATIONS    TABLE VI-2  A,B,C
C          K = 1
C          VC34 = VC3 + VC4
C          VC24 = VC2 + VC4
C          40 GO TO (50,60,70,80,90,100,110,120,130,140,150,160), N
C          600 ALWS = C617
C          WRITE (6,6040) ALWS, VF, C615, EG, C616
C          6040 FORMAT(*MODULATED CONTROL CIRCUIT ALWS TEST CCNDITION FAILED.*
C          1/* ALWS = *,E11.4,* VF = *,E11.4,* C615 = *,E11.4,
C          2 * EG= *,E11.4,* C616 = *,E11.4)
C          CALL EXIT
C          45 K = C
C          VC34 = VC3 + VC4
C          VC24 = VC2 + VC4

```

```

C
C
C      CIRCUIT CONDITION 1
50 AEQ2 = - EGMVCI*C456 - VC34*C457 + C458
51 IF (AEQ2 - C6C7) 51, 51, 53
52 V8 = VC2*CM + AEQ2*C801 - C800
53 IF (V8) 52, 52, 53
54 AC4 = AEQ2 * C806 - VC34 * C804 - C8C7
55 IF (AC4) 52, 53, 54
56 IF (K) 180, 60, 45
57 N = 1
58 GO TO 180
C
C      CIRCUIT CONDITION 2
60 AEQ2 = VC2*C461 - EGMVCI*C459 - VC34*C46C + C462
61 IF (AEQ2 - C607) 61, 61, 63
62 IF (AEQ2 .LT. 0.0) AEQ2 = 0.0
63 V8 = VC2*CM + AEQ2*C801 - C800
64 IF (V8) 63, 63, 62
65 AC4 = AEQ2 * C8C6 - VC34 * C804 - C807
66 IF (AC4) 63, 63, 64
67 IF (K) 180, 70, 45
68 N = 2
69 GO TO 180
C
C      CIRCUIT CONDITION 3
70 AEQ2 = - EGMVCI*C446 - VC34*C447 + C448
71 IF (AEQ2 - C607) 73, 73, 71
72 IF (AEQ2 .GT. C802) AEQ2 = C802
73 V8 = VC2*CM + AEQ2*C801 - C800
74 IF (V8) 72, 72, 73
75 AC4 = AEQ2 * C803 - VC34 * C804 - C805
76 IF (AC4) 73, 73, 74
77 IF (K) 180, 80, 45
78 N = 3
79 GO TO 180
C
C      CIRCUIT CONDITION 4

```

A6AL081  
 A6AL082  
 A6AL083  
 A6AL084  
 A6AL085  
 A6AL086  
 A6AL087  
 A6AL088  
 A6AL089  
 A6AL090  
 A6AL091  
 A6AL092  
 A6AL093  
 A6AL094  
 A6AL095  
 A6AL096  
 A6AL097  
 A6AL098  
 A6AL099  
 A6AL100  
 A6AL101  
 A6AL102  
 A6AL103  
 A6AL104  
 A6AL105  
 A6AL106  
 A6AL107  
 A6AL108  
 A6AL109  
 A6AL110  
 A6AL111  
 A6AL112  
 A6AL113  
 A6AL114  
 A6AL115  
 A6AL116  
 A6AL117  
 A6AL118

80 AEQ2 = VC2\*C450 - EGMVCI\*C449 - VC34\*C451 + C452

IF (AEQ2 - C607) 83, 83, 81

81 IF (AEQ2 .GT. C802) AEQ2 = C8C2

V8 = VC2\*CM + AEQ2\*C801 - C800

IF (V8) 83, 83, 82

82 AC4 = AEQ2 \* C803 - VC34 \* C804 - C8C5

IF (AC4) 83, 83, 84

83 IF (K) 180, 90, 45

84 N = 4

GO TO 180

C

CIRCUIT CONOITION 5

90 AEQ2 = - EGMVCI\*C531 + C532

IF (AEQ2 - C607) 91, 91, 94

91 IF (AEQ2 .LT. 0.0) AEQ2 = 0.0

V8 = VC2\*CM + AEQ2\*C8C1 - C8C0

IF (V8) 92, 92, 94

92 AC4 = 0.0

TEMP1 = AEQ2 \* C806 - VC24 \* C8C4 - C8C7

IF (TEMP1) 93, 93, 94

93 TEMP2 = AEQ2 \* C811 - VC24 \* C809 - C812

IF (TEMP2) 94, 95, 95

94 IF (K) 180, 100, 45

95 N = 5

GO TO 180

C

CIRCUIT CONOITION 6

100 AEQ2 = VC2\*C533 - EGMVCI\*C534 - C535

IF (AEQ2 - C607) 101, 101, 104

101 IF (AEQ2 .LT. 0.0) AEQ2 = 0.0

V8 = VC2\*CM + AEQ2\*C801 - C800

IF (V8) 104, 104, 102

102 AC4 = 0.0

TEMP1 = AEQ2 \* C806 - VC34 \* C8C4 - C8C7

IF (TEMP1) 103, 103, 104

103 TEMP2 = AEQ2 \* C811 - VC24 \* C809 - C812

IF (TEMP2) 104, 105, 105

104 IF (K) 180, 110, 45

105 N = 6

GO TO 180

A6AL119  
A6AL120  
A6AL121  
A6AL122  
A6AL123  
A6AL124  
A6AL125  
A6AL126  
A6AL127  
A6AL128  
A6AL129  
A6AL130  
A6AL131  
A6AL132  
A6AL133  
A6AL134  
A6AL135  
A6AL136  
A6AL137  
A6AL138  
A6AL139  
A6AL140  
A6AL141  
A6AL142  
A6AL143  
A6AL144  
A6AL145  
A6AL146  
A6AL147  
A6AL148  
A6AL149  
A6AL150  
A6AL151  
A6AL152  
A6AL153  
A6AL154  
A6AL155  
A6AL156  
A6AL157  
A6AL158

```

C
C      CIRCUIT CONDITION 7
110 AEQ2 = - EGMVCI*C526 + C527
    IF (AEQ2 - C6C7) 114, 114, 111
111 IF (AEQ2 .GT. C802) AEQ2 = C802
    V8 = VC2*CM + AEQ2*C801 - C800
    IF (V8) 112, 112, 114
112 AC4 = 0.0
    TEMP1 = AEQ2 * C803 - VC34 * C804 - C805
    IF (TEMP1) 113, 113, 114
113 TEMP2 = AEQ2 * C808 - VC24 * C809 - C810
    IF (TEMP2) 114, 115, 115
114 IF (K) 180, 120, 45
115 N = 7
    GO TO 180

C
C      CIRCUIT CONDITION 8
120 AEQ2 = VC2*C528 - EGMVCI*C529 - C530
    IF (AEQ2 - C607) 124, 124, 121
121 IF (AEQ2 .GT. C802) AEQ2 = C802
    V8 = VC2*CM + AEQ2*C801 - C800
    IF (V8) 124, 124, 122
122 AC4 = 0.0
    TEMP1 = AEQ2 * C803 - VC34 * C804 - C805
    IF (TEMP1) 123, 123, 124
123 TEMP2 = AEQ2 * C808 - VC24 * C809 - C810
    IF (TEMP2) 124, 125, 125
124 IF (K) 180, 130, 45
125 N = 8
    GO TO 180

C
C      CIRCUIT CONDITION 9
130 AEQ2 = - EGMVCI*C565 - VC24*C566 + C567
    IF (AEQ2 - C607) 131, 131, 133
131 IF (AEQ2 .LT. 0.) AEQ2 = 0.0
    V8 = VC2*CM + AEQ2*C801 - C800
    IF (V8) 132, 132, 133
132 AC4 = AEQ2 * C811 - VC24 * C809 - C812
    IF (AC4) 134, 133, 133

```

A6AL159  
A6AL160  
A6AL161  
A6AL162  
A6AL163  
A6AL164  
A6AL165  
A6AL166  
A6AL167  
A6AL168  
A6AL169  
A6AL170  
A6AL171  
A6AL172  
A6AL173  
A6AL174  
A6AL175  
A6AL176  
A6AL177  
A6AL178  
A6AL179  
A6AL180  
A6AL181  
A6AL182  
A6AL183  
A6AL184  
A6AL185  
A6AL186  
A6AL187  
A6AL188  
A6AL189  
A6AL190  
A6AL191  
A6AL192  
A6AL193  
A6AL194  
A6AL195  
A6AL196  
A6AL197

A6AL198  
A6AL199  
A6AL200  
A6AL201  
A6AL202  
A6AL203  
A6AL204  
A6AL205  
A6AL206  
A6AL207  
A6AL208  
A6AL209  
A6AL210  
A6AL211  
A6AL212  
A6AL213  
A6AL214  
A6AL215  
A6AL216  
A6AL217  
A6AL218  
A6AL219  
A6AL220  
A6AL221  
A6AL222  
A6AL223  
A6AL224  
A6AL225  
A6AL226  
A6AL227  
A6AL228  
A6AL229  
A6AL230  
A6AL231  
A6AL232  
A6AL233  
A6AL234  
A6AL235  
A6AL236

133 IF (K) 180, 140, 45  
134 N = 9  
GO TO 180

C  
C CIRCUIT CONDITION 10  
140 AEQ2 = VC2\*C568 - EGMVCI\*C569 - VC24\*C570 - C571  
IF (AEQ2 - C607) 141, 141, 143  
141 IF (AEQ2 .LT. 0.0) AEQ2 = 0.0  
V8 = VC2\*CM + AEQ2\*C801 - C800  
IF (V8) 143, 143, 142  
142 AC4 = AEQ2 \* C811 - VC24 \* C809 - C812  
IF (AC4) 144, 143, 143  
143 IF (K) 180, 150, 45  
144 N = 10  
GO TO 180

C  
C CIRCUIT CONDITION 11  
150 AEQ2 = - EGMVCI\*C575 - VC24\*C576 + C577  
IF (AEQ2 - C607) 153, 153, 151  
151 IF (AEQ2 .GT. C802) AEQ2 = C802  
V8 = VC2\*CM + AEQ2\*C801 - C800  
IF (V8) 152, 152, 153  
152 AC4 = AEQ2 \* C808 - VC24 \* C809 - C810  
IF (AC4) 154, 153, 153  
153 IF (K) 180, 160, 45  
154 N = 11  
GO TO 180

C  
C CIRCUIT CONDITION 12  
160 AEQ2 = VC2\*C578 - EGMVCI\*C579 - VC24\*C580 - C581  
IF (AEQ2 - C607) 163, 163, 161  
161 IF (AEQ2 .GT. C802) AEQ2 = C802  
V8 = VC2\*CM + AEQ2\*C801 - C800  
IF (V8) 163, 163, 162  
162 AC4 = AEQ2 \* C808 - VC24 \* C809 - C810  
IF (AC4) 164, 163, 163  
163 IF (K) 180, 170, 45  
164 N = 12  
GO TO 180

```

170 K = -1
GO TO 40
180 CONTINUE
C
C EQUATION (LW-1)
AVAL = AEQ2 + ALWS
C
C EQUATION (N5) TABLE VI-3
GO TO (190,190,200,200,210,210,220,220,230,230,240,240), N
190 AD5 = AVAL*C606 - AC4
GO TO 250
200 AD5 = AVAL*C606*C404 - C405 - AC4
GO TO 250
210 AD5 = AVAL + C606
GO TO 250
220 AD5 = AVAL*C606*C404 - C405
GO TO 250
230 AD5 = AVAL*C606 - AC4
GO TO 250
240 AD5 = AVAL*C606*C404 - C405 - AC4
250 IF (A05 .LT. 0.) AD5 = 0.
C
C EQUATION (N4)
EV = A05 + C406 + C407
C
C EQUATION (N10)
AR3 = AEQ2*C612 + (EV - EGMVC1)*C613
C
C EQUATION (N11)
AC1 = AC8 - AR3 - ACQ1
C
C EQUATION (A1)
VC10 = AC1 + C608
C
C EQUATION (N14)
IF (AC4) 260, 270, 270
260 AC2 = ABQ4 + C614 + AC4 - VC2 + C618
GO TO 280

```

A6AL237  
A6AL238  
A6AL239  
A6AL240  
A6AL241  
A6AL242  
A6AL243  
A6AL244  
A6AL245  
A6AL246  
A6AL247  
A6AL248  
A6AL249  
A6AL250  
A6AL251  
A6AL252  
A6AL253  
A6AL254  
A6AL255  
A6AL256  
A6AL257  
A6AL258  
A6AL259  
A6AL260  
A6AL261  
A6AL262  
A6AL263  
A6AL264  
A6AL265  
A6AL266  
A6AL267  
A6AL268  
A6AL269  
A6AL270  
A6AL271  
A6AL272  
A6AL273  
A6AL274  
A6AL275



```

GO TO 350
340 VC1 = FN(VC1D,VC1D1,VC1D2,VC11,TD)
VC2 = FN(VC2D,VC2D1,VC2D2,VC21,TD)
VC3 = FN(VC3D,VC3D1,VC3D2,VC31,TD)
VC4 = FN(VC4D,VC4D1,VC4D2,VC41,TD)

C 350 WRITE (6,1005) N, VC1, VC2, VC3, VC4
1005 FORMAT (*0*,T14,*SUBROUTINE CONSYS*,T31,* N=*,I2,*
1 * VC2=*,E11.4/ * *,T30, *
2 /)
IF (FLG5.NE.0.) GO TO 360
FLG5 = 1.
GO TO 1C
360 RETURN
END

```

```

A6AL315
A6AL316
A6AL317
A6AL318
A6AL319
A6AL320
A6AL321
A6AL322
A6AL323
A6AL324
A6AL325
A6AL326
A6AL327
A6AL328
A6AL329

```



```

GO TO 18
17 READ (5,5010) GMOC, ESN, EG
18 CONTINUE
C
  CONTROLLER
  READ (5,5020) ICPT(2)
  IF (ICPT(2).EQ.2) GO TO 20
  READ (5,5010) CS, C, EV
  GO TO 24
20 READ (5,5010) CC, VC1, VC10, EV
24 CALL EJECT
25 WRITE (6,6000) IO, TSTEP, TENO, TRITE, MICRC, TINTP
6000 FORMAT (//IHO,T55,I9HI N P U T O A T A//IHO,TLO,
1 *TIME BETWEEN*,T30,*SYSTEM*,T60,*SYSTEM PRINT*,T88,
2 3A10/ * *,TLO,*STEPS=*,E11.4,T30,*FUA TIME = *,
3 E11.4,T60,*INTERVAL = *,E11.4,T88,*MICROFILM OPT= *,I2//
4 * *,TLO,*INTERNAL PRINT INTERVAL =*,E11.4//)
  WRITE (6,5007) ACVRO, ACVSO, PCVB, VMIN, NR
5007 FORMAT (IHO, * ACVRC = *,E11.4, 5X, * ACVSO = *,E11.4, 5X, * PCVB
1= *,E11.4, 5X, * VMIN = *,E11.4, 5X, * NR = *,I3//)
  WRITE (6,6020) SIMP
6020 FORMAT (IHO,T44,*S I M P L I F I E D B R A K E C O N T R O L*/A6AM060
1 *0*,TLO,* ALPHA=*,E11.4,* ALPH8=*,E11.4,* ABP=*,E11.4,
2 * *,TLO,* ABPS=*,E11.4,* ACR=*,E11.4,* ACVO=*,E11.4/
3 * *,TLO,* ACVL=*,E11.4,* CBPL=*,E11.4,* CBPU=*,E11.4,
4 * *,TLO,* CG=*,E11.4,* CSCVR=*,E11.4,* OG=*,E11.4/
5 * *,TLO,* ET=*,E11.4,* FAP=*,E11.4,* GCV=*,E11.4,
6 * *,TLO,* P80=*,E11.4,* PCP=*,E11.4,* PF8=*,E11.4/
7 * *,TLO,* PR=*,E11.4,* R8T=*,E11.4,* RR=*,E11.4,
8 * *,TLO,* RTO=*,E11.4,* SCL=*,E11.4,* SCVC=*,E11.4,
9 * *,TLO,* SCVA=*,E11.4,* SCVR=*,E11.4,* TCP=*,E11.4,
A * *,TLO,* UBL=*,E11.4,* UB2=*,E11.4,* UT1=*,E11.4/
B * *,TLO,* UT2=*,E11.4,* VF=*,E11.4,* VRO=*,E11.4,
C * *,TLO,* WG=*,E11.4,* WIT=*,E11.4/
D * *,TLO,* XCV0=*,E11.4,* XSCP=*,E11.4,* XSCR=*,E11.4,
E * *,TLO,* XBO=*,E11.4,* XGO=*,E11.4,* XGO0=*,E11.4/
F * *,TLO,* XFO=*,E11.4,* XFD0=*,E11.4/)
C
  WHEEL SPEED SENSOR
  IF (ICPT(1).EQ.2) GO TO 83
  WRITE (6,6050) ICPT(1), CCGV, CMG, CHS, DMS, GWS, MWS,ESN,

```

```

1 XWS, XWSD, EG
6050 FORMAT(1H ,T10,6HOPTION,13,T41,35HW T E E L S P E E O S E N S
10 R/
2 1H0,T10,8H CCGV=,E11.4,8H CMG=,E11.4,8H CWS=,E11.4,
3 DWS=,E11.4,8H GWS=,E11.4,8H WWS=,E11.4/
4 1H0,T1C,8H ESN=,E11.4,8H XWS=,E11.4,8H XWSC=,E11.4,
5 EG=,E11.4///)
GC TO 84
83 WRITE (6,6051) IOPT(1), GWOC, ESN, EG
6051 FORMAT(1H ,T10,6HOPTION,13,T41,35HW H E E L S P E E O S E N S
10 R/
2 1H0,T10,8H GWOC=,E11.4,8H ESN=,E11.4,8H EG=,E11.4///)
C
C CONTROL SYSTEM
84 IF (IOPT(2).EQ.2) GO TO 90
WRITE (6,6060) (CS(L),L=1,29)
6060 FORMAT(10*,T46,*CONTROLLER*,
1 *0*,T10,* CM=,E11.4,
2 * C404=,E11.4,* C405=,E11.4,*
3 * *,T10,* C407=,E11.4,* C446=,E11.4,*
4 * *,T10,* C448=,E11.4,* C449=,E11.4,*
5 * *,T10,* C451=,E11.4,* C452=,E11.4,*
6 * *,T10,* C457=,E11.4,* C458=,E11.4,*
7 * *,T10,* C460=,E11.4,* C461=,E11.4,*
8 * *,T1C,* C526=,E11.4,* C527=,E11.4,*
9 * *,T1C,* C529=,E11.4,* C530=,E11.4,*
A * *,T10,* C532=,E11.4,* C533=,E11.4,*
B * *,T10,* C535=,E11.4*)
WRITE (6,6065) (CS(L),L=30,43)
6065 FORMAT(
1 * *,T10,* C565=,E11.4,* C566=,E11.4,*
2 * *,T10,* C568=,E11.4,* C569=,E11.4,*
3 * *,T1C,* C571=,E11.4,* C575=,E11.4,*
4 * *,T10,* C577=,E11.4,* C578=,E11.4,*
5 * *,T10,* C580=,E11.4,* C581=,E11.4)
WRITE (6,6069) (CS(L),L=44,76), C, EV
6069 FORMAT(
1 * *,T1C,* C604=,E11.4,* C605=,E11.4,*
2 * *,T10,* C607=,E11.4,* C608=,E11.4,*
C606=,E11.4,
C609=,E11.4/

```

A6AM118  
A6AM119  
A6AM120  
A6AM121  
A6AM122  
A6AM123  
A6AM124  
A6AM125  
A6AM126  
A6AM127  
A6AM128  
A6AM129  
A6AM130  
A6AM131  
A6AM132  
A6AM133  
A6AM134  
A6AM135  
A6AM136  
A6AM137  
A6AM138  
A6AM139  
A6AM140  
A6AM141  
A6AM142  
A6AM143  
A6AM144  
A6AM145  
A6AM146  
A6AM147  
A6AM148  
A6AM149  
A6AM150  
A6AM151  
A6AM152  
A6AM153  
A6AM154  
A6AM155  
A6AM156

C612=\*,E11.4,  
C615=\*,E11.4/  
C618=\*,E11.4,  
C621=\*,E11.4/  
C800=\*,E11.4,  
C8C3=\*,E11.4/  
C8C6=\*,E11.4,  
C809=\*,E11.4/  
C812=\*,E11.4,  
VC3=\*,E11.4/  
VC2D=\*,E11.4,  
EV=\*,E11.4//)

C7C2=\*,E11.4/  
C707=\*,E11.4,  
C710=\*,E11.4/  
VC1D=\*,E11.4,

C611=\*,E11.4,\*  
C614=\*,E11.4,\*  
C617=\*,E11.4,\*  
C620=\*,E11.4,\*  
C623=\*,E11.4,\*  
C8C2=\*,E11.4,\*  
C805=\*,E11.4,\*  
C8C6=\*,E11.4,\*  
C811=\*,E11.4,\*  
VC2=\*,E11.4,\*  
VC1D=\*,E11.4,\*  
VC4C=\*,E11.4,\*

C701=\*,E11.4,\*  
C706=\*,E11.4,\*  
C7C5=\*,E11.4,\*  
VC1=\*,E11.4,\*

C610=\*,E11.4,\*  
C613=\*,E11.4,\*  
C616=\*,E11.4,\*  
C619=\*,E11.4,\*  
C622=\*,E11.4,\*  
C801=\*,E11.4,\*  
C804=\*,E11.4,\*  
C8C7=\*,E11.4,\*  
C810=\*,E11.4,\*  
VC1=\*,E11.4,\*  
VC4=\*,E11.4,\*  
VC3D=\*,E11.4,\*

C700=\*,E11.4,\*  
C7C5=\*,E11.4,\*  
C7C8=\*,E11.4,\*  
C711=\*,E11.4,\*  
EV=\*,E11.4)

3 \* \*,T10,\*  
4 \* \*,  
5 \* \*,T10,\*  
6 \* \*,  
7 \* \*,T10,\*  
8 \* \*,  
9 \* \*,T10,\*  
A \* \*,  
B \* \*,T10,\*  
C \* \*,  
D \* \*,T10,\*  
E \* \*,

GO TO 55

90 WRITE (6,6080) CC, VC1, VC1D, EV

6C8C FORMAT (\* \*,T46,\*CCNTRCLLER\*)

1 \*0\*,T10,\*  
2 \* \*,

3 \* \*,T1C,\*  
4 \* \*,

5 \* \*,T10,\*  
6 \* \*,

95 CALL EJECT

C

C ERROR CHECKS

100 IF (MICRC .GT. 0 .AND. MICRO .LT. 4) GO TO 110

IT= 100

WRITE (6,6100) IT

6100 FORMAT(\*0 ERROR \*, I3, \* CCCURRED. \* )

110 IF (TEND .GT. 0.) GO TO 120

IT= 101

WRITE (6,6100) IT

120 IF (TRITE .GT. 0.) GO TO 130

IT= 102

WRITE (6,6100) IT

130 IF (TSTEP.GT.0.) GO TO 140

IT = 103

WRITE (6,6100) IT

140 IF (IOPT(1).EQ.1.OR.IOPT(1).EQ.2) GO TO 15C

IT = 104

```

WRITE (6,6100) IT
150 IF (IOPT(2).EQ.1.OR.IOPT(2).EQ.2) GO TO 200
IT # 105
WRITE (6,6100) IT
C
200 N = 1
RETURN
210 CALL EJECT
WRITE(6,6600)
6600 FORMAT(22H0THIS JOB IS CCMPLETE. )
CALL EXIT
RETURN
END

```

```

A6AM157
A6AM158
A6AM159
A6AM160
A6AM161
A6AM162
A6AM163
A6AM164
A6AM165
A6AM166
A6AM167
A6AM168
A6AM169

```



A6AN040  
A6AN041  
A6AN042  
A6AN043  
A6AN044  
A6AN045  
A6AN046  
A6AN047  
A6AN048  
A6AN049  
A6AN050  
A6AN051  
A6AN052  
A6AN053  
A6AN054  
A6AN055  
A6AN056  
A6AN057  
A6AN058  
A6AN059  
A6AN060  
A6AN061  
A6AN062  
A6AN063  
A6AN064  
A6AN065  
A6AN066  
A6AN067  
A6AN068  
A6AN069

```

C      IF (ABQ1 .GE. C700) EV = VS
C      EQUATION (N1)
      AD2 = ABQ1 + AR1
      IF (AD2 .LT. 0.) AD2 = 0.
      AC1 = AD1 + AR4 - AD2

C      EQUATION (A1)
      VC10 = AC1 * C705

C      CHECK FOR PRINTCUT
      IF (FLG6.EQ.0.) GO TO 30
      IF (FLG3.EQ.0.) GO TO 30

      20 WRITE(22,6010) T, VC1, VC10, ABQ1, AC1, AD1, AR1, AR4, EV ,EG
      6010 FORMAT (#0 CONTROLLER INTERNAL DATA*/
      1* T=*,E15.8,* VC1=*,E11.4,* VC10=*,E11.4,
      2* ABQ1=*,E11.4,* AC1=*,E11.4,* AD1=*,E11.4/
      3* AR1=*,E11.4,* AR4=*,E11.4,* EV=*,E11.4,
      4 8H EG=,E11.4)

C      30 IF (FLG1.NE.0.) GO TO 40
      VC1 = TSTEP*.5*(VC10+VC1D1) + VC11
      GO TO 50
      40 VC1 = (TSTEP/12.) * (5.*VC10 + 8.*VC1D1 - VC1C2) + VC11

C      50 IF (FLG6.NE.0.) GO TO 70
      FLG6 = 1.
      GO TO 10
      70 RETURN
      END

```

```

C
C
C
      S U B R O U T I N E   E J E C T

      COMMON /DAT/ JCB, DAY, IPAGE, PAGE(2)

      IPAGE = IPAGE + 1
      ENCODE(14,50,PAGE)IPAGE
      50 FORMAT(114)
      WRITE(6,60) JOB, DAY, PAGE(2)
      60 FORMAT(78HIGENERAL DYNAMICS
      1 FORT WORTH OPERATION /37H 6600 PROCEDURE AIC
      2 A9,11X,A10,2X,5HPAGE ,A4/)
      RETURN
      END

```

A6AP001  
A6AP002  
A6AP003  
A6AP004  
A6AP005  
A6AP006  
A6AP007  
A6AP008  
A6AP009  
A6AP010  
A6AP011  
A6AP012  
A6AP013  
A6AP014

CC = 00871